Characterizing and engineering a dengue refractory phenotype in *Aedes aegypti*

by

Heather Grace Coatsworth

B.Sc., University of Guelph, 2012

Thesis Submitted in Partial Fulfillment of the
Requirements for the Degree of
Doctor of Philosophy

in the
Department of Biological Sciences
Faculty of Science

© Heather Coatsworth 2019
SIMON FRASER UNIVERSITY
Summer 2019

Copyright in this work rests with the author. Please ensure that any reproduction or re-use is done in accordance with the relevant national copyright legislation.

Approval

Name:	**Heather Grace Coatsworth**
Degree:	**Doctor of Philosophy (Biology)**
Title:	**Characterizing and engineering a dengue refractory phenotype in *Aedes aegypt*i**
Examining Committee:	**Chair:** Jenny Cory Professor
	Carl Lowenberger Senior Supervisor Professor
	Jim Mattsson Supervisor Associate Professor
	David Theilmann Supervisor Research Manager and Research Scientist in Molecular Insect Virology Agriculture and Agri-Food Canada
	Dawn Cooper Supervisor Associate Dean for Accreditation, Assessment and Evaluation University of Washington
	Julian Christians Internal Examiner Associate Professor
	Steve Perlman External Examiner Professor Department of Biology University of Victoria
Date Defended/Approved:	June 25, 2019

Abstract

Dengue viruses infect ~400 million people annually and are transmitted principally by *Aedes aegypti*. Severe dengue (dengue hemorrhagic fever and dengue shock syndrome) can be fatal, and there are no efficient drugs or vaccines to prevent the disease. Not all *Ae. aegypti* transmit dengue viruses; in Cali, Colombia, approximately 30% of feral populations are naturally refractory to all four viral serotypes through midgut mechanisms (Cali-MIB), while the remaining 70% are susceptible (Cali-S) and transmit the viruses. We used a combination of molecular biology and bioinformatic methods to identify differences between the refractory and susceptible strains. RNA sequencing, 16S rRNA bacterial profiling, and a genome wide association study (GWAS) were used to identify a subset of genes thought to contribute to the Cali-MIB and Cali-S phenotypes. Genes from this subset that were able to 'flip' the phenotype from susceptible to refractory through RNAi based knockdowns were further tested with gene-editing technology to knock-out these genes using clustered regularly interspaced palindromic repeats (CRISPR) – CRISPR-associated protein 9 (Cas9) guide RNA complexes. This research identified multiple genes we believe contribute to vector competence, created a DNA based assay for identifying Cali-MIB and Cali-S mosquitoes, and edited the germ-line of *Ae. aegypti*. This information could allow us to create lines of permanently refractory mosquitoes to dampen dengue transmission.

Keywords: *Aedes aegypti*; refractory mechanisms; dengue; insect immunity; mosquito genetic engineering

To all who brought lemonade into my life.

Cheers.

Acknowledgements

There are so many people who have made this PhD possible. First and foremost, I need to thank Dr. Mosquito himself, Carl, for all his help, patience and guidance for the last few years. Carl, from long conversations in your office full of sarcastic droll, to scientific debates, hockey bets, lacrosse games, and many a beer, I cannot thank you enough for helping me get to this point. You put up with my blasting rap music, obsessive colour matching, lack of green thumb and need to name every object in our lab. Your attendance and kind words at the burials of Spotty, Fin and Yeezy (my fish) were greatly appreciated. I truly feel that my writing, wet lab skills and teaching abilities have vastly improved since I joined the lab. I'm a better scientist and human because of you.

I'm extremely grateful for my committee members, Dr's. Jim Mattsson, Dawn Cooper and Dave Theilmann. Their support and guidance throughout my degree was extremely appreciated. I know much more about virology and bioinformatics thanks to our committee discussions and hallway run-ins.

At the start of my degree I was the sole member of the Lowenberger lab. I have Cassandra Carroll and Jen McFarlane to thank for bringing me into two labs as an adoptive lab member. Cassandra introduced me to the Moore lab; Margo, Liz Steves and company, and to great lunchtime discussions and crosswords over tea. Those lunches were my first taste of community at SFU – thanks for that Cass! Jen brought me to the Cory lab meetings, which I still attended to the end of my time at SFU. The Cory lab was a second home to me and introduced me to some of the best folks I know, Paul MacDonald, Joyce Leung, Kevin Colmenares and Pauline Deschodt. Our cabin trips, late night Clue playing, and happy hour Ilia visits were always raucous good times. These labs were both headed by amazing women – Margo Moore and Jenny Cory. Both of these women have become academic mentors to me, advising me about academics and life (and even reality TV!). Thank you both so much.

Two years into my degree, the Lowenberger lab started to fill up. First with Shir Yi Toh, Maleni Ramirez, and Nicolas Salcedo, and then with numerous undergraduates, many of whom helped collect much of the data in this thesis: Jazmin Flores, Jaime Chalissery, Lea Sanchez-Milde, Sujani Gomes, Iman Baharmand, Luke Nicholls, Rachel Cooper, Rachel Blair, Jeffery Yung, Chris Combe, William Shen, Madeline Eeles, Laura

Barth, and Liliana Lopez. This meant many a weekend, countless late nights and holidays spent in the lab. Nicolas Salcedo, Iman Baharmand, Rachel Blair, Laura Barth and Lea Sanchez-Milde all became extremely good friends. Some of my best grad school memories (and quotes!) come from these great times. A special shout-out to my lab ride or die, Nico, for always knowing how to pick me up when I was down, entertaining my tiny house rants and re-igniting my scientific curiosity. I wouldn't have made it through without you Nic.

As a graduate student I quickly learned how important community was. I was first exposed to this graduate community with sports, drinks and lunchtime debates with Sebastian Ibarra, Matt Holl, Nathan Derstine and Kyle Bobiwash. As time passed, and my comrades defended and moved away, the community shifted, and Jaime Chalissery, Lea Sanchez-Milde, Kevin Colmenares, Nicolas Salcedo, Pauline Deschodt, Don Wiggins, Ranah Chavoshi and Liz Steves became my go-to homies. Lunchtimes were usually sunny and funny, board games were played, dogs were pet, and beer was a plenty. This graduate community was integral to overcoming the emotional toils of graduate school – thank you guys!

I have so many numerous other individuals and labs at SFU to thank for their consultation and help in building this thesis – thank you to the Brinkman, Cory, Gries, Guttman, Hutter, Mattsson, Morin, and Quarmby labs and the SFU machine shop. The equipment loaned to us from the Molday lab at UBC made Chapter 5 of this thesis possible – thank you so much.

My time at SFU was not solely spent on my thesis, as I also acted as a teaching assistant and sessional lecturer. I learned a great deal about how to teach and became a much better educator from my interactions with Tiia Haapalainen, Kevin Lam, Erin Barley, and Megan Barker. Years of TAing Parasitology with Tammy McMullan and Carl Lowenberger helped prepare me for a sessional position teaching the course with my own TA. I learned a lot about myself through this process!

As part of my degree I spent 3 months in Cali, Colombia, learning from the Vector Biology and Control team at CIDEIM. Mildred Serrato, Julieth Mina, Mabel Moreno, Angélica Aponte, Ana Lucia Jaramillo, Paola Caicedo, and Clara Ocampo taught me much of what I now know about a functioning vector biology lab and viral infections. Everyone

at CIDEIM was extremely kind and hospitable to me during my stay. This thesis would not have been possible without the hard work and sample collection completed by Dr. Paola Caicedo. Much of the data contained in this thesis was prepared by Paola – Paola you are a force to be reckoned with! During my time in Colombia I stayed with Jackeline Bravo Chamorro and her daughter Sofia Gomez. These two women quickly became like sisters to me and travelling across the country with them was a major highlight of my trip. It feels very comforting to know that I always have another home in Colombia.

Anyone who knew me at SFU knew that I functioned primarily on chana masala, samosas and hazelnut coffee from Renaissance café. Renaissance – thank you for sustaining me for the duration of my graduate career at SFU.

A large part of graduate school was understanding how to cope with stress and maintain some resemblance of work-life balance. This balance was extremely difficult, and I often found myself teetering. Through this entire process my friends never wavered – they were constant pillars of support. Whether it be through dog walks, movies, trash TV, sports, walks or talks, Jasmine McCulligh, Rachel Blair, Lea Sanchez-Milde, Don Wiggins, Paul MacDonald, Lydia Stepanovic, Joyce Leung, Ahdia Hassan, Pauline Deschodt, Megan McPhee, Emily Allan and Liz Steves were real G's. To my roomies P and Ahds, thank you for a million dance parties, deep talks, and good eats – you made Vancouver a true home for me. To Emily Allan, thank you for accepting me immediately for who I am always fully understanding that; our time with vegan cardamom ice cream, basketball and falafel house are always with me. To Kyle Bobiwash, thank you for all the amazing times throughout the years - the bike rides, the skateboarding, the tennis playing, the snakes, the tortoises, the traveling, the cooking, the wine and all the times with our pup, Acorn. I love you! To my gerfie, Megan McPhee, thank you for everything that is impossible to capture here – I've never grown as much as a person as I have from our friendship. You welcomed me into your family with an open heart and defined what being a true friend is – thank you and love you!

Lastly, I want to thank my amazing family for always being available for support, whether it be financially, emotionally, comedically or nutritionally. Nana – our talks always bring sunshine into every day. Laura – your understanding and empathy have helped me to be a much more whole human, I'm so happy you are my sibling – hold that purse close! Mom – thank you for your concern, and your nurturing ways always – you always know

exactly what to say. Dad – thank you for your verboseness, attention to detail and willingness to learn new subjects – you always challenge me and although I may always resist it, I have legitimately grown from it. Acorn – thank you for all the face licks, snuggles, chases and hugs – you are and will always be the best puppy ever.

Thank you all so much!

Table of Contents

Approval ii
Abstract iii
Dedication iv
Acknowledgements v
Table of Contents ix
List of Tables xiii
List of Figures xvi
List of Acronyms xviii

Chapter 1. Introduction 1
Author Contributions 1
1.1. Abstract 1
1.2. Introduction 2
1.2.1. Dengue: the virus 2
1.2.2. Dengue: in the human host 2
1.2.3. Transmission to human hosts: vectors 4
1.2.4. Dengue virus in the vector: innate immune responses 5
1.2.5. Toll pathway 6
1.2.6. Immune deficiency (IMD) pathway 7
1.2.7. Janus kinase–signal transducer and activator of transcription (JAK-STAT) pathway 7
1.2.8. RNA interference (RNAi) 8
1.2.9. Autophagy 9
1.2.10. Apoptosis 10
1.2.11. Interactions among pathways 11
1.2.12. Dengue virus in the vector: midgut microbes 12
1.2.13. Vector competence in *Ae. aegypti* 12
1.2.14. Refractory *Aedes aegypti* 13
1.2.15. Mitigating dengue: control measures 15
1.2.16. Conclusion 18
1.3. Thesis objectives 19
1.4. References 21
Figures 34
Connecting Statement 1 36

Chapter 2. RNA sequencing shows differential expression between field derived dengue refractory and susceptible strains of *Aedes aegypti* 37
Author Contributions 37
2.1. Abstract 37
2.2. Introduction 38
2.3. Methods 40
2.3.1. Ethics statement 40

2.3.2. Mosquito rearing 40
2.3.3. Virus propagation and mosquito infections 40
2.3.4. Mosquito dissections 41
2.3.5. RNA extraction, library preparation, and RNA sequencing 41
2.3.6. Processing of raw sequencing reads 41
2.3.7. Read alignment and mapping 42
2.3.8. Differential expression tests 42
2.3.9. Analysis of differential expression data 43
2.3.10. Validation of differential gene expression using quantitative PCR 44
2.4. Results 44
2.4.1. Raw sequencing reads processing, alignment and mapping 44
2.4.2. Differential expression analysis 45
2.4.3. Statistical and systems analysis of differential expression data 45
2.4.4. Choosing a candidate gene shortlist 46
2.4.5. Differential expression validation 46
2.5. Discussion 47
2.5.1. Differential expression analysis 47
2.5.2. Statistical and systems analysis of differential expression data 50
2.5.3. Differential expression validation 51
2.5.4. Candidate Gene Analysis 51
2.6. Data Availability 53
2.7. Acknowledgements 53
2.8. References 55
Tables 63
Figures 72
Connecting Statement 2 75

Chapter 3. Polymorphisms determining phenotypic differences in field derived refractory and susceptible strains of *Aedes aegypti* 76
Author Contributions 76
3.1. Abstract 76
3.2. Introduction 77
3.3. Methods 79
3.3.1. Mosquito collection and maintenance 79
3.3.2. Exposure to dengue virus and phenotype determination 79
3.3.3. DNA sample preparation 80
3.3.4. Variant calling and filtering 81
3.3.5. Genome-Wide Association Study (GWAS) 81
3.3.6. Genome-Wide Epistasis Study (GWES) 82
3.3.7. Identifying phenotypic markers 82
3.3.8. Effect prediction 82
3.4. Results 83
3.4.1. Genome-Wide Association Study 83
3.4.2. Genome-Wide Epistasis Study 83

3.4.3. Identifying phenotypic markers 84
3.4.4. Effect Prediction 84
3.5. Discussion 84
3.6. References 89
Tables 94
Figures 100
Connecting Statement 3 104

Chapter 4. The composition of midgut bacteria in *Aedes aegypti* (Diptera: Culicidae) that are naturally susceptible or refractory to dengue viruses .. 105
Author Contributions 105
4.1. Abstract 105
4.2. Introduction 106
4.3. Methods 108
4.3.1. Ethics statement 108
4.3.2. Mosquito rearing and maintenance 108
4.3.3. Sample preparation 108
4.3.4. Amplicon library preparation and sequencing 109
4.3.5. Amplicon data analysis 109
4.4. Results 110
4.4.1. Analyzing negative and positive controls 110
4.4.2. Bacterial abundance and community composition 111
4.4.3. Alpha and beta diversity metrics 112
4.5. Discussion 112
4.6. Acknowledgements 115
4.7. Data availability 115
4.8. References 116
Tables 121
Figures 123
Connecting Statement 4 125

Chapter 5. Engineering resistance to dengue virus in *Aedes aegypti* via CRISPR-Cas-9 mediated techniques 126
Author Contributions 126
5.1. Abstract 126
5.2. Introduction 127
5.3. Methods 129
5.3.1. Mosquito collection and maintenance 129
5.3.2. Guide design and construction 130
5.3.3. Embryo collection and microinjections: *cathepsin-b* 131
5.3.4. Embryo collection and microinjections: *xylosyltransferase* 133
5.3.5. Genomic DNA extraction 133
5.3.6. Analysis of CRISPR-Cas9 induced mutations 133
5.3.7. Fitness evaluations 133
5.4. Results 134

5.4.1. Embryo collection and microinjections 134
5.4.2. Genomic DNA extraction 135
5.4.3. Analysis of CRISPR-Cas9 induced mutations 135
5.4.4. Fitness evaluations 135
5.5. Discussion 136
5.5.1. Embryonic microinjections 136
5.5.2. Fitness effects on injected individuals 137
5.5.3. Analysis of CRISPR-Cas9 induced mutations 137
5.5.4. Future Directions 138
5.6. References 140
Tables 144
Figures 157

Chapter 6. Conclusions 162
6.1. Summary 162
6.2. Future directions 164
6.3. The challenges of vector control 165
6.4. References 167

Appendix A. Supplementary data for Chapter 2 169

Appendix B. RNAi mediated knock down of *Aedes aegypti xylosyltransferase oxt*, *heparan sulfate N-deacetylase/N-sulfotransferase*, and clip-domain serine protease easter 34, family B 187
Author Contributions 187
Abstract 187
Introduction 188
Methods 189
Mosquito maintenance 189
Synthesis of double-stranded RNA 189
Mosquito microinjections 190
Mosquito dissections 190
RNA extraction and cDNA synthesis 191
Knockdown assessment 191
Results 192
Mosquito microinjections 192
Knockdown assessment 192
Discussion 192
References 195
Tables 197
Figures 199

List of Tables

Table 2.1 Full factorial treatment design outlining all twelve experimental treatments. Each treatment consists of one replicate (n=1), containing 36 pooled mosquito midguts. 63

Table 2.2 List of candidate genes (candidate gene table). Table includes VectorBase gene ID, gene name, functional group, general gene function, possible association with pathogens, and associated references. 'Up' refers to up-regulated in the Cali-MIB strain, while 'Down' refers to down-regulated in the Cali-MIB strain. 64

Table 2.3 Shared genes between differentially expressed genes at 24 and 48 hours (comparing the Cali-Susceptible and Cali-Refractory mosquitoes infected with virus) herein and those already documented in the literature. GOLD differential expression values are displayed from this study, and compared with differential expression values obtained from (Behura and Severson 2012; Bonizzoni et al. 2012a; Chauhan et al. 2012; Colpitts et al. 2011). GOFLD value is the normalized GFOLD log2-fold change value, the first RPKM (reads per kilobase of transcript per million mapped reads values) represents the susceptible mosquitoes, while the second RPKM corresponds to the refractory mosquitoes. Panel A is a comparison after 24 hours, while panel B is after 48 hours. 66

Table 3.1 Primer pair sequences. These primers were designed to flank each of the three markers identified as phenotypically unique by the Lasso regression. 94

Table 3.2 Accuracy of the three markers AX-93240282, AX-93240283, and AX-93220550) in predicting the dengue-susceptible (Cali-S) or refractory (Cali-MIB) phenotypes of *Aedes aegypti*. The mosquitoes used in this test are from the second selection of Cali-S and Cali-MIB mosquitoes, and were not the same ones used in the GWAS and GWES studies. 95

Table 3.3 Genotype ratios from the first selection of dengue-refractory (Cali-MIB, n=17) and dengue-susceptible individuals (Cali-S, n=19). Results are from the three candidate marker variants (AX-93240282, AX-93240283, AX-93220550) identified as phenotypically associated through the stepwise LASSO regression. 96

Table 3.4 Sequence results from the accuracy testing of each of the three markers (AX-93240282, AX-93240283, and AX-93220550). The results are from the second selection of Cali-S (dengue-susceptible, S) and Cali-MIB (dengue-refractory, R) mosquitoes. Text colour represents the observed phenotype of the mosquito (green for S, red for R), while nucleotide shading represents the marker genotype of the mosquito (again, green for the S variant, red for the R variant) 97

Table 3.5 Summary of Vector Base's effect prediction. Only variants predicted to have a high (start loss) or moderate (missense variant or in-frame insertion) impact were included here. 98

Table 4.1 Primer sequences used for 16S amplification 121

Table 4.2 Beta diversity statistical outputs, where the composition of bacteria between Cali-S and Cali-MIB midguts was compared using four beta diversity metrics. 122

Table 5.1 CRISPR guide RNA names and sequences. Guides were created using the Zhang Lab and MIT's CRISPR designe tool (crispr.mit.edu) to target exons (in order to disrupt translation) within two genes of interest: *xylosyltransferase* (AAEL007409) and *cathepsin-b* (AAEL007585) in *Aedes aegpyti*. 144

Table 5.2 Primer names and sequences designed to flank at least 100bp of the cut site for both *cathepsin-b* (AAEL007585) and *xylosyltransferase* (AAEL007409). The For1 and For2 primers for *cathepsin-b* are RNase H-dependant PCR (rhPCR) primers, while the rest of the primers are traditional PCR primers. 145

Table 5.3 Measured continuous fitness parameters (pupal lifespan, time to hatching, larval lifespan, adult male lifespan, adult female lifespan and number of males and females hatched) from the *cathepsin-b* CRISPR-Cas9 injection experiment. Each line represents one biological replicate (separate injection experiment) for each of our four experimental treatments: wildtype control (un-injected, not handled), handled control (un-injected, handled), buffer injected (injected, handled), and *cathepsin-b* RNP injected (injected, handled). Injection date is included to aid in the separation of biological replicates. 146

Table 5.4 Measured proportional fitness parameters (proportion of larvae hatched, proportion of pupae emerged, proportion of adults that ecolsed) from the *cathepsin-b* CRISPR-Cas9 injection experiment. Each line represents one biological replicate (separate injection experiment) for each of our four experimental treatments: wildtype control (un-injected, not handled), handled control (un-injected, handled), buffer injected (injected, handled), and *cathepsin-b* RNP injected (injected, handled). 150

Table 5.5 Measured egg-laying parameters (number of gonotrophic cycles per female, number of eggs from each gonotrophic cycle per female (1^{st}, 2^{nd}, and 3^{rd}, and average egg size of eggs from each gonotrophic cycle (1^{st}, 2^{nd}, and 3^{rd}) from the *cathepsin-b* CRISPR-Cas9 injection experiment. Each line represents one biological replicate (separate mating pair(s)) for each of our four experimental treatments: wildtype (wt) control (un-injected, not handled), handled control (un-injected, handled), buffer injected (injected, handled), and *cathepsin-b* RNP injected (injected, handled). The buffer injected, and handled pair mates remained within treatment (i.e. only buffer males and females mated, and only handled males and females mated). To create separate *cathepsin-b* KO lines (homozygous KO, heterozygous KO), *cathepsin-b* injected individuals were out-crossed with wt males or females. 153

Table 5.6 Statistical analyses completed on the fitness parameter data collected from *cathepsin-b* CRISPR-Cas9 injection experiment. All statistical analyses were completed using R (Team 2018). Panel A represents results from one-way ANOVAs completed on continuous data that passed Levene's Test for Homogeneity of Variance (time to hatching, number of eggs from each gonotrophic cycle, size of eggs from each gonotrophic cycle, larval lifespan, male lifespan, female lifespan, and pupal lifespan).

Panel B shows the results from one-way ANOVAs completed on generalized linear model (family = quasibinomial, link=logit) results used to analyze proportional data (proportion of males and female, proportion of pupae hatched, proportion of adults hatched, proportion of larvae hatched). A generalized linear model (family=poisson, link=log) with another one-way ANOVA was used to investigate the number of gonotrophic cycles per females. *denotes statistically significant ($p<0.05$) parameters.....156

List of Figures

Figure 1.1 Development of dengue viruses in *Aedes aegypti* and the locations on natural infection barriers that prevent virus development, replication, or transmission. 34

Figure 1.2 Mosquito immune signaling and RNAi pathways involved in mosquito–dengue interactions. Figure from Sim S, Jupatanakul N, Dimopoulos G. Mosquito immunity against arboviruses. Viruses 2014;6:4479–504. Reproduced with permission. 35

Figure 2.1 Modified and adapted RNA rocket Galaxy portal bioinformatics workflow. 72

Figure 2.2 Significantly differentially expressed genes between Cali-S and Cali-MIB strains at 24, 36 and 48 h after ingesting dengue virus serotype 2, arranged by broad functional groups denoted by ImmunoDB. 73

Figure 2.3 Consensus hierarchical clustering result from DESeq2 (v. 1.16.0), Cuffdiff (v. 2.2.1) and GFOLD (v. 1.1.1) generated using R (v. 3.1.1). Clustering shows the phylogenetic relationship between all 12 treatment expression profiles (S: Cali-S, R: Cali-MIB, v: virus fed, b: blood fed, numbers represent time points). Euclidian distances were generated to compute Complete Linkage clustering. 74

Figure 3.1 Data processing and bioinformatics workflows for the genome wide association study (GWAS), in blue, and the genowide wide epistatis study (GWES), in purple. 100

Figure 3.2 Q-Q plots of all three association tests created using R v. 3.4.3. The red line is the 1:1 relationship between the expected and observed data, while the black dots are our data. Panel A shows the association test without any correction for population structure, B depicts the data structure after co-variate correction, and panel C is the structure after co-variate and kinship adjustment. The genomic inflation factor, λ (ratio of observed: expected values) is displayed on the bottom right hand corner of each plot. 101

Figure 3.3 Manhattan plot of the association test after population correction. The plot was created using R v. 3.4.3. Each dot represents one of the 15,084 SNPs analyzed. Black dots (n=15,082) are statistically non-significant (p-value $\geq 3.31e^{-6}$), while teal dots (n=2) are statistically significant (p-value <3.31e-6). The teal line depicts the p-value significance cut-off of $3.31e^{-6}$. 102

Figure 3.4 Cross-validation misclassification error rates (with standard error bars) of the Lasso logistic regression model. The model was tuned using λ (log-scale, x-axis). The minimum misclassification error was reached when the log of λ is -1.61, incorporating three SNPs. 103

Figure 4.1 Bacterial taxa organized by order, expressed per sample. Bars on the left are from Cali-MIB samples (R1-R8), while bars on the right are from Cali-S samples (S1-S8). 123

Figure 4.2 Alpha diversity boxplots. A: Pielou's evenness, B: Observed number of ASVs, C: Faith's Phylogenetic Diversity, D: Shannon. 124

Figure 5.1 Methods flowchart detailing *Aedes aegpyti* CRISPR-Cas9 embroyonic injection experiments. All the steps in the *cathepsin-b* RNP injection experiment were completed at Simon Fraser University, while the embro injections for the *xylosyltransferase* RNP injection experiment were completed at the Insect Transformation Facility at the University of Maryland. Red denotes the *cathepsin-b* RNP injected treatment, orange is the buffer injected treatment, green is the handled treatment control, blue is the wildtype (uninjected, unhandled) treatment control, and purple is the *xylosyltransferase* RNP injected treatment.....157

Figure 5.2 A one-way ANOVA with Tukey's post-hoc test was used to investigate differences between pupal lifespan (in days) across treatments in the *cathepsin-b* injection experiment (df=3, F=4.551, p<0.01).....158

Figure 5.3 A generalized linear quasibinomial model with a logit link function was used to analyze differences between the proportion of larvae hatched across treatments in the *cathepsin-b* embryo injection experiment (df=3, p<0.001).....159

Figure 5.4 Heteroduplex assay (Alt-R Genome Editing Detection Kit, IDT) analyzing *cathepsin-b* gRNA targets. The leftmost lane is a 100bp ladder (100bp Opti-DNA Marker, abm), while the other four lanes each represent one individual mosquito. The *wt* control is an uninjected Liverpool *Aedes aegypti.* PCR projects were seperated in a 3% agarose gel. *Cathepsin-b* RNP injected individuals 14 and 31 show multiple bands (heteroduplexes), while the *wt* control and catepsin-b RNP injected individual 20 only show one band (homoduplexes). 160

Figure 5.5 Heteroduplex assay (Alt-R Genome Editing Detection Kit, IDT) analyzing *xylosyltransferase* gRNA targets. The leftmost lane is a 100bp ladder (100bp Opti-DNA Marker, abm), while the other lanes each represent one individual mosquito injected with *xylosyltransferase* gRNA 1. The *wt* control is an uninjected Liverpool *Aedes aegypti*. PCR projects were seperated in a 3% agarose gel. *Xylosyltransferase* RNP injected individuals 93A, 97A, 99A, 106A, 108A, 110A, 114A and 122A show multiple bands (heteroduplexes), while the *wt* control and remaining *xylo*syltrasferase RNP injected individuals only show one band (homoduplexes). The kit homoduplex control shows one single band, while the kit heteroduplex control shows multiple bands.....161

List of Acronyms

ADE	Antibody-dependant enhancement
Ago2	Argonaute-2
AMP	Antimicrobial peptide
ANCOM	Analysis of composition of microbiome
ANT	*Arabidopsis thaliana* Integrase-type DNA-binding superfamily protein
ASV	Amplicon sequence variants
ATG	Autophagy
BHK	Baby hamster kidney
Cas9	CRISPR-associated protein
cDNA	complementary DNA
CFAV	Cell fusion agent virus
CIDEIM	Centro Internacional de Entrenamiento e Investigaciones Médicas
CIEIA	Comité de Ética para la Investigación en Animales Experimentales
CLIPB34	Clip-domain serine protease easter 34, family B
cM	Centimorgan
CRISPR	Clustered regularly interspaced short palindromic repeats
crRNA	CRISPR RNA
Ct	Cycle threshold
CTL	C-type lectin
ddPCR	Droplet digital PCR
ddRAD-seq	Double digest RAD-seq
DE	Differential expression
DENV	Dengue viruses
DEPC	Diethylpyrocarbonate
DF	Dengue fever
DHF	Dengue hemorrhagic fever
Dome	Domeless receptor
dpi	Days post infection
DREDD	Death-related ced-3/Nedd2-like protein
dsRNA	Double stranded RNA

DSS	Dengue shock syndrome
DVRF	Dengue virus restriction factor
E	Envelope protein
EIP	Extrinsic incubation period
EPA	Environmental Protection Agency
FADD	FASS-associated death domain
FDA	US Food and Drug Administration
FPKM	Fragments per kilobase of transcript per million mapped reads
FREP1	Fibrinogen-related protein 1
GEO	Gene expression omnibus
GI	Gastrointestinal
GM	Genetically modified
GNBP	Gram negative binding protein
GO	Gene ontology
gRNA	Guide RNA
GWAS	Genome wide association study
GWES	Genome wide epistasis study
HDR	Homology-directed repair
HIV	Human immunodeficiency virus
Hop	*HS*p70-*HS*p90 organizing protein
HS	*Heparan sulfate N-deacetylase/N-sulfotransferase*
IAP	Inhibitor of apoptosis
IFI	Immunofluorescence assay
IMD	Immune deficiency
JAK-STAT	Janus kinase signal transducer and activator of transcription
JNK	C-Jun N-terminal kinase
KD	Knock-down
KEGG	Kyoto encyclopedia of genes and genomes
KO	Knock-out
LAC	Library and Archives Canada
LEfSe	Linear discriminant analysis effect size
MEB	Midgut escape barrier
MIB	Midgut infection barrier

miRNA	Micro RNA
MMP	Matrix metalloproteinase
MOYO-D	MOYO-In-Dry
MOYO-R	MOYO Refractory
MOYO-S	MOYO Susceptible
mRNA	Messenger RNA
MYD88	Myeloid differentiation primary response 88
NF-κB	Nuclear factor kappa-light-chain-enhancer of activated B cells
NGS	Next-generation sequencing
NHEJ	Non-homologous end joining
NS1	Non-structural protein 1
NS4B	Non-structural protein 4B
OBP	Odorant binding protein
OTU	Operational taxonomic unit
PAM	Protospacer adjacent motif
PAMP	Pathogen-associated molecular pattern
PBM	Post blood meal
PBS	Phosphate buffered saline
PCA	Principal component analysis
PCR	Polymerase chain reaction
PIAS	Protein inhibitor of activated STAT
PRR	Pattern recognition receptor
qPCR	Quantitative-real time PCR
Q-Q	Quantile-quantile
QTL	Quantitative trait loci
R	Refractory
RAD-seq	Restriction-site associated DNA sequencing
RAPD	Random amplification of polymorphic DNA
Rel	Relish
RFLP	Restriction fragment length polymorphism
rhPCR	RNase H-dependant PCR
RIDL	Release of insects carrying a dominant lethal
RISC	RNA-induced silencing complex
RNA seq	RNA sequencing

RNAi	RNA interference
RNP	Ribonucleoprotein
RPKM	Reads per kilobase of transcript per million mapped reads
RPS7	*40S ribosomal protein S7*
S	Susceptible
SD	Severe dengue
SEB	Salivary gland escape barrier
SFU	Simon Fraser University
SIB	Salivary gland infection barrier
siRNA	Small interfering RNA
SIT	Sterile insect technique
SNP	Single nucleotide polymorphism
SSCP	Single strand conformation polymorphism
TALEN	Transcription activator-like effector nuclease
TCID50	Median tissue culture infectious dose
tracrRNA	Trans-activating RNA
Upd	Unpaired ligand
VC	Vector competence
WHO	World Health Organization
wt	Wildtype
xylo	*Xylosyltransferase oxt*
ZFN	Zing-finger nuclease

Chapter 1. Introduction

A modified version of Chapter 1 has been published as: Schonhofer, C., Coatsworth, H.*, Caicedo, P., Ocampo, C., Lowenberger, C. 2016. Aedes aegypti immune responses to dengue virus. Lessons in Immunity. Chapter 10: 129-143.*

** these authors contributed equally to this work and are co-first authors*

Author Contributions

Cole Schonhofer and Heather Coatsworth completed the literature review. Cole Schonhofer, Heather Coatsworth, and Carl Lowenberger designed and wrote the paper. All authors (Cole Schonhofer, Heather Coatsworth, Paola Caicedo, Clara Ocampo and Carl Lowenberger) edited manuscript drafts.

1.1. Abstract

Mosquitoes, especially *Aedes aegypti*, transmit dengue viruses (DENV) to humans. Some strains of *Ae. aegypti* recognize and eliminate DENV through aspects of innate barriers that do not allow the virus to enter or escape infected cells. Within these cells, components of the innate immune responses of the vectors are expressed by the insects and manipulated by the virus: Toll, immune deficiency, Janus kinase—signal transducer and activator of transcription, apoptosis, autophagy, and RNAi act individually or in concert to eliminate or reduce DENV titers in the vectors (Huang et al. 2019). Because many of these pathways share common molecules, it is difficult to know if they have been activated directly by DENV or if their activation is secondary. Nonetheless, the overall response to DENV is a general activation of all immune pathways that may modulate DENV titers but does not eliminate DENV infection in the majority of vectors.

Keywords: *Aedes aegypti*, dengue virus, host–pathogen interactions, innate immunity

1.2. Introduction

1.2.1. Dengue: the virus

Dengue viruses (DENV) are structured, enveloped, single stranded positive sense RNA viruses belonging to the Flavirviridae family. These flaviviruses (named after the Latin *flavus* for the jaundice caused by yellow fever) include some of the most important vector-transmitted human viruses including yellow fever, dengue, West Nile, Zika, and multiple encephalitis viruses (Halstead et al. 1997). Dengue is a single viral species with four viral serotypes. The DENV genome encodes three structural proteins (capsid, pre-membrane, and envelope) and seven non-structural proteins (NS1, NS2A, NS2B, NS3, NS4A, NS4B, and NS5) (Wilder-Smith et al. 2019). Usually the envelope (E) or non-structural protein 1 (NS1) genes are sequenced to identify the serotype due to the lack of overall sequence homology between serotypes (<70%) in these regions. It is generally assumed that, evolutionarily speaking, DENV-4 diverged first, followed by DENV-2, and finally by DENV-1 and DENV-3, which are closely related (Halstead et al. 1997).

Once in a host (vertebrate or vector), DENV attach to host receptors (DC-SIGN and Fc receptors in humans) and use clathrin-dependent endocytosis to enter cells (Guzman and Harris 2015). Once inside, the virus fuses with an endosomal vesicle, where the acidic, negatively charged endosomal environment induces viral nucleocapsid release (Wilder-Smith et al. 2019). DENV then hijack the host's endoplasmic reticulum in order to translate and assemble its genome, creating a negative RNA template to synthesize multiple positive viral RNA strands. The ER membrane envelopes the replicated virus, and immature virus particles pass to the Golgi apparatus to undergo pre-membrane cleavage, producing mature virions. The virus is then released from the cell via exocytosis (Rodenhuis-Zybert et al. 2010), allowing it infect and replicate further.

1.2.2. Dengue: in the human host

Although some infections with dengue virus may be asymptomatic, humans infected with dengue virus often develop dengue fever (DF), colloquially known as "break-bone fever". The disease affects 50-400 million people each year (Messina et al. 2015), and is characterized by muscle and joint pain, fever, headaches, nausea, and rashes (Rigau-Pérez et al. 1998). Most infected people recover completely 5-12 days after initial

infection (Srikiatkhachorn 2009). Primary infection with one DENV serotype provides lifelong protection to subsequent infections with that same serotype. Subsequent infection with a different serotype, however, may result in severe dengue (SD), which encompasses both dengue hemorrhagic fever (DHF) and dengue shock syndrome (DSS), which cause approximately 25,000 deaths annually. Although the exact mechanisms that cause DHF and DSS are under debate, they are clearly linked to a previous DENV exposure (Srikiatkhachorn 2009, Guzman et al. 2013), and are the result of a phenomenon known as antibody-dependant enhancement (ADE) (Whitehead et al. 2007). ADE is a rare immune reaction, found in dengue patients as well as some patients infected with human immunodeficiency virus (HIV), that results in increased viral infectivity. This is caused by the production of non-neutralizing antibodies, as well as the inhibition of naïve B cells, allowing the infective viral serotype to efficiently sub-vert host immune responses (Guzman et al. 2013).

Despite significant effort, there are no efficient vaccines or dengue-specific drugs currently available (Mairuhu et al. 2004, Srikiatkhachorn 2009). While vaccines have been developed, such as Sanofi Pastueur's Dengvaxia, issues have arisen over the production of non-protective dengue infection enhancing antibodies in individuals who are seronegative for dengue, issues which caused an uproar in the Philippines when over 800,000 school children were vaccinated (Dyer 2017). Although Dengvaxia is still available commercially for purchase, it is no longer recommended by the World Health Organization (WHO) for this reason. Despite these set-backs, tetravalent vaccine development continues, with multiple candidates in the development pipeline (Pedrique et al. 2013).

The immune responses and the life threatening potential problems associated with DHF and DSS have challenged the development of a tetravalent vaccine against DENV that must protect equally well against all four serotypes at once (Thomas 2014). A potential fifth DENV serotype was recently reported, making vaccine development efforts even more problematic (Normile 2013, Mustafa et al. 2014). With 2-4 billion people around the world at risk of the disease, Dengue is currently the world's most significant arthropod-borne virus (arbovirus) (Messina et al. 2015). Recent epidemiological and climate change models predict future dengue outbreaks in areas that currently are considered–dengue free (Morin et al. 2013).

1.2.3. Transmission to human hosts: vectors

DENV are transmitted by adult female mosquitoes of the genus *Aedes*, primarily *Aedes aegypti* and, to a lesser extent, *Aedes albopictus*. Both species breed in small water filled containers around human habitation, and are extremely well adapted to urban human environments (Halstead 2008, David et al. 2009). Female *Ae. aegypti* and *Ae. albopictus* bite during the daytime or in crepuscular periods, and therefore sleeping under bed nets at night, which reduces the incidence of *Plasmodium* infection (malaria), transmitted by night biting mosquitoes, will not reduce DENV transmission. With no available vaccines or drugs to combat this disease, dengue control measures have emphasized vector control programs that eradicate or reduce mosquito populations, and therefore transmission. While short term or regional successes of these programs have been reported, *Ae. aegypti* populations have rebounded and expanded their global distribution, contributing to the expansion of DENV transmission to new geographical and dengue-naïve regions (Halstead et al. 1997, Morin et al. 2013). The ease and speed of international commerce and human travel between endemic and non-endemic regions has contributed directly to the spread of mosquito vectors and the constant circulation of multiple DENV serotypes. Whereas previously the 4 serotypes of DENV were geographically separated, there are now areas where all 4 serotypes occur, increasing the prevalence and incidence of severe dengue.

Adult *Ae. aegypti* have a median lifespan of 38 days at optimal temperatures (Brady et al. 2013) and the vast majority of adults die from environmental conditions, predation, or host defences rather than succumbing to old age (Maciel-de-Freitas et al. 2007, David et al. 2009). Female *Ae. aegypti* feed on human blood to obtain the proteins required to develop and lay a batch of eggs. During this blood feeding, females may obtain DENV which enter the mosquito's midgut for digestion. DENV leave the blood bolus and infect and replicate within midgut epithelial cells. Two to three days post infection (dpi), DENV exit midgut cells and disseminate throughout the vector via the hemolymph, infecting and replicating within cells of the fat body, trachea, and nervous tissues (Salazar et al. 2007, Sim et al. 2014). Although DENV can be found in the salivary glands as early as 4 dpi, there is an extrinsic incubation period (EIP) of 7-14 days during which the virus disseminates throughout the mosquito, infects the salivary gland, and replicates to a high enough titre to infect humans during a subsequent blood meal (Salazar et al. 2007, Sim

et al. 2014). After this EIP, females are capable of transmitting DENV for the rest of their lives (Halstead et al. 1997).

Vector competence (VC), the intrinsic ability of a vector to transmit a pathogen, is determined by the dynamics between DENV and the vector. Different mosquito species and strains show different responses to DENV infection in terms of susceptibility (Vazeille-Falcoz et al. 1999, Salazar et al. 2007, Schneider and Mori 2007, Xiao-Xia et al. 2013). A competent or susceptible vector will allow viral infection, dissemination, and transmission, as described above, whereas a refractory vector will not. There are four accepted barriers to virus development (Black et al. 2002). If DENV are unable to infect midgut cells, or cannot replicate within them, the mosquito is considered refractory via a midgut infection barrier (MIB), and if the midgut is infected, but the virus is unable to replicate and disseminate into the hemocoel, a midgut escape barrier (MEB) is present. Additional barriers may exist in the salivary glands, in which the virus escapes the midgut but cannot enter the salivary glands, a salivary gland infection barrier (SIB), or is unable to disseminate into the salivary gland lumen, a salivary gland escape barrier (SEB) (Romoser et al. 2005, Sim et al. 2012, 2013). These barriers represent selective pressures for DENV to overcome (Khoo et al. 2013). The presence of these barriers in some mosquito strains, and their absence in others, is likely genetically pre-determined.

1.2.4. Dengue virus in the vector: innate immune responses

There are other processes and factors that also contribute to VC, such as the inducible immune responses of individual mosquitoes (Molina-Cruz et al. 2005, Cox et al. 2011, Sim et al. 2013, Hill et al. 2014). All invertebrates, including mosquitoes, rely exclusively on their innate immune system to eliminate microbial pathogens. In order to initiate classical innate immune responses, pattern recognition receptors (PRRs) (Medzhitov and Janeway 1997) must recognize conserved pathogen-associated molecular patterns (PAMPs) on the outer surfaces of pathogens. Subsequently, components of the humoral and cellular responses are activated via multiple signalling cascades, including the Toll, IMD, RNA Interference (RNAi), JNK and JAK-STAT pathways (Boutros et al. 2002, Leclerc and Reichhart 2004, Tsakas and Marmaras 2010). These responses culminate in numerous effector mechanisms, including phagocytosis (Kocks et al. 2005), encapsulation (Lemaitre and Hoffmann 2007), melanisation (Christensen et al. 2005), the expression of reactive oxygen intermediates (Nappi and

Carton 2001, Christensen et al. 2005, Kocks et al. 2005), and the expression of multiple antimicrobial peptides (AMPs) that target and kill microorganisms (Lowenberger et al. 1995, 1999, Bulet et al. 1999, Lowenberger 2001, Lopez et al. 2003, Boulanger et al. 2004, 2006, Ursic-Bedoya and Lowenberger 2007, Ursic-Bedoya et al. 2011). The strongest immune responses are expressed in the hemocoel of insects (Lowenberger et al. 1995, Lowenberger 2001, Lee et al. 2019), but many AMPs also are expressed in the GI tract of insects to eliminate or prevent the over proliferation of non-desirable symbionts (Lowenberger et al. 1995, Ursic-Bedoya and Lowenberger 2007, Ursic-Bedoya et al. 2011). DENV, however, are intracellular pathogens and, as such, they are not exposed to classic extracellular insect immune responses. Nonetheless, DENV infection in mosquitoes results in the activation of multiple pathways including Toll, IMD, JAK-STAT, RNA Interference (RNAi), autophagy and apoptosis. These pathways have been reported to control, regulate, or modulate DENV success in mosquitoes and are described in more detail below.

1.2.5. Toll pathway

The Toll pathway, first described in *Drosophila melanogaster* in the innate immune defence against Gram-positive bacteria and fungi, is also activated during DENV infection in *Ae. aegypti* (Zambon et al. 2005, Xi et al. 2008). In response to microbes, PRRs at the cell surface recognize PAMPs and initiate an intracellular signalling cascade that leads to the eventual activation of *Rel* proteins via degradation of the inhibitory binding protein *Cactus*. Activated *Rel* is an NF-κB transcription factor that enters the cell nucleus and initiates transcription of multiple effector AMP genes, such as *drosomycin* and *defensin*s (Waterhouse et al. 2007). Transcriptional profiling of DENV-2-infected *Ae. aegypti* midguts and carcasses revealed increased expression of genes linked to the Toll pathway, including *toll*, *spatzle*, and *Rel1A*, as well as a decrease in transcription of the negative regulator, *cactus* (Xi et al. 2008). Additionally, targeted RNAi silencing of *cactus* resulted in a decreased midgut viral load, while RNAi silencing of *MYD88*, an activator of the Toll pathway, resulted in an increased midgut viral load (Xi et al. 2008). Consistent results were obtained when the experiments were performed 3-7 dpi using different mosquito and viral serotypes (Ramirez and Dimopoulos 2010). The overall contribution of the Toll pathway activation in DENV infected mosquitoes is not clear; despite *toll* activation, and the expression of *toll* mediated responses, dengue was not eliminated.

1.2.6. Immune deficiency (IMD) pathway

The IMD pathway is often considered the principal immune response against Gram-negative bacteria, and also results in activation of an NF-kB transcription factor, *Rel2*. The IMD pathway is initiated by different PRR-PAMP interactions, involves different signalling cascades, and activates a variety of effector AMPs. In *Ae. aegypti*, *Rel2*, is held inactive in the cytosol by *caspar*, which is degraded during IMD signal transduction, allowing *Rel2* to be translocated to the nucleus, leading to the transcription of several AMPs (Kingsolver et al. 2013).

Although there is evidence that IMD activation protects against viral infection in *D. melanogaster* (Costa et al. 2009), similar IMD-mediated protection against DENV infection in *Ae. aegypti* is unclear. RNAi silencing of caspar in DENV-2-infected mosquitoes at 7 dpi had no effect on viral titres in midgut or carcass tissues (Xi et al. 2008). DENV infection of *Ae. aegypti* salivary glands induces the expression of *cecropin*, an IMD-related AMP that reduces DENV titres in *Ae. albopictus* cells (Luplertlop et al. 2011). RNAi silencing of IMD in two strains of moderately susceptible *Ae. aegypti* significantly increased midgut DENV-2 titres to levels comparable with more susceptible strains, whereas RNAi silencing of *caspar* did not reduce viral titres significantly (Sim et al. 2013). These data suggest that Caspar silencing during DENV infection is ineffective because the IMD pathway is already activated to its full extent (Sim et al. 2013). As was the case with *toll* activation, the significance of IMD activation, and the expression of IMD-induced AMPs does not eliminate DENV from infected mosquitoes.

1.2.7. Janus kinase–signal transducer and activator of transcription (JAK-STAT) pathway

The JAK-STAT pathway is a signalling pathway involved in development, immunity, and multiple other processes. Activation of the pathway begins with the extracellular binding of the unpaired ligand (*Upd*) to the domeless receptor (*Dome*), which leads to the self-phosphorylation of JAKs (*Hop*) and the creation of binding sites on *Dome*. These sites induce dimerization of *STAT*s, which then translocate to the nucleus and affect the expression of target genes (Kingsolver et al. 2013).

Although the JAK-STAT pathway has been studied predominately in *D. melanogaster*, *Ae. aegypti* possesses orthologs of key JAK-STAT pathway molecules that

likely function in a similar manner (Waterhouse et al. 2007). The JAK-STAT pathway is intricately integrated into multiple pathways and relatively few of the genes directly induced by JAK-STAT are involved in immunity (Souza-Neto et al. 2009), suggesting that their contribution to immune responses are possibly indirect (Dostert et al. 2005, Hillyer 2010). The JAK-STAT pathway, however, is activated during DENV infection in *Ae. aegypti*, as measured by up regulation of pathway genes such as *Dome* and *Hop*, among others, in midguts and carcasses at 3 h, 18 h, and 7 days post infection (Xi et al. 2008, Behura et al. 2011). Inhibition of the pathway via RNAi silencing of either *Hop* or *Dome* resulted in increased midgut DENV titres in infected *Ae. aegypti* at 3 and 7 dpi, respectively (Souza-Neto et al. 2009). Additionally, RNAi depletion of *PIAS*, a JAK-STAT inhibitor, led to decreased midgut titres. These effects were consistent across several *Ae. aegypti* strains, and led to the identification of two putative anti-dengue restriction factors (DVRFs) regulated by the JAK-STAT pathway (Souza-Neto et al. 2009). While the JAK-STAT pathway is initiated during DENV infection, and DENV titres may be modulated, the virus is not eliminated.

1.2.8. RNA interference (RNAi)

RNA interference is considered the predominant antiviral immune response used by insects (Kingsolver et al. 2013, Lee et al. 2019). In contrast to classic extracellular signalling pathways, RNAi acts as an intracellular defence mechanism against foreign RNA. RNA viruses such as DENV form double stranded RNA (dsRNA) structures during replication, although dsRNA also can be generated via the creation of intra-strand secondary structures (Lee et al. 2019). Long dsRNA structures are recognized by *Dicer* proteins and are cleaved to generate small interfering RNAs (siRNAs) of 20-23 nucleotides (Blair and Olson 2015). These siRNAs occur in a relatively equal ratio of positive and negative sense strands, suggesting that *Dicer-2* targets replicative dsRNA (Scott et al. 2010). Once generated, these siRNAs are loaded onto the RNA-induced silencing complex (*RISC*) by the *R2D2* protein and are unwound. One siRNA strand is degraded via the RNase activity of one of *RISC*'s constitutive proteins, *Argonaute-2*, while the other is used to target complementary viral RNA for degradation (Kingsolver et al. 2013).

Specific siRNAs are generated in *Ae. aegypti* midguts during DENV infection, confirming that components of the RNAi pathway are activated (Sánchez-Vargas et al. 2009, Scott et al. 2010). Cells with non-functioning *Dicer-2* are extremely susceptible to

DENV (Scott et al. 2010), and RNAi inhibition of key pathway genes such as *dicer-2*, *argonaute-2*, and *R2D2* leads to increased viral replication and a decreased EIP in infected mosquitoes (Sánchez-Vargas et al. 2009). However, RNAi does not eliminate DENV-2 completely, suggesting that DENV suppress or evade RNAi in some manner. Only 0.05% of the small RNAs harvested from whole DENV infected *Ae. aegypti* carcasses at 9 dpi were induced by the presence of DENV-2 (Sánchez-Vargas et al. 2009).

DENV replication involves the rearrangement of host cell membranes to form vesicle packets which enclose replicative structures (Uchil and Satchidanandam 2003). If Dicer-2 is unable to reach replicative dsRNA (its preferred target), due to these double membrane barriers, RNAi measures will be inefficient. Additionally, indirect evidence suggests that West Nile Virus has RNAi-suppressing properties within its subgenomic RNA, a property that might be conserved in other flaviviruses such as dengue (Schnettler et al. 2012). DENV-2 protein NS4B can also suppress RNAi in mammalian and non-mosquito insect cell lines (Kakumani et al. 2013). However, these responses have not been reported in DENV infections of *Aedes spp*., and thus remain conjecture.

The siRNA pathway is not the only pathway in mosquito cells that utilizes RNAi machinery. The micro RNA (miRNA) pathway uses RNAi to influence gene expression at the translational level (Blair and Olson 2015). Although miRNA levels are modified during and following DENV infection of *Ae. aegypti*, their role in infection dynamics is unclear (Campbell et al. 2014). PIWI-interacting RNAs (piRNAs) are longer than siRNAs and are generated independently of *Dicer-2* (Blair and Olson 2015). They are thought to be involved in maintenance of the cell genome through preventing transposon movement (Steinert and Levashina 2011), but appear to be generated in *Ae. aegypti* in response to DENV infection (Hess et al. 2011). However, their potential role in antiviral defences remains unknown.

1.2.9. Autophagy

Autophagy involves the creation of an autophagosome that encloses cellular components targeted for degradation, which then fuses with lysosomes in order to destroy the cell contents. Autophagy is used to recycle molecules, especially during times of nutritional starvation, and can destroy non-functioning entities such as damaged

organelles and malfunctioning proteins. Numerous autophagy regulators and factors (ATG proteins) also coordinate with components of the innate immune response, such as *toll*-like receptors, to target intracellular pathogens (Deretic and Levine 2009, Nakamoto et al. 2012). Under the regulation of the phosphatidylinositol 3-kinase-Akt pathway, autophagy is activated and prevents viral infection in *D. melanogaster*, while the inhibition of autophagy leads to increased viral replication (Shelly et al. 2009).

Some viruses manipulate the autophagy pathway to facilitate viral replication, and DENV rely on autophagy to replicate efficiently within mammalian cells. Autophagosomes generated during DENV infection target lipid droplets, leading to the release of stored triglycerides and energy generation via β-oxidation (Heaton and Randall 2010, 2011, Mateo et al. 2013, Raquin et al. 2013). The pro-viral role of autophagy during DENV infection can be replicated in autophagy-deficient cells by adding exogenous fatty acids (Heaton and Randall 2010). Although these processes have not been demonstrated in whole mosquitoes, a potential role of autophagy against chikungunya virus in mosquito cells has been reported (Raquin et al. 2013), and as ATG proteins are conserved among metazoans, these process also may occur in DENV infected *Ae. aegypti*.

1.2.10. Apoptosis

Apoptosis is a highly regulated process responsible for the destruction of abnormal or infected cells. It can be triggered by intracellular signals such as DNA replication failure, DNA or mitochondrial damage, or a host of other events including viral infection (Clarke and Clem 2003). Virus replication causes large changes within the cell, many of which can trigger apoptosis at various stages of infection. Early apoptosis can eliminate infected cells before the virus can replicate, and thus can be protective for the host. Apoptosis is carried out by a series of caspases; initiator caspases initiate apoptosis, while effector caspases are the executioners and work towards the organized degradation of cellular components (Clarke and Clem 2003). Finally, the resulting cell fragments are recognized and removed by phagocytic cells.

Although much of our knowledge of apoptosis in the invertebrate immune response has been derived from studies with *D. melanogaster*, the apoptotic machinery is highly conserved in mosquitoes. Several studies have characterised caspases in *Ae. aegypti*, including the initiator caspases *Dronc* and *Dredd* (Cooper, Pio, et al. 2007, Cooper, Thi,

et al. 2007). Additionally, several studies have demonstrated that apoptotic genes are upregulated in DENV infected cells in refractory, but not in susceptible, mosquitoes, suggesting that apoptosis contributes to the refractory phenotype (Xi et al. 2008, Barón et al. 2010, Behura et al. 2011, Ocampo et al. 2013, Behura et al. 2014). Furthermore, RNAi knockdown of the pro-apoptotic caspases, *Dronc* and *caspase-16*, in a refractory strain of *Ae. aegypti*, significantly increased susceptibility to DENV-2 (Ocampo et al. 2013). In general, apoptosis of virus-infected cells is detrimental to virus replication and represents an effective method of eliminating DENV infected cells. Many viruses, however, encode factors that block or arrest host apoptotic machinery and thus avoid destruction (Clarke and Clem 2003), while some viruses such as Sindbis virus appear to require some level of apoptosis for efficient dissemination in *Ae. aegypti* (Wang et al. 2012). There is still much to be elucidated regarding the role of apoptosis in mosquito immune responses to DENV infection.

1.2.11. Interactions among pathways

DENV infection in mosquitoes activates the Toll, IMD, JAK-STAT, RNAi, autophagy, and apoptosis pathways through means that are not well understood. Although most studies have been conducted on individual pathways, it is apparent that the immune pathways do not act completely independently of one another. The interactions between pathways and the mechanisms driving these interactions are varied, complex, and largely uncharacterized.

Activation of the JAK-STAT pathway in the midguts of DENV infected *Ae. aegypti* was linked to the down-regulation of NF-kB-responsive genes and the transcriptional repression of several AMPs (Souza-Neto et al. 2009). There is intriguing evidence that DENV may actively repress AMP production. DENV infected *Ae. aegypti* cells produce lower levels of cecropins and defensins when challenged with either Gram-positive or Gram-negative bacteria than uninfected cells (Sim and Dimopoulos 2010), suggesting that DENV can suppress both the Toll and IMD pathway's antibacterial responses, and that this repression is in some way beneficial to the virus. Why a virus would repress the antibacterial response of its host and make it susceptible to microbial infection is unclear.

The apoptosis and IMD signalling pathways also interact through a shared molecule, *Fadd*. As an upstream regulator of *Rel2*, *Fadd*, is necessary for IMD function

and the expression of cecropins and defensins during bacterial challenge (Cooper et al. 2009). *Fadd* also serves as an adapter required by the initiator caspase *Dredd* for apoptosis. Knockdown of *Fadd* stops *Dredd* activity, and also renders the insect incapable of eliminating bacterial infections (Cooper et al. 2009). It is difficult to determine if a specific measured response has been induced directly by DENV, or whether if it is an indirect consequence of activating a shared molecule that then activates downstream events in multiple pathways. Teasing apart the timing and control of these responses is complex and challenging.

1.2.12. Dengue virus in the vector: midgut microbes

The makeup of an insect's midgut microbiome has variable effects on multiple physiological parameters including the innate immune system responses to pathogens (Jupatanakul et al. 2014) that ultimately determine the vector competence of mosquitoes to specific pathogens. Whereas some insects such as the kissing bug, *Rhodnius prolixus*, rely on obligate intestinal symbionts to provide essential vitamins and nutrients (Beard et al. 2002), the role and contribution of most facultative microbes in the intestinal tracts of insects is unknown. There are, however, differences in the makeup and abundance of midgut microbial communities between strains of *Ae. aegypti* that are susceptible or refractory to DENV (Charan et al. 2013), and eliminating midgut bacteria using antibiotics can reduce AMP expression and increase midgut DENV titres (Xi et al. 2008). Additionally, specific strains of bacteria have been linked to an increased or decreased susceptibility to pathogens (Gonzalez-Ceron et al. 2003, Wang et al. 2009, Gusmão et al. 2010, Cirimotich et al. 2011, Apte-Deshpande et al. 2012, Pan et al. 2012, Ramirez et al. 2012). How bacteria and viruses interact, and whether they compete directly in the midgut for resources or space, or indirectly through immune system modulation is unknown, but has become an exciting area of research (Rosenberg and Zilber-Rosenberg 2011). These microorganisms may change the VC of a mosquito by increasing available resources (acting as nutritional supplements), producing secondary metabolites, as well as immune priming the mosquito against future pathogen encounters (Dennison et al. 2014).

1.2.13. Vector competence in *Ae. aegypti*

Strains of *Ae. aegypti* differ in their susceptibility to DENV, producing high, medium, low, or zero DENV titres in the salivary glands. This is due, in part, to the immune

responses and barriers described previously. This discrepancy in VC is affected by interacting genetic loci, age, body size, larval conditions, and environmental factors (Bosio et al. 2000, Bennett, Flick, et al. 2005, Alto, Lounibos, et al. 2008, Alto, Reiskind, et al. 2008, Schneider et al. 2011, Sylvestre et al. 2013, Souza-neto et al. 2019). Undoubtedly, variation in immune responses also impacts VC directly. Understanding the physiological basis of VC will allow a greater understanding of innate immune responses and might identify targets for novel control measures. These complex interactions between DENV and *Ae. aegypti* also may be affected by specific genotype-by-genotype interactions (Lambrechts 2011), and influenced by genetic-environmental interactions that combine to contribute to the VC (Schneider et al. 2011).

1.2.14. Refractory *Aedes aegypti*

Laboratory strains of *Ae. aegypti* have been selected specifically to generate DENV refractory phenotypes. The Moyo-In-Dry (MOYO-D) strain of *Ae. aegypti* was used to select strains of *Ae. aegypti* susceptible (MOYO-S) or refractory (MOYO-R) to *Plasmodium gallinaceum* (Thathy et al. 1994). These selected strains are also 53.60% and 19% susceptible to DENV-2, respectively (Schneider and Mori 2007, Behura et al. 2011). These two strains differ significantly in expression levels of several immune-related genes when exposed to DENV-2 (Chauhan et al. 2012). Compared with the MOYO-S strain, MOYO-R mosquitoes demonstrated an elevated expression of genes related to the JAK-STAT and apoptotic pathways (Behura et al. 2011), suggesting that the refractory phenotype was related to the expression of specific immune related genes.

A separate laboratory selection process generated the *Ae. aegypti* D2S3 strain that features a weak MIB and MEB, thus generating high midgut infection and dissemination rates (Bennett, Beaty, et al. 2005). Subsequently, a D2MEB strain was selected with a weak MIB and a strong MEB, proving that these phenotypes could be selected and manipulated independently (Bennett, Beaty, et al. 2005). These strains were crossed, and the progeny were mapped to identify quantitative trait loci (QTL) that contribute to the phenotype (Bennett, Flick, et al. 2005) as has been done for the MIB barrier in other *Ae. aegypti* strains (Bosio et al. 2000). The D2S3 strain (45.95% susceptible) and the MOYO-D strain (13% susceptible) were exposed to DENV (Behura et al. 2014) and a differential pattern of gene expression, similar to the comparison between MOYO-R and MOYO-S was observed (Chauhan et al. 2012). Although mosquito

strains respond to infection differently, there seems to be a core set of genes that undergo a similar expression change in refractory and susceptible mosquitoes that may be required for DENV development.

The studies cited above represent long established laboratory strains used to select specific phenotypes. There are, however, feral strains of *Ae. aegypti* that are naturally refractory to DENV (Souza-neto et al. 2019). In Cali, Colombia, approximately 30% of feral *Ae. aegypti* are refractory to all four serotypes of DENV (Ocampo and Wesson 2004, Barón et al. 2010, Serrato et al. 2017). Subsequent analysis and selection identified both MIB and MEB barriers in the feral populations (Barón et al. 2010, Caicedo et al. 2013), and differential gene expression in the midguts and carcasses of these different phenotypes (Barón et al. 2010, Caicedo et al. 2013, 2018). Both anti- and pro-apoptotic genes were activated in both strains, suggesting that the phenotype may be a result of competing pro- and anti-apoptotic responses, as well as manipulation of host apoptosis factors by DENV to facilitate viral dissemination. Many differentially expressed genes were identified, characterized, and subsequently assigned to an immune function. Non immune-related genes, including a trypsin inhibitor gene, were differentially expressed in the MIB strain (Barón et al. 2010, Caicedo et al. 2018). Trypsin inhibition has been shown to reduce both DENV titres and dissemination rates (Molina-Cruz et al. 2005) and, as such, trypsin may represent a non-immune-related contributor to the refractory phenotype.

The expression levels of selected apoptosis-related genes (*Caspase-16*, *Dronc*, *Dredd,* and *Inhibitor of Apoptosis* (*IAP1*)) and one RNAi-related gene (*Argonaute-2*) were compared in the midguts and fat body tissues of Cali-S (susceptible), Cali-MIB and Cali-MEB 12-48 hours after initial dengue infection (Caicedo et al. 2013, 2018, Ocampo et al. 2013). The pro-apoptotic caspases, *Dronc*, *Dredd*, and *caspase-16*, were up regulated in midgut tissues 24-48 hours post infection in the Cali-MIB strain. The authors proposed that upon infection, mosquito cells initiated apoptosis, but DENV subsequently induced the expression of *IAP1* to stop this apoptotic process. In the Cali-S strain, *IAP1* prevented apoptosis, whereas in the Cali-MIB strain, the over expression of pro-apoptotic caspases could not be regulated by low levels of *IAP1*. Knocking down *Dronc* and *caspase-16* in the Cali-MIB strain using RNAi increased the proportion of Cali-MIB mosquitoes that were susceptible to DENV-2. Although these studies demonstrate that apoptosis contributes to the refractory phenotype, it is clear that there are other, yet unidentified, factors that also contribute to this phenotype (Ocampo et al. 2013, Serrato et al. 2017, Caicedo et al. 2018).

Feral Cali-S, Cali-MIB and Cali-MEB strains were selected to generate phenotypically consistent strains. While the Cali-S strain became 99% susceptible, the prevalence of the refractory individuals never exceeded 50% in the Cali-MIB or Cali-MEB strains (Caicedo et al. 2013). Refractory mosquitoes were slightly smaller, had a slightly reduced lifespan, and produced slightly fewer eggs than their Cali-S counterparts. It is generally assumed that trade-offs will evolve when the cost of having a pathogen exceeds the costs of eliminating the pathogen. The effects of DENV on *Aedes spp*. are not universal; several studies have indicated no detrimental effects (Putnam and Scott 1995, Sim et al. 2012), while others have demonstrated a shorter life span, reduced fecundity, increased locomotion, and lower feeding efficiencies (Platt et al. 1997, Lima-Camara et al. 2011, Maciel-de-Freitas et al. 2011), but DENV-2 infection appears to present no significant or measurable costs to Cali-S mosquitoes. It is unclear from an evolutionary perspective why a Cali-MIB phenotype would evolve and be maintained if there is a trade off with overall fitness in the refractory phenotype, especially when no observable fitness effects seem to exist in Cali-S mosquitoes, in the presence or absence of DENV (Caicedo et al. 2013). This refractory nature may have arisen due to closely related insect specific flaviviruses, such as cell fusion agent virus (CFAV), that may harm and affect the fitness of *Ae. aegypti* (Yamanaka et al. 2013, Contreras-Gutierrez et al. 2017, Zhang et al. 2017); being refractory to viruses could confer significant fitness advantages (i.e. increased lifespan and fertility) compared to susceptible individuals. The prevalence of arboviruses in *Ae. aegypti* in Cali could also help to explain why we see a general 30:70 ratio of dengue-refractory: dengue-susceptible individuals even in the absence of DENV outbreaks. Whether these viruses are co-circulating with DENV in Cali remains unknown.

1.2.15. Mitigating dengue: control measures

Dengue can be a debilitating disease and represents an enormous economic cost to endemic areas and countries. Accordingly, there are many efforts underway to curb the spread of both DENV and its mosquito vectors, including vaccine development and vector control measures. Traditional mosquito eradication programs based on insecticides have not proven sufficiently effective (Halstead et al. 1997, Maciel-de-Freitas and Valle 2014) and alternative approaches are essential. Outside of a highly effective vaccine that prevents infection from all DENV serotypes, it is unlikely that any single control measure

will be sufficient, and thus interdisciplinary approaches and combinations of efforts will be required.

Until an effective vaccine becomes available, disease control efforts against all mosquito-transmitted pathogens will continue to focus on vector control. Conventional insecticide applications are used routinely, usually after initial dengue cases appear, and thus represent a retroactive rather than a proactive strategy. There are, however, several novel and sophisticated strategies being used to reduce or eliminate dengue transmission that fall under two primary goals: population suppression, aiming to decrease the overall mosquito population and thus reduce the number of virus transmitting individuals, and population replacement, aiming to replace virus transmitting individuals with non-virus transmitting individuals (Kean et al. 2015).

Genetic modification of vectors is the primary means to create genetically stable, DENV refractory mosquitoes (Franz et al. 2006, 2014, Mathur et al. 2010), as well as sterile or sex-skewing mosquitoes (Alphey 2014, Kyrou et al. 2018). However, transgenic mosquitoes face many challenges, including acceptance by the general public. The potential benefits of vector population suppression or replacement systems, especially those that are species specific and insecticide-independent, towards the reduction of dengue or other vector-borne diseases warrant further discussion.

One such approach, known as the Sterile Insect Technique (SIT), involves producing large numbers of fit, but sterile males that are released to compete with fertile males for mating opportunities. This environmentally friendly method reduces the mating potential of *Ae. aegypti* females and thus suppresses the population (Lacroix et al. 2012). Another approach developed by a British biotechnology company, Oxitec, uses the Release of Insects carrying a Dominant Lethal (RIDL) strategy, in which a genetically engineered *Ae. aegypti* strain (OX513A) carries both a dominant lethal gene and a genetic marker for easy identification. During larval development tetracycline is included in the diet, which allows the transgenic insects to survive (Phuc et al. 2007, Lacroix et al. 2012). Adult males are released in massive numbers into the field to mate with females and the resultant offspring die due to the lack of tetracycline in their diet, thus reducing overall populations (Phuc et al. 2007, Harris et al. 2011, Lacroix et al. 2012). Oxitec has also created an *Ae. albopictus* strain (OX3688) featuring a transgene that renders adult females flightless when they develop without tetracycline (Oxitec 2015). These

approaches, while promising, require constant production and release of the transgenic males.

Other more ecologically stable approaches have focused on reducing vector competence for DENV rather than eliminating the vector itself. Population replacement by mosquitoes that are refractory to DENV would theoretically reduce the VC of the population as a whole. One such approach uses bacterial symbionts to reduce longevity and VC of *Ae. aegypti*. The intracellular bacterium *Wolbachia pipientis* is a natural endosymbiont of arthropods that induces cytoplasmic incompatibility that selects strongly for *Wolbachia*-infected offspring, and is transmitted vertically from mother to progeny resulting in very fast rates of infection throughout entire populations (Rainey et al. 2014). In fact, *W. pipientis* may manipulate the gene expression, including miRNAs, of its *Ae. aegypti* hosts to facilitate the establishment and colonization of the bacterium (Hussain et al. 2011, Zhang et al. 2013, 2014). Highly virulent strains of *W. pipientis* shorten mosquito life spans, which ultimately should reduce DENV transmission (Brownstein et al. 2003, McMeniman et al. 2009). Less virulent strains of *W. pipientis* reduce DENV replication in *Ae. aegypti*, thus reducing VC (Blagrove et al. 2012, Sinkins 2013). *Wolbachia*-mediated protection against DENV appears to be density dependant, as higher *W. pipientis* infections provide greater resistance (Frentiu et al. 2010, Rainey et al. 2014). The exact means by which *W. pipientis* reduces the lifespan of *Ae. aegypti* and reduces DENV replication in infected mosquitoes is not well understood. It appears to be mediated through components of the immune system and gene regulation (Hussain et al. 2011, Pan et al. 2012, Rainey et al. 2014, Zhang et al. 2014), and influenced by direct competition between DENV and *W. pipientis* for resources such as specific amino acids (Caragata et al. 2014). Field trials of *W. pipientis* infected mosquitoes currently underway in Australia, Asia, and Latin America will provide data on the feasibility of using such para-transgenic mosquitoes to reduce or eliminate DENV transmission (Hoffmann et al. 2011, Walker et al. 2011, Frentiu et al. 2014). While this system remains promising, recent research suggests that the exclusion of DENV from *Wolbachia* infected individuals may be genotype and titre specific, reducing some *Wolbachia* infected mosquitoes VC (Terradas et al. 2017).

Species specific, highly targeted genome editing has recently become possible through employing new genetic engineering technologies; specifically, clustered, regularly interspaced, short palindromic repeats (CRISPR), which utilizes a *Streptococcus*

pyogenes CRISPR-associated nuclease, Cas9. Sequence specific guides can be created, which the CRISPR-Cas9 system then uses to complementarily pair to, subsequently inducing double stranded breaks in the DNA. The cell can then use one of two repair mechanisms, non-homologous end joining (NHEJ), which is error prone and will cause small insertions or deletions (indels) at the break site, or homology-directed repair (HDR), which allows for a donor piece of DNA to be inserted at the cut site (Gaj et al. 2013, Sander and Joung 2014). Unlike older genome editing technologies such as zinc-finger nuclease (ZFNs) and transcription activator-like effector nucleases (TALENs), CRISPR-Cas9 utilizes targeted nucleases and overcomes the recognition difficulties and transfection necessities of TALENs and ZFNs (Gaj et al. 2013). This system has now been used in a wide variety of organisms, including plants (Shan et al. 2013), humans (Mali et al. 2013), fruit flies (Yu et al. 2013) and in mosquitoes (Dong et al. 2015, Kistler et al. 2015, Li et al. 2017).

In mosquitoes, CRISPR-Cas9 has been used in *Anopheles* sp. (the vectors for *Plasmodium* sp) (Gantz et al. 2015, Galizi et al. 2016, Hammond et al. 2016, Dong et al. 2018, Kyrou et al. 2018), *Aedes aegypti* (the vector for dengue, Zika, chikungunya and yellow fever) (Dong et al. 2015, Kistler et al. 2015, Li et al. 2017), and also recently in *Culex quinquefasciatus* (the vector for West Nile and St. Louis encephalitis virus) (Li et al. 2019). Most of these studies aim to use CRISPR-Cas to achieve a population suppression goal (Galizi et al. 2016, Hammond et al. 2016, Kyrou et al. 2018) by skewing the sex-ratio of a population, or changing the expression of sex-determining genetic elements (i.e. *doublesex*). They have also been used to alter the vector competence of *Anopheles gambiae*, reducing *Plasmodium* infection by creating a fibrinogen-related protein 1 (*FREP1*) mutant *An. gambiae* line. Although these studies provide proof of principle for using CRISPR-Cas in mosquitoes, these techniques still cause fitness effects in the altered mosquitoes, remain cost-limiting, and will require a large shift in public perception before they are able to be deployed as a viable means of vector control.

1.2.16. Conclusion

The interactions between dengue viruses, their principal vector, *Ae. aegypti*, and humans, are complex and intricate. There is substantial variation in vector competence between strains of virus and vector, based on genetic compatibility and environmental factors. Dengue and other arboviruses represent a huge burden on global society and

affect billions of people. Controlling both the spread of DENV and their vectors requires an in-depth knowledge of the molecular and immunological interactions between individual vectors and viruses, especially regarding how mosquito vectors recognize DENV, anti-viral mechanisms used by the vectors, as well as strategies used by DENV to circumvent vector immune responses to ensure its own survival. It is becoming increasingly clear that the innate immune system of insects reacts directly to specific types of pathogens rather than employing a generalized response to all infections. Multiple immune pathways work in concert rather than in isolation to eliminate pathogens. Our detailed understanding of DENV-vector interactions is a relatively new, but rapidly evolving, field of research that is expanding from molecular interactions between vector and virus to understanding the effects of climate change on vector-virus-human interactions. However, until an effective efficient tetravalent (or possibly pentavalent) vaccine is available worldwide, species specific, immune-related, vector control strategies to limit DENV development or to reduce the vector competence of feral vectors will continue to rely on our knowledge and understanding of the innate immune responses in these vectors.

1.3. Thesis objectives

The overall goal of this thesis was to identify and characterize genes associated with the dengue-refractory (Cali-MIB) and dengue-susceptible (Cali-S) phenotypes, with the ultimate goal of using gene editing tools to alter the phenotype of dengue-susceptible *Aedes aegypti*. Although previous research has identified numerous genes contributing to these established phenotypes, these studies focused on single gene effects, and were biased by limitations. The main objectives for this thesis were to:

(1) Use bioinformatic tools to identify differentially expressed genes that contribute to the Cali-MIB or Cali-S phenotype using RNA sequencing techniques,

(2) Identify phenotype-specific genetic variants and characterize their effect on vector competence, and

(3) Characterize the bacterial communities present in Cali-S and Cali-MIB mosquito midguts, determining bacterial effects on vector competence for dengue,

(4) Use gene editing techniques to permanently eliminate gene function in the germline of mosquitoes to create dengue-refractory *Aedes aegypti*.

We used a combination of molecular biology and bioinformatic methods to identify the differences between Cali-MIB and Cali-S mosquitoes. RNA sequencing (Chapter 2) and a genome wide association study (GWAS) (Chapter 3) were used to flag a subset of genes thought to contribute to the two phenotypes, while 16S rRNA bacterial profiling (Chapter 4) was used to flag microbes of interest. Selected genes from this subset that were able to 'flip' the phenotype of mosquitoes from susceptible to refractory through RNAi based knockdowns were further tested with gene-editing technology (Chapter 5). Mosquito embryos were injected with CRISPR-Cas9 guide RNA complexes, and DNA was extracted and sequenced from these mosquitoes to determine transformation success. We identified multiple genes contributing to vector competence (Chapters 2 and 3), created a DNA based assay for identifying refractory and susceptible mosquitoes (Chapter 3), and successfully edited the germ-line of *Ae. aegypti* (Chapter 5).

1.4. References

Alphey, L. 2014. Genetic control of mosquitoes. Annu. Rev. Entomol. Rev. Entomol. 59: 205–224.

Alto, B. W., L. P. Lounibos, C. N. Mores, and M. H. Reiskind. 2008. Larval competition alters susceptibility of adult *Aedes mosquitoes* to dengue infection. Proc Biol Sci. 275: 463–471.

Alto, B. W., M. H. Reiskind, and L. P. Lounibos. 2008. Size Alters Susceptibility of Vectors to Dengue Virus Infection and Dissemination. Am J Trop Med Hyg. 79: 688–695.

Apte-Deshpande, A., M. Paingankar, M. D. Gokhale, and D. N. Deobagkar. 2012. *Serratia odorifera* a midgut inhabitant of *Aedes aegypti* mosquito enhances its susceptibility to dengue-2 virus. PLoS One. 7(7): e40401.

Barón, O., R. Ursic-Bedoya, C. Lowenberger, and C. Ocampo. 2010. Differential gene expression from midguts of refractory and susceptible lines of the mosquito, *Aedes aegypti*, infected with Dengue-2 virus. J. Insect Sci. 10: 41.

Beard, B. C., C. Cordon-Rosales, and R. V. Durvasula. 2002. Bacterial symbionts of the triatominae and their potential use in control of Chagas disease transmission. Annu Rev Entomol. 47: 123–141.

Behura, S. K., C. Gomez-Machorro, B. Debruyn, D. D. Lovin, B. W. Harker, J. Romero-Severson, A. Mori, and D. W. Severson. 2014. Influence of mosquito genotype on transcriptional response to dengue virus infection. Funct. Integr. Genomics. 14: 581–589.

Behura, S. K., C. Gomez-Machorro, B. W. Harker, B. deBruyn, D. D. Lovin, R. R. Hemme, A. Mori, J. Romero-Severson, and D. W. Severson. 2011. Global cross-talk of genes of the mosquito *Aedes aegypti* in response to dengue virus infection. PLoS Negl. Trop. Dis. 5(11): e1385.

Bennett, K. E., B. J. Beaty, and W. C. Black. 2005. Selection of D2S3, an *Aedes aegypti* (Diptera: Culicidae) strain with high oral susceptibility to Dengue 2 virus and D2MEB, a strain with a midgut barrier to Dengue 2 escape. J. Med. Entomol. 42: 110–119.

Bennett, K. E., D. Flick, K. H. Fleming, R. Jochim, B. J. Beaty, and W. C. Black IV. 2005. Quantitative Trait Loci That Control Dengue-2 Virus Dissemination in the Mosquito *Aedes aegypti*. Genetics. 194: 185–194.

Black, W. C., K. E. Bennett, N. Gorrochótegui-Escalante, C. V. Barillas-Mury, I. Fernández-Salas, M. D. L. Muñoz, J. a. Farfán-Alé, K. E. Olson, and B. J. Beaty. 2002. Flavivirus susceptibility in *Aedes aegypti*. Arch. Med. Res. 33: 379–388.

Blagrove, M. S. C., C. Arias-Goeta, F. A. B., and S. P. Sinkins. 2012. *Wolbachia* strain wMel induces cytoplasmic incompatibility and blocks dengue transmission in *Aedes albopictus*. Proc Natl Acad Sci. 109: 255–260.

Blair, C., and K. Olson. 2015. The Role of RNA Interference (RNAi) in Arbovirus-Vector Interactions. Viruses. 7: 820–843.

Bosio, C., R. Fulton, M. Salasek, B. Beaty, and W. Iv. 2000. Quantitative trait loci that control vector competence for dengue-2 virus in the mosquito *Aedes aegypti*. Genetics. 156: 687–698.

Boulanger, N., P. Bulet, and C. Lowenberger. 2006. Antimicrobial peptides in the interactions between insects and flagellate parasites. Trends Parasitol. 22: 262–268.

Boulanger, N., C. Lowenberger, P. Volf, R. Ursic, L. Sigutova, L. Sabatier, M. Svobodova, S. M. Beverley, G. Späth, R. Brun, B. Pesson, and P. Bulet. 2004. Characterization of a *defensin* from the sand fly *Phlebotomus duboscqi* induced by challenge with bacteria or the protozoan parasite *Leishmania major*. Infect Immun. 72: 7140–7146.

Boutros, M., H. Agaisse, and N. Perrimon. 2002. Sequential activation of signaling pathways during innate immune responses in *Drosophila*. Dev Cell. 3: 711–722.

Brady, O. J., M. A. Johansson, C. A. Guerra, S. Bhatt, N. Golding, D. M. Pigott, H. Delatte, M. G. Grech, P. T. Leisnham, R. Maciel-de-Freitas, L. M. Styer, D. L. Smith, T. W. Scott, P. W. Gething, and S. I. Hay. 2013. Modelling adult *Aedes aegypti* and *Aedes albopictus* survival at different temperatures in laboratory and field settings. Parasit. Vectors. 6: 351.

Brownstein, J., E. Hett, and S. O'Neill. 2003. The potential of virulent *Wolbachia* to modulate disease transmission by insects. J Invertebr Patol. 84: 24–29.

Bulet, P., C. Hetru, J. L. Dimarcq, and D. Hoffmann. 1999. Antimicrobial peptides in insects; structure and function. Dev Comp Immunol. 23: 329–344.

Caicedo, P. A., O. L. Barón, M. Pérez, N. Alexander, C. Lowenberger, and C. B. Ocampo. 2013. Selection of *Aedes aegypti* (Diptera: Culicidae) strains that are susceptible or refractory to Dengue-2 virus. Can. Entomol. 145: 273–282.

Caicedo, P. A., I. M. Serrato, S. Sim, G. Dimopoulos, H. Coatsworth, C. Lowenberger, and C. B. Ocampo. 2018. Immune response-related genes associated to blocking midgut dengue virus infection in *Aedes aegypti* strains that differ in susceptibility. Insect Sci. 26: 635–648.

Campbell, C. L., T. Harrison, A. M. Hess, and G. D. Ebel. 2014. MicroRNA levels are modulated in *Aedes aegypti* following exposure to Dengue-2. Insect Mol Biol. 23: 132–139.

Caragata, E. P., E. Rancès, S. L. O'Neill, and E. A. McGraw. 2014. Competition for Amino Acids Between *Wolbachia* and the Mosquito Host, *Aedes aegypti*. Microb. Ecol. 67: 205–218.

Charan, S. S., K. D. Pawar, D. W. Severson, M. S. Patole, and Y. S. Shouche. 2013. Comparative analysis of midgut bacterial communities of *Aedes aegypti* mosquito strains varying in vector competence to dengue virus. Parasitol. Res. 112: 2627–2637.

Chauhan, C., S. K. Behura, B. deBruyn, D. D. Lovin, B. W. Harker, C. Gomez-Machorro, A. Mori, J. Romero-Severson, and D. W. Severson. 2012. Comparative Expression Profiles of Midgut Genes in Dengue Virus Refractory and *Susceptible Aedes aegypti* across Critical Period for Virus Infection. PLoS One. 7(10): e47350.

Christensen, B. M., J. Li, C. C. Chen, and A. J. Nappi. 2005. Melanization immune responses in mosquito vectors. Trends Parasitol. 21: 192–199.

Cirimotich, C. M., Y. Dong, A. M. Clayton, S. L. Sandiford, J. A. Souza-Neto, M. Mulenga, and G. Dimopoulos. 2011. Natural microbe - mediated refractoriness to Plasmodium infection in *Anopheles gambiae*. Science. 332(6031): 855–858.

Clarke, T. E., and R. J. Clem. 2003. Insect Defenses Against Virus Infection: The Role of Apoptosis. Int J Mol Sci. 22: 402–424.

Contreras-Gutierrez, M. A., D. M. Watts, D. Perera, A. P. A. Travassos da Rosa, M. R. T. Nunes, D. Fish, N. Vasilakis, J. F. Cardoso, V. L. Popov, T. G. Wood, R. B. Tesh, H. Guzman, K. I. Young, S. G. Widen, K. A. Hanley, and C. Savit. 2017. Characterization of Three New Insect-Specific Flaviviruses: Their Relationship to the Mosquito-Borne Flavivirus Pathogens. Am. J. Trop. Med. Hyg. 98(2): 410-419.

Cooper, D. M., C. M. Chamberlain, and C. Lowenberger. 2009. *Aedes* FADD: a novel death domain-containing protein required for antibacterial immunity in the yellow fever mosquito, *Aedes aegypti*. Insect Biochem Mol Biol. 39: 47–54.

Cooper, D. M., F. Pio, E. P. Thi, D. Theilmann, and C. Lowenberger. 2007. Characterization of *Aedes* Dredd: A novel initiator caspase from the yellow fever mosquito, *Aedes aegypti*. Insect Biochem. Mol. Biol. 37: 559–569.

Cooper, D. M., E. P. Thi, C. M. Chamberlain, F. Pio, and C. Lowenberger. 2007. *Aedes* Dronc: A novel ecdysone-inducible caspase in the yellow fever mosquito, *Aedes aegypti*. Insect Mol. Biol. 16: 563–572.

Costa, A., E. Jan, P. Sarnow, and D. Schneider. 2009. The Imd pathway is involved in antiviral immune responses in *Drosophila*. PLoS One. 4(10): e7436.

Cox, J., H. E. Brown, and R. Rico-Hesse. 2011. Variation in vector competence for dengue viruses does not depend on mosquito midgut binding affinity. PLoS Negl. Trop. Dis. 5(5): e1172.

David, M. R., R. Lourenço-de-Oliveira, and R. Maciel-de-Freitas. 2009. Container productivity, daily survival rates and dispersal of *Aedes aegypti* mosquitoes in a high-income dengue epidemic neighbourhood of Rio de Janeiro: presumed influence of differential urban structure on mosquito biology. Mem Inst Oswaldo Cruz. 104: 927–932.

Dennison, N. J., N. Jupatanakul, and G. Dimopoulos. 2014. The mosquito microbiota influences vector competence for human pathogens. Curr. Opin. Insect Sci. 3: 6–13.

Deretic, V., and B. Levine. 2009. Autophagy, immunity, and microbial adaptations. Cell Host Microbe. 5: 527–549.

Dong, S., J. Lin, N. L. Held, R. J. Clem, A. L. Passarelli, and A. W. E. Franz. 2015. Heritable CRISPR/Cas9-mediated genome editing in the yellow fever mosquito, *Aedes aegypti*. PLoS One. 10(3): e0122353.

Dong, Y., M. L. Simões, E. Marois, and G. Dimopoulos. 2018. CRISPR/Cas9 - mediated gene knockout of *Anopheles gambiae* FREP1 suppresses malaria parasite infection. PLoS Pathog. 14(3): e1006898.

Dostert, C., E. Jouanguy, P. Irving, L. Troxler, D. Galiana-Arnoux, C. Hetru, J. A. Hoffmann, and J. L. Imler. 2005. The Jak-STAT signaling pathway is required but not sufficient for the antiviral response of *Drosophila*. Nat Immunol. 6: 946–953.

Dyer, O. 2017. Philippines halts dengue immunisation campaign owing to safety risk. BMJ. 359: j5759.

Franz, A. W. E., I. Sanchez-Vargas, Z. N. Adelman, C. D. Blair, B. J. Beaty, A. A. James, and K. E. Olson. 2006. Engineering RNA interference-based resistance to dengue virus type 2 in genetically modified *Aedes aegypti*. Proc. Natl. Acad. Sci. 103: 4198–4203.

Franz, A. W. E., I. Sanchez-Vargas, R. R. Raban, W. C. Black IV, A. A. James, and K. E. Olson. 2014. Fitness Impact and Stability of a Transgene Conferring Resistance to Dengue-2 Virus following Introgression into a Genetically Diverse *Aedes aegypti* Strain. PLoS Negl. Trop. Dis. 8(5): e2833.

Frentiu, F. D., J. Robinson, P. R. Young, E. A. McGraw, and S. L. O'Neill. 2010. *Wolbachia*-mediated resistance to dengue virus infection and death at the cellular level. PLoS One. 5(10): e13398.

Frentiu, F. D., T. Zakir, T. Walker, J. Popovici, A. T. Pyke, A. van den Hurk, E. A. McGraw, and S. L. O'Neill. 2014. Limited dengue virus replication in field-collected *Aedes aegypti* mosquitoes infected with *Wolbachia*. PLoS Negl. Trop. Dis. 8(2): e2688.

Gaj, T., C. A. Gersbach, and C. F. Barbas. 2013. ZFN, TALEN, and CRISPR/Cas-based methods for genome engineering. Trends Biotechnol. 31: 397–405.

Galizi, R., A. Hammond, K. Kyrou, C. Taxiarchi, F. Bernardini, S. M. O. Loughlin, P. Papathanos, T. Nolan, N. Windbichler, and A. Crisanti. 2016. A CRISPR-Cas9 sex-ratio distortion system for genetic control. Sci. Rep. 6: 31139.

Gantz, V. M., N. Jasinskiene, O. Tatarenkova, A. Fazekas, V. M. Macias, E. Bier, and A. A. James. 2015. Highly efficient Cas9-mediated gene drive for population modification of the malaria vector mosquito *Anopheles stephensi*. Proc. Natl. Acad. Sci. 112: E6736–E6743.

Gonzalez-Ceron, L., F. Santillan, M. H. Rodriguez, D. Mendez, and J. E. Hernandez-Avila. 2003. Bacteria in midguts of field-collected *Anopheles albimanus* block *Plasmodium vivax* sporogonic development. J. Med. Entomol. 40: 371–374.

Gusmão, D. S., A. V. Santos, D. C. Marini, M. Bacci, M. A. Berbert-Molina, and F. J. A. Lemos. 2010. Culture-dependent and culture-independent characterization of

microorganisms associated with *Aedes aegypti* (Diptera: Culicidae) (L.) and dynamics of bacterial colonization in the midgut. Acta Trop. 115: 275–281.

Guzman, M. G., M. Alvarez, and S. B. Halstead. 2013. Secondary infection as a risk factory for dengue hemorrhagic fever/dengue shock syndrome: an historical perspective and role of antibody-dependent enhancement of infection. Arch Virol. 158: 1445–1459.

Guzman, M. G., and E. Harris. 2015. Dengue. Lancet. 385: 453–465.

Halstead, S. B. 2008. Dengue. Imperial College Press, London.

Halstead, S. B., D. J. Gubler, and G. Kuno. 1997. Dengue and dengue hemorrhagic fever. Handb. Zoonoses. 8: 45–60.

Hammond, A., R. Galizi, K. Kyrou, A. Simoni, C. Siniscalchi, D. Katsanos, M. Gribble, D. Baker, E. Marois, S. Russell, A. Burt, N. Windbichler, A. Crisanti, and T. Nolan. 2016. A CRISPR-Cas9 gene drive system targeting female reproduction in the malaria mosquito vector *Anopheles gambiae*. Nat. Biotechnol. 34: 78–83.

Harris, A. F., D. Nimmo, A. R. McKemey, N. Kelly, S. Scaife, C. A. Donnelly, C. Beech, W. D. Petrie, and L. Alphey. 2011. Field performance of engineered male mosquitoes. Nat Biotechnol. 29: 1034–1037.

Heaton, N. S., and G. Randall. 2010. Dengue virus-induced autophagy regulates lipid metabolism. Cell Host Microbe. 8: 422–432.

Heaton, N. S., and G. Randall. 2011. Dengue virus and autophagy. Viruses. 3: 1332–1341.

Hess, A. M., A. N. Prasad, A. Ptitsyn, G. D. Ebel, K. E. Olson, C. Barbacioru, C. Monighetti, and C. L. Campbell. 2011. Small RNA profiling of Dengue virus-mosquito interactions implicates the PIWI RNA pathway in anti-viral defense. BMC Microbiol. 11: 45.

Hill, C. L., A. Sharma, Y. Shouche, and D. W. Severson. 2014. Dynamics of midgut microflora and dengue virus impact on life history traits in *Aedes aegypti*. Acta Trop. 140: 151–157.

Hillyer, J. F. 2010. Mosquito immunity. Adv. Exp. Med. Biol. 708: 218–238.

Hoffmann, A. A., B. L. Montgomery, J. Popovici, I. Iturbe-Ormaetxe, P. H. Johnson, F. Muzzi, M. Greenfield, M. Durkan, Y. S. Leong, Y. Dong, H. Cook, J. Axford, A. G. Callahan, H. Kenny, C. Omodei, E. A. McGraw, P. A. Ryan, S. A. Ritchie, M. Turelli, and S. L. O'Neill. 2011. Successful establishment of *Wolbachia* in *Aedes* populations to suppress dengue transmission. Nature. 476: 454–457.

Huang, Y., S. Higgs, and D. L. VanLandingham. 2019. Arbovirus-Mosquito Vector-Host Interactions and the Impact on Transmission and Disease Pathogenesis of Arboviruses. Front. Microbiol. 10.

Hussain, M., F. D. Frentiu, L. A. Moreira, S. L. O'Neill, and S. Asgari. 2011. *Wolbachia* uses host microRNAs to manipulate host gene expression and facilitate colonization of the dengue vector *Aedes aegypti*. Proc Natl Acad Sci. 108: 9250–9255.

Jupatanakul, N., S. Sim, and G. Dimopoulos. 2014. The insect microbiome modulates vector competence for arboviruses. Viruses. 6: 4294–4313.

Kakumani, P. K., S. S. Ponia, R. K. S, V. Sood, M. Chinnappan, A. C. Banerjea, G. R. Medigeshi, P. Malhotra, S. K. Mukherjee, and R. K. Bhatnagar. 2013. Role of RNA interference (RNAi) in dengue virus replication and identification of NS4B as an RNAi suppressor. J Virol. 87: 8870–8883.

Kean, J., S. M. Rainey, M. McFarlane, C. L. Donald, E. Schnettler, A. Kohl, and E. Pondeville. 2015. Fighting arbovirus transmission: Natural and engineered control of vector competence in *Aedes* mosquitoes. Insects. 6: 236–278.

Khoo, C. C. H., J. B. Doty, N. L. Held, K. E. Olson, and A. W. E. Franz. 2013. Isolation of midgut escape mutants of two American genotype dengue 2 viruses from *Aedes aegypti*. Virol J. 10: 257.

Kingsolver, M. B., Z. Huang, and R. W. Hardy. 2013. Insect antiviral innate immunity: Pathways, effectors, and connections. J. Mol. Biol. 425: 4921–4936**.**

Kistler, K. E., L. B. Vosshall, and B. J. Matthews. 2015. Genome engineering with CRISPR-Cas9 in the mosquito *Aedes aegypti*. Cell Rep. 11: 51–60.

Kocks, C., J. H. Cho, N. Nehme, J. Ulvila, A. M. Pearson, M. Meister, C. Strom, S. L. Conto, C. Hetru, L. M. Stuart, T. Stehle, J. A. Hoffmann, J.-M. Reichhart, D. Ferrandon, M. Rämet, and R. A. B. Ezekowitz. 2005. Eater, a Transmembrane Protein Mediating Phagocytosis of Bacterial Pathogens in Drosophila. Cell. 123: 335–346.

Kyrou, K., A. M. Hammond, R. Galizi, N. Kranjc, A. Burt, A. K. Beaghton, T. Nolan, and A. Crisanti. 2018. A CRISPR – Cas9 gene drive targeting doublesex causes complete population suppression in caged *Anopheles gambiae* mosquitoes. Nat. Biotechnol. 36(11): 1062-1066.

Lacroix, R., A. R. McKemey, N. Raduan, L. Kwee Wee, W. Hong Ming, T. Guat Ney, S. Rahidah A. A., S. Salman, S. Subramaniam, O. Nordin, N. Hanum, A. T., C. Angamuthu, S. Marlina Mansor, R. S. Lees, N. Naish, S. Scaife, P. Gray, G. Labbé, C. Beech, D. Nimmo, L. Alphey, S. S. Vasan, L. Han Lim, N. Wasi A., and S. Murad. 2012. Open field release of genetically engineered sterile male *Aedes aegypti* in Malaysia. PLoS One. 7(8): e42771.

Lambrechts, L. 2011. Quantitative genetics of *Aedes aegypti* vector competence for dengue viruses: towards a new paradigm? Trends Parasitol. 27: 111–114.

Leclerc, V., and J.-M. Reichhart. 2004. The immune response of *Drosophila melanogaster*. Immunol Rev. 198: 59–71.

Lee, W., J. A. Webster, E. T. Madzokere, E. B. Stephenson, and L. J. Herrero. 2019. Mosquito antiviral defense mechanisms: a delicate balance between innate immunity and persistent viral infection. Parasit. Vectors. 12.

Lemaitre, B., and J. Hoffmann. 2007. The Host Defense of *Drosophila melanogaster*. Annu. Rev. Immunol. 25: 697–743.

Li, M., M. Bui, T. Yang, C. S. Bowman, B. J. White, and O. S. Akbari. 2017. Germline Cas9 expression yields highly efficient genome engineering in a major worldwide disease vector, *Aedes aegypti*. Proc. Natl. Acad. Sci. 201711538.

Li, M., T. Li, N. Liu, R. Raban, X. Wang, and O. S. Akbari. 2019. Methods for the generation of heritable germline mutations in the disease vector *Culex quinquefasciatus* using CRISPR/Cas9. bioRxiv. April 16.

Lima-Camara, T. N., R. V. Bruno, P. M. Luz, M. G. Castro, R. Lourenço-de-Oliveira, M. H. F. Sorgine, and A. A. Peixoto. 2011. Dengue infection increases the locomotor activity of *Aedes aegypti* females. PLoS One. 6(3): e17690.

Lopez, L., G. Morales, R. Ursic, M. Wolff, and C. Lowenberger. 2003. Isolation and characterization of a novel insect *defensin* from *Rhodnius prolixus*, a vector of Chagas disease. Insect Biochem Mol Biol. 33: 439–447.

Lowenberger, C. 2001. Innate immune response of *Aedes aegypti*. Insect Biochem. Mol. Biol. 31: 219–229.

Lowenberger, C., P. Bulet, M. Charlet, C. Hetru, B. Hodgeman, B. M. Christensen, and J. A. Hoffmann. 1995. Insect immunity: isolation of three novel inducible antibacterial *defensins* from the vector mosquito, *Aedes aegypti*. Insect Biochem Mol Biol. 25: 867–873.

Lowenberger, C., M. Charlet, J. Vizioli, S. Kamal, a Richman, B. M. Christensen, and P. Bulet. 1999. Antimicrobial activity spectrum, cDNA cloning, and mRNA expression of a newly isolated member of the cecropin family from the mosquito vector *Aedes aegypti*. J. Biol. Chem. 274: 20092–20097.

Luplertlop, N., P. Surasombatpattana, D. Patramool, E. Dumas, L. Wasinpiyamongkol, L. Saune, R. Hamel, E. Bernard, D. Sereno, F. R. Thomas, D. Piquemal, H. Yssel, L. Briant, and D. Missé. 2011. Induction of a peptide with activity against a broad spectrum of pathogens in the *Aedes aegypti* salivary gland, following infection with Dengue Virus. PLoS Pathog. 7(1): e1001252.

Maciel-de-Freitas, R., C. T. Codeço, and R. Lourenço-de-Oliveira. 2007. Daily survival rates and dispersal of *Aedes aegypti* females in Rio de Janeiro, Brazil. Am J Trop Med Hyg. 76: 659–665.

Maciel-de-Freitas, R., J. C. Koella, and R. Lourenço-de-Oliveira. 2011. Lower survival rate, longevity and fecundity of *Aedes aegypti* (Diptera: Culicidae) females orally challenged with dengue virus serotype 2. Trans. R. Soc. Trop. Med. Hyg. 105: 452–458.

Maciel-de-Freitas, R., and D. Valle. 2014. Challenges encountered using standard vector control measures for dengue in Boa Vista, Brazil. Bull World Heal. Organ. 92: 685–689.

Mairuhu, A. T. A., J. Wagenaar, D. P. M. Brandjes, and E. C. M. Van Gorp. 2004. Dengue: An arthropod-borne disease of global importance. Eur. J. Clin. Microbiol. Infect. Dis. 23: 425–433.

Mali, P., L. Yang, K. Esvelt, J. Aach, M. Guell, J. DiCarlo, J. Norville, and G. Church. 2013. RNA-Guided Human Genome Engineering via Cas9. Science. 339(6121): 823–826.

Mateo, R., C. M. Nagamine, J. Spagnolo, E. Méndez, M. Rahe, M. Gale, J. Yuan, and K. Kirkegaard. 2013. Inhibition of cellular autophagy deranges dengue virion maturation. J. Virol. 87: 1312–1321.

Mathur, G., I. Sanchez-Vargas, D. Alvarez, K. E. Olson, O. Marinotti, and A. A. James. 2010. Transgene-mediated suppression of dengue viruses in the salivary glands of the yellow fever mosquito, *Aedes aegypti*. Insect Mol Biol. 19: 753–763.

McMeniman, C. J., R. V. Lane, B. N. Cass, A. W. Fong, M. Sidhu, Y. F. Wang, and S. L. O'Neill. 2009. Stable Introduction of a Life-Shortening *Wolbachia* Infection into the Mosquito *Aedes aegypti*. Science. 323(5910): 141–144.

Medzhitov, R., and C. A. Janeway. 1997. Innate immunity: impact on the adaptive immune response. Curr Opin Immunol. 9: 4–9.

Messina, J. P., O. J. Brady, D. M. Pigott, N. Golding, M. U. G. Kraemer, T. W. Scott, G. R. Wint, D. L. Smith, and S. I. Hay. 2015. The many projected futures of dengue. Nat Rev Microbiol. 13: 230–239.

Molina-Cruz, A., L. Gupta, J. Richardson, K. Bennett, W. Black IV, and C. Barillas-Mury. 2005. Effect of mosquito midgut trypsin activity on dengue-2 virus infection and dissemination in *Aedes aegypti*. Am. J. Trop. Med. Hyg. 72: 631–637.

Morin, C. W., A. C. Comrie, and K. Ernst. 2013. Climate and Dengue Transmission: Evidence and Implications. Environ. Heal. Perspect. 121: 1264–1272.

Mustafa, M. S., V. Rasotgi, S. Jain, and V. Gupta. 2014. Discovery of fifth serotype of dengue virus (DENV-5): A new public health dilemma in dengue control. Med J Armed Forces India. 71: 67–70.

Nakamoto, M., R. H. Moy, J. Xu, S. Bambina, A. Yasunaga, S. S. Shelly, B. Gold, and S. Cherry. 2012. Virus recognition by Toll-7 activates antiviral autophagy in *Drosophila*. Immunity. 36: 658–667.

Nappi, A. J., and Y. Carton. 2001. Immunogenetic aspects of the cellular immune response of *Drosophila* against parasitoids. Immunogenetics. 52: 157–164.

Normile, D. 2013. Surprising New Dengue Virus Throws A Spanner in Disease Control Efforts. Science. 342(6157): 415.

Ocampo, C. B., P. A. Caicedo, G. Jaramillo, R. Ursic Bedoya, O. Baron, I. M. Serrato, D. M. Cooper, and C. Lowenberger. 2013. Differential Expression of Apoptosis Related Genes in Selected Strains of *Aedes aegypti* with Different Susceptibilities to Dengue Virus. PLoS One. 8(4): e61187.

Ocampo, C. B., and D. M. Wesson. 2004. Population dynamics of *Aedes aegypti* from a dengue hyperendemic urban setting in Colombia. Am. J. Trop. Med. Hyg. 71: 506–513.

Oxitec. 2015. *Aedes albopictus* OX3688.

Pan, X., G. Zhou, J. Wu, G. Bian, P. Lu, A. S. Raikhel, and Z. Xi. 2012. *Wolbachia* induces reactive oxygen species (ROS)-dependent activation of the Toll pathway to control dengue virus in the mosquito *Aedes aegypti*. Proc. Natl. Acad. Sci. 109: E23–E31.

Pedrique, B., N. Strub-Wourgaft, C. Some, P. Olliaro, P. Trouiller, N. Ford, B. Pécoul, and J. Bradol. 2013. The drug and vaccine landscape for neglected diseases (2000–11): a systematic assessment. Lancet Glob. Heal. 1: e371-379.

Phuc, H. K., M. H. Andreasen, R. S. Burton, C. Vass, M. J. Epton, G. Pape, G. Fu, K. C. Condon, S. Scaife, C. A. Donnelly, P. G. Coleman, H. White-Cooper, and L. Alphey. 2007. Late-acting dominant lethal genetic systems and mosquito control. BMC Biol. 5: 11.

Platt, K. B., K. J. Linthicum, K. S. Myint, B. L. Innis, K. Lerdthusnee, and D. W. Vaughn. 1997. Impact of dengue virus infection on feeding behavior of *Aedes aegypti*. Am J Trop Med Hyg. 57: 119–125.

Putnam, J. L., and T. W. Scott. 1995. Blood-feeding behavior of dengue-2 virus-infected *Aedes aegypti*. Am J Trop Med Hyg. 52: 225–227.

Rainey, S. M., P. Shah, A. Kohl, and I. Dietrich. 2014. Understanding the *Wolbachia*-mediated inhibition of arboviruses in mosquitoes: progress and challenges. J Gen Virol. 95: 517–530.

Ramirez, J. L., and G. Dimopoulos. 2010. The Toll immune signaling pathway control conserved anti-dengue defenses across diverse *Ae. aegypti* strains and against multiple dengue virus serotypes. Dev Comp Immunol. 34: 625–629.

Ramirez, J. L., J. Souza-Neto, R. T. Cosme, J. Rovira, A. Ortiz, J. M. Pascale, and G. Dimopoulos. 2012. Reciprocal tripartite interactions between the *Aedes aegypti* midgut microbiota, innate immune system and dengue virus influences vector competence. PLoS Negl. Trop. Dis. 6(3): e1561.

Raquin, V., C. V. Moro, C. Bernardin, F. Tran, V. T. Van, P. Potier, D. Lavillette, and P. Mavingui. 2013. Potential role of autophagy during *Wolbachia* antiviral interference against chikungunya virus in mosquito cells. In 5th Eur. Congr. Virol.

Rigau-Pérez, J. G., G. G. Clark, D. J. Gubler, P. Reiter, E. J. Sanders, and A. V Vorndam. 1998. Dengue and dengue haemorrhagic fever. Lancet. 352: 971–7.

Rodenhuis-Zybert, I. A., J. Wilschut, and J. M. Smit. 2010. Dengue Virus Lifecycle: Viral and Host Factors Modulating Infectivity. Cell Mol Life Sci. 67: 2773–2786.

Romoser, W. S., M. J. Turell, K. Lerdthusnee, M. Neira, D. Dohm, G. Ludwig, and L. Wasieloski. 2005. Pathogenesis of Rift Valley fever virus in mosquitoes-tracheal conduits & the basal lamina as an extra-cellular barrier. Arch Virol Suppl. (19): 89–100.

Rosenberg, E., and I. Zilber-Rosenberg. 2011. Symbiosis and development: The hologenome concept. Birth Defects Res. Part C - Embryo Today Rev. 93: 56–66.

Salazar, M. I., J. H. Richardson, I. Sánchez-Vargas, K. E. Olson, and B. J. Beaty. 2007. Dengue virus type 2: Replication and tropisms in orally infected *Aedes aegypti* mosquitoes. BMC Microbiol. 7: 1–13.

Sánchez-Vargas, I., J. C. Scott, B. K. Poole-Smith, A. W. E. Franz, V. Barbosa-Solomieu, J. Wilusz, K. E. Olson, and C. D. Blair. 2009. Dengue virus type 2 infections of *Aedes aegypti* are modulated by the mosquito's RNA interference pathway. PLoS Pathog. 5(2): e1000299.

Sander, J. D., and J. K. Joung. 2014. CRISPR-Cas systems for editing, regulating and targeting genomes. Nat. Biotechnol. 32: 347–350.

Schneider, J. R., D. D. Chadee, A. Mori, J. Romero-Severson, and D. W. Severson. 2011. Heritability and adaptive phenotypic plasticity of adult body size in the mosquito *Aedes aegypti* with implications for dengue vector competence. Infect Genet Evol. 11: 11–16.

Schneider, J. R., and A. Mori. 2007. Investigations of dengue-2 susceptibility and body size among *Aedes aegypti* populations. Med. Vet. Entomol. 21: 370–376.

Schnettler, E., M. G. Sterken, J. Y. Leung, S. W. Metz, C. Geertsema, R. W. Goldbach, J. M. Vlak, A. Kohl, A. A. Khromykh, and G. P. Pijlman. 2012. Noncoding Flavivirus RNA Displays RNA Interference Suppressor Activity in Insect and Mammalian Cells. J. Virol. 86: 13486–13500.

Scott, J. C., D. E. Brackney, C. L. Campbell, V. Bondu-Hawkins, B. Hjelle, G. D. Ebel, K. E. Olson, and C. D. Blair. 2010. Comparison of Dengue Virus Type 2-Specific Small RNAs from RNA Interference-Competent and –Incompetent Mosquito Cells. PLoS Negl. Trop. Dis. 4(10): e848.

Serrato, I. M., P. A. Caicedo, Y. Orobio, C. Lowenberger, and C. B. Ocampo. 2017. Vector competence and innate immune responses to dengue virus infection in selected laboratory and field-collected *Stegomyia aegypti* (= *Aedes aegypti*). Med. Vet. Entomol. 31: 312–319.

Shan, Q., Y. Wang, J. Li, Y. Zhang, K. Chen, Z. Liang, K. Zhang, J. Liu, J. Xi, J. Qiu, and C. Gao. 2013. Targeted genome modification of crop plants using a CRISPR-Cas system. Biotechnology. 31: 686–688.

Shelly, S., N. Lukinova, S. Bambina, A. Berman, and S. Cherry. 2009. Autophagy is an essential component of *Drosophila* immunity against vesicular stomatitis virus. Immunity. 30: 588–598.

Sim, S., and G. Dimopoulos. 2010. Dengue virus inhibits immune responses in *Aedes aegypti* cells. PLoS One. 5(5): e10678.

Sim, S., N. Jupatanakul, and G. Dimopoulos. 2014. Mosquito immunity against arboviruses. Viruses. 6: 4479–4504.

Sim, S., N. Jupatanakul, J. L. Ramirez, S. Kang, C. M. Romero-Vivas, H. Mohammed, and G. Dimopoulos. 2013. Transcriptomic Profiling of Diverse *Aedes aegypti* Strains Reveals Increased Basal-level Immune Activation in Dengue Virus-

refractory Populations and Identifies Novel Virus-vector Molecular Interactions. PLoS Negl. Trop. Dis. 7(7): e2295.

Sim, S., J. L. Ramirez, and G. Dimopoulos. 2012. Dengue virus infection of the *Aedes aegypti* salivary gland and chemosensory apparatus induces genes that modulate infection and blood-feeding behavior. PLoS Pathog. 8(3): e1002631.

Sinkins, S. P. 2013. *Wolbachia* and arbovirus inhibition in mosquitoes. Futur. Microbiol. 8: 1249–1256.

Souza-neto, J. A., J. R. Powell, and M. Bonizzoni. 2019. Infection, Genetics and Evolution *Aedes aegypti* vector competence studies: A review. Infect. Genet. Evol. 67: 191–209.

Souza-Neto, J. A., S. Sim, and G. Dimopoulos. 2009. An evolutionary conserved function of the JAK-STAT pathway in anti-dengue defense. Proc. Natl. Acad. Sci. 106: 17841–17846.

Srikiatkhachorn, A. 2009. Plasma leakage in dengue haemorrhagic fever. Thromb. Haemost. 102: 1042–1049.

Steinert, S., and E. A. Levashina. 2011. Intracellular immune responses of dipteran insects. Immunol. Rev. 240: 129–140.

Sylvestre, G., M. Gandini, and R. Maciel-de-Freitas. 2013. Age-Dependent Effects of Oral Infection with Dengue Virus on *Aedes aegypti* (Diptera: Culicidae) Feeding Behavior, Survival, Oviposition Success and Fecundity. PLoS One. 8(3): e59933.

Terradas, G., S. L. Allen, S. F. Chenoweth, and E. A. McGraw. 2017. Family level variation in *Wolbachia*-mediated dengue virus blocking in *Aedes aegypti*. Parasit. Vectors. 10(1): 622.

Thathy, V., D. W. Severson, and B. M. Christensen. 1994. Reinterpretation of the genetics of susceptibility of *Aedes aegypti* to *Plasmodium gallinaceum*. J Parasitol. 80: 705–712**.**

Thomas, S. J. 2014. Developing a dengue vaccine: progress and future challenges. Ann NY Acad Sci. 1323: 140–159.

Tsakas, S., and V. J. Marmaras. 2010. Insect immunity and its signalling: an overview. Invertebr. Surviv. J. 7: 228–238.

Uchil, P. D., and V. Satchidanandam. 2003. Architecture of the flaviviral replication complex. Protease, nuclease, and detergents reveal encasement within double-layered membrane compartments. J Biol Chem. 278: 24388–24398.

Ursic-Bedoya, R., J. Buchhop, J. B. Joy, R. Durvasula, and C. Lowenberger. 2011. Prolixicin: A novel antimicrobial peptide isolated from *Rhodnius prolixus* with differential activity against bacteria and *Trypanosoma cruzi*. Insect Mol. Biol. 20: 775–786.

Ursic-Bedoya, R. J., and C. A. Lowenberger. 2007. *Rhodnius prolixus*: Identification of immune-related genes up-regulated in response to pathogens and parasites using suppressive subtractive hybridization. Dev. Comp. Immunol. 31: 109–120.

Vazeille-Falcoz, M., L. Mousson, F. Rodhain, E. Chungue, and A. Failloux. 1999. Variation in oral susceptibility to dengue type 2 virus of populations of *Aedes aegypti* from the islands of Tahiti and Moorea, French Polynesia. Am J Trop Med Hyg. 60: 292–299.

Walker, T., P. H. Johnson, I. I. Ormaetxe, F. D. Frenitu, C. J. McMeniman, Y. S. Leong, Y. Dong, J. Axford, P. Kriesner, A. L. Lloyd, S. A. Ritchie, S. L. O'Neill, and A. Hoffmann. 2011. The wMel *Wolbachia* strain blocks dengue and invades caged *Aedes aegypti* populations. Nature. 476: 450–453.

Wang, H., T. Gort, D. L. Boyle, and R. J. Clem. 2012. Effects of Manipulating Apoptosis on Sindbis Virus Infection of *Aedes aegypti* Mosquitoes. J. Virol. 86: 6546–6554.

Wang, J., Y. Wu, G. Yang, and S. Aksoy. 2009. Interactions between mutualist *Wigglesworthia* and tsetse peptidoglycan recognition protein (PGRP-LB) influence trypanosome transmission. Proc. Natl. Acad. Sci. U. S. A. 106: 12133–12138.

Waterhouse, R. M., E. V. Kriventseva, S. Meister, Z. Xi, K. S. Alvarez, L. C. Bartholomay, C. Barillas-Mury, G. Bian, S. Blandin, B. M. Christensen, Y. Dong, H. Jiang, M. R. Kanost, A. C. Koutsos, E. A. Levashina, J. Li, P. Ligoxygakis, R. M. MacCallum, G. F. Mayhew, A. Mendes, K. Michel, M. A. Osta, S. Paskewitz, W. S. Sang, D. Vlachou, L. Wang, Q. Wei, L. Zheng, Z. Zou, D. W. Severson, A. S. Raikhel, F. C. Kafatos, G. Dimopoulos, E. M. Zdobnov, and G. K. Christophides. 2007. Evolutionary dynamics of immune-related genes and pathways in disease-vector mosquitoes. Science. 316(5832): 1738–1743.

Whitehead, S. S., J. E. Blaney, A. P. Durbin, and B. R. Murphy. 2007. Prospects for a dengue virus vaccine. Nat Rev Microbiol. 5: 518–528.

Wilder-Smith, A., E. E. Ooi, O. Horstick, and B. Wills. 2019. Dengue. Lancet. 393: 350–363.

Xi, Z., J. L. Ramirez, and G. Dimopoulos. 2008. The *Aedes aegypti* toll pathway controls dengue virus infection. PLoS Pathog. 4(7): e1000098.

Xiao-Xia, G., Z. Xiao-Juan, L. Chun-Xiao, D. Yan-De, Z. Ying-Mei, D. Xing, X. Rui-De, Q. Cheng-Feng, and Z. Tong-Yan. 2013. Vector competence of *Aedes albopictus* and *Aedes aegypti* (Diptera: Culicidae) for DEN2-43 and New Guinea C virus strains of dengue 2 virus. Acta Trop. 128: 566–570.

Yamanaka, A., S. Thongrungkiat, P. Ramasoota, and E. Konishi. 2013. Genetic and evolutionary analysis of cell-fusing agent virus based on Thai strains isolated in 2008 and 2012. Infect. Genet. Evol. 19: 188–194.

Yu, Z., M. Ren, Z. Wang, B. Zhang, Y. S. Rong, R. Jiao, and G. Gao. 2013. Highly efficient genome modifications mediated by CRISPR/Cas9 in *Drosophila*. Genetics. 195: 289–291.

Zambon, R. A., M. Nandakumar, V. N. Vakharia, and L. P. Wu. 2005. The Toll pathway is important for an antiviral response in *Drosophila*. Proc Natl Acad Sci. 102: 7257–7262.

Zhang, G., S. Asad, A. A. Khromykh, and S. Asgari. 2017. Cell fusing agent virus and dengue virus mutually interact in Aedes aegypti cell lines. Sci. Rep. 7(1): 6935.

Zhang, G., M. Hussain, and S. Asgari. 2014. Regulation of arginine methyltransferase 3 by a *Wolbachia*-induced microRNA in *Aedes aegypti* and its effect on *Wolbachia* and dengue virus replication. Insect Biochem Mol Biol. 53: 81–88.

Zhang, G., M. Hussain, S. L. O'Neill, and S. Asgari. 2013. *Wolbachia* uses a host microRNA to regulate transcripts of a methyltransferase, contributing to dengue virus inhibition in *Aedes aegypti*. Proc Natl Acad Sci. 110: 10276–10281.

Figures

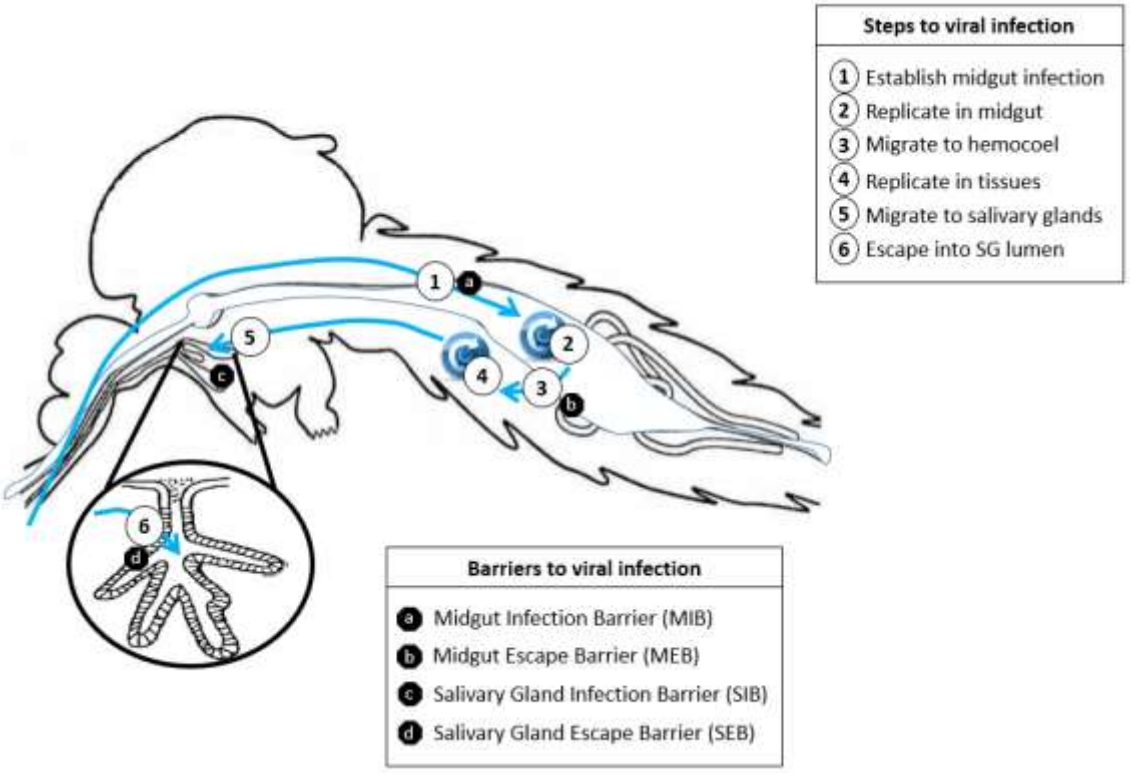

Figure 1.1 Development of dengue viruses in *Aedes aegypti* and the locations on natural infection barriers that prevent virus development, replication, or transmission.

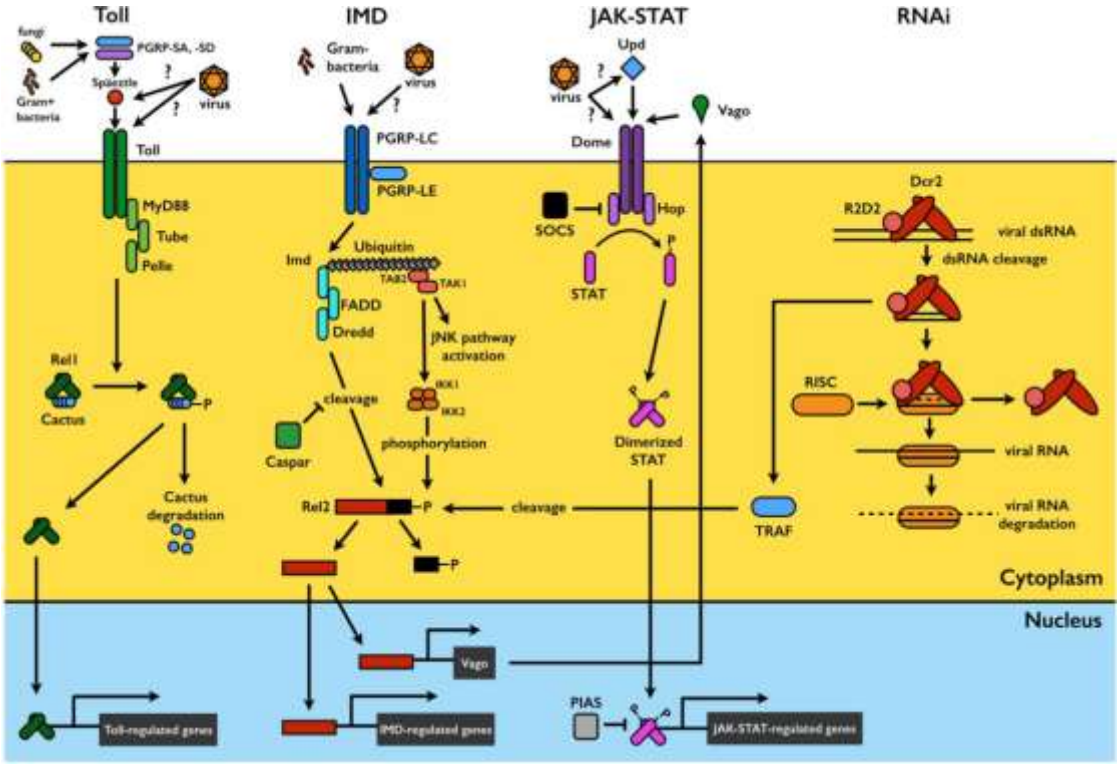

Figure 1.2 Mosquito immune signaling and RNAi pathways involved in mosquito–dengue interactions. Figure from Sim S, Jupatanakul N, Dimopoulos G. Mosquito immunity against arboviruses. Viruses 2014;6:4479–504. Reproduced with permission.

Connecting Statement 1

In Chapter 1 we described two strains of *Aedes aegypti* found in Cali, Colombia that are naturally refractory (Cali-MIB) or susceptible (Cali-S) to dengue viruses. While the mechanisms behind these differences in vector competence are not well understood, several studies, including ours, have implicated differences in gene expression between strains that contribute to refractory or susceptible phenotypes. Some studies have predicted *a priori* what genes might be involved in creating these phenotypes and have studied them in isolation. In order to carry out a global overview of all genes expressed in the midguts of Cali-MIB and Cali-S females, we completed a full-factorial RNA sequencing study to examine differential gene expression between our two phenotypes. The next chapter describes this study and identifies differentially expressed genes between the Cali-MIB and Cali-S strains of *Ae. aegypti*.

Chapter 2. RNA sequencing shows differential expression between field derived dengue refractory and susceptible strains of *Aedes aegypti*

Author Contributions

Carl Lowenberger conceived and designed the analysis. Paola Caicedo collected and prepared the samples and RNAseq libraries for analysis. Geoff Windsor assisted Heather Coatsworth in creating a bioinformatics pipeline and helped write scripts to easily parse through data. Heather Coatsworth completed all bioinformatic analyses. Heather Coatsworth and Carl Lowenberger wrote the manuscript. Paola Caicedo, Clara Ocampo, Fiona Brinkman, Geoff Windsor, Heather Coatsworth and Carl Lowenberger edited manuscript drafts for submission.

2.1. Abstract

Dengue viruses (serotypes 1-4), are the most prevalent arboviruses that affect humans, causing fever and rash, as well as severe dengue (dengue hemorrhagic fever and dengue shock syndrome) which may be lethal. Dengue viruses are transmitted primarily by the mosquito vector, *Aedes aegypti*. In Cali, Colombia, approximately 30% of field collected *Ae. aegypti* are naturally refractory to all 4 serotypes of dengue. We used RNA-sequencing to identify differentially expressed genes in the midguts of field derived refractory and susceptible mosquitoes. We employed a full factorial design, analyzing differential gene expression across time (24, 36 and 48 hours post blood meal), feeding treatment (blood or blood + dengue-2) and strain (susceptible or refractory). Resultant sequences were aligned to the reference *Ae. aegypti* genome (18,317 transcripts) for identification and assembled to visualize transcript structure and to analyze dynamic gene expression changes. A variety of clustering techniques was used to identify differentially expressed genes. We found the highest number of differentially expressed genes between susceptible and refractory mosquitoes at 24 and 36 hours post feeding. We found that both strains differentially expressed digestive genes (trypsins and serine endopeptidases); Cali-MIB mosquitoes had higher levels of metalloproteinases and autophagy related genes, while Cali-S mosquitoes had a higher expression of cell transport and odorant binding genes. These differentially expressed genes may contribute to the susceptible and

refractory phenotypes. Down regulated genes in Cali-S might help DENV enter and replicate in midgut cells, while up-regulated genes in Cali-MIB might kill the virus or prevent viral entry into cells.

Keywords: dengue, *Aedes aegypti*, yellow fever mosquito, RNA sequencing, refractory mechanisms, innate immunity

2.2. Introduction

Vector-borne pathogens are responsible for a significant proportion of the world's most debilitating and devastating human diseases (Mairuhu et al. 2004). In their role as vectors of protozoans (Plasmodium sp.) and viruses (West Nile, Japanese encephalitis, dengue, chikungunya, yellow fever, Zika) (Barnes 2005), mosquitoes are the indirect cause of more than 2 million deaths a year (Oxitec 2014). Of these, dengue is the most widespread arbovirus disease, infecting up to 390 million people each year throughout tropical and subtropical regions (Mairuhu et al. 2004; Bhatt et al. 2013). Dengue is transmitted primarily by *Aedes aegypti*, and to a lesser extent by *Aedes albopictus* (Barnes 2005). Changes in global travel, urbanization, as well as climate have facilitated *Ae. aegypti* population expansion, and consequently have allowed dengue to thrive. Half of the world's population is at risk of contracting dengue, a statistic that could increase as the effects of climate change mount (Bhatt et al. 2013).

Although insecticides, larvicides, and source reduction are used widely to reduce mosquito populations, none seem able to dampen dengue transmission significantly (Barnes 2005). This has resulted in an emphasis on mosquito bio-manipulation or genetic modification techniques to induce sterility, decrease lifespan, or reduce vector competence (McGraw and O'Neill 2013). These have shown great promise towards effective vector control and are based on understanding the molecular interactions between vector and virus, as well as vector genetics (Oxitec 2014; McGraw and O'Neill 2013).

Although *Ae. aegypti* is the principal vector of dengue viruses (DENV), not all *Ae. aegypti* females transmit the virus. In Cali, Colombia, approximately 30% of field collected *Ae. aegypti* are refractory to all 4 dengue serotypes (Ocampo and Wesson 2004; Serrato et al. 2017). Approximately 48% of their offspring in field-derived colonies are refractory

to dengue virus 2 (DENV-2) (Barón et al. 2010; Ocampo et al. 2013; Caicedo et al. 2013), through one or more of the established barriers to flavivirus development; a midgut infection barrier (MIB) in which DENV is unable to replicate within midgut cells, or a midgut escape barrier (MEB) in which the virus cannot escape the midgut cells (Ocampo et al. 2013). Other barriers include a salivary gland infection barrier (SIB) in which the virus cannot enter the salivary glands, or a salivary gland escape barrier (SEB) in which DENV is unable to disseminate into the salivary gland lumen (Sim et al. 2012, 2013). These refractory mechanisms and general immune responses to DENV have been studied principally in long established, specifically selected laboratory strains of *Ae. aegypti* (Behura et al. 2011; Behura and Severson 2012; Bonizzoni et al. 2012a). In Cali, Colombia we can collect mosquitoes in the field with one of three phenotypes; susceptible (Cali-S), refractory with a midgut infection barrier (Cali-MIB) and refractory with a midgut escape barrier (Cali-MEB). All three phenotypes can be collected within the same communities, and inside the same houses or oviposition sites within different neighborhoods. These have been raised in the laboratory and selected to increase the proportion of each phenotype, giving rise to the field derived strains (Caicedo et al. 2013).

We have described significant differences in the expression of apoptosis related genes in the Cali-MIB and Cali-S strains (Barón et al. 2010; Ocampo et al. 2013; Caicedo et al. 2013), based on laboratory studies and literature on general immune responses to intracellular viruses (Cooper 2008, 2011; Ocampo et al. 2013). Knocking down apoptosis related genes altered the phenotype of *Ae. aegypti*, but could only explain ~30% of the refractory phenotype (Ocampo et al. 2013; Caicedo et al. 2013). We undertook a midgut transcriptome analysis, using RNA sequencing (RNA-seq) technology, to identify all transcripts in the midguts of Cali-S and Cali-MIB females at three different time points (24, 36 and 48 hours post feeding) that are relevant to the period when the virus is entering, replicating in, and then exiting the midgut epithelial cells respectively. The aim of this study was to identify, in an unbiased manner, all differentially expressed genes that might contribute to the refractory or susceptible phenotype.

Other studies have examined *Ae. aegypti* transcriptome changes after exposure to DENV in long established susceptible laboratory strains (Sim et al. 2012; Colpitts et al. 2011; Bonizzoni et al. 2012a; Hess et al. 2011; Campbell et al. 2014), and some have investigated semi-refractory laboratory strains (Zou et al. 2011; Behura et al. 2011, 2014; Bonizzoni et al. 2012a; Chauhan et al. 2012; Sim et al. 2013). Our study is unique in that

it analyzes mosquitoes that have evolved the refractory and susceptible phenotypes in the field with no human directed laboratory selection specifically for refractoriness to dengue.

2.3. Methods

2.3.1. Ethics statement

All female mosquitoes were exposed to dengue virus through an artificial membrane feeder. Adults in colonies were fed on hamsters at CIDEIM (Cali, Colombia) under protocols approved by the CIDEIM institutional review committee for research in animals (CIEIA).

2.3.2. Mosquito rearing

The collection, rearing and selection of the Cali-S and Cali-MIB strains of *Ae. aegypti* have been described (Caicedo et al. 2013). The strains used here were maintained under standard laboratory conditions: 28 ± 2ºC, 70% relative humidity, and a 12:12 hour light-dark cycle. Adults were fed with a 10% sugar solution.

2.3.3. Virus propagation and mosquito infections

DENV-2 New Guinea C strain was propagated in *Ae. albopictus* (Skuse) C6/36HT cells. Infected cells were incubated for 14 days at 32°C in L15 medium supplemented with 2% heat-inactivated fetal bovine serum, 1% penicillin/streptomycin, and 1% L-glutamine. Virus and cells were harvested and collected in a 15mL conical centrifuge tube. The viral suspension was mixed 1:1 with defibrinated rabbit blood to create an infectious blood meal. Aliquots of the infected cell suspension, and the mixture of blood and virus were titred before and after the infection process as described previously (Bennett et al. 2002). Titers in the cell suspensions ranged from 108 to 108.5 TCID50/mL in all oral challenges. Five to eight-day old adult female laboratory raised *Ae. aegypti* Cali-S and Cali-MIB were exposed for 2 hours to the infectious blood meal via an artificial membrane feeder (Ocampo et al. 2013). All infections were carried out in Bio Safety Level 2+ facilities. After exposure to a blood meal with or without DENV-2, females that had fed to repletion were transferred to 300mL containers, covered with mesh (~20 mosquitoes/container), and

were given access to 10% sucrose solution ad libitum. Containers were maintained under the laboratory conditions described above.

2.3.4. Mosquito dissections

Midguts from adult females were dissected from each strain (Cali-S and Cali-MIB) under each feeding treatment (blood meal or blood meal with DENV) and at each time point (24, 36 and 48 hours post blood meal (PBM)) (Table 2.1). In order to obtain enough RNA, midguts from three biological replicates were pooled, leaving one sample for RNA sequencing for each of the 12 treatments. All dissections were performed in DEPC sterile water on a cold table, and dissected tissues were immediately transferred to a microcentrifuge tube containing 200µL of RNAlater® Stabilization Solution (Ambion, Austin, Texas). All samples were subsequently transported from CIDEIM (Cali, Colombia) to Simon Fraser University (Burnaby, British Columbia), and stored at -20°C.

2.3.5. RNA extraction, library preparation, and RNA sequencing

Total RNA was extracted from each pool of midguts and carcasses using Trizol (Sigma, Oakville, Ontario) as described (Lowenberger et al. 1999). RNA concentrations were determined using a spectrophotometer (NanoDrop, ND-1000). Poly-A mRNA purification was performed with the Micro Poly A Purist Kit (Ambion, Austin, Texas) following the manufacturer's protocols. From each mRNA sample, 100ng was used to generate cDNAs using the Ultra RNA Library Prep Kit for Illumina (New England BioLabs, Ipswich, Massachusetts). All purification reactions were completed using AMPure XP Beads (Beckman Coulter, Brea, California). Fragment length analyses and overall library quality were completed on the final libraries using a Bioanalyzer (Agilent High Sensitivity Chip, Agilent Santa Clara, California). Libraries were diluted to 2nM and were sequenced at 100X depth as technical duplicates across two lanes using an Illumina miSeq platform at Fusion Genomics (Burnaby, BC).

2.3.6. Processing of raw sequencing reads

A basic bioinformatics workflow, obtained from the Galaxy portal RNA-Rocket (Blankenberg et al. 2010), was modified to accommodate newer programs and multiple analyses (Figure 2.1). The quality of the sequence data from each of the 12 treatments

was checked using FastQC (v. 0.11.1) (Andrews 2010), and a sequence trimmer, Trimmomatic (v. 0.30) (Bolger et al. 2014), was used on each of the 12 files to reduce overrepresented sequences, as well as to remove sequences less than 90bp in length.

2.3.7. Read alignment and mapping

The *Ae. aegypti* genome and associated gene annotation files were obtained from VectorBase (http://www.vectorbase.org) (Megy et al. 2012): AaegL3 Scaffolds was used as the genome, while AaegL3 Basefeatures was used for gene annotation. Tophat2 (Kim et al. 2013) was used to align and map reads as previously outlined (Rinker et al. 2013). Alignments then were visualized using the Integrative Genomics Viewer (IGV) (v. 2.3.32) (Thorvaldsdóttir et al. 2013) to examine read alignments manually. Samstat (v.1.09) (Lassmann et al. 2011) subsequently was used to check mapping quality.

2.3.8. Differential expression tests

Twenty-four separate differential expression (DE) tests were run to investigate the effects of time, viral presence and mosquito strain (Table A1). Because our MIB strain is only ~50% refractory, we assumed, based on Caicedo et al. 2013, that 50% of the refractory mosquitoes were indeed phenotypically refractory. As such, strain comparisons were made between a pool of susceptible mosquitoes, and a pool of half refractory and half susceptible mosquitoes. Due to a lack of biological replicates, three different programs were used to analyze the RNA-seq data. Cuffdiff (v. 2.2.1) (Trapnell et al. 2010) was used to test differential expression at both the gene and transcript level. Cuffdiff differential expression tests without replicates were run using the ‘blind’ method, while tests with replicates were run using the ‘pooled’ method. Alongside Cuffdiff, DESeq2 (v. 1.16.0) (Anders and Huber 2010), was also used to test for differential expression at the gene level. Tests without biological replicates were run under the ‘blind’ method, ‘fit-only’ sharing mode, and the ‘parametric’ fit-type, while tests with replicates were run using the ‘pooled’ method, the ‘maximum’ sharing mode, and the ‘parametric’ fit-type. Both programs generate a p-value from analyzing if the variance present in a group of samples is beyond what is expected from a simple Poisson model of the RNA sequencing data. Fold change values from Cuffdiff and DESeq2 are generated from Fragments Per Kilobase of transcript per Million mapped reads (FPKM) values, specifically, log2(FPKMsample1/FPKMsample2). A third differential expression program, GFOLD (v.

1.1.1) (Feng et al. 2012), which is specifically designed for RNA-seq analyses without replicates, was used with default parameters. GFOLD reports a GFOLD value, which acts as a reliable log2-fold change value, calculated using Reads per Kilobase of transcript per Million mapped reads (RPKM) values. GFOLD values of zero show no differential expression. DE files were output alongside corresponding gene annotations including gene names, GO (Gene Ontology) terms (Ashburner et al. 2000), and KEGG (Kyoto Encyclopedia of Genes and Genomes) terms (Kanehisa and Goto 2000), obtained using Biomart (VectorBase).

2.3.9. Analysis of differential expression data

Two separate sub-analyses were completed on each DE output; one general, which included only significantly differentially expressed genes, and one immune-related, which included non-significantly expressed genes ranked from highest to lowest according to log2-fold change values. The immune related analysis was completed to identify genes with lower expression differentials, where even small changes in expression can have serious biological implications (Liesecke et al. 2018). To complete the immune specific analysis, an *Ae. aegypti*-specific immune related list of genes was downloaded from ImmunoDB (Waterhouse et al. 2007) (Table A2). Functional classifications were assessed using a concatenated list of GO terms obtained through ImmunoDB. The second analysis was performed in a similar manner, excluding the ImmunoDB gene filtering step.

Clustering analyses and functional enrichment tests were completed on data obtained from all treatments, without incorporating a variance scaling factor, as data were found to be homoscedastic (Figure A1). To investigate how closely the expression profiles from each sample compared, a principal component analysis (PCA) plot using Euclidian distances was created using DESeq2 by log transforming the merged read count. Aedes aegypti GO (gene ontology) terms were used to complete functional over-representation analyses via Ontologizer (v. 2.0) (Bauer et al. 2008).

Two main types of clustering were performed through R (v. 3.1.1) (Team 2011): hierarchical and partitioning (k-means) clustering. Dendrogram cutting was used to determine the optimal number of clusters for k-means clustering.

2.3.10. Validation of differential gene expression using quantitative PCR

As we did not have true biological replicates for our RNA sequencing study, we completed validation tests on biologically replicated cDNAs. These cDNAs were generated in an identical manner from different generations of mosquitoes than those used to create the RNA-seq libraries. Droplet digital PCR (ddPCR) and quantitative real time PCR (qPCR) were used to validate expression values. These values were then directly compared to our RNA-sequencing expression values for comparison. Thermocycling conditions for ddPCR were: 95°C for 10s, 55°C for 10s, and 72°C for 30s in 20µL reactions (containing 1 µL of cDNA) using QX200 ddPCR EvaGreen Supermix (Bio-Rad Laboratories, Hercules, California, USA) on an automated QX200 Droplet Digital PCR System (Bio-Rad Laboratories, Hercules, California, USA). QuantaSoft v1.7.4 (Bio-Rad Laboratories, Hercules, California, USA) was used to obtain an absolute expression quantification. qPCR was performed on a Light Cycler® 96 system (Roche, Basel, Switzerland) using PerfeCTa SYBR® (Quantabio, Massachusetts, USA). Thermocycling conditions for qPCR were: 95°C for 10s, 55°C for 10s, and 72°C for 30s in 10µL reactions (containing 4µL of 1:50 diluted cDNA). LightCycler® 96 Application Software Version 1.1.1 (Roche, Basel, Switzerland) was used to obtain relative gene expression comparisons against a constitutively expressed housekeeping gene, 40S ribosomal protein RPS17 (AAEL004175). All RNA-seq GFOLD001 values were divided by the corresponding ddPCR or qPCR values in order to test the similarity between the two datasets. Comparisons were made between ddPCR or log2 qPCR values and RNA-seq GFOLD001 values were made, noting the direction and magnitude of change. Genes were considered as validated if their direction and magnitude of change was the same between both datasets.

2.4. Results

2.4.1. Raw sequencing reads processing, alignment and mapping

Each RNA-seq library generated between 14 and 28 million reads >90 bp for each of the 12 treatments (Table 2.1). Eighty three percent of all reads mapped to the genome (17% unmapped), and 63% of the mapped reads had an error rate of less than 0.001% (Table A3).

2.4.2. Differential expression analysis

All three programs identified the same genes as being the highest differentially expressed (>$\log_2$ fold difference). All time point comparisons under the Cali-S blood and virus versus Cali-MIB blood and virus tests yielded similar functional group profiles (Figure 2.2). Diverse and unknown functional groups represented the largest proportion of genes, followed by transcription/translation, transport, metabolism, redox/stress/mitochondrial and finally the immune group. The remaining groups each represented less than three percent of the total number of differentially expressed genes.

2.4.3. Statistical and systems analysis of differential expression data

Hierarchical clustering produced a dendrogram (Figure 2.3), with a clear separation between treatments analyzed at the 48-hour time point (right branch) and all other treatments (left branch). The further splits within this right branch were based on the viral treatment of the sample (either blood fed or blood and virus fed). The left branch however displayed an initial splitting of the Cali-S and Cali-MIB strains, with further branching into separate blood fed and virus fed treatments, and a final branching event at the 24 and 36h time points, showing us that the Cali-S and -MIB strains were the most different at these 24 and 36h time points.

The functional over-representation analysis again highlighted the 48h time point as more diverse and dissimilar to the other time points. There was a large number of terms associated with cellular localization and transport across all comparisons. Comparisons at earlier time points (24 and 36h) represented generation of precursor metabolites, envelope proteins, and ion binding; while later time points (36 and 48h), invoked intracellular signal transduction and small molecule metabolic processes (Table A4).

Based on dendrogram cutting, the k-means analysis (Figure A2) clustered all the gene count data into seven distinct clusters. The first cluster represented 98% of the genes (17,254), and as such, was tied to a wide variety of functional classes. Cluster 2 (44 genes) was primarily associated with ribosomal intracellular and translation functions, as well as RNA transport and degradation activity. Cluster 3 (1 gene, AAEL013284) was specifically related to serine-type peptidase activity, as was cluster 7 (1 gene, AAEL007818), and cluster 6 (10 genes). Similar to cluster 2, cluster 4 (162 genes) contained genes with many

ribosomal functions, as well as functions associated with ATP binding and transport, metabolic pathways, and carbohydrate metabolism. Finally, cluster 5 (7 genes) was solely made up of genes representing metallopeptidases, GTP binding and GTPase activity.

2.4.4. Choosing a candidate gene shortlist

We further selected 15 genes (Table 2.2) for further study based on three criteria: i) differentially expressed, ii) differentially expressed and immune related, and iii) marked as intriguing by other published research papers (Table 2.3). Genes were chosen from both the top significantly DE list, as well as the DE immune list. Only genes with documented or putative unique functions were chosen. Genes were classified as up-regulated when expression was higher in virus fed Cali-MIB versus virus fed Cali-S or blood fed Cali-MIB. Conversely, genes were labeled as down-regulated when expression was higher in virus fed Cali-S versus virus fed Cali-MIB or blood fed Cali-S. Up-regulated genes might be expressed to block viral cell entry and exit, stop replication or aid in immune viral clearance, while down-regulated genes may do the opposite, aiding in DENV entry, exit, and replication.

2.4.5. Differential expression validation

Four candidate genes (*autophagy related target of rapamycin*, *TOR*, AAEL000693, a *40S ribosomal gene*, AAEL013694, *a low-density lipoprotein receptor gene*, AAEL014222, and a *bumetanide-sensitive Na-K-Cl co-transport*, AAEL009888), and five non-candidate genes (*60S ribosomal protein L15*, AAEL012736, *60S ribosomal protein L35a*, AAEL000823, *Eukaryotic translation initiation factor 3 subunit G*, AAEL012661, an uncharacterized gene, AAEL002930, and *4-nitro*, AAEL007097) were chosen as representatives for differential expression validation. ddPCR was used to validate candidate genes, as their expression levels were smaller and could not be detected using qPCR. Non-candidate gene validation was completed using qPCR, as the overall expression levels of these genes was high enough for reliable detection. After comparing the datasets (RNAseq, ddPCR and qPCR), genes displaying discordant correlations (AAEL012661, AAEL013694, AAEL014222 and AAEL000693) were removed from the candidate gene list. All remaining genes had good correlation between the RNA-seq data with regards to the magnitude and direction of change (Figure A3).

2.5. Discussion

2.5.1. Differential expression analysis

All three programs (Cuffdiff, DESeq2 and GFOLD) identified the same top differentially expressed genes. Due to the lack of biological replicates, Cuffdiff and DESeq2 are both extremely conservative in their list of differentially expressed genes compared to GFOLD. We used GFOLD rank log2-fold change values to help us overcome our issues with replicability. It is not uncommon for immunologically relevant genes to rank below others in the list of the greatest differentials in gene expression. This trend is further highlighted in immune genes, where even slight changes in expression may have large downstream effects. As such, the ordering of gene expression differences (from highest to lowest) may have resulted in ranking biologically relevant genes lower in importance based solely on expression level differences (Chen et al. 2007). To overcome this quandary, two lists of candidate genes were generated: one based on the top DE genes (shared amongst all three programs), and one based on the most expressed immune related genes (as identified by ImmunoDB, still shared amongst all three programs).

There were some general trends within the dataset. Both Cali-S and Cali-MIB mosquitoes infected with DENV-2 had increased expression of digestive genes such as trypsins, serine endopeptidases and metalloproteinases compared with their counterparts fed solely on blood. These digestive enzymes are likely important early regulators of infection (Palmer et al. 2018); an increase in these digestive enzymes could assist in the dampening of dengue's ability to enter and replicate in cells, as the level of degradation within the midgut could be higher.

In Cali-MIB females exposed to DENV, we observed higher levels of matrix metalloproteinases (MMPs), as well as increases in the expression of a *Niemann-pick type C2 gene*. *Niemann-pick-C2* is a cholesterol transporter and has been identified in various studies as a viral agonist that may enhance, or be required for, the entry of DENV-2 into cells (Jupatanakul et al. 2014). However, our results in refractory mosquitoes seem to suggest the opposite. It is possible, that in response to other mechanisms expressed to decrease viral titres in the midgut of refractory mosquitoes, that DENV upregulates *Niemann-pick C2* expression to remain viable.

In Cali-S females, we see higher expression levels of several *odorant binding proteins* (*OBP*s) (AAEL006176-*OBP27*, AAEL002606-*OBP35*, AAEL012377-*OBP55*, AAEL009449-*OBP39*, AAEL010666-*OBP42*, AAEL013018-*OBP56*) as well as an anti-apoptosis gene (AAEL009074-Inhibitor of Apoptosis, *AeIAP1*). The role of OBPs in the midgut is unclear, although it has been proposed that they act as signalling mechanisms for odorant binding proteins in the salivary glands (Smartt and Erickson 2009), inducing the mosquito to bite repeatedly and enhancing virus transmission. *AeIAP1*, on the other hand, is involved in inhibiting apoptosis, and has been characterized as being pro-viral, preventing cells from undergoing apoptosis and eliminating the virus before it replicates. Unfortunately, knock-downs of *AeIAP1* were lethal to the mosquitoes, and cannot be the sole mechanism driving refractoriness in Cali-MIB mosquitoes (Cooper 2008). Lethal genes have, however, proven useful in developing techniques to reduce vector populations (Oxitec 2014).

There were notable temporal differences in the expression of genes within each treatment and strain. Most digestive function ontology terms correlate directly with mosquito blood meal processing. We observed trypsins and sodium and potassium co-transporters at 24h post blood meal, serine endopeptidases, carboxypeptidases and lipases at 36h PBM, and heme peroxidases, cytochrome p450s and sucrose transporters at 48h PBM. Insects rapidly produce digestive enzymes upon feeding, and these decrease in production as absorption occurs within the midgut (Marquardt 2005). Specifically, late trypsin is activated 12-48 hours post blood meal, during which lipid digestion occurs via phospholipases and phosphatases, which hydrolyze ester bonds, solubilizing cell membranes for the passage of lipids into the hemolymph (Marquardt 2005). This may result in the spike of expression in these enzymes at earlier time points, and lower expressions at later time points. The digestion of the blood meal produces toxic heme as a by-product, and this toxic heme has specific binding sites on the peritrophic matrix where it is bound and excreted after blood digestion has occurred. As a result, heme cannot interact with and damage the midgut epithelial cells. Mosquitoes also use p450-like enzymes such as CYP6 and CYP9 to assist in heme detoxification (Feyereisen 2006). This is likely why higher levels of heme peroxidases and cytochrome p450s start to appear around 48h PBM. Sucrose transports may have higher expression levels at 48h as the mosquito is likely in the process of digesting, and subsequently transporting, these carbohydrates.

Eighty-five of the genes identified in this RNA sequencing study have been implicated in previous refractory mosquito expression studies (Behura and Severson 2012; Chauhan et al. 2012; Bonizzoni et al. 2012a; Bonizzoni et al. 2011), including a microarray study on Cali-MIB and Cali-S at one time point only; 30 h after blood feeding (Caicedo et al. 2018). These correlations centered on digestive genes such as trypsins and serine-endopeptidases, as well as signalling and cell entry genes such as lectins and lipoproteins. A smaller subset of immune related genes was also common, including a variety of anti-microbial peptides, CLIP domains, apoptotic genes, and small RNA pathway molecules. Although many genes were common between these datasets, some genes had difference in their direction of differential expression. These differences were mostly evident between our refractory strain (Cali-MIB) and the MOYO-D strain, and primarily encompassed cell signalling, processing and transport genes such as *ubiquitin*, *dynein*, *adenylyl cyclase*, *clathrin*, *dishevelled*, and multiple vitellogenin precursors.

A large proportion of differentially expressed genes are matrix metalloproteinases (MMPs), which have a strong association with immunity. MMPs play important roles in pathogen infection, acting as both agonists and antagonists. In humans, increased MMP activity is associated with increased pathogenicity, as MMPs assist in breaking down the basal lamina of tissues, allowing for subsequent viral entry and replication, often resulting in increased vascular leakage (Leaungwutiwong et al. 2016). In mosquitoes, MMPs have been implicated in extracellular matrix remodelling, potentially allowing virions to pass through an altered basal lamina (Kantor et al. 2017). MMPs also have been annotated as anti-viral, acting as apoptotic effectors in the JAK-STAT pathway, an important anti-viral pathway (Cheng et al. 2016; Jupatanakul et al. 2017; Palmer et al. 2018), as well as pro-viral, preventing cell death (Zuo et al. 2014). MMPs often act in tissue specific manners. In *Anopheles gambiae*, a midgut specific matrix metalloproteinase, *MT-MMP1*, was shown to enrich cell attachment sites and increased the mean intensity of *Plasmodium sp*. ookinete infections (Goulielmaki et al. 2014). In baculovirus-infected arthropods, fibroblast growth factors caused MMPs to adopt effector caspase functions, degrading the midgut basal lamina and allowing for increased viral midgut passage (Means and Passarelli 2010). In theory, decreasing these pervasive midgut specific MMPs would assist an insect in creating a tissue specific barrier to migrating pathogens. A down regulation of MMPs in *Ae. aegypti* was correlated with decreased viral titre, or elimination of DENV (Bonizzoni et al. 2011; Chauhan et al. 2012; Sim et al. 2013).

We have reported trends observed within the dataset. Some genes in the *Ae. aegypti* genome have not been annotated, and their expression will appear in the dataset as 'conserved hypothetical proteins' or 'hypothetical proteins', and as such, the role of these genes was not examined. Further work should be completed to look at the functional roles of these hypothetical proteins using protein prediction software programs to search for conserved protein domains. It should also be noted that the differences observed here are based on transcripts and may not accurately reflect protein levels due to post-transcriptional or post translational modifications.

2.5.2. Statistical and systems analysis of differential expression data

The outputs from the hierarchical clustering and PCA analysis were, as expected, similar, as both involve distance matrix measures to scale and visualize data sets. In both analyses the 48-hour time point appears much more isolated than the 24- and 36-hour time points, likely because the mosquito has finished or is near the end point of blood digestion, and thus different regulatory genes are at play. In Cali-S mosquitoes, by 48 hours, the virus will have started to migrate into and replicate within other mosquito tissues, and as such, different genes may be expressed. Conversely, DENV does not enter the hemocoel of Cali-MIB mosquitoes and therefore it is likely that these expression differences are related to the process of viral elimination. Furthermore, the lack of expression differences in Cali-S and Cali-MIB fed solely on blood at 48h PBM suggests that the major differences between these strains are directly related to their response towards DENV.

The partitioning (k-means) analysis allowed us to view the functional clustering of the differentially expressed genes, while the Ontologizer completed a functional over-representation analysis. Both outputs yielded similar trends. We observed many genes with a wide variety of functions, with many genes at 24h and 36h PBM associated with blood meal processing, suggesting differences in blood meal digestion between the two mosquito strains. Other studies have found that the strongest modulation of midgut gene expression occurs between 18-24 hours post DENV exposure (Raquin et al. 2017). Many ribosomal, RNA transport and degradation terms clustered together, which could suggest dengue is utilizing host mechanisms to help in its own replication. Since the virus itself utilizes the host endoplasmic reticulum for transport and assembly, these changes in expression could reflect efficient viral infection and propagation.

2.5.3. Differential expression validation

Our RNA sequencing study did not have biological replication, while our ddPCR/qPCR assays did. While our RNA sequencing study captured biological variation through sample pooling, differential and statistical comparisons without replicates is extremely difficult. To try and overcome these difficulties we used multiple differential expression programs to assess differences, and compared our RNA sequencing expression differences with separate, biologically replicated data analyzed using ddPCR and qPCR. While we obtained very similar differential expression results across all three DE programs (Cuffdiff, DESeq2, and GFOLD) we found that many of our candidate genes did not display a good correlation between ddPCR/qPCR and our RNA-seq data (Figure A3). This could be due to actual biological differences as the samples obtained for the studies were from different founder populations. The lack of correlation could also be from the difference in statistical power between our two studies. In our ddPCR/qPCR assays (that used biological replicates) we were able to verify that inter-treatment differences exceeded intra-treatment differences. Since we did not have biological replicates for our RNA sequencing data, we could not complete this same verification step. As such, differences in the direction and magnitude of change between these two datasets may be due to incorrect expression assessments (i.e. false positives) from our RNA sequencing study.

2.5.4. Candidate Gene Analysis

Most of these candidate genes (5/15) were immune related; a *c-type lysozyme* (AAEL003712), and three *dead box ATP dependant RNA helicases* (AAEL001769, AAEL002083, and AAEL 004978) may limit DENV replication as part of the mosquito's innate immune response (Ramirez et al. 2012; Hussain and Asgari 2014), while the remaining gene, *CLIBB34* (AAEL000028) may be manipulated by the virus to interfere with cell surface proteins (Clements 2012). Multiple digestive genes (a *serine-type endopeptidase*, AAEL002360, a *pyrokinin*, AAEL005444, and a *trypsin*, AAEL010195) were also in the list, and have been proposed to limit viral infectivity due to their high proteolytic activity and role in absorption (Brackney et al. 2008; Paluzzi and O'Donnell 2012), although some studies have shown the opposite to be true (Molina-Cruz et al. 2005). Candidate genes related to cell signaling, growth, binding and transport (a *sphingolipid delta 4 desaturase*, AAEL002992, a *40S ribosomal protein*, AAEL008083, a

c-type lectin, AAEL005641, and a *low-density lipoprotein*, AAEL014222, respectively) may play roles in assisting or inhibiting viral cell entry (van Gorp et al. 2002; Guo et al. 2010; Liu et al. 2014). Lastly, two autophagy candidate genes, an *autophagy related target of rapamycin*, AAEL000693, and an *autophagy related gene*, AAEL013063, both up-regulated in Cali-MIB mosquitoes may play a role in viral replication (Lee and Iwasaki 2008; Heaton and Randall 2010; Shertz and Cardenas 2011; Lee et al. 2013). A summary of all our candidate genes, their function as well as possible DENV association can be found in Table 2.2. We have focused on four of these genes (validated using ddPCR) in more detail below.

Although *NaK* (a *bumetanide-sensitive Na-K-Cl co-transport*, AAEL009888) has not been reported previously as important within the mosquito-dengue literature, it plays a vital role in regulating ionic balance and cell volume (Gillen et al. 2015). *NaK* may be localized in the apical membrane of midgut epithelial cells in *Ae. aegypti*, as was demonstrated by an ortholog of AAEL009888 in *Manduca sexta* (Gillen et al. 2006). Furthermore, sodium transporters are needed to maintain intracellular pH (Pullikuth et al. 2006), and changes in the expression of these transporters could result in changes to cell homeostasis. *NaK* could be necessary for the maintenance of intracellular homeostasis, and this could be why we see a higher expression of the *NaK* transcript in susceptible infected mosquitoes.

Conversely, we observed a higher transcript expression of *CTL*, a *c-type lysozyme* (AAEL003712) in refractory mosquitoes. Lysozymes have historically been implicated as anti-bacterial agents. When lysozyme-c was silenced, mosquitoes had a higher titre of dengue virus, suggesting that lysozymes may exert an inhibitory effect on the virus itself (Ramirez et al. 2012).

We found higher expression of autophagy related genes, which are normally associated with organelle recycling and destruction, but recently have been implicated in reducing viral titres (Cooper 2011; Schonhofer et al. 2016). The opposite seems to be true for DENV infections, where autophagy related genes (*APG*s) augment viral infection and replication (Lee and Iwasaki 2008). Silencing *Aedronc*, an initiator caspase, decreased autophagy and DENV titres in *Ae. aegypti*, suggesting an apoptotic basis of autophagy control (Eng et al. 2016). DENV may induce autophagy and subsequent autophagosome formation, using virus induced double membrane vesicles as replication sites (Lee and

Iwasaki 2008), although mechanisms using lipid metabolism, lipid droplets, virion maturation and dsRNA localization also have been proposed (Jordan and Randall 2015; Barletta et al. 2016; Palmer et al. 2018). This pro-viral effect is consistent with reports describing significant increases in *APG* expression in susceptible mosquitoes exposed to DENV (Colpitts et al. 2011; Chauhan et al. 2012; Ocampo et al. 2013; Sim et al. 2013). There is a trend in DENV-refractory mosquitoes to have increased expression of *Inhibitor of Apoptosis* (*IAP*), *Buffy*, and anti-apoptotic genes (Chauhan et al. 2012; Sim et al. 2013), suggesting that the autophagy pathway may contribute to the DENV refractory phenotype.

It is evident that there are proximate differences in DENV processing by Cali-S and Cali-MIB mosquitoes, although the selective advantage for this is unclear because many studies suggest no significant impact of DENV on *Ae. aegypti* fitness (Lambrechts and Scott 2009; Lambrechts and Failloux 2012; Maciel-de-Freitas et al. 2011; Sylvestre et al. 2013). Understanding whether these responses are restricted to DENV, to other flaviviruses such as Zika, and yellow fever or to other arboviruses such as chikungunya, will help us recognize the extent of differential gene expression as a general antiviral response in *Ae. aegypti*. As this study employed a single replicate approach, we were only able to flag a smaller subset of genes that might play a role in determining vector competence in *Ae. aegypti.* Future studies will use RNAi based gene knockdown studies to examine the phenotypic function of candidate genes identified in this study. Identifying which genes play a role in determining vector competence might help us understand and manipulate vector competence for vector control.

2.6. Data Availability

All relevant data are within the paper and its Supplementary Appendices. The raw sequencing data as well as processed differential expression data is available to the public through NCBI's Gene Expression Omnibus (GEO) database (GSE90974).

2.7. Acknowledgements

The authors thank the Vector Biology and Control team at CIDEIM for training and technical support, as well as Rachel Blair and Iman Baharmand (SFU) for technical assistance. This research was funded in part by COLCIENCIAS (Contract 2229-519-28645 to CB), an NSERC Discovery grant to CL (RGPIN261940), Emerging Leaders in

the Americas Program (ELAP) scholarships to PC, and Graduate Fellowships (SFU) and the H.R. MacCarthy Scholarship (SFU) to HC.

2.8. References

Anders, S., and W. Huber. **2010**. Differential expression analysis for sequence count data. Genome Biol. 11: R106.

Andrews, S. 2010. FastQC: A quality control tool for high throughput sequence data.

Ashburner, M., C. Ball, J. Blake, D. Botstein, H. Butler, J. Cherry, P. Davis, J. Dolinski, S. Dwight, J. Eppig, M. Harris, D. Hill, L. Issel-Tarver, A. Kasarskis, S. Lewis, J. Matese, J. Richardson, M. Ringwald, G. Rubin, and G. Sherlock. **2000**. Gene ontology: tool for the unification of biology. The Gene Ontology Consortium. Nat. Genet. 25: 25–29.

Barletta, A. B. F., L. R. Alves, M. C. L. Nascimento Silva, S. Sim, G. Dimopoulos, S. Liechocki, C. M. Maya-Monteiro, and M. H. F. Sorgine. **2016**. Emerging role of lipid droplets in *Aedes aegypti* immune response against bacteria and Dengue virus. Sci. Rep. 6: 1–13.

Barnes, E. 2005. Diseases and Human Evolution. University of New Mexico Press, Albuquerque, N.Y.

Barón, O., R. Ursic-Bedoya, C. Lowenberger, and C. Ocampo. **2010**. Differential gene expression from midguts of refractory and susceptible lines of the mosquito, *Aedes aegypti*, infected with Dengue-2 virus. J. Insect Sci. 10: 41.

Bauer, S., S. Grossmann, M. Vingron, and P. Robinson. **2008**. Ontologizer 2.0--a multifunctional tool for GO term enrichment analysis and data exploration. Bioinformatics. 24: 1650–1.

Behura, S., C. Gomez-Machorro, B. DeBruyn, D. Lovin, B. Harker, J. Romero-Severson, A. Mori, and D. Severson. **2014**. Influence of mosquito genotype on transcriptional response to dengue virus infection. Funct. Integr. Genomics. 14: 581–9.

Behura, S. K., C. Gomez-Machorro, B. W. Harker, B. deBruyn, D. D. Lovin, R. R. Hemme, A. Mori, J. Romero-Severson, and D. W. Severson. **2011**. Global cross-talk of genes of the mosquito *Aedes aegypti* in response to dengue virus infection. PLoS Negl. Trop. Dis. 5(11): e1385.

Behura, S., and D. Severson. **2012**. Intrinsic features of *Aedes aegypti* genes affect transcriptional responsiveness of mosquito genes to dengue virus infection. Infect Genet Evol. 12: 1413–1418.

Bennett, K., K. Olson, M. Munoz, I. Fernandez-Salas, J. Farfan, S. Higgs, W. Black IV., and B. Beaty. **2002**. Variation in vector competence for dengue-2 virus among 24 collections of *Aedes aegypti* from Mexico and the United States. Am. J. Trop. Med. Hyg. 67: 84–92.

Bhatt, S., P. Gething, O. Brady, J. Messina, A. Farlow, C. Moyes, J. Drake, J. Brownstein, A. Hoen, O. Sankoh, M. Myers, D. George, T. Jaenisch, G. Wint, C. Simmons, T. Scott, J. Farrar, and S. Hay. **2013**. The global distribution and burden of dengue. Nature. 496(7446): 504–7.

Blankenberg, D., G. Von Kuster, N. Coraor, G. Ananda, R. Lazarus, M. Mangan, A. Nekrutenko, and J. Taylor. **2010**. Galaxy, a web-based genome analysis tool for experimentalists. Curr. Protoc. Mol. Biol. 29: 997–1003.

Bolger, A., M. Lo*HS*e, and B. Usadel. **2014**. Trimmomatic: a flexible trimmer for Illumina sequence data. Bioinformatics. 30: 2114–2120.

Bonizzoni, M., W. A. Dunn, C. L. Campbell, K. E. Olson, O. Marinotti, and A. a James. **2012a**. Strain Variation in the Transcriptome of the Dengue Fever Vector, *Aedes aegypti*. G3 (Bethesda). 2: 103–14.

Bonizzoni, M., W. Dunn, C. Campbell, K. Olson, M. Dimon, O. Marinotti, and A. James. **2011**. RNA-seq analyses of blood-induced changes in gene expression in the mosquito vector species, *Aedes aegypti*. BMC Genomics. 12: 82.

Bonizzoni, M., W. Dunn, C. Campbell, K. Olson, O. Marinotti, and A. James. **2012b**. Complex Modulation of the *Aedes aegypti* Transcriptome in Response to Dengue Virus Infection. PLoS One. 7(11): e50512.

Brackney, D. E., B. D. Foy, and K. E. Olson. **2008**. The effects of midgut serine proteases on dengue virus type 2 infectivity of *Aedes aegypti*. Am. J. Trop. Med. Hyg. 79: 267–274.

Caicedo, P. A., I. M. Serrato, S. Sim, G. Dimopoulos, H. Coatsworth, C. Lowenberger, and C. B. Ocampo. **2018**. Immune response-related genes associated to blocking midgut dengue virus infection in *Aedes aegypti* strains that differ in susceptibility. Insect Sci. 26: 635–648.

Caicedo, P., O. Barón, M. Pérez, N. Alexander, C. Lowenberger, and C. Ocampo. **2013**. Selection of *Aedes aegypti* (Diptera: Culicidae) strains that are susceptible or refractory to Dengue-2 virus. Can. Entomol. 145: 273–282.

Campbell, C. L., T. Harrison, A. M. Hess, and G. D. Ebel. **2014**. MicroRNA levels are modulated in *Aedes aegypti* following exposure to Dengue-2. Insect Mol Biol. 23: 132–139.

Chauhan, C., S. Behura, B. DeBruyn, D. Lovin, B. Harker, C. Gomez-Machorro, A. Mori, J. Romero-Severson, and D. Severson. **2012**. Comparative Expression Profiles of Midgut Genes in Dengue Virus Refractory and Susceptible *Aedes aegypti* across Critical Period for Virus Infection. PLoS One. 7(10): e47350.

Chen, J. J., S. J. Wang, C. A. Tsai, and C. J. Lin. **2007**. Selection of differentially expressed genes in microarray data analysis. Pharmacogenomics J. 7: 212–220.

Cheng, G., Y. Liu, P. Wang, and X. Xiao. **2016**. Mosquito Defense Strategies against Viral Infection. Trends Parasitol. 32: 177–186.

Cheng, J., Y. Wang, F. Li, J. Liu, Y. Sun, and J. Wu. **2014**. Cloning and characterization of a mannose binding C-type lectin gene from salivary gland of *Aedes albopictus*. Parasit. Vectors. 7: 337.

Clements, A. N. 2012. The Biology of Mosquitoes Volume 3: Transmission of Viruses and Interactions with Bacteria.

Colpitts, T., J. Cox, D. VanLandingham, F. Feitosa, G. Cheng, S. Kurscheid, P. Wang, M. Krishnan, S. Higgs, and E. Fikrig. **2011**. Alterations in the *Aedes aegypti* transcriptome during infection with west nile, dengue and yellow fever viruses. PLoS Pathog. 7(9): e1002189.

Cooper, D. 2008. Apoptosis and Immunity: Characterizing the Cell Death Machinery in the Yellow Fever Mosquito, *Aedes aegpyti*. SFU Research Repository. PhD Thesis

Cooper, D., and K. Mitchell-Foster. 2011. Death for survival : what do we know about innate immunity and cell death in insects? Invertebrate Survival Journal. 8(2): 162-172.

Eng, M. W., M. N. van Zuylen, and D. W. Severson. **2016**. Apoptosis-related genes control autophagy and influence DENV-2 infection in the mosquito vector, *Aedes aegypti*. Insect Biochem. Mol. Biol. 76: 70–83.

Feng, J., C. Meyer, Q. Wang, J. Liu, X. Liu, and Y. Zhang. **2012**. GFOLD: A generalized fold change for ranking differentially expressed genes from RNA-seq data. Bioinformatics. 28: 2782–2788.

Feyereisen, R. 2006. Evolution of insect P450. Biochem. Soc. Trans. 34: 1252–1255.

Gillen, C., D. Akuma, and P. Piermarini. **2015**. Expression Pattern and RNAi Inhibition of Putative Sodium-coupled Cation-chloride Cotransporters in the Mosquito *Aedes aegypti*. Faseb. 29.

Gillen, C. M., C. R. Blair, N. R. Heilman, M. Somple, M. Stulberg, R. Thombre, N. Watson, K. M. Gillen, and H. Itagaki. **2006**. The cation-chloride cotransporter, masBSC, is widely expressed in *Manduca sexta* tissues. J. Insect Physiol. 52: 661–668.

van Gorp, E. C., C. Suharti, a T. Mairuhu, W. M. Dolmans, J. van Der Ven, P. N. Demacker, and J. W. van Der Meer. **2002**. Changes in the plasma lipid profile as a potential predictor of clinical outcome in dengue hemorrhagic fever. Clin Infect Dis. 34: 1150–1153.

Goulielmaki, E., I. Sidén-Kiamos, and T. G. Loukeris. **2014**. Functional characterization of *Anopheles* matrix metalloprotease 1 reveals its agonistic role during sporogonic development of malaria parasites. Infect. Immun. 82: 4865–4877.

Guo, X., Y. Xu, G. Bian, A. D. Pike, Y. Xie, and Z. Xi. **2010**. Response of the mosquito protein interaction network to dengue infection. BMC Genomics. 11: 1–15.

Heaton, N. S., and G. Randall. **2010**. Dengue virus-induced autophagy regulates lipid metabolism. Cell Host Microbe. 8: 422–432.

Hess, A., A. Prasad, A. Ptitsyn, G. Ebel, K. Olson, C. Barbacioru, C. Monighetti, and C. Campbell. **2011**. Small RNA profiling of Dengue virus-mosquito interactions implicates the PIWI RNA pathway in anti-viral defense. BMC Microbiol. 11: 45.

Hussain, M., and S. Asgari. **2014**. MicroRNA-like viral small RNA from Dengue virus 2 autoregulates its replication in mosquito cells. Proc. Natl. Acad. Sci. 111: 2746–2751.

Jordan, T. X., and G. Randall. **2015**. Flaviviruses and Autophagy, pp. 81–100. *In* Jackson, W.T., Swanson, M. (eds.), Autophagy, Infect. Immune Response. Wiley-Blackwell, Hoboken, New Jersey.

Jupatanakul, N., S. Sim, Y. I. Angleró-Rodríguez, J. Souza-Neto, S. Das, K. E. Poti, S. L. Rossi, N. Bergren, N. Vasilakis, and G. Dimopoulos. **2017**. *Engineered Aedes aegypti* JAK/STAT Pathway-Mediated Immunity to Dengue Virus. PLoS Negl. Trop. Dis. 11(1): e0005187.

Jupatanakul, N., S. Sim, and G. Dimopoulos. **2014**. *Aedes aegypti* ML and Niemann-Pick type C family members are agonists of dengue virus infection. Dev. Comp. Immunol. 43: 1–9.

Kanehisa, M., and S. Goto. **2000**. KEGG: kyoto encyclopedia of genes and genomes. Nucleic Acids Res. 28: 27–30.

Kantor, A. M., S. Dong, N. L. Held, E. Ishimwe, A. Lorena Passarelli, R. J. Clem, and A. W. E. Franz. **2017**. Identification and Initial Characterization of Matrix Metalloproteinases in the Yellow Fever Mosquito, *Aedes aegypti*. Insect Mol Biol. 26: 113–126.

Kim, D., G. Pertea, C. Trapnell, H. Pimentel, R. Kelley, and S. L. Salzberg. **2013**. TopHat2: Accurate alignment of transcriptomes in the presence of insertions, deletions and gene fusions. Genome Biol. 14: R36.

Lambrechts, L., and A. B. Failloux. **2012**. Vector biology prospects in dengue research. Mem. Inst. Oswaldo Cruz. 107: 1080–1082.

Lambrechts, L., and T. W. Scott. **2009**. Mode of transmission and the evolution of arbovirus virulence in mosquito vectors. Proc. R. Soc. B Biol. Sci. 276: 1369–1378.

Lassmann, T., Y. Hayashizaki, and C. Daub. **2011**. SAMStat: Monitoring biases in next generation sequencing data. Bioinformatics. 27: 130–131.

Leaungwutiwong, P., J. F. Kelley, A. Sachair, A. Jittmittraphap, and N. Luplertlop. **2016**. Relationship between MMP expression and virulence of dengue virus type-2 in infected mosquito and mammalian cells. Jpn. J. Infect. Dis. 69: 45–50.

Lee, H. K., and A. Iwasaki. **2008**. Autophagy and antiviral immunity. Curr. Opin. Immunol. 20: 23–29.

Lee, Y.-R., H.-Y. Hu, S.-H. Kuo, H.-Y. Lei, Y.-S. Lin, T.-M. Yeh, C.-C. Liu, and H.-S. Liu. **2013**. Dengue virus infection induces autophagy: an in vivo study. J. Biomed. Sci. 20: 65.

Liesecke, F., D. Daudu, R. D. De Bernonville, S. Besseau, M. Clastre, V. Courdavault, J. O. De Craene, J. Crèche, N. Giglioli-Guivarc'h, G. Glévarec, O. Pichon, and T. D. De Bernonville. **2018**. Ranking genome-wide correlation measurements improves microarray and RNA-seq based global and targeted co-expression networks. Sci. Rep. 8: 1–16.

Liu, Y., F. Zhang, J. Liu, X. Xiao, S. Zhang, C. Qin, Y. Xiang, P. Wang, and G. Cheng. **2014**. Transmission-Blocking Antibodies against Mosquito C-Type Lectins for Dengue Prevention. PLoS Pathog. 10(2): e1003931.

Lowenberger, C., M. Charlet, J. Vizioli, S. Kamal, a Richman, B. M. Christensen, and P. Bulet. **1999**. Antimicrobial activity spectrum, cDNA cloning, and mRNA expression of a newly isolated member of the cecropin family from the mosquito vector *Aedes aegypti*. J. Biol. Chem. 274: 20092–20097.

Maciel-de-Freitas, R., J. C. Koella, and R. Lourenço-de-Oliveira. **2011**. Lower survival rate, longevity and fecundity of *Aedes aegypti* (Diptera: Culicidae) females orally challenged with dengue virus serotype 2. Trans. R. Soc. Trop. Med. Hyg. 105: 452–458.

Mairuhu, A. T. A., J. Wagenaar, D. P. M. Brandjes, and E. C. M. Van Gorp. **2004**. Dengue: An arthropod-borne disease of global importance. Eur. J. Clin. Microbiol. Infect. Dis. 23: 425–433.

Marquardt, W. C. 2005. Biology of Disease Vectors, 2nd ed. Elsevier Inc., Amsterdam.

McGraw, E. A., and S. L. O'Neill. **2013**. Beyond insecticides: new thinking on an ancient problem. Nat. Rev. Microbiol. 11: 181–93.

Means, J. C., and a L. Passarelli. **2010**. Viral fibroblast growth factor, matrix metalloproteases, and caspases are associated with enhancing systemic infection by baculoviruses. Proc. Natl. Acad. Sci. U. S. A. 107: 9825–9830.

Megy, K., S. J. Emrich, D. Lawson, D. Campbell, E. Dialynas, D. S. T. Hughes, G. Koscielny, C. Louis, R. M. MacCallum, S. N. Redmond, A. Sheehan, P. Topalis, D. Wilson, E. Birney, M. Hammond, P. Kersey, N. Langridge, K. S. Campbell, M. Corby, D. Emmert, W. M. Gelbart, P. Zhou, G. K. Christophides, F. C. Kafatos, T. Collier, G. C. Lanzaro, Y. Lee, C. E. Taylor, P. Baker, M. Werner-Washburne, N. J. Besansky, R. Butler, R. Carmichael, D. Cieslak, N. Konopinski, A. Thrasher, G. Madey, and F. H. Collins. **2012**. VectorBase: Improvements to a bioinformatics resource for invertebrate vector genomics. Nucleic Acids Res. 40: 729–734.

Molina-Cruz, A., L. Gupta, J. Richardson, K. Bennett, W. Black IV, and C. Barillas-Mury. **2005**. Effect of mosquito midgut trypsin activity on dengue-2 virus infection and dissemination in *Aedes aegypti*. Am. J. Trop. Med. Hyg. 72: 631–637.

Ocampo, C. B., P. A. Caicedo, G. Jaramillo, R. Ursic Bedoya, O. Baron, I. M. Serrato, D. M. Cooper, and C. Lowenberger. **2013**. Differential Expression of Apoptosis Related Genes in Selected Strains of *Aedes aegypti* with Different Susceptibilities to Dengue Virus. PLoS One. 8(4): e61187.

Ocampo, C. B., and D. M. Wesson. **2004**. Population dynamics of *Aedes aegypti* from a dengue hyperendemic urban setting in Colombia. Am. J. Trop. Med. Hyg. 71: 506–513.

Oxitec. **2014**. Dengue Fever: The fastest growing mosquito-borne disease. Abingdon, UK.

Palmer, W. H., F. S. Varghese, and R. P. Van Rij. **2018**. Natural Variation in Resistance to Virus Infection in Dipteran Insects. Viruses. 10(3): E118.

Paluzzi, J. P., and M. J. O'Donnell. **2012**. Identification, spatial expression analysis and functional characterization of a pyrokinin-1 receptor in the Chagas' disease vector, *Rhodnius prolixus*. Mol. Cell. Endocrinol. 363: 36–45.

Pullikuth, A. K., K. Aimanova, W. Kang, H. R. Sanders, and S. S. Gill. **2006**. Molecular characterization of sodium / proton exchanger 3 (NHE3) from the yellow fever vector, *Aedes aegypti*. J. Exp. Biol. 209(18): 3529–3544.

Ramirez, J. L., J. Souza-Neto, R. T. Cosme, J. Rovira, A. Ortiz, J. M. Pascale, and G. Dimopoulos. **2012**. Reciprocal tripartite interactions between the *Aedes aegypti* midgut microbiota, innate immune system and dengue virus influences vector competence. PLoS Negl. Trop. Dis. 6(3): e1561.

Raquin, V., S. H. Merkling, V. Gausson, I. Moltini-Conclois, L. Frangeul, H. Varet, M. A. Dillies, M. C. Saleh, and L. Lambrechts. **2017**. Individual co-variation between viral RNA load and gene expression reveals novel host factors during early dengue virus infection of the *Aedes aegypti* midgut. PLoS Negl. Trop. Dis. 11(12): e0006152.

Rinker, D. C., X. Zhou, R. J. Pitts, A. Rokas, and L. J. Zwiebel. **2013**. Antennal transcriptome profiles of anopheline mosquitoes reveal human host olfactory specialization in *Anopheles gambiae*. BMC Genomics. 14: 749.

Schonhofer, C., H. Coatsworth, P. Caicedo, C. Ocampo, and C. Lowenberger. **2016**. Aedes aegypti Immune Responses to Dengue Virus, pp. 129–143. *In* Ballarin, L., Cammarata, M. (eds.), Lessons Immun. From Single-Cell Org. to Mamm. Academic Press, London.

Serrato, I. M., P. A. Caicedo, Y. Orobio, C. Lowenberger, and C. B. Ocampo. **2017**. Vector competence and innate immune responses to dengue virus infection in selected laboratory and field-collected *Stegomyia aegypti* (= *Aedes aegypti*). Med. Vet. Entomol. 31: 312–319.

Shertz, C. A., and M. E. Cardenas. **2011**. Exploiting and subverting tor signaling in the pathogenesis of fungi, parasites, and viruses. PLoS Pathog. 7(9): e1002269.

Sim, S., N. Jupatanakul, J. L. Ramirez, S. Kang, C. M. Romero-Vivas, H. Mohammed, and G. Dimopoulos. **2013**. Transcriptomic Profiling of Diverse *Aedes aegypti* Strains Reveals Increased Basal-level Immune Activation in Dengue Virus-refractory Populations and Identifies Novel Virus-vector Molecular Interactions. PLoS Negl. Trop. Dis. 7(7): e2295.

Sim, S., J. L. Ramirez, and G. Dimopoulos. **2012**. Dengue virus infection of the *Aedes aegypti* salivary gland and chemosensory apparatus induces genes that modulate infection and blood-feeding behavior. PLoS Pathog. 8(3): e1002631.

Smartt, C. T., and J. S. Erickson. **2009**. Expression of a novel member of the odorant-binding protein gene family in *Culex nigripalpus* (Diptera: Culicidae). J. Med. Entomol. 46: 1376–1381.

Sylvestre, G., M. Gandini, and R. Maciel-de-Freitas. **2013**. Age-Dependent Effects of Oral Infection with Dengue Virus on *Aedes aegypti* (Diptera: Culicidae) Feeding Behavior, Survival, Oviposition Success and Fecundity. PLoS One. 8(3): e59933.

Team, R. D. C. 2011. R: A language and environment for statistical computing.

Ternes, P., S. Franke, U. Zähringer, P. Sperling, and E. Heinz. **2002**. Identification and characterization of a sphingolipid Δ4-desaturase family. J. Biol. Chem. 277: 25512–25518.

Thorvaldsdóttir, H., J. T. Robinson, and J. P. Mesirov. **2013**. Integrative Genomics Viewer (IGV): High-performance genomics data visualization and exploration. Brief. Bioinform. 14: 178–192.

Trapnell, C., B. A. Williams, G. Pertea, A. Mortazavi, G. Kwan, M. J. Van Baren, S. L. Salzberg, B. J. Wold, and L. Pachter. **2010**. Transcript assembly and quantification by RNA-Seq reveals unannotated transcripts and isoform switching during cell differentiation. Nat. Biotechnol. 28: 511–515.

Waterhouse, R. M., E. V. Kriventseva, S. Meister, Z. Xi, K. S. Alvarez, L. C. Bartholomay, C. Barillas-Mury, G. Bian, S. Blandin, B. M. Christensen, Y. Dong, H. Jiang, M. R. Kanost, A. C. Koutsos, E. A. Levashina, J. Li, P. Ligoxygakis, R. M. MacCallum, G. F. Mayhew, A. Mendes, K. Michel, M. A. Osta, S. Paskewitz, W. S. Sang, D. Vlachou, L. Wang, Q. Wei, L. Zheng, Z. Zou, D. W. Severson, A. S. Raikhel, F. C. Kafatos, G. Dimopoulos, E. M. Zdobnov, and G. K. Christophides. **2007**. Evolutionary dynamics of immune-related genes and pathways in disease-vector mosquitoes. Science. 316(5832): 1738–1743.

Zou, Z., J. Souza-Neto, Z. Xi, V. Kokoza, S. W. Shin, G. Dimopoulos, and A. Raikhel. **2011**. Transcriptome analysis of *Aedes aegypti* transgenic mosquitoes with altered immunity. PLoS Pathog. 7(11): e1002394.

Zuo, X., W. Pan, T. Feng, X. Shi, and J. Dai. **2014**. Matrix metalloproteinase 3 promotes cellular anti-dengue virus response via interaction with transcription factor NFkB in cell nucleus. PLoS One. 9(1): e84748.

Tables

Table 2.1 Full factorial treatment design outlining all twelve experimental treatments. Each treatment consists of one replicate (n=1), containing 36 pooled mosquito midguts.

Hours PBM	24				36				48			
Treatment	Blood		Blood + DENV-2		Blood		Blood + DENV-2		Blood		Blood + DENV-2	
Strain (Cali-)	S	MIB	S	MIB	S	MIB	S	MIB	S	MIB	S	MIB

Table 2.2 List of candidate genes (candidate gene table). Table includes VectorBase gene ID, gene name, functional group, general gene function, possible association with pathogens, and associated references. 'Up' refers to up-regulated in the Cali-MIB strain, while 'Down' refers to down-regulated in the Cali-MIB strain.

Gene ID	Gene Name	Functional Group	Up/ Down	Function	Possible Pathogen Association	Reference
AAEL000693	*TOR*	Autophagy	Up	Inhibits autophagy, promoting cell growth	Inhibition should prevent viral replication	(Shertz and Cardenas 2011)
AAEL003712	*C-Type Lysozyme*	Immunity	Up	Involved in innate immunity specifically in AMP expression	Lysozyme exerts a significant inhibitory effect on DENV	(Ramirez et al. 2012)
AAEL002360	*Serine-Type Endopeptidase*	Digestion	Up	Digestive enzymes which assists in breaking down meals	Proteolytic activity of serine-type endopeptidases limits virus infectivity	(Brackney et al. 2008)
AAEL005444	*Pyrokinin*	Digestion and Ionic Balance	Up	Neuropeptide that regulates growth, metamorphosis, plays a role in anti-diuresis	Inhibits substrate absorption by anterior midgut	(Paluzzi and O'Donnell 2012)
AAEL002992	*Sphingolipid delta 4 desaturase*	Cell Signaling	Up	Control cell proliferation, differentiation, and apoptosis		(Ternes et al. 2002)
AAEL005641	*C-Type Lectin*	Binding	Up	Directly involved in cell galactose binding	Primary candidates for PRRs	(Cheng et al. 2014)
AAEL001769	*RM62B (Dead Box ATP-dependent RNA helicase)*	Immunity	Up	Guides the silencing of target transcripts within small RNA pathway	Small RNA pathway (PIWI) may limit DENV replication	(Hussain and Asgari 2014)
AAEL010195	*Trypsin*	Digestion	Up	Digestive enzyme which assists in breaking down meals	Higher trypsin expression results in higher DENV titers	(Molina-Cruz et al. 2005)

Gene ID	Gene Name	Functional Group	Up/ Down	Function	Possible Pathogen Association	Reference
AAEL013063	*Autophagy Related Gene*	Autophagy	Up	Participates in autophagy, an intracellular degradation system initiated upon stress	Autophagy plays a supportive role in DENV replication	(Lee and Iwasaki 2008, Heaton and Randall 2010, Lee et al. 2013)
AAEL002083	*RM62C (Dead Box ATP-dependent RNA helicase)*	Immunity	Up	Guides the silencing of target transcripts within small RNA pathway	Small RNA pathway may limit DENV replication	(Hussain and Asgari 2014)
AAEL000028	*CLIPB34*	Immunity	Down	Serine protease involved in immune and developmental processes	Malaria parasites utilize CLIPs to sever surface proteins	(Clements 2012)
AAEL014222	*Low-density lipoprotein*	Cell Transport	Down	Mediates receptor endocytosis	A wide variety of viruses utilize LDLs to enter host cells	(van Gorp et al. 2002)
AAEL008083	*40S ribosomal protein*	Cell Growth and Proliferation	Down	Directly involved in protein translation	Putative receptor for the entry of DENV into host cells	(Guo et al. 2010)
AAEL009888	*Bumetanide-sensitive Na-K-Cl cotransport*	Transport	Down	Vital role in regulating ionic balance and cell volume		(Gillen et al. 2015)
AAEL004978	*RM62E (Dead Box ATP-dependent RNA helicase)*	Immunity	Down	Guides the silencing of target transcripts within small RNA pathway	Small RNA pathway may limit DENV replication	(Hussain and Asgari 2014)

Table 2.3 Shared genes between differentially expressed genes at 24 and 48 hours (comparing the Cali-Susceptible and Cali-Refractory mosquitoes infected with virus) herein and those already documented in the literature. GOLD differential expression values are displayed from this study, and compared with differential expression values obtained from (Behura and Severson 2012; Bonizzoni et al. 2012a; Chauhan et al. 2012; Colpitts et al. 2011). GOFLD value is the normalized GFOLD log2-fold change value, the first RPKM (reads per kilobase of transcript per million mapped reads values) represents the susceptible mosquitoes, while the second RPKM corresponds to the refractory mosquitoes. Panel A is a comparison after 24 hours, while panel B is after 48 hours.

A

Vector Base Gene ID	GFOLD value	log2-fold change	FirstRPKM	SecondRPKM	Gene Description
AAEL015458***	1.63429	2.09472	0.482571	4.29899	transferrin
AAEL008019**	1.15154	1.35835	8.45216	44.6763	hypothetical protein
AAEL006911*	1.13906	1.33454	2.89728	15.0603	microtubule-associated protein
AAEL005091**	0.962343	1.23939	2.49015	12.1359	conserved hypothetical protein
AAEL005561***	0.92409	1.06373	4.33529	18.661	plasma membrane calcium-transporting ATPase 3 (pmca3)
AAEL009762****	0.887696	1.40863	0.602798	3.33524	cytochrome P450
AAEL006138**^	0.83831	0.886424	19.4911	74.1502	hypothetical protein
AAEL010434**^	0.800671	0.867546	10.7857	40.5015	Vitellogenin-A1 Precursor (VG)(PVG1)
AAEL000940***	0.71424	0.768284	130.763	458.353	conserved hypothetical protein
AAEL008413**	0.709035	0.988036	1.21075	4.95468	serine/threonine protein kinase
AAEL001503*	0.659975	0.751801	8.16197	28.2886	sodium/hydrogen exchanger 3 (nhe3)

AAEL003609**	0.637787	0.917252	1.18354	4.61077	neurobeachin
AAEL003733**	0.588112	0.805074	0.806103	2.90214	hypothetical protein
AAEL007817**	0.571004	0.857399	0.659328	2.46414	hypothetical protein
AAEL008234***^	0.565555	1.03674	0.559988	2.38295	dishevelled
AAEL017241**	0.540569	0.922035	1.62698	6.37326	
AAEL006126**^	0.528522	0.597776	7.44993	23.2034	conserved hypothetical protein
AAEL006563**^	0.49487	0.670025	7.09483	23.2468	Vitellogenic carboxypeptidase Precursor (EC 3.4.16.-)
AAEL008216***	0.468322	0.548729	15.6068	46.9852	aconitase
AAEL003331***	0.389598	1.01092	0.214398	0.901404	hypothetical protein
AAEL008853***	0.363469	0.515272	7.3669	21.6768	choline/ethanolamine kinase
AAEL000191***	0.358468	0.492464	6.24993	18.0997	conserved hypothetical protein
AAEL006728***^	0.287245	0.577257	2.62092	8.06135	ubiquitin-conjugating enzyme E2 c
AAEL013074***^	0.281054	0.373851	20.7738	55.4011	adenylyl cyclase-associated protein
AAEL006785***	0.275308	0.314515	210.798	539.46	60S ribosomal protein L18a
AAEL009630**	0.267701	0.519107	1.76691	5.21699	high-affinity cgmp-specific 3,5-cyclic phosphodiesterase
AAEL005358****	0.266146	0.571726	0.924488	2.83316	conserved hypothetical protein
AAEL000087***	0.230243	1.8899	0.020329	0.178293	macroglobulin/complement

AAEL001972***	0.213241	0.571861	3.44608	10.5697	TATA box binding protein (TBP)-associated factor, putative
AAEL004699***	0.207845	0.258941	34.393	84.6913	conserved hypothetical protein
AAEL008329***	0.187807	0.239528	207.059	503.059	60S ribosomal protein L24
AAEL011326***^	0.170562	0.563302	0.751053	2.29116	conserved hypothetical protein
AAEL011756***	0.157017	0.213465	68.2496	162.847	aldehyde dehydrogenase
AAEL013614***^	0.138192	0.220292	8.36298	20.0499	clathrin heavy chain
AAEL005706***	0.133593	0.491582	0.733715	2.12793	triacylglycerol lipase
AAEL013694***	0.112597	0.149466	277.193	632.684	40S ribosomal protein SA
AAEL001898***	0.08628	0.243694	3.39235	8.26768	conserved hypothetical protein
AAEL006511***^	0.076473	0.117664	374.017	835.071	ubiquitin
AAEL001158***	0.035571	0.379164	1.78576	4.78794	fructose-1,6-bisphosphatase
AAEL001516***^	0.008267	0.172471	3.04556	7.06473	vesicle associated protein, putative
AAEL011900**	0.007043	0.398599	1.41796	3.85581	N-acetyllactosaminide beta-1,3-Nacetylglucosaminyltransferase, putative
AAEL000026***^	-0.02263	-0.02764	0.382792	0.775454	dynein light chain, putative
AAEL002813***	-0.02916	-0.15403	56.2173	103.968	coupling factor, putative
AAEL013252***	-0.08415	-0.34997	2.47179	3.98877	hypothetical protein

AAEL013407***^	-0.08858	-0.13579	64.4558	120.724	catalase
AAEL007293***^	-0.115	-0.28768	6.79592	11.4547	cAMP-dependent protein kinase catalytic subunit
AAEL011476***^	-0.13368	-0.6027	1.91153	2.58157	conserved hypothetical protein
AAEL009275***	-0.13769	-0.29124	12.5854	21.1615	protein phosphatase-1
AAEL009658***	-0.15448	-0.29219	6.7785	11.3903	alpha,alpha-trehalase
AAEL013979***	-0.21581	-0.6126	1.88957	2.5368	conserved hypothetical protein
AAEL015312****	-0.25461	-0.38054	23.8955	37.7669	cathepsin b
AAEL004181**	-0.26924	-0.45802	1.12191	1.68004	conserved hypothetical protein
AAEL002793***	-0.32904	-0.66303	1.2945	1.67913	conserved hypothetical protein
AAEL001432***	-0.34173	-0.41512	39.1863	60.4723	protein disulfide isomerase
AAEL012245****	-0.44171	-2.28002	0.326285	0.109783	conserved hypothetical protein
AAEL003067****	-0.45827	-1.09195	1.07278	1.02269	conserved hypothetical protein
AAEL002759***	-0.46062	-0.5438	17.766	25.0759	tropomyosin invertebrate
AAEL004958****	-0.46068	-3.56953	0.110887	0	conserved hypothetical protein
AAEL012349****	-0.46068	-3.56953	0.154968	0	lipase 1 precursor
AAEL013566****	-0.48876	-1.91745	0.978856	0.494022	C-Type lectin (CTL) - galactose binding
AAEL015004***	-0.51611	-0.79771	3.27493	3.87027	hypothetical protein
AAEL004027***	-0.59755	-0.70559	26.8693	33.8975	glucose dehydrogenase
AAEL014190****	-0.59899	-2.52514	0.189295	0.048122	elongase, putative

AAEL009244***	-0.61831	-0.6692	195.675	253.206	serine-type enodpeptidase
AAEL013853****	-0.92413	-1.80399	0.947571	0.535306	C-Type Lectin (CTL) - galactose binding
AAEL013648****	-0.93159	-2.59552	0.293348	0.08286	conserved hypothetical protein
AAEL001295****	-1.03599	-1.58042	1.66246	1.1286	conserved hypothetical protein
AAEL002652***	-1.14538	-2.98457	0.129852	0.023579	hypothetical protein
AAEL007942***^	-1.25268	-1.58534	7.32334	4.99762	fibrinogen and fibronectin
AAEL017211**	-1.36322	-1.89536	16.8411	9.17417	cecropin anti-microbial peptide
AAEL001287**	-1.5998	-3.38312	0.620966	0.084568	conserved hypothetical protein
AAEL002796**	-1.78703	-2.66264	0.730636	0.224168	l-asparaginase i
AAEL008046**	-2.28638	-2.73068	4.00053	1.22289	rh antigen
AAEL003290**	-3.47153	-6.25985	1.0477	0	cell wall protein DAN4 precursor, putative
AAEL017110**	-5.13546	-7.88489	7.924	0	
AAEL009888**	-5.69755	-7.44101	1.44731	0.008596	bumetanide-sensitive Na-K-Cl cotransport protein, putative

^ previously detected as differentially expressed (see below for more information), but our results show changes in the opposite direction

* previously detected as differentially expressed in mosquitoes of the MOYO-S or MOYO-R strains infected with DENV2 Jam1409 18h post infection (Behura et al., 2011)

** previously detected as differentially expressed in Chetumal (CTM) mosquito midguts 1dpi with DENV2 Jam1409 or blood (Bonizzoni et al., 2012)

*** previously detected as differentially expressed in mosquitoes of the MOYO-S or MOYO-D strains infected with DENV2 Jam1409 24h post infection (Chauhan et al., 2012)

**** previously detected as differentially expressed in mosquitoes of the Rockefeller strain infected with DENV2 New Guinea C 48h post infection (Colpitts et al., 2011)

B

Vector Base Gene ID	GFOLD value	log2 fold change	FirstRPKM	SecondRPKM	Gene Description
AAEL008392***^	0.812048	1.3925	0.932716	2.58007	conserved hypothetical protein
AAEL006291***	0.57612	0.754547	4.46132	7.84022	cullin
AAEL010798***^	0.303677	0.440852	14.8129	20.9368	ubiquitin-conjugating enzyme E2 g
AAEL000604***^	0.281466	0.478478	4.90627	7.11891	hypothetical protein
AAEL014190****	-0.07837	-2.18723	0.160454	0.020175	elongase
AAEL001295****	-0.10263	-0.4388	4.09937	3.14096	conserved hypothetical protein
AAEL004809****	-0.12691	-0.78669	2.839	1.68835	conserved hypothetical protein
AAEL002908****	-0.27134	-1.89772	1.03566	0.250423	hypothetical protein
AAEL002818***	-0.31054	-0.62888	3.96005	2.6588	splicing factor u2af large subunit

Figures

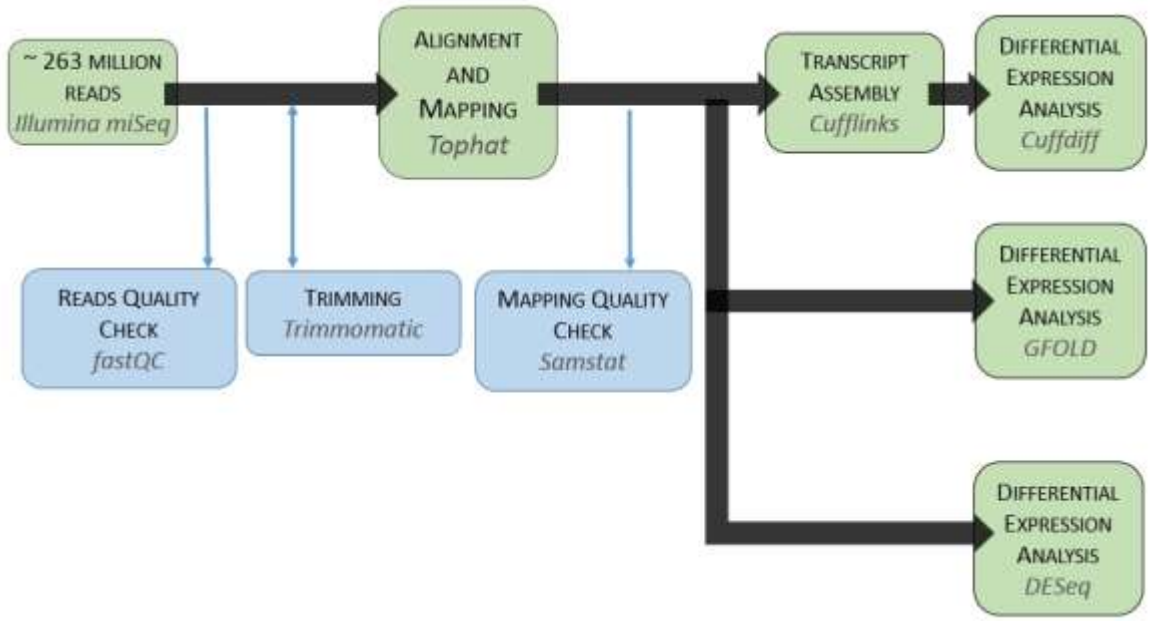

Figure 2.1 Modified and adapted RNA rocket Galaxy portal bioinformatics workflow.

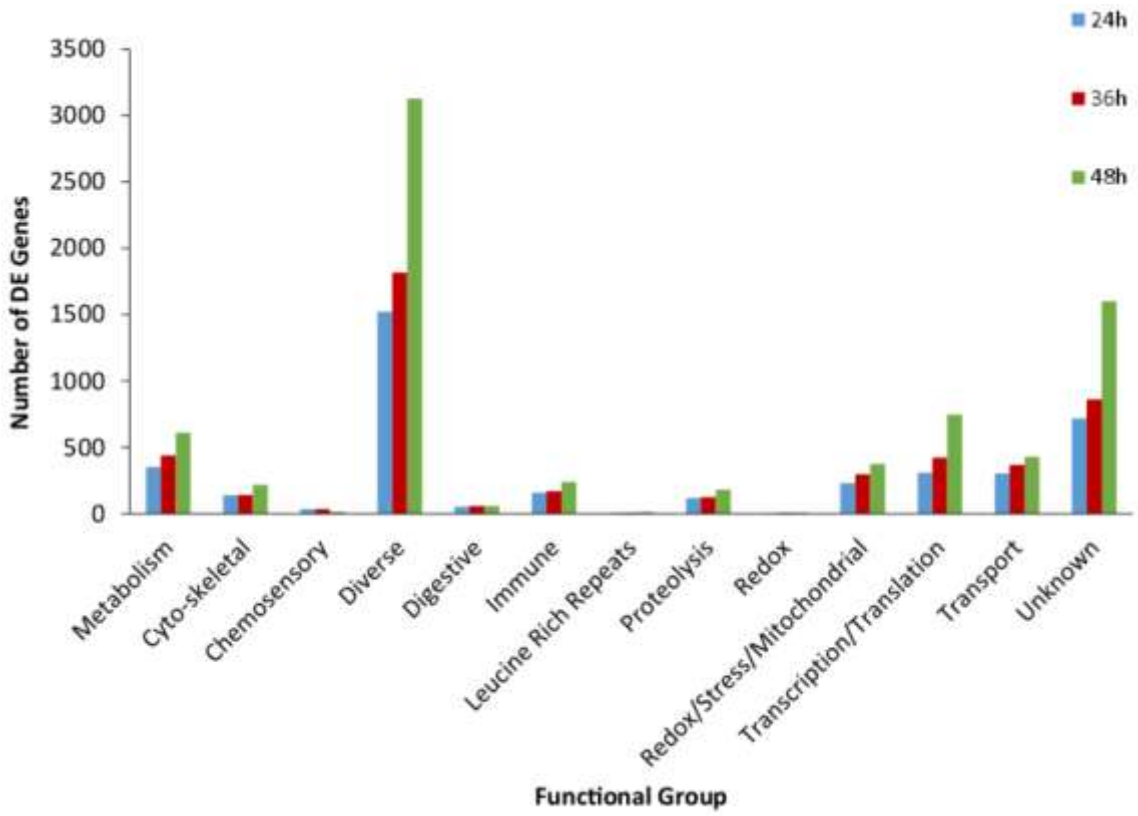

Figure 2.2 Significantly differentially expressed genes between Cali-S and Cali-MIB strains at 24, 36 and 48 h after ingesting dengue virus serotype 2, arranged by broad functional groups denoted by ImmunoDB.

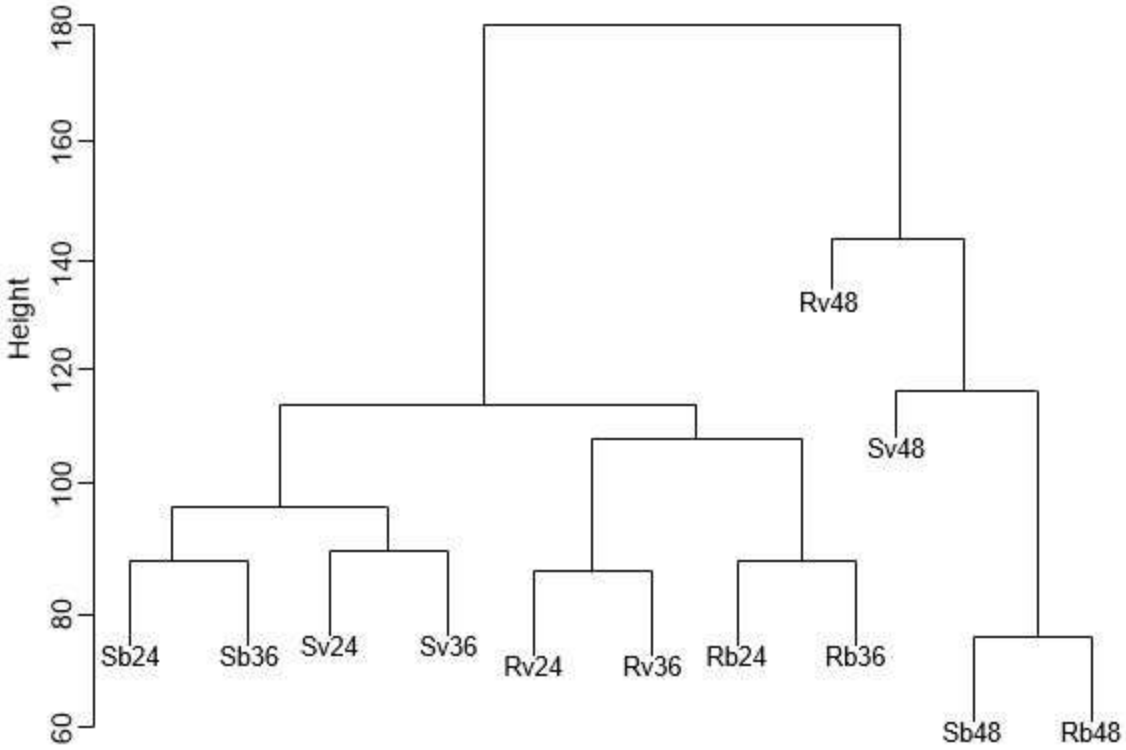

Figure 2.3 Consensus hierarchical clustering result from DESeq2 (v. 1.16.0), Cuffdiff (v. 2.2.1) and GFOLD (v. 1.1.1) generated using R (v. 3.1.1). Clustering shows the phylogenetic relationship between all 12 treatment expression profiles (S: Cali-S, R: Cali-MIB, v: virus fed, b: blood fed, numbers represent time points). Euclidian distances were generated to compute Complete Linkage clustering.

Connecting Statement 2

In Chapter 2 we identified many genes that were differentially expressed between Cali-MIB and Cali-S mosquitoes using RNA sequencing and questioned if any of these differences could be due to differences in the genomes of these mosquitoes. As whole genome sequencing of individual mosquitoes is expensive, and the downstream analyses are laborious, we carried out a genome wide association study (GWAS) to investigate DNA based differences in our strains. This approach allows us to compare thousands of loci and determine if any of these loci are significantly associated with the Cali-MIB or Cali-S phenotypes. This approach can then allow us to hone in on a particular region of the genome for a more detailed analysis on a gene by gene basis. The next chapter describes this GWAS, and also investigates genome wide epistatic effects.

Chapter 3. Polymorphisms determining phenotypic differences in field derived refractory and susceptible strains of *Aedes aegypti*

Author Contributions

Carl Lowenberger and Heather Coatsworth conceived the study. Paola Caicedo collected the samples, and Heather Coatsworth prepared the samples for analysis. Benjamin Evans quality checked the raw genotyping data. Maxwell Libbrecht assisted Heather Coatsworth and Carl Lowenberger in creating a data analysis pipeline. Heather Coatsworth completed all bioinformatic analyses. Heather Coatsworth and Laura Barth completed sequencing prep and analysis. Heather Coatsworth and Carl Lowenberger wrote the manuscript.

3.1. Abstract

Aedes aegypti is the principal vector of dengue viruses, which can cause serious medical problems (dengue hemorrhagic fever and shock syndrome). In Cali, Colombia, approximately 30% of field collected *Ae. aegypti* are dengue-refractory, possessing a midgut infection or midgut escape barrier, while the remaining 70% are dengue-susceptible. We performed a genome-wide association study using 15,084 markers from the Axiom_aegypti1 genotyping chip to elucidate genetic factors that may contribute or identify the dengue-refractory and -susceptible phenotypes. Two markers, AX-93240282 and AX-93240283 have a highly significant association with the Cali-MIB phenotype. AX-93240282 is a synonymous variant occurring within AAEL007409, *xylosyltransferase*, while AX-93240282 is a 5'UTR variant of AAEL007410, a putative protein phosphatase inhibitor 2. A Lasso regression model was created to identify a sub-set of variants that could predict the phenotype of a given mosquito. The model with the lowest misclassification error used three variants, AX-93240282, AX-93240283 and AX-93220550 to differentiate between dengue-refractory and -susceptible *Ae. aegypti*. Accuracy testing of these three variants with a new population of mosquitoes showed that AX-93240282 perfectly discriminates between the two phenotypes, while AX-93220550 and AX-93240283 did not. These results indicate that these specific variants can be used

to identify, quickly and accurately, mosquitoes that are refractory or susceptible to dengue viruses.

Keywords: *Aedes aegypti*, genotyping, vector competence, phenotypic markers

3.2. Introduction

Vector-borne pathogens are responsible for a significant proportion of the world's most debilitating and devastating human diseases (Mairuhu et al. 2004). In their role as vectors of protozoans (*Plasmodium* sp.) and viruses (West Nile, Japanese encephalitis, dengue, chikungunya, yellow fever, Zika) (Barnes 2005), mosquitoes are the indirect cause of more than 2 million deaths a year (Oxitec 2014). Of these, dengue is the most widespread arbovirus disease, infecting 50-390 million people each year throughout tropical and subtropical regions (Mairuhu et al. 2004, Bhatt et al. 2013). Dengue may present as a febrile illness from which patients recover, or as severe dengue (hemorrhagic fever and shock syndrome), which can be fatal.

Dengue viruses are transmitted primarily by *Aedes aegypti*, and to a lesser extent by *Aedes albopictus* (Barnes 2005). Changes in global travel, urbanization, as well as the mounting effects of climate change have facilitated *Ae. aegypti* population expansion, and consequently have allowed dengue to thrive. One half of the world's population is currently at risk of contracting dengue, a statistic that could increase as the effects of climate change mount (Bhatt et al. 2013); we have seen recent large *Ae. aegypti* range expansions into more temperate climates such as the United Kingdom, Australia and the United States of America.

Although insecticides, larvicides, and source reduction are used widely to reduce mosquito populations, none seem to significantly dampen dengue transmission (Barnes 2005), and there are currently no therapeutic drugs or commercially effective vaccines to treat dengue. This has resulted in an emphasis on mosquito bio-manipulation or genetic modification techniques to induce sterility (Catteruccia et al. 2003, 2009, Gabrieli et al. 2014), decrease lifespan (McGraw and O'Neill, 2013) or reduce vector competence, the innate ability of a mosquito to transmit a specific pathogen (Black et al. 2002b). Many of these developments have shown great promise in the laboratory and are based on

understanding the molecular interactions between vector and virus, as well as vector genetics (McGraw and O'Neill, 2013; Oxitec, 2014).

Once ingested by *Ae. aegypti*, DENV first enters and replicates in midgut epithelial cells. The virus later migrates through the midgut to replicate in secondary tissues, finally migrating to the salivary glands, where it continues replicating and is transmitted when the female bites again (Halstead et al. 1997, Black et al. 2002b, Perera-Lecoin et al. 2013).

Although *Ae. aegypti* is the principal vector of dengue viruses, not all females transmit dengue. Naturally refractory strains with varying degrees of vector competence have been observed, and multiple laboratory strains have been selected for reduced vector competence (Bennett, Beaty, et al. 2005b, Dong et al. 2011, Smith et al. 2013, Behura, Gomez-Machorro, DeBruyn, et al. 2014). In Cali, Colombia, approximately 30% of field collected *Ae. aegypti* are refractory to all 4 dengue serotypes (Ocampo and Wesson 2004, Serrato, Caicedo, Orobio, et al. 2017) through a midgut infection barrier (MIB) in which DENV is unable to replicate within midgut cells, or a midgut escape barrier (MEB) in which the virus cannot escape midgut cells (Ocampo et al. 2013). We can collect susceptible (Cali-S) or refractory (Cali-MIB and Cali-MEB) strains within the same communities, and inside the same houses within different neighborhoods and raise them in the laboratory as field derived strains (Caicedo et al. 2013b). We used multiple approaches to discern that differences between the Cali-MIB and Cali-S strains were based on differential gene expression in the midguts of the strains (Barón et al. 2010a, Ocampo et al. 2013, Caicedo et al. 2018), and was not determined by the midgut microbiota (Coatsworth et al. 2018).

For these studies, mosquitoes were collected in the field or raised in the laboratory, and subsequently exposed to DENV, after which there is a 2-week delay before we can determine the phenotype using an IFI antibody procedure. We used a genome wide association study (GWAS) to look at the role of intrinsic genetic variation between the strains to identify markers that will accurately predict the DENV susceptible or refractory phenotype. Single nucleotide polymorphisms (SNPs), are single base variants between two individuals, one reference and one alternate, occurring in at least 1% of the population. SNPs can be used to investigate differences between homozygous and heterozygous individuals in a population using non-reference alleles. Analyzing SNPs in thousands to hundreds of thousands of individuals can generate enough statistical power to investigate

whether any variants or loci are associated with a trait of interest and allows for a whole-genome view of association and linkage patterns. We used a high-throughput genotyping chip, Axiom_aegypti1 (Evans et al. 2015) to screen 50,000 SNPs across Cal-MIB and Cali-S mosquitoes (Evans et al. 2015). This chip has been used to investigate the population structure of mosquitoes from different geographic origins (Gloria-Soria et al. 2018, Kotsakiozi et al. 2018), but not, to our knowledge, to investigate vector competence. Such an approach will untangle the intrinsic genetic variation between the Cali-MIB and Cali-S strains, will identify a sub-set of genetic variants linked to, or responsible for, the phenotype, and if successful, will create a rapid, cost-effective phenotypic diagnostic tool.

3.3. Methods

3.3.1. Mosquito collection and maintenance

Laboratory colonies of *Ae. aegypti* were established at CIDEM from larvae and pupae collected from artificial larval habitats in five locations at least 10 km apart in the city of Cali, Colombia (Ocampo and Wesson 2004). Larvae were maintained in plastic containers at a density of 300 larvae/2 L of water and were fed daily with 2mL of a stock solution (8g/400mL) of beef liver (DIFCO, New Jersey, USA). Adult mosquitoes were maintained under standard laboratory conditions: 27˚C, 70% relative humidity, and a 12:12 hour light: dark cycle, and were maintained with a 10% sucrose solution. Blood feeding was done by allowing the mosquitoes to feed on live hamsters (for colony maintenance), while an artificial membrane feeder using a pig intestine as the membrane and defibrinated rabbit's blood warmed to 37˚C was used for dengue infections. A damp piece of paper towel was provided to the mosquitoes three days post blood-feeding as an oviposition surface. The resultant eggs (F1) were stored and used to begin the phenotype selection process. Experimental protocols and the use of hamsters and rabbit blood to feed and maintain insect colonies at CIDEIM were approved by the CIDEIM institutional review committee for research in animals (Comité de Ética para la Investigación en Animales Experimentales).

3.3.2. Exposure to dengue virus and phenotype determination

To asses their vector competency, adult females were exposed to dengue virus through an artificial membrane feeder. New Guinea C DENV serotype 2 (Colorado State

University) was grown in *Aedes albopictus* C6/36HT cells in Leivovitz 15 medium (L15) with 10% heat inactivated fetal bovine serum (FBS), 1% penicillin/streptomycin, and 1% L-glutamine at 31 ± 1 °C, as described previously (Caicedo et al. 2013b). Infected cells were incubated for 14 days at 32 °C in L15 medium supplemented with 2% heat-inactivated FBS, 1% penicillin/streptomycin, and 1% L-glutamine. The virus and cells were harvested and collected in a 15mL conical centrifuge tube.

The virus suspension was mixed 1:1 with defibrinated rabbit's blood. Eight- to ten-day-old adult female *Ae. aegypti* were exposed for 2 h to an infectious bloodmeal via the membrane feeder. The presence and concentration of virus to which the females were exposed to was determined in: (i) uninfected rabbit blood; (ii) the virus suspension; and a mixture of blood and virus at the beginning (iii) and end (iv) of the exposure period as previously described (Bennett, Beaty, et al. 2005b).

Infected mosquitoes (n=30) were maintained in the insectary for the 14-day extrinsic incubation period for DENV2. At 14 days, the heads and midguts were scored for the presence of disseminated virus using indirect immunofluorescence assays (IFI) to determine each mosquito's phenotype. Mosquitoes with positive head and midgut IFI results were deemed dengue-susceptible (Cali-S) (n=13), while mosquitoes with negative head and midgut IFI results were classified as dengue-refractory (Cali-MIB) (n=12). The carcasses from these mosquitoes were stored individually in 1.5mL centrifuge tubes in 70% ethanol, and were sent to Simon Fraser University (British Columbia, Canada), for further processing. All dengue related work was completed in a BSL-2+ facility at CIDEIM.

3.3.3. DNA sample preparation

The DNA was extracted from confirmed Cali-MIB or Cali-S mosquitoes using a Qiagen DNeasy Blood and Tissue kit (Venlo, Netherlands) following the manufacturer's protocol for insect DNA extraction, with an additional step of adding 10µL of RNase A (Qiagen, Venlo, Netherlands) following the proteinase K digestion. Amicon Ultra 0.5mL – 30K centrifugal columns (Burlington, Massachusetts, USA) were used to concentrate the samples and eluted DNA was quantified using Qubit High Sensitivity dsDNA reagents (Waltham, Massachusetts, USA). Each sample was diluted to 12ng/µL and was sent to Yale University (Powell Lab, New Haven, CT, USA) for genotyping using the Axiom_aegypti1 SNP-Chip 1.

3.3.4. Variant calling and filtering

Raw data files were processed with the Axiom Analysis Suite v.3.1. (Affymetrix, Santa Clara, CA, USA) to call the genotypes. In total, 27,674 loci were called and filtered using PLINK v.1.90, to account for missing genotyping rates for both SNPs and individuals (>0.1), to remove loci with minor allele frequencies <0.1, and those not in Hardy Weinberg equilibrium (p-value of <1e-6). After filtering, a total of 15084 SNPs remained.

3.3.5. Genome-Wide Association Study (GWAS)

After filtering, a workflow was created in order to complete our GWAS study (Figure 3.1). The data from the PLINK analysis were used to complete an association test, analyzing the effect of each SNP individually. A quantile-quantile (Q-Q) plot was made using the ggplot2 package in R (v 3.4.3) to analyze the population structure (Figure 3.2). Most of our data did not follow the expected quantile distribution, showing high population stratification (genomic inflation factor, λ, of 7.35). In order to reduce this inflation, we completed a principal component (PC) analysis on a subset of our data and made a scree plot to examine the relationship between the eigenvalues and number of principal components. As there was a clear drop off in eigenvalues after the first two principal components, we chose to use these two PCs as co-variates in a new association test. Using these co-variates improved our Q-Q plot (Figure 3.2), decreasing inflation bulk inflation in our dataset (λ=1.29). To obtain a genomic inflation factor of <1.1 to further reduce bias, EMMAX v. beta, was used to create a Balding-Nichols kinship matrix, as our dataset had a higher degree of relatedness due to inbreeding within our lab populations. The kinship matrix and covariates then were used to complete an association test, again using EMMAX. The resultant Q-Q plot from the association test accounting for kinship showed a genomic inflation factor (λ) of 1.07 (Figure 3.2), indicating we had adequately adjusted our dataset to account for our population structure, as most of our data matched the expected quantile distribution. R (ggplot2 package) was used to create a Manhattan plot to visualize the results of the association test (Figure 3.3). To create a significance cut-off that account for multiple testing, the α value of 0.05 was divided by the number of variants we analyzed (15084), resulting in a p-value significance cut-off of $3.31e^{-6}$.

3.3.6. Genome-Wide Epistasis Study (GWES)

Similar to our GWAS study, we created a workflow to complete our GWES study (Figure 3.1). A subset of the results from the GWAS study were used in a genome-wide epistasis study to investigate the effects of SNPs in combination rather than individually. We completed a Least absolute shrinkage and selection operator (Lasso) regression analysis to train a model that would predict the phenotype of a given mosquito based on the genotype of the SNPs analyzed. The glmnet package (Friedman et al. 2010) in R was used to determine how many SNPs needed to be included for the optimal model. The remaining data were run on the selected model to test its accuracy in predicting the phenotype.

3.3.7. Identifying phenotypic markers

The results from Lasso were tested empirically for accuracy with additional verified Cali-MIB and Cali-S mosquitoes selected from newly collected field insects, and thus represented a different genetic background than the first set of individuals. The phenotype of each mosquito was determined as described above, and DNA was extracted from the carcass of 10 Cali-S and 10 Cali-MIB mosquitoes as described above. Primer sets were designed for each of the predicted markers (see Table 3.1). Accuracy testing for each marker was completed on the newly selected Cali-S and Cali-MIB DNA using standard PCR with 1µL (5 ng) of template DNA. Thermocycling conditions were: 95°C for 5 mins, 30 cycles of 95°C for 10s, 56°C for 10s, and 72°C for 30s in 25µL reactions. Results were visualized on 1.5% agarose gels and DNA was precipitated from the post-PCR product using sodium acetate. The quality and purity of all resultant DNA samples was assessed using a Nanodrop (NanoDrop, ND-1000), and 10µL (20ng) of DNA was sequenced at GENEWIZ (New Jersey, USA).

3.3.8. Effect prediction

RNA seq data from these Cali-S and Cali-MIB (Chapter 2) were used to detect possible causal polymorphisms between the phenotypes 7,000 bp up- or downstream of each putative marker. Samtools v1.9 (Li et al. 2009, Liu et al. 2012) was used to remove all PCR duplicates, leaving only unique reads, and provided output files for each

phenotype. These files were sorted using samtools, and bcftools v1.9 (Li et al. 2009, Liu et al. 2012) was used to call variants, generating a vcf file for each phenotype.

VectorBase's Variant Effect Predictor (Giraldo-Calderón et al. 2015) was used to analyze the vcf files to predict the effect of each of the variants (low effect – splice region variant, synonymous variant; moderate effect – missense variant, in frame insertion, modifier – 3' UTR variant, 5' UTR variant, downstream gene variant, intergenic variant, non-coding transcript exon variant, upstream gene variant; and high effect – ATG start loss). As the variants are a result of differences between our mosquito phenotypes and the *Ae. aegypti* Liverpool strain geneset 3 release from VectorBase (AaegL3.3, October 2014), we further filtered out variants common in both the Cali-MIB and Cali-S mosquitoes (most likely geographical in origin).

3.4. Results

3.4.1. Genome-Wide Association Study

Our association study identified two variants (AX-93240282, AX-93240283) that were significantly (p-value<$3.31e^{-6}$) associated phenotypically. Both variants displayed a homozygous phenotypic association (Table 3.1). AX-93240282 is a synonymous variant in the coding region of AAEL007409, *xylosyltransferase*, while AX-93240283 is a variant in the 5' UTR region on AAEL007410, uncharacterized in *Ae. aegypti*, but with close similarity to A0A023EJV7, a protein phosphatase inhibitor in *Ae. albopictus*. The two variants are 7000 bp apart and, based on inheritance patterns, appear to be in linkage disequilibrium (LD).

3.4.2. Genome-Wide Epistasis Study

The GWES study identified three variants from the Lasso regression, clearly denoted by the drop in the model's misclassification error after including three variants (Figure 3.4). When provided with blind phenotype data, the model used these three variants to identify the correct phenotype of a mosquito 100% of the time. The three variants were AX-93240282, AX-93240283, and AX-93220550 (see Table 3.1 for genotype distributions). The first two were the same variants identified through the GWAS study, while the third variant was an intergenic variant.

3.4.3. Identifying phenotypic markers

The variants identified through the GWAS and GWES pipelines were tested on a new population of verified Cali-MIB and Cali-S mosquitoes to test the accuracy of these predictions. Expected results were based on the genotypes we observed in the GWAS study (Table 3.1). Variant 1 (AX-93240282) was able to distinguish clearly between dengue-susceptible (Cali-S) and dengue-refractory (Cali-MIB) individuals, as all sequenced Cali-S mosquitoes had the expected 'T' variant, while all Cali-MIB mosquitoes contained the expected 'C' variant (Tables 3.2, 3.4). Variant 2 (AX-93240293) was completely invariant in the second population of mosquitoes we tested; all S and R mosquitoes presented with the same expected dengue-susceptible 'G' variant (Tables 3.2, 3.4). Variant 3 (AX-93220550), correctly identified all Cali-MIB mosquitoes; all contained the 'T' variant, while Cali-S mosquitoes contained both the expected Cali-S 'C' and Cali-MIB 'T' variants (Tables 3.2, 3.4).

3.4.4. Effect Prediction

From our RNAseq study, a total of 410 unique (only in Cali-S or Cali-MIB) variants were identified. Most of the variants (280), were predicted to have a 'modifier' effect, which includes 124 3' UTR variants (21 S, 103 R), 46 5' UTR variants (4 S, 32 R), 83 downstream gene variants (22 S, 61 R), 27 upstream gene variants (2 S, 25 R), 9 non-coding transcript exon variants (2 S, 7 R), and 1 Cali-MIB intergenic variant. Another 105 variants (14 S, 91 R) were predicated to have a 'low' effect, as they were synonymous variants. Of those most likely to induce a protein-coding change, 24 had a 'moderate' effect: 20 were missense variants (6 S, 14 R), and 4 Cali-S variants were in-frame insertions. Only 1 variant in Cali-S mosquitoes was predicted to have a 'high' impact as this variant caused a start codon loss in AAEL008911, an uncharacterized gene (Table 3.5).

3.5. Discussion

In this study we identified loci that were genotypically distinct and associated with our dengue-refractory and dengue-susceptible phenotypes. The GWAS study identified two loci, AX-93240282, and AX-93240283 that were highly associated with our phenotypes of interest. Neither of these loci encoded for changes that could be phenotypically relevant (synonymous exonic, and 5'UTR variants, respectively). Using

RNA sequencing data obtained from the same two dengue mosquito phenotypes, we were able to investigate putative biologically relevant variants (outlined in Table 3.5) by scanning areas around our variants of interest. Since our associated variants were 7,000 bp apart, we scanned the RNA seq data for variants ± 3,500 bp of each associated variant. As the RNA seq data comprised pooled individuals, we do not know how prevalent each of the variants is within a single Cali-MIB or Cali-S mosquito. In Cali-MIB mosquitoes, there are numerous missense variants in AAEL021595 (unknown gene function), and AAEL007409 (*xylosyltransferase*). Most of these variants have not been reported previously, suggesting they may be unique to the Cali-MIB strain. In Cali-S females, many missense variants as well as in-frame mutations were present in AAEL007410 (protein phosphatase inhibitor 2), while a start loss was noted in AAEL008911 (unknown gene function). Variants that putatively affect gene function of AAEL007409 and AAEL021595 in Cali-MIB were not found in Cali-S. Similarly, putative gene altering variants in Cali-S in AAEL007410 and AAEL008911 were not found in Cali-MIB. These data suggest that these 4 genes may be important in determining the phenotype.

These missense and in-frame mutations most likely decrease the efficacy of the gene, although rare cases of mutations increasing gene expression have been noted (Eyre-Walker and Keightley 2007). In Cali-S mosquitoes, these variants were present in AAEL007410, protein phosphatase inhibitor 2, as well as in AAEL008911, a gene with unknown function. Protein phosphatase inhibitors have been shown to decrease dengue virus titres in human liver carcinoma cells (Limjindaporn et al. 2017), as well as titres of hepatitis C virus, in living cells (Georgopoulou et al. 2006). There is evidence that viral infection stimulates phosphatase activity; mosquitoes with impaired phosphatase inhibitor activity, such as the Cali-S strain, might allow high virus replication. In Cali-MIB mosquitoes, variants were observed in AAEL021595, a gene with unknown function, and AAEL007409, *xylosyltransferase*. *Xylosyltransferase* is an enzyme necessary for heparin and chondroitin sulfate production (Esko et al. 1985), substrates deemed essential for viral binding and entry into Vero and BHK (baby hamster kidney) cells (Germi et al. 2002). Cell lines that contained *heparan sulfate* mutations or that were supplied with heparin-lyase resulted in significantly reduced binding of yellow fever and dengue viruses, (up to 97%), indicating that *xylosyltransferase* is necessary for viral entry and subsequent establishment (Chen et al. 1997, Germi et al. 2002, Avirutnan et al. 2007, Dalrymple and Mackow 2011). In mosquitoes, chondroitin sulfates are necessary for *Plasmodium sp.*

entry into midgut epithelial cells (Dinglasan et al. 2007). Mutations in *xylosyltransferase* in dengue-refractory individuals may render downstream substrates such as heparin and chondroitin sulfate non- or sub-functional, preventing viral entry into midgut epithelial cells. Future studies should sequence all four genes to determine causal variants and carry out protein modeling predictions.

Our Lasso regression identified three variants, AX-93240282, AX-93240283, and AX-93220550 that could be used in concert to predict accurately the phenotype of a mosquito. Upon testing these variants with newly selected dengue-refractory and dengue-susceptible field mosquitoes, only AX-93240282 was able to discriminate reliably between the two phenotypes. AX-93220550 accurately identified Cali-MIB individuals, but multiple Cali-S mosquitoes also had the 'refractory' variant, resulting in a high false negative rate. All mosquitoes had the same sequence for AX-93240283, with each individual possessing the variant we originally designated as the 'susceptible' variant. The discrepancies between the results are most likely due to the different population backgrounds of the insects that were tested (discovery and accuracy). Current selection procedures require dengue exposure and phenotype determination using IFI two weeks later. Using this technique, we have established a 99% dengue-susceptible line (Cali-S); and a dengue-refractory line (Cali-MIB) where only 50% of the mosquitoes are truly dengue-refractory (Caicedo et al. 2013b). If AX-93240282 is a true dengue-refractory indicator across multiple Cali-MIB populations, DNA could be extracted from a single pulled leg, and only those with a dengue-refractory variant would be kept in the colony. This might permit a more effective approach to developing a 100% dengue-refractory strain of mosquitoes. Although this variant, and AX-93220550, appear promising for identifying Cali-MIB individuals, our results only examined females. Selecting males with the "correct" genotype for selecting the refractory strain would confirm the role of these variants in determining the phenotype, and potentially allow us to create 'pure' lines of dengue-susceptible and -refractory individuals. Further analyses should be completed on more field-derived individuals from across the city, confirming the presence of the 'refractory' marker in other verified Cali-MIB individuals.

We used a mosquito specific genotyping chip, Axiom_aegypti1 (Evans et al. 2015) to investigate vector competence in *Aedes aegypti.* The chip was designed using next-generation sequencing based (NGS) techniques: restriction-site associated DNA sequencing (RAD-seq) and double digest RAD-seq (ddRAD-seq) principles, which

allowed for a mass amplification of hundreds of thousands of variants. Although this comprehensive chip was designed for multiple utilities, it has only been used thus far to examine geographical differences between mosquitoes (Evans et al. 2015, Gloria-Soria et al. 2018, Kotsakiozi et al. 2018). While other populations of dengue-refractory mosquitoes exist, they have not implemented the same study design as us, and thus we cannot compare our entire dataset to others due to a lack of overlapping genetic data. There was also a significant drop-off in the number of SNPs we were able to include after our filtering steps. The chip analyzes 50,000 loci (25,000 of which were validated in Evans et al. 2015). However, we were only able to use 15,084 of these loci, suggesting further optimization may be needed. We also ran our GWAS study on field-derived laboratory strains of Cali-MIB and Cali-S mosquitoes. As such, we needed to account for inbreeding in our GWAS study, and this may have resulted in a very conservative association test significance cut-off. Future studies should aim to reduce relatedness between individuals as much as possible to identify more phenotypically associated variants.

Studies examining the effects of genetic differences on vector competence in mosquitoes have traditionally used restriction fragment length polymorphisms (RFLPs), random amplification of polymorphic DNA (RAPD), and single strand conformation polymorphisms (SSCPs) to determine quantitative-trait loci (QTLs) and microsatellites that contribute to observed differences in vector competence (Morlais and Severson 2003). Most of these studies were completed prior to the sequencing of the *Ae. aegypti* genome (Nene et al. 2007), and the low abundance of microsatellites and scarcity of simple-sequence repeats made genetic analyses in mosquitoes quite difficult (Fagerberg et al. 2001). As such, genetic positions were confined to centrimorgan (cM) positions on chromosomes, which made subsequent functional interpretations and analyses difficult. Despite these difficulties, multiple studies found continued evidence of a large genetic contribution to midgut specific refractory barriers (both infection and escape), with over 20% of phenotypic variance deriving from genetic elements, although these varied in chromosomal location (Bosio et al. 2000, Gomez-Machorro et al. 2004, Bennett, Flick, et al. 2005). In some systems, vector competence was found to be tightly linked to a cluster of independent genes, with a single locus affecting susceptibility (Severson et al. 1995), a trend which was also evident in our dengue-susceptible and -refractory populations. In some studies, a higher concentration of variants was observed to occur in immune related genes, especially those related to pathogen recognition receptors (Morlais et al. 2004,

Bonizzoni et al. 2013). While we did not observe any large-scale trends among functional groups, this may have been confounded by a lack of functional gene annotations in our identified genes.

In summary, we have identified two variants highly associated with our dengue-refractory and susceptible phenotypes and have flagged four genes for further variant investigation and functional testing. We found that one genetic locus was able to identify Cali-S and Cali-MIB individuals based on a single SNP, and another locus could be used to confirm Cali-MIB mosquitoes. This study is the first step in understanding the natural genetic variation between the Cali-S and Cali-MIB phenotypes and has broad implications for creating DNA-based phenotypic markers to flag specific *Ae. aegypti* populations. These data may be used to generate pure dengue-refractory and -susceptible lines, to continue studies on vector-arbovirus interactions with the aim of identifying factors we might use to dampen dengue transmission.

3.6. References

Avirutnan, P., L. Zhang, N. Punyadee, A. Manuyakorn, and C. Puttikhunt. 2007. Secreted NS1 of Dengue Virus Attaches to the Surface of Cells via Interactions with *Heparan sulfate* and Chondroitin Sulfate E. PLoS Pathog. 3(11): e183.

Barnes, E. 2005. Diseases and Human Evolution. University of New Mexico Press, Albuquerque, N.Y.

Barón, O. L., R. J. Ursic-Bedoya, C. A. Lowenberger, and C. B. Ocampo. 2010. Differential Gene Expression from Midguts of Refractory and Susceptible Lines of the Mosquito, *Aedes aegypti*, Infected with Dengue-2 Virus. J. Insect Sci. 10: 1–23.

Behura, S., C. Gomez-Machorro, B. DeBruyn, D. Lovin, B. Harker, J. Romero-Severson, A. Mori, and D. Severson. 2014. Influence of mosquito genotype on transcriptional response to dengue virus infection. Funct. Integr. Genomics. 14: 581–9.

Bennett, K. E., B. J. Beaty, and W. C. Black. 2005. Selection of D2S3, an *Aedes aegypti* (Diptera: Culicidae) strain with high oral susceptibility to Dengue 2 virus and D2MEB, a strain with a midgut barrier to Dengue 2 escape. J. Med. Entomol. 42: 110–119.

Bennett, K. E., D. Flick, K. H. Fleming, R. Jochim, B. J. Beaty, and W. C. B. Iv. 2005. Quantitative Trait Loci That Control Dengue-2 Virus Dissemination in the Mosquito *Aedes aegypti*. Genetics. 170(1): 185–194.

Bhatt, S., P. W. Gething, O. J. Brady, J. P. Messina, A. W. Farlow, C. L. Moyes, J. M. Drake, J. S. Brownstein, A. G. Hoen, O. Sankoh, M. F. Myers, D. B. George, T. Jaenisch, G. R. William Wint, C. P. Simmons, T. W. Scott, J. J. Farrar, and S. I. Hay. 2013. The global distribution and burden of dengue. Nature. 496: 504–507.

Black, W. C., K. E. Bennett, N. Gorrochótegui-Escalante, C. V. Barillas-Mury, I. Fernández-Salas, M. D. L. Muñoz, J. a. Farfán-Alé, K. E. Olson, and B. J. Beaty. 2002. Flavivirus susceptibility in *Aedes aegypti*. Arch. Med. Res. 33: 379–388.

Bonizzoni, M., M. Britton, O. Marinotti, W. Dunn, J. Fass, and A. A. James. 2013. Probing functional polymorphisms in the dengue vector, *Aedes aegypti*. BMC Genomics. 14: 739.

Bosio, C., R. Fulton, M. Salasek, B. Beaty, and W. Iv. 2000. Dengue-2 Virus in the Mosquito *Aedes aegypti*. Genetics. 156: 687–698.

Caicedo, P. A., I. M. Serrato, S. Sim, G. Dimopoulos, H. Coatsworth, C. Lowenberger, and C. B. Ocampo. 2018. Immune response-related genes associated to blocking midgut dengue virus infection in *Aedes aegypti* strains that differ in susceptibility. Insect Sci. 26(4): 635-648.

Caicedo, P., O. Barón, M. Pérez, N. Alexander, C. Lowenberger, and C. Ocampo. 2013. Selection of *Aedes aegypti* (Diptera: Culicidae) strains that are susceptible or refractory to Dengue-2 virus. Can. Entomol. 145: 273–282.

Catteruccia, F., A. Crisanti, and E. A. Wimmer. 2009. Transgenic technologies to induce sterility. Malar. J. 8: 1–8.

Catteruccia, F., J. C. H. Godfray, and A. Crisanti. 2003. Impact of genetic manipulation on the fitness of *Anopheles stephensi* mosquitoes. Science. 299(5610): 1225–1227.

Chen, Y., T. Maguire, R. Hileman, J. Fromm, J. Esko, R. Linhardt, and R. Marks. 1997. Dengue virus infectivity depends on envelope protein binding to target cell *heparan sulfate*. Nat. Med. 3: 866–871.

Coatsworth, H., P. A. Caicedo, T. Van Rossum, C. B. Ocampo, and C. Lowenberger. 2018. The Composition of Midgut Bacteria in *Aedes aegypti* (Diptera: Culicidae) That Are Naturally Susceptible or Refractory to Dengue Viruses. J. Insect Sci. 18(6). https://doi.org/10.1093/jisesa/iey118.

Dalrymple, N., and E. R. Mackow. 2011. Productive Dengue Virus Infection of Human Endothelial Cells Is Directed by *Heparan sulfate*-Containing Proteoglycan Receptors. J. Virol. 85: 9478–9485.

Dinglasan, R. R., A. Alaganan, A. K. Ghosh, A. Saito, T. H. Van Kuppevelt, and M. Jacobs-lorena. 2007. *Plasmodium falciparum* ookinetes require mosquito midgut chondroitin sulfate proteoglycans for cell invasion. PNAS. 104(40): 15882-15887.

Dong, Y., S. Das, C. Cirimotich, J. A. Souza-Neto, K. J. McLean, and G. Dimopoulos. 2011. Engineered *Anopheles* immunity to *Plasmodium* infection. PLoS Pathog. 7(12): e1002458.

Esko, J. D., T. O. D. E. Stewart, and W. H. Taylor. 1985. Animal cell mutants defective in glycosaminoglycan biosynthesis. Proc Natl Acad Sci. 82: 3197–3201.

Evans, B. R., A. Gloria-Soria, L. Hou, C. McBride, M. Bonizzoni, H. Zhao, and J. R. Powell. 2015. A Multipurpose, High-Throughput Single-Nucleotide Polymorphism Chip for the Dengue and Yellow Fever Mosquito, *Aedes aegypti*. G3 (Bethesda). 5(5): 711–718.

Eyre-Walker, A., and P. D. Keightley. 2007. The distribution of fitness effects of new mutations. Nature Rev. Gen. 8: 610-618.

Fagerberg, A. J., R. E. Fulton, and F. Collins. 2001. Microsatellite loci are not abundant in all arthropod genomes: analyses in the hard tick, *Ixodes scapularis* and the yellow fever mosquito, *Aedes aegypti*. Insect Mol. Biol. 10: 225–236.

Friedman, J., T. Hastie, and R. Tibshirani. 2010. Regularization Paths for Generalized Linear Models via Coordinate Descent. J. Stat. Softw. 36: 1–22.

Gabrieli, P., A. Smidler, and F. Catteruccia. 2014. Engineering the control of mosquito-borne infectious diseases. Genome Biol. 15: 535.

Georgopoulou, U., P. Tsitoura, M. Kalamvoki, and P. Mavromara. 2006. The protein phosphatase 2A represents a novel cellular target for hepatitis C virus NS5A protein. Biochimie. 88: 651–662.

Germi, R., J.-M. Crance, D. Garin, J. Guimet, H. Lortat-Jacob, R. Ruigrok, J.-P. Zarski, and E. Drouet. 2002. *Heparan sulfate*-Mediated Binding of Infectious Dengue Virus Type 2 and Yellow Fever Virus. Virology. 168: 162–168.

Giraldo-Calderón, G. I., S. J. Emrich, R. M. MacCallum, G. Maslen, S. Emrich, F. Collins, E. Dialynas, P. Topalis, N. Ho, S. Gesing, G. Madey, F. H. Collins, D. Lawson, P. Kersey, J. Allen, M. Christensen, D. Hughes, G. Koscielny, N. Langridge, E. L. Gallego, K. Megy, D. Wilson, B. Gelbart, D. Emmert, S. Russo, P. Zhou, G. Christophides, A. Brockman, I. Kirmitzoglou, B. MacCallum, T. Tiirikka, K. Louis, V. Dritsou, E. Mitraka, M. Werner-Washburn, P. Baker, H. Platero, A. Aguilar, S. Bogol, D. Campbell, R. Carmichael, D. Cieslak, G. Davis, N. Konopinski, J. Nabrzyski, C. Reinking, A. Sheehan, S. Szakonyi, and R. Wieck. 2015. VectorBase: An updated Bioinformatics Resource for invertebrate vectors and other organisms related with human diseases. Nucleic Acids Res. 43: D707–D713.

Gloria-Soria, A., A. Lima, D. D. Lovin, J. M. Cunningham, D. W. Severson, J. R. Powell, T. Able, and S. Vincent. 2018. Origin of a High-Latitude Population of *Aedes aegypti* in Washington, DC. Am. J. Trop. Med. Hyg. 98: 445–452.

Gomez-Machorro, C., K. E. Bennet, M. del Lourdes Munoz, and W. C. Black IV. 2004. Quantitative trait loci affecting dengue midgut infection barriers in an advanced intercross line of *Aedes aegypti*. Insect Mol. Biol. 13: 637–648.

Halstead, S. B., D. J. Gubler, and G. Kuno. 1994. Dengue and dengue hemorrhagic fever. Handb. Zoonoses. 8: 89–99.

Kotsakiozi, P., B. R. Evans, D. Ayala, C. Paupy, B. Kamgang, M. Mayanja, J. Lutwama, G. Le, A. Badolo, J. Pinto, C. A. Sousa, A. D. Troco, and J. R. Powell. 2018. Population structure of a vector of human diseases: *Aedes aegypti* in its ancestral range, Africa. Ecol. Evol. 8(16): 7835–7848.

Li, H., B. Handsaker, A. Wysoker, T. Fennell, J. Ruan, N. Homer, G. Marth, G. Abecasis, and R. Durbin. 2009. The Sequence Alignment/Map format and SAMtools. Bioinformatics. 25: 2078–2079.

Limjindaporn, T., J. Panaampon, and S. Malakar. 2017. Biochemical and Biophysical Research Communications Tyrosine kinase / phosphatase inhibitors decrease dengue virus production in HepG2 cells. Biochem. Biophys. Res. Commun. 483: 58–63.

Liu, Q., Y. Guo, J. Li, J. Long, B. Zhang, and Y. Shyr. 2012. Steps to ensure accuracy in genotype and SNP calling from Illumina sequencing data. BMC Genomics. 13 Suppl 8: S8.

Mairuhu, A. T. A., J. Wagenaar, D. P. M. Brandjes, and E. C. M. Van Gorp. 2004. Dengue: An arthropod-borne disease of global importance. Eur. J. Clin. Microbiol. Infect. Dis. 23: 425–433.

Morlais, I., N. Ponc, L. De Lutte, I. Nuisibles, and I. De Recherche. 2004. Intraspecific nucleotide variation in *Anopheles* gambiae: New insights into the biology of malaria vectors. 71: 795 – 802.

Morlais, I., and D. W. Severson. 2003. Intraspecific DNA variation in nuclear genes of the mosquito *Aedes aegypti*. Insect Mol Biol. 12: 631–639.

Nene, V., J. R. Wortman, D. Lawson, B. Haas, C. Kodira, Z. J. Tu, B. Loftus, Z. Xi, K. Megy, M. Grabherr, Q. Ren, E. M. Zdobnov, N. F. Lobo, K. S. Campbell, S. E. Brown, M. F. Bonaldo, J. Zhu, S. P. Sinkins, D. G. Hogenkamp, P. Amedeo, P. Arensburger, P. W. Atkinson, S. Bidwell, J. Biedler, E. Birney, R. V Bruggner, J. Costas, M. R. Coy, J. Crabtree, M. Crawford, B. Debruyn, D. Decaprio, K. Eiglmeier, E. Eisenstadt, H. El-Dorry, W. M. Gelbart, S. L. Gomes, M. Hammond, L. I. Hannick, J. R. Hogan, M. H. Holmes, D. Jaffe, J. S. Johnston, R. C. Kennedy, H. Koo, S. Kravitz, E. V Kriventseva, D. Kulp, K. Labutti, E. Lee, S. Li, D. D. Lovin, C. Mao, E. Mauceli, C. F. M. Menck, J. R. Miller, P. Montgomery, A. Mori, A. L. Nascimento, H. F. Naveira, C. Nusbaum, S. O'leary, J. Orvis, M. Pertea, H. Quesneville, K. R. Reidenbach, Y.-H. Rogers, C. W. Roth, J. R. Schneider, M. Schatz, M. Shumway, M. Stanke, E. O. Stinson, J. M. C. Tubio, J. P. Vanzee, S. Verjovski-Almeida, D. Werner, O. White, S. Wyder, Q. Zeng, Q. Zhao, Y. Zhao, C. a Hill, A. S. Raikhel, M. B. Soares, D. L. Knudson, N. H. Lee, J. Galagan, S. L. Salzberg, I. T. Paulsen, G. Dimopoulos, F. H. Collins, B. Birren, C. M. Fraser-Liggett, and D. W. Severson. 2007. Genome sequence of *Aedes aegypti*, a major arbovirus vector. Science. 316(5832): 1718–1723.

Ocampo, C. B., P. A. Caicedo, G. Jaramillo, R. Ursic Bedoya, O. Baron, I. M. Serrato, D. M. Cooper, and C. Lowenberger. 2013. Differential Expression of Apoptosis Related Genes in Selected Strains of *Aedes aegypti* with Different Susceptibilities to Dengue Virus. PLoS One. 8(4): e61187.

Ocampo, C. B., and D. M. Wesson. 2004. Population dynamics of *Aedes aegypti* from a dengue hyperendemic urban setting in Colombia. Am. J. Trop. Med. Hyg. 71: 506–513.

Oxitec. 2014. Dengue Fever: The fastest growing mosquito-borne disease. Abingdon, UK.

Perera-Lecoin, M., L. Meertens, X. Carnec, and A. Amara. 2013. Flavivirus entry receptors: An update. Viruses. 6: 69–88.

Serrato, I. M., P. A. Caicedo, Y. Orobio, C. Lowenberger, and C. B. Ocampo. 2017. Vector competence and innate immune responses to dengue virus infection in selected laboratory and field-collected *Stegomyia aegypti* (= *Aedes aegypti*). Med. Vet. Entomol. 31: 312–319.

Severson, D. W., V. Thathy, A. Mori, Y. Bang, and B. M. Christensen. 1995. Restriction Fragment Length Polymorphism Mapping of Quantitative Trait Loci for Malaria Parasite Susceptibility in the Mosquito *Aedes aegypti*. Genetics. 139(4): 1711–1717.

Smith, R. C., C. Kizito, J. L. Rasgon, and M. Jacobs-Lorena. 2013. Transgenic Mosquitoes Expressing a Phospholipase A2 Gene Have a Fitness Advantage When Fed *Plasmodium falciparum* - Infected Blood. PLoS One. 8(10): e76097.

Tables

Table 3.1 Primer pair sequences. These primers were designed to flank each of the three markers identified as phenotypically unique by the Lasso regression.

Marker	Forward Primer (5'→3')	Reverse Primer (5'→3')
AX-93240282	GCACCGAAGCCAAACAGTTC	CGATAACGGTCGTGGTCCAA
AX-93240283	AAACAAACCCCCGAAGTCGT	CTCTTACGCCGGATGTGTGA
AX-93220550	CTGCTTGTCCCATTCAGCCT	TCCGGATCTGTTTTGGACGG

Table 3.2 Accuracy of the three markers AX-93240282, AX-93240283, and AX-93220550) in predicting the dengue-susceptible (Cali-S) or refractory (Cali-MIB) phenotypes of *Aedes aegypti*. The mosquitoes used in this test are from the second selection of Cali-S and Cali-MIB mosquitoes, and were not the same ones used in the GWAS and GWES studies.

AX-93240282			
		Observed Phenotype	
		S	R
Marker Result	S	13	0
	R	0	8

AX-93240283			
		Observed Phenotype	
		S	R
Marker Result	S	13	4
	R	0	0

AX-93220550			
		Observed Phenotype	
		S	R
Marker Result	S	4	0
	R	6	5

Table 3.3 Genotype ratios from the first selection of dengue-refractory (Cali-MIB, n=17) and dengue-susceptible individuals (Cali-S, n=19). Results are from the three candidate marker variants (AX-93240282, AX-93240283, AX-93220550) identified as phenotypically associated through the stepwise LASSO regression.

AX-93240282		
	Cali-S	Cali-MIB
CC	0	15
CT	1	2
TT	18	0

AX-93240283		
	Cali-S	Cali-MIB
AA	0	15
AG	1	2
GG	18	0

AX-93220550		
	Cali-S	Cali-MIB
CC	17	0
CT	1	0
TT	1	17

Table 3.4 Sequence results from the accuracy testing of each of the three markers (AX-93240282, AX-93240283, and AX-93220550). The results are from the second selection of Cali-S (dengue-susceptible, S) and Cali-MIB (dengue-refractory, R) mosquitoes. Text colour represents the observed phenotype of the mosquito (green for S, red for R), while nucleotide shading represents the marker genotype of the mosquito (again, green for the S variant, red for the R variant).

AX-93240282	
Expected	
S SNP	---------T-----
R SNP	---------C-----
Observed	
Sample	Sequence
S4	CAATGCTAAG
S8	CAATGCTAAG
S11	CAATGCTAAG
S17c	CAATGCTAAG
S10c	CAATGCTAAG
S49c	CAATGCTAAG
S39c	CAATGCTAAG
S15	CAATGCTAAG
S42c	CAATGCTAAG
S35c	CAATGCTAAG
S2c	CAATGCTAAG
S13c	CCATGCTAAN
S16	CAATGCTAAG
25R	CAATGCCAAG
36R	CAATGCCAAG
40R	CAATGCCAAG
53R	CAATGCCAAG
73R	CAATGCCAAG
76R	CAATGCCAAG
97R	CAATGCCAAG
R4	CAATGCCAAG
51R	

AX-93240283	
Expected	
S SNP	----------G-------
R SNP	----------A-------
Observed	
Sample	Sequence
S4	GACTGATACGGATTC
S8	GACTGATACGGATTC
S11	GACTGATACGGATTC
S17c	GACTGATACGGATTC
S10c	GAGTGATACGGATTC
S49c	GACTGATACGGATTC
S39c	GANTGATACGGATTC
S15	GACTGATACGGATTC
S42c	GACTGATACGGATTC
S35c	GACTGATACGGATTC
S2c	GACTGATACGGATTC
S13c	GACTGATACGGATTC
S16	GACTGATACGGATTC
25R	
36R	GACTGATACGGATTC
40R	
53R	
73R	
76R	GACTGATACGGATTC
97R	GACTGATACGGATTC
R4	
51R	GACTGATACGGATTC

AX-93220550	
Expected	
S SNP	----------C-----
R SNP	----------T-----
Observed	
Sample	Sequence
S4	CCCATTTACTGACT
S8	CCCATTTACCGACT
S11	
S17c	CCCATTTACTGACT
S10c	CCCATTTACCGACT
S49c	
S39c	CCCATTTACCGACT
S15	CCCATTTACTGACT
S42c	CCCATTTACTGACT
S35c	CCCATTTACTGACT
S2c	
S13c	CCCATTTACTGACT
S16	CCCATTTACCGACT
25R	
36R	CCCATTTACTGACT
40R	
53R	CCCATTTACTGACT
73R	CCCATTTACTGACN
76R	
97R	CCCATTTACTGACT
R4	
51R	CCCATTTACTGACT

Table 3.5 Summary of Vector Base's effect prediction. Only variants predicted to have a high (start loss) or moderate (missense variant or in-frame insertion) impact were included here.

Variant phenotype	Gene	Strand	Transcript	Impact	Consequence	Chromosome	Nucleotide Position	Allele	Codons	Amino acids	Existing?
S	AAEL008911	1	RA	High	Start loss	2	12692530-12692530	T	atG/atT	M/I	No
				Moderate	Missense variant		12692545-12692545	T	caG/caT	Q/H	Yes
	AAEL007409	-1	RB		Missense variant		12665455-12665455	T	aGt/aAt	S/N	No
	AAEL007410	-1	RA		Missense variant		12636522-12636522	G	cAa/cCa	Q/P	Yes
					In-frame insertion		12636514-12636514	TGG	-/CCA	-/P	No
			RB		Missense variant		12636522-12636522	G	cAa/cCa	Q/P	Yes
					In-frame insertion		12636514-12636514	TGG	-/CCA	-/P	No
			RC		Missense variant		12636522-12636522	G	cAa/cCa	Q/P	Yes
					In-frame insertion		12636514-12636514	TGG	-/CCA	-/P	No
			RD		Missense variant		12636522-12636522	G	cAa/cCa	Q/P	Yes
					In-frame insertion		12636514-12636514	TGG	-/CCA	-/P	No
R	AAEL021595	1	RA		Missense variant		12663631-12663631	C	gTt/gCt	V/A	No
							12663802-12663802	C	gAa/gCa	E/A	
							12664012-12664012	A	gTg/gAg	V/E	

							12664056-12664056	G	Aac/Gac	N/D	
							12663606-12663606	A	Tgc/Agc	C/S	
							12664041-12664041	T	Acg/Tcg	T/S	Yes
	AAEL007409	-1	RB		Missense variant		12665375-12665375	T	Ttt/Att	F/I	No
							12665405-12665405	T	Cta/Ata	L/I	
							12665459-12665459	A	Ccc/Tcc	P/S	
							12665635-12665635	G	aAc/aCc	N/T	
							12666478-12666478	T	cCa/cAa	P/Q	
							12678666-12678666	T	aGa/aAa	R/K	
							12678867-12678867	G	gTc/gCc	V/A	
							12678890-12678890	C	gaT/gaG	D/E	Yes

Figures

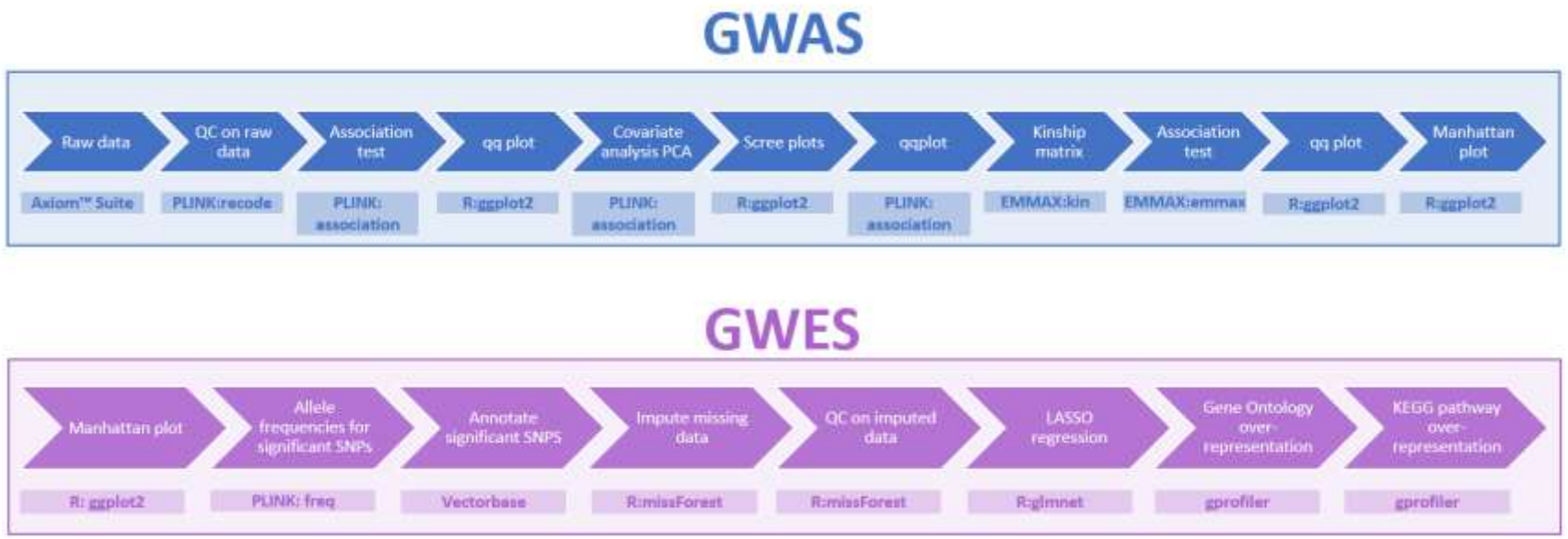

Figure 3.1 Data processing and bioinformatics workflows for the genome wide association study (GWAS), in blue, and the genowide wide epistatis study (GWES), in purple.

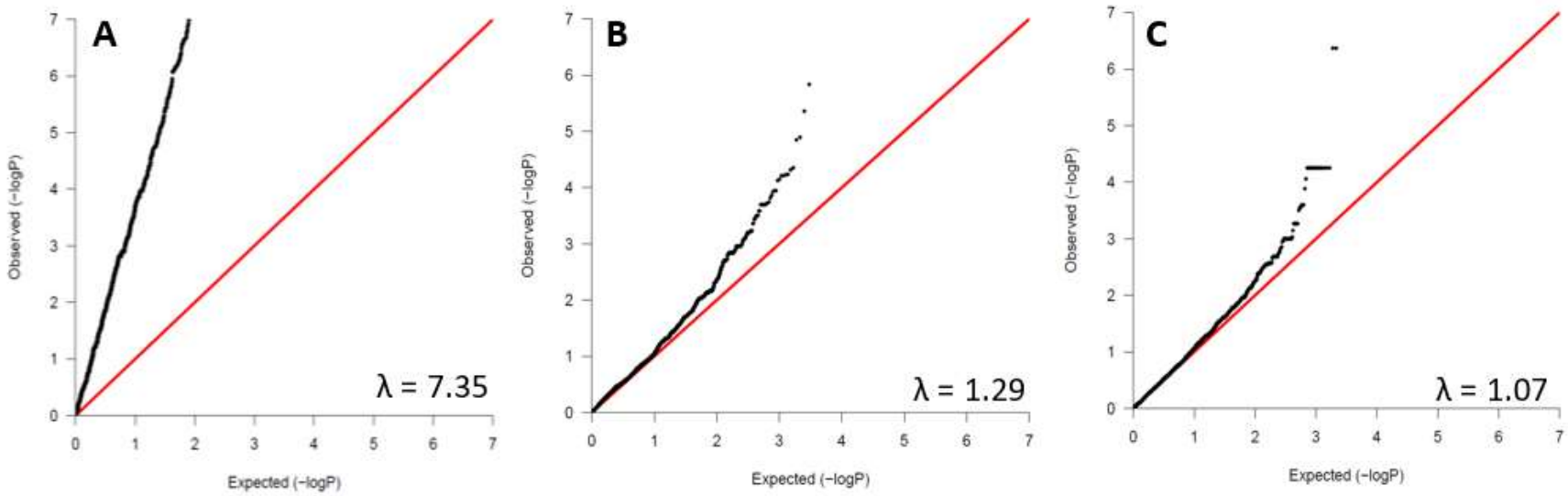

Figure 3.2 Q-Q plots of all three association tests created using R v. 3.4.3. The red line is the 1:1 relationship between the expected and observed data, while the black dots are our data. Panel A shows the association test without any correction for population structure, B depicts the data structure after co-variate correction, and panel C is the structure after co-variate and kinship adjustment. The genomic inflation factor, λ (ratio of observed: expected values) is displayed on the bottom right hand corner of each plot.

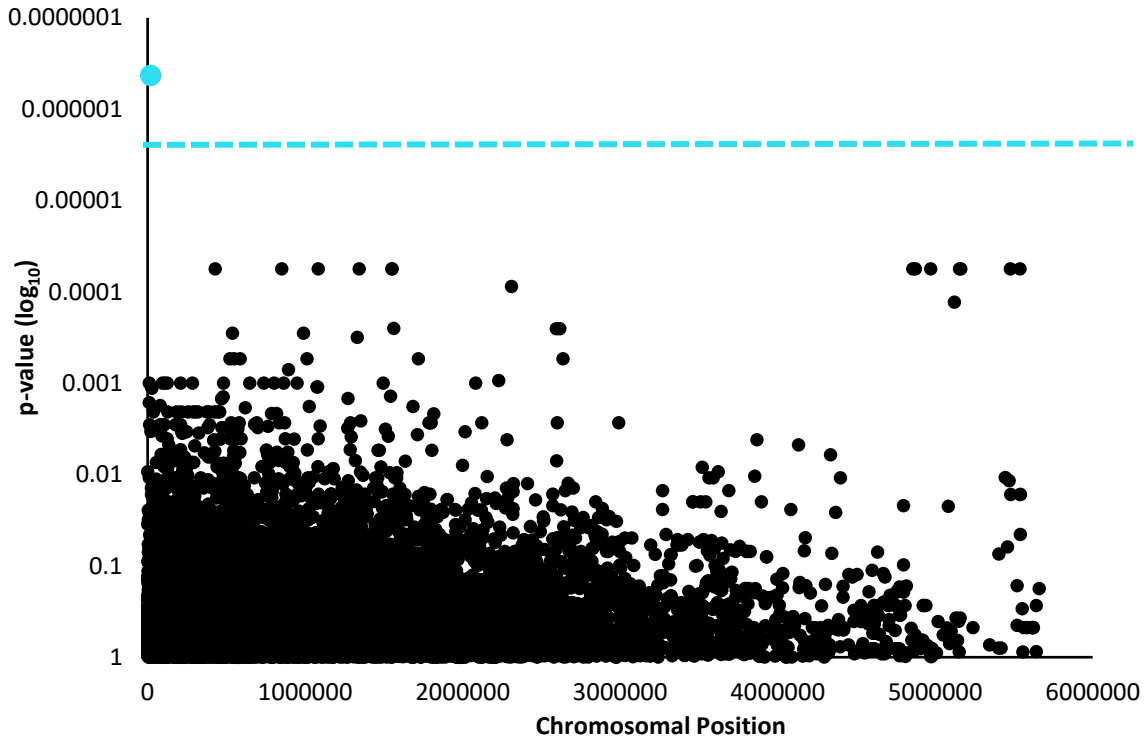

Figure 3.3 Manhattan plot of the association test after population correction. The plot was created using R v. 3.4.3. Each dot represents one of the 15,084 SNPs analyzed. Black dots (n=15,082) are statistically non-significant (p-value ≥3.31e^{-6}), while teal dots (n=2) are statistically significant (p-value <3.31e-6). The teal line depicts the p-value significance cut-off of 3.31e^{-6}.

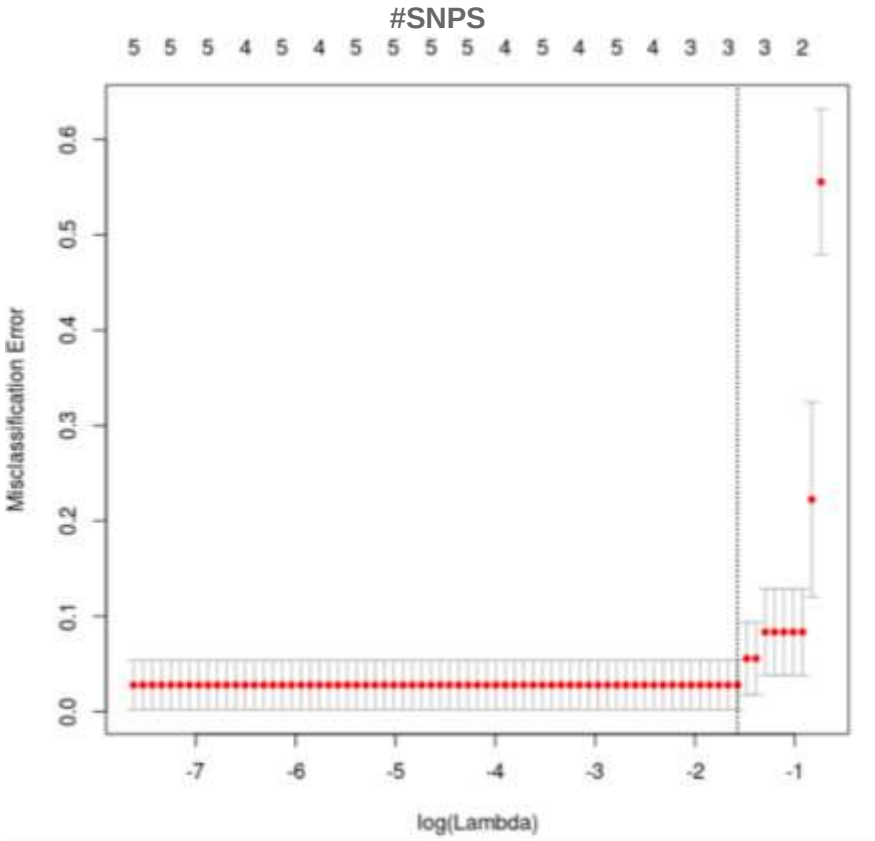

Figure 3.4 Cross-validation misclassification error rates (with standard error bars) of the Lasso logistic regression model. The model was tuned using λ (log-scale, x-axis). The minimum misclassification error was reached when the log of λ is -1.61, incorporating three SNPs.

Connecting Statement 3

In Chapters 2 and 3 we identified genes that were differentially expressed between Cali-MIB and Cali-S mosquitoes, as well as variants significantly associated with these phenotypes. The midgut of *Aedes aegypti* is much more dynamic and complex than its genetic components. As a mosquito grows and develops, it forms its own gut microbiota from its environment, diet and maternal line. These microorganisms form an interconnected community that can interact directly with other gut constituents, including pathogens such as dengue viruses. Secondary metabolites produced by *Ae. aegypti* gut microbiomes have been shown to alter dengue titres, and thus the overall vector competence of the mosquito. As such, in Chapter 4, we compare the microbiomes of our Cali-S and Cali-MIB mosquitoes, using 16S rRNA sequencing to identify different microbes that might contribute to the susceptible or refractory phenotype.

Chapter 4. The composition of midgut bacteria in *Aedes aegypti* (Diptera: Culicidae) that are naturally susceptible or refractory to dengue viruses

A modified version of Chapter 4 has been published as: Coatsworth, H., Caicedo, P., Van Rossum, T., Ocampo, O., and Lowenberger, C. 2018. The composition of midgut bacteria in Aedes aegypti (Diptera: Culicidae) that are naturally susceptible or refractory to dengue viruses. Journal of Insect Science. 18(6): https://doi.org/10.1093/jisesa/iey118.

Author Contributions

Carl Lowenberger and Heather Coatsworth conceived the study. Paola Caicedo collected the samples, and Heather Coatsworth and Iman Baharmand prepared the samples for analysis. Thea Van Rossum assisted Heather Coatsworth in creating a bioinformatics pipeline. Heather Coatsworth completed all bioinformatic analyses. Heather Coatsworth and Carl Lowenberger wrote the manuscript. All authors (Heather Coatsworth, Paola Caicedo, Thea Van Rossum, Carl Ocampo and Carl Lowenberger) reviewed the manuscript.

4.1. Abstract

The composition, abundance, and diversity of midgut bacteria in mosquitoes can influence pathogen transmission. We used 16S rRNA microbiome profiling to survey midgut microbial diversity in pooled samples of lab colonized dengue-refractory, Cali-MIB, and dengue-susceptible, Cali-S *Aedes aegypti*. The 16S rRNA sequences from the sugar fed midguts of adult females clustered to 63 amplicon sequence variants (ASVs), primarily from Proteobacteria, Firmicutes, Flavobacteria, and Actinobacteria. An average of five ASVs dominated the midguts, and most ASVs were present in both Cali-MIB and Cali-S midguts.

No differences in abundance were noted at any phylogenetic level (Phylum, Class, Order, Family, Genus) by analysis of composition of microbiome (ANCOM) (w=0). No community diversity metrics were significantly different between refractory and susceptible mosquitoes. These data suggest that phenotypic differences in the susceptibility to

dengue virus between Cali-MIB and Cali-S are not likely due to major differences in midgut bacterial communities.

Keywords: vector competence, microbiome, midgut infection barrier

4.2. Introduction

Tripartite interactions between host, pathogens, and vectors are extremely important in determining the ultimate outcome of pathogen transmission and host disease. A variety of studies has demonstrated the effects of genetic variation, gene expression, and the environment on vector susceptibility to pathogens at both individual and population levels (Palmer et al. 2018). Many of these intriguing relationships have been studied in mosquito systems due to their importance in the field of human health, as vectors for pathogens that cause some of the world's most prevalent and widespread diseases such as malaria, dengue, chikungunya, Zika, filariasis, and West Nile fever.

Symbiotic relationships between individuals and their microbiomes have long been known. These relationships have spurred interest into microbiome research as a possible primary and secondary driver of disease and pathogen susceptibility. These interactions manifest in individuals in one of two possible manners: obligate systems, typically older, more evolutionary stable systems where bacterial presence is fundamental for systemic function, or non-obligate systems, typically newer, more diverse and flexible, where bacterial presence is determined by extrinsic factors such as the environment, or intrinsic variable factors such as familial lineage and mating partners. As with most symbiotic relationships, these close interactions can increase (nutritionally supplement), impede (increase pathogen susceptibility) or remain neutral with regards to their hosts through resource competition, production of secondary metabolites and immune priming (Dennison et al. 2014).

Mosquito-microbiome interactions may change a mosquito's susceptibility to pathogen invasion; increasing bacterial diversity and abundance tends to decrease susceptibility to pathogens (Dennison et al. 2014). Bacterial symbionts that are new in mosquitoes, seem to increase resistance in *Ae. aegypti* to dengue virus (DENV). While the exact mechanisms are not known, this could be accomplished by promoting the defensive abilities of the mosquito via increased antimicrobial peptides (*Proteus sp.*) and

reactive oxygen species production (*Wolbachia sp.*) (Pan et al. 2012, Ramirez et al. 2012, Rancès et al. 2012). These *Ae. aegypti* – DENV studies have thus far been conducted solely on long established lab reared colonies of susceptible mosquitoes. In contrast, we aimed to investigate these symbiotic relationships in naturally susceptible (Cali-S) and refractory (via a midgut infection barrier (MIB), Cali-MIB) mosquitoes to determine the relationship between mosquito microbiota and vector competence. These two strains originated from field collected mosquitoes in the city of Cali, Colombia where approximately 30% of field collected mosquitoes are refractory to DENV-2 (Ocampo and Wesson 2004b, Caicedo et al. 2013b). Subsequent studies hypothesized that the DENV-susceptible or -refractory phenotype was determined in the midgut of these mosquitoes within 48 hours of blood being ingested by the mosquitoes (Ocampo et al. 2013, Serrato, Caicedo, Lowenberger, et al. 2017, Caicedo et al. 2018). Although microbiota may exist in a variety of mosquito tissues and organs (salivary glands, ovaries, Malpighian tubules, and midgut), we examined only the gut microbiome, which serves as the first barrier to virus infection, to determine if changes in abundance or diversity of the microbiota contributed to the differential susceptibility to DENV between the Cali-MIB and Cali-S phenotypes.

Metagenomics projects typically investigate the diversity and presence of a variety of symbionts, including (but not limited to) archaea, bacteria and various eukaryotic species. Due to their previously identified effects in mosquito-pathogen interactions (Gonzalez-Ceron et al. 2003, Wang et al. 2009, Gusmão et al. 2010, Cirimotich, Ramirez, et al. 2011, Chauhan, Behura, DeBruyn, et al. 2012, Pan et al. 2012, Ramirez et al. 2012), bacteria were chosen as the focus of this study. Eukaryotes such as yeast and fungi have been isolated from mosquitoes, but their effects remain unknown, and they were excluded from analysis. Non-culture dependent techniques were used to gain bacterial abundance and diversity values without technique- or medium-related biases. Sequencing was completed on the hyper-diverse 16S V4-V5 region using the Illumina platform for its superior read depth (at the cost of read length), to tease apart rare operational taxonomic units (OTUs). Midgut bacterial diversity and composition were compared within and between Cali-S and Cali-MIB mosquitoes to determine if differences in microbiota composition could explain differences in susceptibility to DENV.

4.3. Methods

4.3.1. Ethics statement

All protocols were approved by the Centro Internacional de Entrenamiento e Investigaciones Médicas (CIDEIM) institutional review committee for research in animals (1021), governed by law 84 (1989) and resolution 8430 (1993) of the National Ministry of Agriculture in Colombia.

4.3.2. Mosquito rearing and maintenance

Cali-S and Cali-MIB strains of *Ae. aegypti* were selected from field collected larvae and pupae from artificial larval habitats in five locations in and around the city of Cali, Colombia (Caicedo et al. 2013b). Strains were selected after exposure to DENV-2 using an isofamily selection technique, where only eggs from verified susceptible or refractory females were hatched (Ocampo and Wesson 2004b, Caicedo et al. 2013b, Ocampo et al. 2013). $F_{<30}$ mosquitoes were maintained under standard laboratory conditions: 28 ± 2ºC, 70% relative humidity, and a 12:12 hour light: dark cycle. Larvae were maintained at a density of 300 larvae/2 L of distilled water in plastic pans and were fed daily with 2mL of a stock solution (8g/400mL) of beef liver (DIFCO, Becton, Dickinson and Company, Franklin Lakes, NJ). Adults were fed with 10% sugar solution ad libitum.

4.3.3. Sample preparation

Four days after emergence, sugar fed Cali-S and Cali-MIB females were surface sterilized individually through a series of four washes, each performed in a new 1.5mL microcentrifuge tube. First, each female was placed in a 70% ethanol bath for 5 mins, followed by 3 mins of vortexing, then a 1-min nuclease free water bath, followed by 1 min of vortexing, a second 1 min 70% ethanol bath, followed by 1 min of vortexing, and a last 1-min nuclease free water bath, followed by 1 min of vortexing. Midguts were dissected in 30µL of sterilized phosphate buffer solution (PBS). Midguts (n=80) were pooled into groups of 5 each (8 susceptible pools, S1-8, and 8 refractory pools, R1-8) (n=16). A negative control of 10 µL of PBS used for dissections, and a positive control of 10 µL of a pure *Escherichia coli* culture were also created. DNA was extracted from each sample using Qiagen's DNeasy Blood and Tissue Kit (Hilden, Germany) following the

manufacturer's instructions for the extraction of bacteria. DNA concentration was evaluated using a Qubit® 2.0 Fluorometer (ThermoFisher Scientific, Waltham, MA, USA). A portion of the DNA obtained from each sample was used in a polymerase chain reaction (PCR) with two conserved 16S primers (S-D-Bact-0564-a-S-15: 5′-AYT GGG YDT AAA GNG-3′, and S-D-Bact-0785-b-A-18: 5′-TAC NVG GGT ATC TAA TCC-3′ (Klindworth et al. 2013) to verify that bacterial DNA had been extracted from each sample pool. Each PCR contained: 6 µL of nuclease free water, 10 µL of 5 Prime Hot Master Mix (5 Prime, Gaithersburg, MD, USA), 2 µL of 25 µM forward primer, 2 µL of 25 µM reverse primer, and 5 µL of the template DNA. PCRs were performed in duplicate on a PTC-200 Peltier Thermocycler (Bio-Rad, Hercules, CA, USA) with the following program: hot start of 94°C for 3mins, 35 cycles of 94°C for 45s, 45°C for 60s, and 72°C for 90s, with a final extension of 72°C for 10mins. Any sample with a concentration higher than 20 ng/µL was considered acceptable for sequencing.

4.3.4. Amplicon library preparation and sequencing

All DNA was sequenced at MR DNA (Shallowater, TX, USA) using an Illumina MiSeq platform (San Diego, CA, USA) to sequence the bacterial 16S rRNA gene. Briefly, the V4-V5 hyper variable region was targeted via PCR (see primers in Table 4.1), adding treatment specific barcodes to each sample. The PCR was performed using the HotStartTaq Plus Master Mix Kit (Qiagen, Hilden, Germany) under the following conditions: 94°C for 3mins, 28 cycles of 94°C for 30sec, 53°C for 40sec and 72°C for 1min, after which a final elongation step at 72°C for 5min was performed. After amplification, PCR products were checked for relative intensity on a 2% agarose gel. Samples were then purified using calibrated Agencourt AMPure XP beads (Brea, CA, USA). A Nextera DNA Sample Preparation Kit was then used (Illumina, CA, USA) to prepare the samples. Paired end (2x300bp) sequencing was performed on a MiSeq platform by loading pooled samples (at 12pM) onto a 600 cycle v3 reagent cartridge (Illumina, CA, USA).

4.3.5. Amplicon data analysis

(DADA2) (Callahan et al. 2016) and Quantitative Insights Into Microbial Ecology 2 (QIIME2) (release 2018.8) (Caporaso et al. 2010) were used to analyze all resultant FASTQ files obtained from MR DNA (Shallowater, TX, USA). First, using QIIME2, FASTQ

files were demultiplexed (*cutadapt demux-paired*), and the adapters were trimmed off (*cutadapt trim-paired*) (Martin 2011). Next, DADA2 (v1.8.0) was used to create read quality profiles, and reads were truncated to avoid low quality scores (>240bp for forward, >200bp for reverse reads) (*maxN=0, truncQ=2, maxEE=2*). Error rates were then learned (*err*) and dereplication was completed (*derepFastq*). The *dada* core sample inference algorithm was then applied to the filtered and dereplicated forward and reverse data. Reads were merged (*mergePairs*) with a minimum overlap of 12bp. An amplicon sequence variant (ASV) table was made (*makeSequenceTable*) for all 16 (8 Refractory and 8 Susceptible) samples, and chimeric samples were removed (*removeBimeraDenovo*). Silva (v132) (Callahan 2018) was used as the taxonomic training set (via *assignTaxonomy* and *addSpecies*). The feature table, representative fasta sequences, taxonomy data and sample metadata were then imported into QIIME2 (*tools import*).

In order to complete downstream diversity and composition analyses, rooted and unrooted phylogenetic trees were created (*phylogeny align-to-tree-mafft-fasttree*) in QIIME2. Samples with a sampling depth of less than 1000 sequences/sample were removed to retain an acceptable sequence coverage. ASVs with an abundance of less than 0.01% were also removed. Alpha rarefraction (McDonald et al. 2012) and diversity (Faith's phylogenetic diversity, Pielou's evenness, Shannon and species richness) (Kruskal and Wallis 1952, McKinney 2010), as well as beta diversity (Jaccard, unweighted unifrac, weighted unifrac and Bray-Curtis) (Anderson 2001) were calculated. Taxa were grouped by abundance (McKinney 2010, McDonald et al. 2012), and analysis of composition of microbiome (ANCOM) was used to test for differential abundance across multiple taxonomic levels (Phylum, Class, Order, Family, and Genus) (Mandal et al. 2015). Linear discriminant analysis effect size (LEfSe) was used to detect potential phenotype-specific bacterial markers (Segata et al. 2011).

4.4. Results

4.4.1. Analyzing negative and positive controls

As expected, our negative PBS control did result in some bacterial reads (Salter et al. 2014), however, the abundance of these reads was substantially lower than those obtained from any of our samples or our positive control. To control for contamination, the read counts for the negative control were subtracted from all sample counts (which

resulted in the elimination of negative control specific ASVs). Furthermore, the composition of bacteria in the negative control was different than the ASVs noted in any of our experimental samples or in our positive control. Our positive control primarily showed one highly abundant *Shigella* ASV. As 16S sequencing is often unable to differentiate between *Shigella* and *Escherichia coli* species (Khot and Fisher 2013), we completed an *Escherichia* and *Shigella* specific PCR on the positive control DNA which verified that our positive control was indeed *E. coli* bacterial DNA.

4.4.2. Bacterial abundance and community composition

After quality filtering, samples R1, R2, R5 and S2 were removed due to low depth of sampling (≤1000 sequences/sample), while the remaining samples were rarefied to a sampling depth of 1,333 sequences. Chimeric filtering removed 13% of sequences. The remaining sequences clustered into 63 ASVs from 6 phyla, 9 classes, 13 orders, 19 families, and 27 genera (some classified further into sub-species), although only 21 ASVs had an overall abundance greater than 1%. Most of the sequences were from Proteobacteria (40.5%), comprised of Alphaproteobacteria (22%), Betaproteobacteria (10%), and Gammaproteobacteria (8.5%), then Flavobacteria (23%), Bacilli (21%), and Actinobacteria (8.5%) (Figure 4.1). As 16S sequencing is unable to differentiate between *Swaminathania* and *Asaia*, and *Asaia* sp. are commonly associated with insect guts, it is likely that the *Swaminathania* ASVs observed here are actually *Asaia* sp. (Deutscher et al. 2018).

An average of five ASVs dominated both the Cali-S and Cali-MIB midguts (≥5% total abundance). Actinobacteria and Bacilli (Bacillales) dominated the susceptible midguts, while Alphaproteobacteria and Flavobacteriia made up most bacteria in refractory midguts. The majority of ASVs were present in both Cali-S and Cali-MIB midguts. Only a few low abundance OTUs were exclusively found in either phenotype.

The analysis of composition of microbiome (ANCOM) tests at all levels of analysis (Phylum, Class, Order, Family, and Genus) did not yield any significantly different results (w=0). The linear discriminant analysis effect size (LEfSe) did not identify any taxonomic biomarkers specific to the Cali-MIB or Cali-S phenotype ($p \geq 0.00005$) at different hierarchical levels.

4.4.3. Alpha and beta diversity metrics

In all measured alpha diversity metrics (Faith's phylogenetic diversity, species richness, Pielou's evenness, and Shannon index), no significant differences were found between Cali-MIB and Cali-S mosquitoes (p-value ≥ 0.05, Figure 4.2). All alpha rarefraction plots reached saturation. Similarly, no significant differences were observed between Cali-S and Cali-MIB mosquitoes in terms of beta diversity metrics (p-≥0.05, Table 4.2).

4.5. Discussion

Overall, we found a low number of dominant bacterial ASVs present in each midgut (average of five), a trend that has been observed in other midgut composition studies (Yun et al. 2014, Ngo et al. 2016, Muturi et al. 2017). No diversity differences were found to exist between Cali-S and Cali-MIB mosquitoes using any of the metrics examined here, nor were there any significant differences between the abundance of bacteria in Cali-S and Cali-MIB midguts, identified both by LEfSe, and via ANCOM tests completed in QIIME2. It is possible that these differences are biologically relevant yet masked by the lack of difference in overall inter-phenotype composition and diversity.

In Cali-S, bacteria from the phylum Firmicutes, and Actinobacteria were high in abundance. In other studies their presence was noted in mosquitoes treated with low doses of *Bacillus thuringiensis* (Demisse 2013), and species from Firmicutes have been shown to inhibit gut algal growth (Engel and Moran 2017). Firmicutes bacteria are quite common Gram-positive anaerobic insect gut symbionts, although their role in the midgut is largely unknown. Bacteria from the order Burkholderiales were also abundant in Cali-S midguts. These are usually observed in hemipterans such as kissing bugs (Triatominae species) and bean bugs (*Riptortus spp*.), and contribute to the detoxification of insecticides, enabling these insects to resist or tolerate insecticides (Kikuchi et al. 2012). Two transcriptome studies identified multiple genes tied to insecticide resistance that were highly expressed in Cali-S but not in Cali-MIB mosquitoes, an observation that may be indirectly linked to the presence of Burkholderiales species in Cali-S midguts. Lastly, Actinobacteria were highly abundant in the Cali-S midgut. Actinobacteria have been characterized in beetles and hemipterans as important nutrient processors, aiding in the

digestion of sugar and blood meals (Zucchi et al. 2012). Actinobacteria are part of the core microbiota of *Ae. aegypti* (David et al. 2016).

In Cali-MIB mosquitoes, higher numbers of ASVs were observed in Flavobacteriaceae. Flavobacteria are extremely ubiquitous Gram-negative mosquito gut symbionts, most likely due to their wide range of metabolic activities (Terenius et al. 2012, Yadav et al. 2018). They have no reported links to vector competence in mosquitoes, but are a common larval food source (Chen et al. 2014). They are commonly found in lab reared mosquito guts, and can be transferred by transstadial means (Boissière et al. 2012, Chen et al. 2015). Due to their high abundance across a variety of mosquito genera, a variety of Flavobacteria have been proposed as a biological control technique, manipulating them to express and deliver *Bacillus thuringiensis* proteins (Chen et al. 2014, 2015).

To complete functional tests, studies have traditionally used retraction experiments to render the gut aseptic, and reintroduce a single species of bacteria (Ramirez et al. 2012, Jupatanakul et al. 2014, Koskella et al. 2017). The introduction of individual species identified through culture dependant methods did not significantly change the vector competence of Cali-MIB or Cali-S mosquitoes (Molina-Henao and Ocampo unpublished). Although this gives us useful information about the putative role of a single bacterial species, it negates the large interplay between and among all members of the midgut microbiota (Koskella et al. 2017). We could use a similar technique to functionally assess abundance trends we noted but understanding the indirect effects of individual bacterial species and the rest of the microbiome would be theoretically challenging. Future studies should aim for a more inclusive metagenomic technique, giving a more holistic view of all microbiota (including fungi, protozoans and viruses), rather than solely bacteria.

Other studies have shown that mosquitoes from different geographical localities harbour differ microbiomes (Ngo et al. 2016, Muturi et al. 2017). When mosquitoes from different localities were raised in a laboratory environment, there were no differences in their gut microbiomes, suggesting environmental factors as the primary driver in mosquito gut microbiome differences (Dickson et al. 2017). Multiple studies in mosquitoes and other insects have, however, shown that microbiota contribute to vector competence, even within lab settings (Joyce et al. 2011, Ramirez et al. 2012, Jupatanakul et al. 2014, Muturi

et al. 2017). This dichotomy could persist due to the intrinsic differences in physiology between different susceptible and refractory strains.

Although bacterial species associated with changes in vector competence for viruses (*Proteus* sp., *Chromobacterium sp., Pseudomonas rhodesiae*, *Enterobacter ludwigii*, and *Vagococcus salmoninarium*) (Dong et al. 2011, Joyce et al. 2011, Apte-Deshpande et al. 2012, Boissière et al. 2012, Ramirez et al. 2012, Jupatanakul et al. 2014) were not detected in any of the midgut samples in this study, some bacterial ASVs from the same family (Enterobacteriaceae) were found. This suggests that the Cali-MIB refractory phenotype does not stem from previously characterized microbe dependant factors.

As observed in Figure 4.1., intra phenotype variability in midgut microbiota was larger than the variability observed between phenotypes. Despite this intra-phenotype variability, the diversity captured within this study seemed to be sufficient, as all diversity index rarefaction curves were at or near saturation. The large disparity between samples observed in this study may have been due, in part, to the make-up of the refractory samples. While the selection process allows for the creation of 100% susceptible lines, only 50% of the Cali-MIB line are 100% refractory to dengue. This means that half of the refractory samples in this study are most likely susceptible in nature.

All the compositional differences examined in this study are based on sugar fed mosquitoes. There seems to be evidence suggesting that the microbiota composition changes upon blood feeding, as there is an increase in bacterial abundance, which could result in cases of competition among bacterial species (Gaio et al. 2011, Jupatanakul et al. 2014, Coon et al. 2016). As a blood meal provides a different, more proteinaceous nutritional profile, midgut bacterial abundances post blood feeding would likely be much different than those observed here. DENV moves from the bolus to enter midgut epithelial cells as early as 8 hours after ingestion (Junjhon et al. 2014), which may be too short a period for significant proliferation of bacteria to affect DENV viability directly. As a result, the holo-immune concept has been proposed (Dheilly 2014), whereby bacteria exert indirect effects on viral replication and dissemination mediated through host innate immunity, secondary metabolite production, resource competition, or via the secretion of miRNAs. Blood-feeding may be an important trigger to re-structure the gut microbiota, which we were unable to detect in this study. Further research investigating the gut

microbiome through blood and virus feeding, as well as basal metabolomics studies to assess the characteristics of the midgut environment, would augment our current understanding of differences in Cali-S and Cali-MIB midguts.

Microbiome studies are important tools that help us identify communities and highlight differences between microbiomes and the environments that support microbial proliferation. These studies have helped us identify potential biological control agents, novel RNAi delivery systems, and prospective anti-viral compounds. The results from this study help augment our current understanding of mosquito midgut microbiomes, and aid in curating microbiome data from susceptible and refractory *Ae. aegypti* phenotypes with the aim of identifying factors that might shift the balance towards mosquitoes that do not transmit arboviruses to humans.

4.6. Acknowledgements

The authors would like to thank the entire Vector Biology and Control team at CIDEIM for training and technical support, as well as Iman Baharmand (SFU) for technical assistance. This research was funded in part by the Departamento Administrativo de Ciencia, Tecnología e Innovación (http://www.colciencias.gov.co/), Contract 2229-519-28645 to CB, and a Discovery Grant to CL (RGPIN261940) from the Natural Sciences and Engineering Research Council of Canada (http://www.nserc-crsng.gc.ca/).

4.7. Data availability

The raw sequence data has been uploaded onto NCBI's SRA database (SRA Accession: SRP149364, Bio Project ID: PRJNA473810).

4.8. References

Anderson, M. J. 2001. A new method for non-parametric multivariate analysis of variance. Austral Ecol. 26: 32–46.

Apte-Deshpande, A., M. Paingankar, M. D. Gokhale, and D. N. Deobagkar. **2012**. *Serratia odorifera* a midgut inhabitant of aedes aegypti mosquito enhances its susceptibility to dengue-2 virus. PLoS One. 7(7): e40401.

Boissière, A., M. T. Tchioffo, D. Bachar, L. Abate, A. Marie, S. E. Nsango, H. R. Shahbazkia, P. H. Awono-Ambene, E. A. Levashina, R. Christen, and I. Morlais. **2012**. Midgut microbiota of the malaria mosquito vector *Anopheles gambiae* and interactions with *Plasmodium falciparum* infection. PLoS Pathog. 8(5): 1–12.

Caicedo, P. A., I. M. Serrato, S. Sim, G. Dimopoulos, H. Coatsworth, C. Lowenberger, and C. B. Ocampo. **2018**. Immune response-related genes associated to blocking midgut dengue virus infection in *Aedes aegypti* strains that differ in susceptibility. Insect Sci. 26: 635–648.

Caicedo, P., O. Barón, M. Pérez, N. Alexander, C. Lowenberger, and C. Ocampo. **2013**. Selection of *Aedes aegypti* (Diptera: Culicidae) strains that are susceptible or refractory to Dengue-2 virus. Can. Entomol. 145: 273–282.

Callahan, B. 2018. Silva taxonomic training data formatted for DADA2.

Callahan, B. J., P. J. Mcmurdie, M. J. Rosen, A. W. Han, A. J. A. Johnson, and S. P. Holmes. **2016**. DADA2 : High-resolution sample inference from Illumina amplicon data. Nat. Methods. 13(7): 581-583.

Caporaso, J. G., J. Kuczynski, J. Stombaugh, K. Bittinger, F. D. Bushman, E. K. Costello, N. Fierer, A. G. Peña, J. K. Goodrich, J. I. Gordon, G. a Huttley, S. T. Kelley, D. Knights, J. E. Koenig, R. E. Ley, C. a Lozupone, D. Mcdonald, B. D. Muegge, M. Pirrung, J. Reeder, J. R. Sevinsky, P. J. Turnbaugh, W. a Walters, J. Widmann, T. Yatsunenko, J. Zaneveld, and R. Knight. **2010**. QIIME allows analysis of high- throughput community sequencing data. Nat. Publ. Gr. 7: 335–336.

Chauhan, C., S. Behura, B. DeBruyn, D. Lovin, B. Harker, C. Gomez-Machorro, A. Mori, J. Romero-Severson, and D. Severson. **2012**. Comparative Expression Profiles of Midgut Genes in Dengue Virus Refractory and Susceptible *Aedes aegypti* across Critical Period for Virus Infection. PLoS One. 7(10): e47350.

Chen, S., M. Bagdasarian, and E. D. Walker. **2015**. *Elizabethkingia anophelis*: Molecular manipulation and interactions with mosquito hosts. Appl. Environ. Microbiol. 81: 2233–2243.

Chen, S., M. G. Kaufman, M. L. Korir, and E. D. Walker. **2014**. Ingestibility, digestibility, and engineered biological control potential of *Flavobacterium hibernum*, isolated from Larval mosquito habitats. Appl. Environ. Microbiol. 80: 1150–1158.

Cirimotich, C. M., J. L. Ramirez, and G. Dimopoulos. **2011**. Native microbiota shape insect vector competence for human pathogens. Cell Host Microbe. 10: 307–310.

Coon, K. L., M. R. Brown, and M. R. Strand. **2016**. Gut bacteria differentially affect egg production in the anautogenous mosquito *Aedes aegypti* and facultatively autogenous mosquito *Aedes atropalpus* (Diptera: Culicidae). Parasites and Vectors. 9: 1–12.

David, M. R., L. Maria, A. Carolina, P. Vicente, and R. Maciel-de-freitas. **2016**. Effects of environment , dietary regime and ageing on the dengue vector microbiota : evidence of a core microbiota throughout *Aedes aegypti* lifespan. Mem Inst Oswaldo Cruz. 111: 577–587.

Demisse, D. D. 2013. Influence of Nutrients and Integrated Mosquito Management Tactics on Mosquitoes and Their Habitat Microbiomes.

Dennison, N. J., N. Jupatanakul, and G. Dimopoulos. **2014**. The mosquito microbiota influences vector competence for human pathogens. Curr. Opin. Insect Sci. 3: 6–13.

Deutscher, A. T., C. M. Burke, A. E. Darling, M. Riegler, O. L. Reynolds, and T. A. Chapman. **2018**. Near full-length 16S rRNA gene next-generation sequencing revealed *Asaia* as a common midgut bacterium of wild and domesticated Queensland fruit fly larvae. Microbiome. 6: 1–22.

Dheilly, N. M. 2014. Holobiont – Holobiont Interactions : Redefining Host – Parasite Interactions. PLoS Pathogens. 10(7): 1–4.

Dickson, L. B., A. Ghozlane, S. Volant, C. Bouchier, L. Ma, A. Vega-Rúa, I. Dusfour, D. Jiolle, C. Paupy, M. N. Mayanja, A. Kohl, J. J. Lutwama, V. Duong, and L. Lambrechts. **2017**. Diverse laboratory colonies of *Aedes aegypti* harbor the same adult midgut bacterial microbiome. Parasites and Vectors. 11(1): 207.

Dong, Y., S. Das, C. Cirimotich, J. A. Souza-Neto, K. J. McLean, and G. Dimopoulos. **2011**. Engineered *Anopheles* immunity to *Plasmodium* infection. PLoS Pathog. 7(12): e1002458.

Engel, P., and N. A. Moran. **2017**. The gut microbiota of insects – diversity in structure and function. FEMS Microbiol. Rev. 37(5): 699–735.

Gaio, A., D. Gusmão, A. Santos, M. Berbert-Molina, P. Pimenta, and F. Lemos. **2011**. Contribution of midgut bacteria to blood digestion and egg production in *Aedes aegypti* (diptera: culicidae) (L.). Parasit. Vectors. 4: 105.

Gonzalez-Ceron, L., F. Santillan, M. H. Rodriguez, D. Mendez, and J. E. Hernandez-Avila. **2003**. Bacteria in midguts of field-collected *Anopheles albimanus* block *Plasmodium vivax* sporogonic development. J. Med. Entomol. 40: 371–374.

Gusmão, D. S., A. V. Santos, D. C. Marini, M. Bacci, M. A. Berbert-Molina, and F. J. A. Lemos. **2010**. Culture-dependent and culture-independent characterization of microorganisms associated with *Aedes aegypti* (Diptera: Culicidae) (L.) and dynamics of bacterial colonization in the midgut. Acta Trop. 115: 275–281.

Joyce, J. D., J. R. Nogueira, A. A. Bales, K. Pittman, and J. R. Anderson. **2011**. Interactions between La Crosse Virus and Bacteria Isolated from the Digestive Tract of *Aedes albopictus* (Diptera : Culicidae) Interactions Between La Crosse Virus and Bacteria Isolated From the Digestive Tract of *Aedes albopictus* (Diptera : Culicidae). J Med Entomol. 48: 389–394.

Junjhon, J., J. G. Pennington, T. J. Edwards, R. Perera, J. Lanman, and J. Kuhn. **2014**. Ultrastructural Characterization and Three-Dimensional Architecture of Replication Sites in Dengue Virus-Infected Mosquito Cells. J. Virol. 88: 4687–4697.

Jupatanakul, N., S. Sim, and G. Dimopoulos. **2014**. The insect microbiome modulates vector competence for arboviruses. Viruses. 6: 4294–4313.

Khot, P. D., and M. A. Fisher. **2013**. Novel Approach for Differentiating *Shigella* Species and *Escherichia coli* by Matrix-Assisted Laser Desorption Ionization – Time of Flight. J. Clin. Microbiol. 51: 3711–3716.

Kikuchi, Y., M. Hayatsu, T. Hosokawa, A. Nagayama, and K. Tago. **2012**. Symbiont-mediated insecticide resistance. Proc. Natl. Acad. Sci. U. S. A. 109: 8618–8622.

Klindworth, A., E. Pruesse, T. Schweer, J. Peplies, C. Quast, M. Horn, and F. O. Glöckner. **2013**. Evaluation of general 16S ribosomal RNA gene PCR primers for classical and next-generation sequencing-based diversity studies. Nucleic Acids Res. 41: 1–11.

Koskella, B., L. J. Hall, and J. E. Metcalf. **2017**. The microbiome beyond the horizon of ecological and evolutionary theory. Nat. Ecol. Evoltuion. 1: 1606–1615.

Kruskal, W. H., and W. A. Wallis. **1952**. Use of ranks in one-criterion variance analysis. J. Am. Stat. Assoc. 47: 583–621.

Mandal, S., W. Van Treuren, R. A. White, M. Eggesbø, R. Knight, and S. D. Peddada. **2015**. Analysis of composition of microbiomes: a novel method for studying microbial composition. Microb. Ecol. Health Dis. 26: 27663.

Martin, M. 2011. Cutadapt removes adapter sequences from high-throughput sequecning reads. EMBnet.journal. 17: 10–12.

McDonald, D., J. C. Clemente, J. Kuczynski, J. R. Rideout, J. Stombaugh, D. Wendel, A. Wilke, S. Huse, J. Hufnagle, F. Meyer, R. Knight, and J. G. Caporaso. **2012**. The Biological Observation Matrix (BIOM) format or: how I learned to stop worrying and love the ome-ome. Gigascience. 1: 7.

McKinney, W. 2010. Data Structures for Statistical Computing in Python, pp. 51–56. *In* van der Walt, S., Millman, J. (eds.), Proc. 9th Python Sci. Conf.

Molina-Henao, E. H., I. M. Serrato, L. V. Romero, P. A. Caicedo, M. Y. Graffe, E. P. De La Cadena, A. Correa, and C. B. Ocampo. **2018**. Evaluation of the microbial composition present in the midgut of *Aedes aegypti* strains with different susceptibility to dengue virus infection.

Muturi, E. J., J. L. Ramirez, A. P. Rooney, and C.-H. Kim. **2017**. Comparative analysis of gut microbiota of mosquito communities in central Illinois. PLoS Negl. Trop. Dis. 11(2): e0005377.

Ngo, C. T., S. Romano-Bertrand, S. Manguin, and E. Jumas-Bilak. **2016**. Diversity of the bacterial microbiota of *Anopheles* mosquitoes from binh Phuoc Province, Vietnam. Front. Microbiol. 7: 1–11.

Ocampo, C. B., P. A. Caicedo, G. Jaramillo, R. Ursic Bedoya, O. Baron, I. M. Serrato, D. M. Cooper, and C. Lowenberger. **2013**. Differential Expression of Apoptosis Related Genes in Selected Strains of *Aedes aegypti* with Different Susceptibilities to Dengue Virus. PLoS One. 8(4): e61187.

Ocampo, C. B., and D. M. Wesson. **2004**. Population dynamics of *Aedes aegypti* from a dengue hyperendemic urban setting in Colombia. Am. J. Trop. Med. Hyg. 71: 506–513.

Palmer, W. H., F. S. Varghese, and R. P. Van Rij. **2018**. Natural Variation in Resistance to Virus Infection in Dipteran Insects. Viruses. 10(3): E118.

Pan, X., G. Zhou, J. Wu, G. Bian, P. Lu, A. S. Raikhel, and Z. Xi. **2012**. *Wolbachia* induces reactive oxygen species (ROS)-dependent activation of the Toll pathway to control dengue virus in the mosquito *Aedes aegypti*. Proc. Natl. Acad. Sci. 109: E23–E31.

Ramirez, J. L., J. Souza-Neto, R. T. Cosme, J. Rovira, A. Ortiz, J. M. Pascale, and G. Dimopoulos. **2012**. Reciprocal tripartite interactions between the *Aedes aegypti* midgut microbiota, innate immune system and dengue virus influences vector competence. PLoS Negl. Trop. Dis. 6(3): e1561.

Rancès, E., Y. H. Ye, M. Woolfit, E. A. McGraw, and S. L. O'Neill. **2012**. The relative importance of innate immune priming in *Wolbachia*-mediated dengue interference. PLoS Pathog. 8(2): e1002548.

Salter, S. J., M. J. Cox, E. M. Turek, S. T. Calus, W. O. Cookson, M. F. Moffatt, P. Turner, J. Parkhill, N. J. Loman, and A. W. Walker. **2014**. Reagent and laboratory contamination can critically impact sequence-based microbiome analyses. BMC Biol. 12: 87.

Segata, N., J. Izard, L. Waldron, D. Gevers, L. Miropolsky, W. S. Garrett, and C. Huttenhower. **2011**. Metagenomic biomarker discovery and explanation. Genome Biol. 12.

Serrato, I. M., P. A. Caicedo, C. A. Lowenberger, and C. Ocampo. **2017**. Vector competence and innate immune responses to dengue virus infection in selected laboratory and field-collected *Stegomyia aegypti* (= *Aedes aegypti*).. Med. Vet. Entomol. 31(3): 312-319.

Terenius, O., J. M. Lindh, K. Eriksson-Gonzales, L. Bussière, A. T. Laugen, H. Bergquist, K. Titanji, and I. Faye. **2012**. Midgut bacterial dynamics in *Aedes aegypti*. FEMS Microbiol. Ecol. 80: 556–565.

Wang, J., Y. Wu, G. Yang, and S. Aksoy. **2009**. Interactions between mutualist *Wigglesworthia* and tsetse peptidoglycan recognition protein (PGRP-LB) influence trypanosome transmission. Proc. Natl. Acad. Sci. U. S. A. 106: 12133–12138.

Yadav, K. K., K. Chandel, D. Organisation, and S. S. Bhagyawant. **2018**. Midgut Bacterial Microbiota of Important Mosquito Disease Vectors and Its Role in Control of Parasite Transmission, pp. 245–299. *In* Kishore Tyagi, B., Dhanasekaran, D. (eds.), Microb. Control Vector-Borne Dis. CRC Press, Boca Raton, Florida, USA.

Yun, J., W. Roh, W. Whon, M. Jung, M. Kim, D. Park, and C. Yoon. **2014**. Insect Gut Bacterial Diversity Determined by Environmental Habitat , Diet , Developmental Stage , and Phylogeny of Host. Appl. Environ. Microbiol. 80: 5254–5264.

Zucchi, T. D., S. S. Prado, and F. L. Cônsoli. **2012**. The gastric caeca of pentatomids as a house for actinomycetes. BMC Microbiol. 12: 101.

Tables

Table 4.1 Primer sequences used for 16S amplification.

Primer Name	Sequence
515F	GTGCCAGCMGCCGCGGTAA
926R	CCGYCAATTYMTTTRAGTTT
NC	GAGATCAG
PC	GAGAGTGT
R1	GAGATCTC
R2	GAGATGAC
R3	GAGATGTG
R4	GAGTACAG
R5	GAGTACTC
R6	GAGTAGAC
R7	GAGTAGTG
R8	GAGTCACT
S1	GAGTCAGA
S2	GAGTCTCA
S3	GAGTCTGT
S4	GAGTGACA
S5	GAGTGAGT
S6	GAGTGTCT
S7	GAGTGTGA
S8	GAGTTCAC

Table 4.2 Beta diversity statistical outputs, where the composition of bacteria between Cali-S and Cali-MIB midguts was compared using four beta diversity metrics.

	Sample Size	Permutations	pseudo-F	p-value	q-value
Bray-Curtis	12	999	0.627477	0.881	0.881
Jaccard	12	999	0.714433	0.931	0.931
Unweighted	12	999	3.01566	0.098	0.098
Weighted	12	999	1.08424	0.41	0.41

Figures

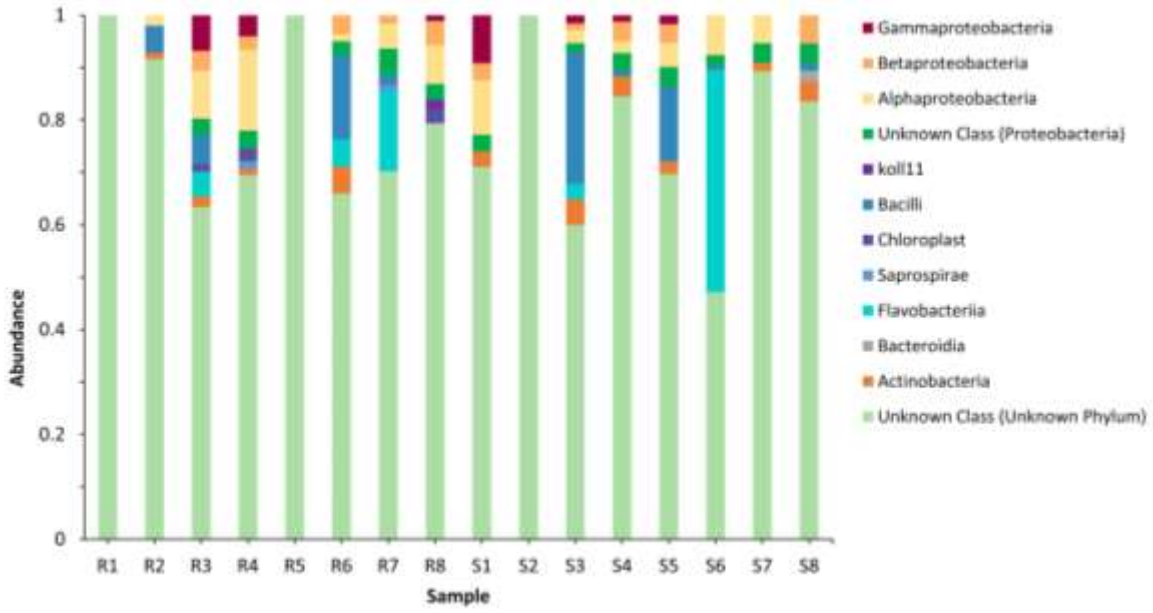

Figure 4.1 Bacterial taxa organized by order, expressed per sample. Bars on the left are from Cali-MIB samples (R1-R8), while bars on the right are from Cali-S samples (S1-S8).

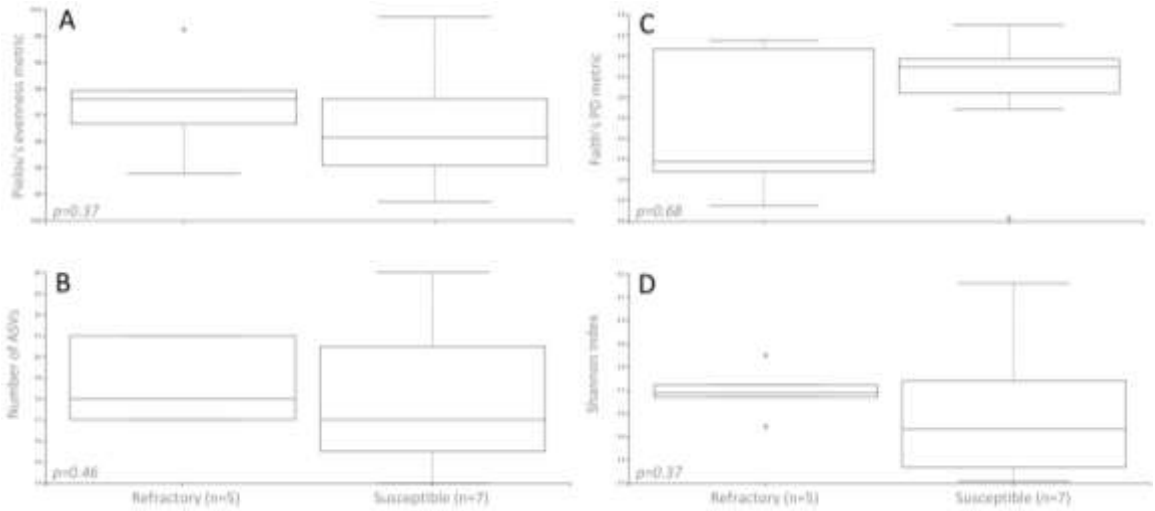

Figure 4.2 Alpha diversity boxplots. A: Pielou's evenness, B: Observed number of ASVs, C: Faith's Phylogenetic Diversity, D: Shannon.

Connecting Statement 4

In Chapters 2, 3 and 4 we identified factors that might be important in determining the vector competence of the Cali-MIB and Cali-S strains of *Aedes aegypti*. We wanted to determine if we could use gene editing approaches to modify mosquitoes and genetically alter their vector competence. Would these permanent changes affect the overall fitness of modified mosquitoes? In the next chapter we describe our approach to use a new gene editing technology, clustered regularly interspaced palindromic repeats (CRISPR), to knock-out two genes, a *cathepsin-b* (identified in Chapter 2), and *xylosyltransferase oxt* (identified in Chapter 3), both of which have an increased expression level in the Cali-S strain, and which have been implicated in other reports to be required for DENV to enter and replicate in mosquito cells.

Chapter 5. Engineering resistance to dengue virus in *Aedes aegypti* via CRISPR-Cas-9 mediated techniques

Author Contributions

Carl Lowenberger and Heather Coatsworth conceived the study. Heather Coatsworth completed guide design and off target analyses. Heather Coatsworth, Lea Sanchez-Milde and Carl Lowenberger completed embryo injections. Lea Sanchez-Milde, Heather Coatsworth and Laura Barth maintained and collected mosquito life history data, as well as analyzed mosquitoes for genetic modifications. Heather Coatsworth completed statistical analyses on mosquito life history data. Heather Coatsworth and Carl Lowenberger wrote the manuscript.

5.1. Abstract

Aedes aegypti is the vector for dengue viruses, which affect 100 million people each year. As traditional insecticide programs have proved unsuccessful in decreasing vector populations, novel approaches are required. Gene editing strategies have been proposed to permanently modify vector reproduction and competence in an overall effort to reduce population size and replace susceptible populations with pathogen-resistant individuals, respectively. Here we describe the use of Clustered Regularly Interspaced Short Palindromic Repeats/CRISPR-associated sequence 9 (CRISPR/Cas9) genome editing to modify the vector competence of *Ae. aegypti*. We created multiple guide RNAs for Cas9 mediated dsDNA cutting of two target genes, *xylosyltransferase*, a mosquito protein required by dengue viruses to bind to cells, and *cathepsin-b*, a lysosomal cysteine protease predicted to aid in virus-mediated apoptosis. These guides along with Cas9 protein were injected directly into embryos. In insects that were injected with the *xylosyltransferase* knockout construct and survived to adulthood, approximately 19% were modified, while in insects injected with the *cathepsin-b* knockout construct, approximately 5.4% of emerging adults were modified. We observed that injected embryos had lower hatching rates, and that *cathepsin-b* injected embryos spent more time as pupae than their non-injected counterparts. These data support the concept of using CRISPR/Cas9 based genetic modification techniques to permanently knock-out genes of interest in *Ae. aegypti*.

5.2. Introduction

Dengue is the most widespread of the arthropod-borne viruses (arboviruses), infecting 50-100 million people each year throughout the Americas, Africa, Asia and Australia (Mairuhu et al. 2004, Bhatt et al. 2013). Dengue is primarily transmitted by the anthropophilic mosquito *Aedes aegypti* (Halstead et al. 1997). To manage dengue, vector control measures including insecticides, larvicides and source reduction are used commonly to reduce transmission (McGraw and O'Neill 2013). However, due to the long-term ineffectiveness of insecticide programs, there is a significant interest in mosquito bio-manipulation techniques such as genetic modifications that confer sterility, the introduction of endosymbionts that decrease lifespan, and the generation of refractory strains that prevent pathogen transmission. Some of these approaches have shown great promise towards effective vector control and are being used commercially (Barnes 2005, McGraw and O'Neill 2013). These approaches and techniques require an in-depth understanding of vector biology and up to date knowledge regarding the current available tools to modify these vectors.

Despite the importance of *Ae. aegypti* in the transmission of DENV, not all *Ae. aegypti* transmit DENV; strains of *Ae. aegypti* that are refractory to DENV have been identified or generated in research laboratories (Bennett, Beaty, et al. 2005a, Chauhan, Behura, deBruyn, et al. 2012b). We have a unique situation in that approximately 30% of feral *Ae. aegypti* in Cali, Colombia are naturally refractory to DENV. These mosquitoes manifest their phenotype through a midgut infection barrier (MIB) (Caicedo et al. 2013a), whereby DENV is unable to replicate within midgut cells (Black et al. 2002b).

Previous studies collected mosquitoes in the field and carried out selection procedures to rear field derived strains of dengue-refractory (Cali-MIB) and dengue-susceptible (Cali-S) mosquitoes (Caicedo et al. 2013a). Only ~47% of the Cali-MIB population was refractory, while the Cali-S population was 98% susceptible (Caicedo et al. 2013a). These strains were exposed to dengue virus every other generation for over 30 generations but did not significantly change their proportions of refractoriness.

Previous research demonstrated a differential expression of midgut genes between the Cali-S and Cali-MIB strains (Cooper 2008, Barón et al. 2010a, Ocampo et al. 2013, Caicedo et al. 2018) (Chapter 2), including genes associated with autophagy,

apoptosis, serine proteases and lysosomal peptides. When selected genes from these functional groups were knocked down in the Cali-S strain using RNAi, susceptible individuals became refractory (Caicedo et al. 2018). In parallel to the gene knockdown studies, we investigated the effects that genetic variants had on determining or identifying susceptible and refractory individuals (Chapter 3). We found a single nucleotide polymorphism (SNP) that identified Cali-MIB or Cali-S mosquitoes as well as other variants that might render some genes non-functional and contribute to the Cali-S or Cali-MIB phenotype.

While we can now predict the phenotype based on SNPs, and alter the phenotype using temporary knockdown strategies, we want to create permanent changes to the expression of these characterized genes so that they remain altered at a population level. Such a system would allow us to create lines of dengue refractory individuals for further study.

One recently developed approach to edit genomes utilizes a family of DNA sequences known as Clustered Regularly Interspaced Short Palindromic Repeats (CRISPRs) alongside a CRISPR-Associated protein 9 (Cas 9) nuclease, isolated from *Streptococcus pyogenes* to make a double stranded break in a targeted area of the genome. The CRISPR complex is guided to an area of interest using a 4-20nt long RNA moiety known as the guide RNA (gRNA), which contains a trans-activating CRISPR RNA (tracrRNA), as well as a specific complementary CRISPR RNA (crRNA). The cut resulting from the complex typically is repaired by endogenous nonhomologous end joining (NHEJ), which is an error-prone repair process, often leading to small indels at the repair site. Cells also can repair the break using homology directed repair (HDR), which uses a homologous piece of DNA, often referred to as a donor to guide the repair process. Although HDR maintains genomic stability, it is much less common. Both these repair processes offer great promise for disrupting and eliminating gene function by deletions or insertions using NHEJ or adding in new nonsense or alternatively functional genes with HDR.

CRISPR-Cas technology has been used to create mosquitoes with different traits that can be used in different approaches to affect disease transmission (Dong et al. 2015, Gantz et al. 2015, Kistler et al. 2015, Galizi et al. 2016, Hammond et al. 2016). These approaches fall into two broad categories: population suppression and population replacement techniques. Population suppression systems aim to reduce or eliminate an

entire vector population, whereas replacement techniques are geared towards changing the population make-up over time until an entire population contains a specific trait, i.e. pathogen-resistance (Kean et al. 2015). To increase the success of these systems, gene drives, another genetic engineering technology, may be used to skew inheritance patters towards the alleles of interest. This technology results in offspring that only contain the gene edits of interest, and as such, allows these edits to integrate quickly and spread within a population of interest (Gantz et al. 2015, Hammond et al. 2016, Kyrou et al. 2018).

In this study we used an NHEJ CRISPR-Cas9 based approach to render two genes of interest non-functional in dengue-susceptible *Ae. aegypti*. The first of these genes, *xylosyltransferase* (AAEL007409), is an enzyme involved in the biosynthesis of chondroitin and heparan sulfate. Previous studies have suggested that *xylosyltransferase* is necessary for dengue virus to bind to, and enter, cells (Avirutnan et al. 2007). Our work has shown that the naturally refractory Cali-MIB strain possess numerous non-synonymous mutations within the coding regions of this gene (Chapter 3). Orthologues of a second *Ae. aegypti* gene, *cathepsin-b* (AAEL007585), a lysosomal cysteine protease, has been shown in humans to enhance the establishment and replication of DENV (Morchang et al. 2013). When this gene was knocked down in susceptible *Ae. aegypti* using RNAi, 80% of the dsRNA treated females became refractory to DENV (Caicedo et al. 2018). Creating indels within these genes using an NHEJ CRISPR-Cas9 based approach may decrease the vector competence of the modified mosquitoes, and of their offspring.

5.3. Methods

5.3.1. Mosquito collection and maintenance

A laboratory colony of the black-eyed Liverpool strain of *Ae. aegypti* has been maintained at Simon Fraser University for 16 years. Filter paper containing eggs was placed in widemouthed 237mL glass Mason jars (ULINE, Pleasant Prairie, WI, USA) and submerged in 60mL of deoxygenated water kept at room temperature with 2 g of ground Nutrafin® basix Staple Food, a commercial grade tropical fish food (Hagen, Montreal, QC, Canada). Larvae were maintained in enamel pans at a density of approximately 300 larvae/2 L of water and were fed daily with a slurry of Nutrafin® basix Staple Food (Hagen, Montreal, QC, Canada). Pupae were transferred to 207mL wax coated cups (Solo Cup,

Lake Forest, IL, USA) containing 100mL water, and housed as individuals to control mating.

Adult mosquitoes were maintained under standard laboratory conditions: 27˚C, 70% relative humidity, and a 12:12 hour light: dark cycle, and fed daily with a 10% sucrose solution. Male and female mosquitoes from the same cohort were transferred into the same cup (via manual aspiration) and allowed to mate. Six days post eclosion, mated females were blood fed through an artificial membrane feeder using Parafilm (Bemis, Neenah, WI, USA) and defibrinated sterile sheep's blood (Cedarlane, Burlington, ON, Canada) warmed to 37˚C. A damp piece of grade 1 filter paper (Whatman plc, Maidstone, UK) was provided to the mosquitoes in 35 x 10mm plastic petri dishes (Sarstedt, Sarstedtstraße 1, Germany) three days post blood-feeding as an oviposition surface and these surfaces were changed daily until egg laying commenced. This process was repeated until the mosquito died or no longer took a blood meal. Eggs were collected, labelled, and stored in enclosed cups to prevent the paper from drying out. Individuals were monitored daily, and the life history parameters of each individual (time to hatching, larval lifespan, pupal lifespan, adult lifespan, mating partner, and number of gonotrophic cycles) were recorded. Dead mosquitoes were transferred to 1.5mL centrifuge tubes containing 70% ethanol for storage and preservation.

5.3.2. Guide design and construction

The Alt-RT CRISPR-Cas9 system manufactured by Integrated DNA Technologies (IDT, Coralville, IA, USA) was used to perform the knockouts. The kit contained three components: a guide specific 36nt Alt-R CRISPR RNA (crRNA), a 67nt trans-activating crRNA (tracrRNA), and the *Streptococcus pyogenes* Cas9 nuclease 3 nucleic localization signal (NLS). Three crRNAs were designed for cathepsin B (AAEL007585), while two crRNAs were created for *xylosyltransferase* (AAEL007409). Each crRNA targeted an exonic region of the gene to disrupt gene function. To minimize off target effects, the CRISPR Design tool developed by the Zhang lab at MIT (http://crispr.mit.edu/) was used to blast each crRNA against the *Ae. aegypti* genome. Guides were chosen to minimize off target effects while optimizing protospacer adjacent motif (PAM) sites (Table 5.1).

The RNP complex was created following IDT's Zebrafish Alt-R microinjection protocol (Dr. Jeffrey Essner, Iowa State University) using guide and Cas9 concentrations

as suggested (Kistler et al. 2015). For each reaction, the crRNA and tracrRNA were diluted to a final concentration of 100µM each in Nuclease-Free IDTE Buffer (IDT). A guideRNA (gRNA) solution was then created by mixing 0.3ul of the crRNA and tracrRNA with 9.4ul of Nuclease-Free IDTE Buffer. The gRNA solution was heated at 95°C for 5 mins and allowed to cool to room temperature (15-25°C) to produce a 3 µM gRNA solution. The Cas9 protein was diluted to a working concentration of 0.5 µg/µL in Cas9 working buffer (20 mM HEPES; 150 mM KCl, pH 7.5) and was mixed in equal volumes with the gRNA solution. The reaction was incubated at 37°C for 10 min and allowed to cool at room temperature to produce the ribonucleoprotein (RNP) complex.

5.3.3. Embryo collection and microinjections: *cathepsin-b*

Prior to injections, needles were pulled from aluminosilicate glass capillary tubing (1 mm OD, x 0.64mm ID, Sutter Instrument, Novato, CA, USA) using a P-1000 micropipette puller. The needle pulling settings were obtained from (Li et al. 2017) (heat: 605, velocity: 130, delay: 80, pull: 70, pressure: 500).

For each set of injections, ~ 15 gravid female Liverpool strain *Ae. aegypti* were transferred into 50mL Falcon tubes containing a cotton ball soaked with distilled water, covered with grade 1 filter paper arranged in a cone as an oviposition site. Each tube of mosquitoes was placed in a dark container at 27°C and 70% humidity for one hour to encourage egg-laying. The filter paper was then inspected for eggs. Filter papers containing recently laid light gray to dark grey eggs were transferred onto a moistened sponge to maintain humidity. Eggs were aligned manually in parallel rows of 40 – 60 eggs on the filter paper strip under a dissection microscope. Dissecting scissors were used to cut out the portion of the filter paper containing the line of eggs and was placed atop a dry piece of filter paper. The space around the egg line was pressed using the back of a fine paintbrush to remove residual water from the egg strip. Double-sided transparent Scotch tape was used to transfer the eggs onto a transparent microscope slide by gently applying pressure onto the line of eggs. Once transferred, the eggs dried at room temperature until dimples began to appear on their surface (~30 seconds post-transfer). A few drops of Halocarbon 700 oil (Sigma, St. Louis, MO, USA) were then deposited on the egg line (Jasinskiene et al. 2007, Kistler et al. 2015).

Injections were carried out under a compound microscope, using an Eppendorf FemtoJet® microinjector set to an injection pressure (pi) of 600 hPa, a compensation pressure (pc) of 250 hPa, and time set to manual. 18ul of the RNP complex was backfilled into each needle using Eppendorf Microloader Femtotips (Eppendorf, Mississauga, ON, Canada). The needle was then secured into the collet of the FemtoJet unit and secured onto a micromanipulator. Embryos were horizontally injected through the posterior, narrow pole, with approximately 0.2-0.5nL of RNP solution until a small amount of cytoplasm was displaced. Once a row of injections was complete, the microscope slides were placed vertically into a slide box filled with water for 5 hours, allowing the oil to slowly run off the eggs. A water dipped fine paintbrush was then used to individually transfer eggs from the glass slide onto a damp piece of circular grade 1 filter paper placed inside a plastic petri dish. The eggs were maintained in the petri dishes for 3-5 days and then were hatched and raised according to standard procedures (see above).

As eggs were handled and injected during this process, three control treatments were completed alongside the RNP injections: i) a wildtype control, where the filter paper was removed from the Falcon tube and directly placed into a petri dish for later hatching, ii) a handled control, in which the eggs were aligned and transferred but not injected, and iii) an injected buffer control, in which the eggs were aligned, injected with the Cas9 working buffer (20 mM HEPES; 150 mM KCl, pH 7.5), and transferred as above to Petri plates.

Hatched larvae were reared and kept separately by treatment. Pupae were housed individually until the adults emerged, at which point we carried out 1:1 matings with another individual from the same treatment group (*cathepsin-b* RNP guide 1, 2, and 3 injected, buffer injected, handled, *wt* control). Due to low hatching rates within our *cathepsin-b* RNP guide treatment groups, *cathepsin-b* RNP injected adults were outcrossed to *wt* mosquitoes to secure potential future heterozygous individuals (Figure 5.1). Egg laying, and collection were completed as described above. Adults were monitored daily, and any deceased individuals were collected and individually stored in 1.5mL microcentrifuge tubes containing 70% ethanol.

5.3.4. Embryo collection and microinjections: *xylosyltransferase*

The second round of CRISPR-Cas9 injections using *xylosyltransferase* guides was done at the Insect Transformation Facility (University of Maryland), following the same protocol as used in the *cathepsin-b* injections above. As the injections were not done in house, there were only two treatment groups: *xylo* 1 gRNA and *xylo* 2 gRNA injected. As such, pairings were completed within each guide treatment group.

5.3.5. Genomic DNA extraction

To determine if the gene of interest had been modified, the head of each deceased adult (or entire larvae or pupae) was collected and its DNA was extracted using a Qiagen DNeasy Blood and Tissue kit (Venlo, Netherlands) following the manufacturer's protocol. DNA concentrations were assessed using a Nanodrop2000 (Thermo Fischer Scientific, Waltham, MA, USA).

5.3.6. Analysis of CRISPR-Cas9 induced mutations

Due to the high similarity with other cathepsin and vitellogenein genes, highly specific RNase H-dependant PCR (rhPCR) primers were designed to target AAEL007585 (Table 5.2) in traditional PCR based reactions, while standard PCR primers were used to amplify the *xylosyltransferase* product. The rhPCR primers contain RNA bases and are used alongside an RNase H2 enzyme to block non-specific product formation through a 3' blocking moiety. The amplified gene-specific DNA was used in heteroduplex reactions (Alt-R Genome Editing Detection Kit, IDT, Coralville, IA, USA) to verify if changes existed within our targeted locus. Results were visualized in a 3% agarose gel to inspect for homozygous mutants, homozygous wildtypes and heterozygous individuals.

5.3.7. Fitness evaluations

In order to collect fecundity data, each oviposition substrate sheet was photographed. Eggs were counted, and 5 eggs/sheet were randomly measured using ImageJ v2 (Rueden et al. 2017). Longevity, fecundity, egg hatching success, survival of larvae, blood-feeding success and number of gonotrophic cycles were recorded for each mosquito from each treatment that hatched. Biological replicates consisted of each

separate injection round. Statistical analyses on the fitness data were completed using R (Team 2018) (packages: ggplot2 (Wickham 2016), multcomp (Hothorn et al. 2008), car (Fox and Weisberg 2011), and agricolae (de Mendiburu and Simon 2015). One-way ANOVAs using Tukey's post-hoc tests were completed on continuous data that passed Levene's Test for Homogeneity of Variance (pupal lifespan, time to hatching, number of eggs/gonotrophic cycle, size of eggs/gonotrophic cycle, male lifespan, female lifespan). For proportional data (proportion of larvae hatched, proportion of females hatched, proportion of males hatched, proportion of pupae hatched, proportion of adults hatched) a generalized linear model (family = quasibinomial, link=logit) was used. One-way ANOVAs were performed on the results from the linear model. Lastly, another generalized linear model (family=poisson, link=log) was used to investigate the number of gonotrophic cycles/female with subsequent one-way ANOVAs being performed on the results from the linear model.

5.4. Results

5.4.1. Embryo collection and microinjections

In total, 7218 embryos were RNP injected for the *cathepsin-b* experiment, and 1485 were injected with the buffer control. 421 embryos were injected for the *xylosyltransferase* experiment.

Although the *cathepsin-b* experiment produced edited individuals (n=3), the overall success of our injections was low (3 successful modifications/7218 injections). The *xylosyltransferase* injection process yielded 14/33 and 15/43 edited adult individuals (*xylo* 2 and *xylo* 1 guides, respectively).

Most RNP injected treatments produced equal adult sex ratios (*cathepsin-b* RNP1, 9 ♀: 8 ♂, *cathepsin-b* RNP 2, 11 ♀: 8 ♂, *xylosyltransferase* RNP 1, 59 ♀: 64 ♂). However, two treatments resulted in different sex ratios, *cathepsin-b* RNP 3, 5 ♀: 10 ♂, and *xylosyltransferase* RNP 2, 20 ♀: 11♂.

5.4.2. Genomic DNA extraction

We extracted DNA from 159 mosquitoes from the *cathepsin-b* experiment: 16 RNP1 adults, 1 RNP1 pupa, 18 RNP2 adults, 1 RNP2 pupae, 3 RNP2 larvae, 15 RNP3 adults, 2 RNP3 larvae, and 103 control (buffer injected, handled and *wt*) adults. For the *xylosyltransferase* experiment we extracted DNA from 158 mosquitoes: 31 RNP1 adults, 1 RNP1 pupa, 1 RNP1 larva, 123 RNP2 adults, 1 RNP2 pupa, and 1 RNP2 larva. All individuals had at least 20µL of 10ng/µL DNA, which was considered acceptable for downstream analyses.

5.4.3. Analysis of CRISPR-Cas9 induced mutations

When a cell has been modified by the CRISPR/Cas-9 complex, the NHEJ repair pathway will cause small indels to be introduced into the resultant sequence. When run in a gel, these PCR amplified indels appear as heteroduplexes, or multiple bands. Conversely, in un-edited individual's PCR amplicons migrate as single bands or homoduplexes in a gel. We observed three heteroduplex individuals from our *cathepsin-b* RNP injected experiment (Figure 5.4), and 29 heteroduplex individuals from our *xylosyltransferase* RNP injected experiment (Figure 5.5), indicating that our CRISPR/Cas-9 experiments were indeed successful in creating indels.

5.4.4. Fitness evaluations

Fitness data were obtained across all four treatments for all fitness parameters measured (Tables 5.3, 5.4, 5.5). Only two parameters were statistically significant between treatments; the proportion of larvae hatched ($p<0.001$) (Figure 5.3), and pupal lifespan ($p<0.05$) (Figure 5.3). Fewer individuals injected with CRISPR constructs or buffer hatched, and CRISPR-injected individuals spent more time as pupae than their non-injected counterparts. One-way ANOVA analyzing the time to hatching, number of eggs/gonotrophic cycle, size of eggs/gonotrophic cycle, male lifespan, female lifespan, number of gonotrophic cycles/female were not significantly different among treatments ($p\geq0.05$) (Table 5.6). Generalized linear models used to asses treatment differences between the proportion of females hatched, males hatched, pupae hatched, and adults hatched were also not statistically significantly different ($p\geq0.05$) (Table 5.6).

5.5. Discussion

5.5.1. Embryonic microinjections

We used the CRISPR-Cas9 system to make changes in two genes of interest in *Ae. aegypti*. Although we were able to make these changes using our in-house injection system, the system was much more efficient when we employed a professional injection service. As the procedure requires an extreme amount of dexterity, there was a steep learning curve associated with manipulating, handling and injecting the embryos. It would be advisable to use a professional injection service for future experiments to maximize time and injection success.

Although embryonic injection is still the gold standard for genomic editing in mosquitoes, recent studies employing other means of germline editing look promising. Instead of injecting embryos, researchers have used an ovary-specific ligand to allow for injection of RNPs into adult female mosquitoes, which then lay mutated individuals (Chaverra-Rodriguez et al. 2018). This technique targets an earlier embryonic phase of development, reducing the chances of obtaining mosaic individuals, and eliminates the arduous and delicate step of microinjecting individual embryos directly. Other techniques such as nanoparticle CRISPR-Cas9 delivery systems could also help overcome embryonic injection issues (Kulkarni, personal communication).

Our direct embryo injection technique targeting NHEJ based repair allowed us to examine whether small indels were present in our genes of interest and helped determine which guide RNA was the most successful at creating a double stranded break. These small indels can be hard to track, especially since our system generates mosaic individuals (possessing mutated and unmutated gene copies) due to the large number of cells present in the embryos. Similar results have been reported from numerous other insect microinjection studies (Li et al. 2017, Zhang and Reed 2017, Chaverra-Rodriguez et al. 2018). In order to overcome these issues with mosaic individuals, we would need to complete injections on cell lines (Yu et al. 2013) or target earlier embryonic developmental stages within the female mosquito (Gutierrez-Triana et al. 2018).

Screening for modifications could be made easier by creating an HDR based construct that incorporates a visible marker that indicates a genetic change has occurred.

This approach has been used previously in a number of mosquito gene editing studies; researchers have used homology arms with promoter systems to express eGFP and dsRed fluorescent constructs in whole bodies, eyes, and cuticle (Kistler et al. 2015, Li et al. 2017).These homology arms also have been used to express novel proteins of interest, such as anti-*Plasmodium* effector genes in *Anopheles stephensi* (Gantz et al. 2015) or gene drive systems in *Anopheles gambiae* (Hammond et al. 2016). It would be ideal to add a fluorescent reporter and possible a gene-drive construct into our future CRISPR-Cas9 studies to easily screen large numbers of larvae for successful mutants and track the heritability of the genetic change.

5.5.2. Fitness effects on injected individuals

In the *cathepsin-b* injection experiment, the proportion of larvae hatched, and pupal lifespan were significantly affected by the injection process (Figures 5.2 and 5.3). These are likely effects brought on by the intrusive injection procedure, as we also observed these effects in both the CRISPR and buffer treatments. The embryos may need more time to heal from the wound and stress of the injection process. Lower hatching of modified embryos and lower proportions of mosquitoes surviving to adulthood (i.e. higher larval and pupal mortality) have been found in other CRISPR-mosquito studies (Gantz et al. 2015, Galizi et al. 2016) . It is likely that in future generations (F1 onwards) the proportion of larvae hatched, and pupal lifespan would not be different among treatments, as the mosquitoes would no longer undergo the injection process.

5.5.3. Analysis of CRISPR-Cas9 induced mutations

Our modification and hatching success were much higher for *xylosyltransferase* guide injected individuals (421 injected, 155 hatched, 19% modification rate (number modified/number hatched)) than for our *cathepsin-b* guide injected individuals (7218 injected, 56 hatched, 5.4% modification rate). Most mosquito CRISPR-based study systems use HDR mediated techniques, with modification successes of 5% or lower (Dong et al. 2015, Gantz et al. 2015, Kistler et al. 2015, Hammond et al. 2016, Chaverra-Rodriguez et al. 2018). The NHEJ systems surveyed in mosquitoes have had an approximate success rate of 25% (Kistler et al. 2015). These numbers are hard to estimate, as modification analysis techniques are still being developed to properly assess individuals for potential germ-line modifications. The heteroduplex assays used in this

study are used commonly to asses for changes during guide development. Sanger sequencing techniques are difficult to employ with G_0 mosaic individuals, as single base pairs may be deleted at a variety of loci, which makes analyzing resultant sequences difficult. As such, more precise sequencing techniques are needed to assess single base pair modifications. Assessing potential changes in HDR-cassette systems is much easier, as searches for insert DNA can easily be detected through traditional Sanger sequencing.

5.5.4. Future Directions

Although we attempted to mate the modified individuals we obtained in both our studies, we were unable to use these primary experiments to establish lines of *cathepsin-b* or *xylosyltransferase* knock-out individuals. Future experiments should aim to inject more individuals using a professional service and incorporate a fluorescent marker for easy sorting. Once these lines are established, the vector competence of the verified knock-out mosquitoes towards dengue viruses could be assessed. We would predict that knock-out *cathepsin-b* individuals would have a decreased vector competence based on our RNAi experiments (Caicedo et al. 2018). *Xylosyltransferase* knock-outs have been completed in cell line systems (Avirutnan et al. 2007), but not yet in whole organisms such as *Ae. aegypti*. As *xylosyltransferase* is necessary for dengue virus to bind to cells (Avirutnan et al. 2007), a *xylosyltransferase* knock-out in mosquitoes should, in theory, create dengue-refractory individuals. Conceptually our approach using these gene targets aligns with a population replacement vector control method, where wildtype, dengue-susceptible individuals are replaced with modified, dengue-refractory individuals.

There is a significant effort in the scientific community to use genetically modified mosquitoes to decrease pathogen transmission and associated disease incidence (Alphey 2014). Although modified mosquitoes appear to be the latest ‘best option’ for vector control, larger issues stemming from a lack of legislative framework and societal acceptance has curbed their deployment (Panjwani and Wilson 2016). This was the case in 2015, when Oxitec, a British biotechnology company that commercially creates genetically modified mosquitoes with a goal of population suppression, attempted to release their GM mosquitoes in the Florida Keys (USA), a potential hot-bed for Zika transmission, and in Miami during a period of mosquito-borne transmission of Zika virus in 2017. Although the Florida Keys Mosquito Control District, and the US Food and Drug Administration (FDA) approved the project, some residents started a petition against the

project, and concerns were raised over a lack of regulatory approval from the Environmental Protection Agency (EPA) (Chakradhar 2015, West et al. 2015). As a result, these plans were halted, and GM mosquitoes have yet to be released within the Florida Keys or the Miami region, despite successful Oxitec program deployments in the Cayman Islands and Brazil (Chakradhar 2015). Despite all the recent scientific advancements using genetic modification technologies such as CRISPR to curb the spread of mosquito-borne pathogens, it is clear that there are numerous societal and political barriers that need to be addressed (Panjwani and Wilson 2016, Lull and Scheufele 2017) before these approaches may be used. *Wolbachia* infected dengue refractory mosquitoes are not genetically modified, and same reservations have not been observed or expressed during release programs of *Wolbachia* infected mosquitoes, possibly due to the extensive public consultation and media communication that has been used in the various countries in which these mosquitoes have been released (Kolopack et al. 2015).

5.6. References

Alphey, L. 2014. Genetic control of mosquitoes. Annu. Rev. Entomol. Rev. Entomol. 59: 205–224.

Avirutnan, P., L. Zhang, N. Punyadee, A. Manuyakorn, and C. Puttikhunt. 2007. Secreted NS1 of Dengue Virus Attaches to the Surface of Cells via Interactions with *Heparan sulfate* and Chondroitin Sulfate E. PLoS Pathog. 3(11): e183.

Barnes, E. 2005. Diseases and Human Evolution. University of New Mexico Press, Albuquerque, N.Y.

Barón, O. L., R. J. Ursic-Bedoya, C. A. Lowenberger, and C. B. Ocampo. 2010. Differential Gene Expression from Midguts of Refractory and Susceptible Lines of the Mosquito, *Aedes aegypti*, Infected with Dengue-2 Virus. J. Insect Sci. 10: 1–23.

Bennett, K. E., B. J. Beaty, and W. C. Black. 2005. Selection of D2S3, an *Aedes aegypti* (Diptera: Culicidae) strain with high oral susceptibility to Dengue 2 virus and D2MEB, a strain with a midgut barrier to Dengue 2 escape. J. Med. Entomol. 42: 110–119.

Bhatt, S., P. W. Gething, O. J. Brady, J. P. Messina, A. W. Farlow, C. L. Moyes, J. M. Drake, J. S. Brownstein, A. G. Hoen, O. Sankoh, M. F. Myers, D. B. George, T. Jaenisch, G. R. William Wint, C. P. Simmons, T. W. Scott, J. J. Farrar, and S. I. Hay. 2013. The global distribution and burden of dengue. Nature. 496: 504–507.

Black, W. C., K. E. Bennett, N. Gorrochótegui-Escalante, C. V. Barillas-Mury, I. Fernández-Salas, M. D. L. Muñoz, J. a. Farfán-Alé, K. E. Olson, and B. J. Beaty. 2002. Flavivirus susceptibility in *Aedes aegypti*. Arch. Med. Res. 33: 379–388.

Caicedo, P. A., O. L. Barón, M. Pérez, N. Alexander, C. Lowenberger, and C. B. Ocampo. 2013. Selection of *Aedes aegypti* (Diptera: Culicidae) strains that are susceptible or refractory to Dengue-2 virus. Can. Entomol. 145: 273–282.

Caicedo, P. A., I. M. Serrato, S. Sim, G. Dimopoulos, H. Coatsworth, C. Lowenberger, and C. B. Ocampo. 2018. Immune response-related genes associated to blocking midgut dengue virus infection in *Aedes aegypti* strains that differ in susceptibility. Insect Sci. 26(4): 635-648.

Chakradhar, B. S. 2015. Buzzkill: Regulatory uncertainty plagues rollout of genetically modified mosquitoes. Nat. Publ. Gr. 21: 416–418.

Chauhan, C., S. K. Behura, B. deBruyn, D. D. Lovin, B. W. Harker, C. Gomez-Machorro, A. Mori, J. Romero-Severson, and D. W. Severson. 2012. Comparative Expression Profiles of Midgut Genes in Dengue Virus Refractory and Susceptible *Aedes aegypti* across Critical Period for Virus Infection. PLoS One. 7(10): e47350.

Chaverra-Rodriguez, D., V. M. Macias, G. L. Hughes, S. Pujhari, Y. Suzuki, D. R. Peterson, D. Kim, S. McKeand, and J. L. Rasgon. 2018. Targeted delivery of CRISPR-Cas9 ribonucleoprotein into arthropod ovaries for heritable germline gene editing. Nat. Commun. 9: 3008.

Cooper, D. 2008. Apoptosis and Immunity: Characterizing the Cell Death Machinery in the Yellow Fever Mosquito, *Aedes aegypti*.

Dong, S., J. Lin, N. L. Held, R. J. Clem, A. L. Passarelli, and A. W. E. Franz. 2015. Heritable CRISPR/Cas9-mediated genome editing in the yellow fever mosquito, *Aedes aegypti*. PLoS One. 10(3): 1–13.

Fox, J., and S. Weisberg. 2011. An {R} Companion to Applied Regression, Second. ed. Sage, Thousand Oaks.

Galizi, R., A. Hammond, K. Kyrou, C. Taxiarchi, F. Bernardini, S. M. O. Loughlin, P. Papathanos, T. Nolan, N. Windbichler, and A. Crisanti. 2016. A CRISPR-Cas9 sex-ratio distortion system for genetic control. Sci. Rep. 6: 31139.

Gantz, V. M., N. Jasinskiene, O. Tatarenkova, A. Fazekas, V. M. Macias, E. Bier, and A. A. James. 2015. Highly efficient Cas9-mediated gene drive for population modification of the malaria vector mosquito *Anopheles stephensi*. Proc. Natl. Acad. Sci. 112: E6736–E6743.

Gutierrez-Triana, J. A., T. Tavhelidse, T. Thumberger, I. Thomas, B. Wittbrodt, T. Kellner, K. Anlas, E. Tsingos, and J. Wittbrodt. 2018. Efficient single-copy HDR by 5’ modified long dsDNA donors. Elife. 7: 1–15.

Halstead, S. B., D. J. Gubler, and G. Kuno. 1994. Dengue and dengue hemorrhagic fever. Handb. Zoonoses. 8: 89–99.

Hammond, A., R. Galizi, K. Kyrou, A. Simoni, C. Siniscalchi, D. Katsanos, M. Gribble, D. Baker, E. Marois, S. Russell, A. Burt, N. Windbichler, A. Crisanti, and T. Nolan. 2016. A CRISPR-Cas9 gene drive system targeting female reproduction in the malaria mosquito vector *Anopheles gambiae*. Nat. Biotechnol. 34: 78–83.

Hothorn, T., F. Bretz, and P. Westfall. 2008. Simultaneous Inference in General Parametric Models. Biometrical J. 50: 346–363.

Jasinskiene, N., J. Juhn, and A. A. James. 2007. Microinjection of *A. aegypti* Embryos to Obtain Transgenic Mosquitoes. J. Vis. Exp. (5): 219.

Kean, J., S. M. Rainey, M. McFarlane, C. L. Donald, E. Schnettler, A. Kohl, and E. Pondeville. 2015. Fighting arbovirus transmission: Natural and engineered control of vector competence in *Aedes* mosquitoes. Insects. 6: 236–278.

Kistler, K. E., L. B. Vosshall, and B. J. Matthews. 2015. Genome engineering with CRISPR-Cas9 in the mosquito *Aedes aegypti*. Cell Rep. 11: 51–60.

Kolopack, P. A., J. A. Parsons, and J. V Lavery. 2015. What Makes Community Engagement Effective?: Lessons from the Eliminate Dengue Program in Queensland Australia. PLoS Negl. Trop. Dis. 9(4): 1–19.

Kyrou, K., A. M. Hammond, R. Galizi, N. Kranjc, A. Burt, A. K. Beaghton, T. Nolan, and A. Crisanti. 2018. A CRISPR – Cas9 gene drive targeting doublesex causes complete population suppression in caged *Anopheles gambiae* mosquitoes. Nat. Biotechnol. 36(11): 1062-1066.

Li, M., M. Bui, T. Yang, C. S. Bowman, B. J. White, and O. S. Akbari. 2017. Germline Cas9 expression yields highly efficient genome engineering in a major worldwide disease vector, *Aedes aegypti*. Proc. Natl. Acad. Sci. 114(49): E10540-E10549.

Lull, R. B., and D. A. Scheufele. 2017. Understanding and Overcoming Fear of the Unnatural in Discussion of GMOs, pp. 409–420. In Jamieson, K.H., Kahan, D., Scheufele, D.A. (eds.), Oxford Handb. Sci. Sci. Commun. Oxford University Press, Oxford.

Mairuhu, A. T. A., J. Wagenaar, D. P. M. Brandjes, and E. C. M. Van Gorp. 2004. Dengue: An arthropod-borne disease of global importance. Eur. J. Clin. Microbiol. Infect. Dis. 23: 425–433.

McGraw, E. A., and S. L. O'Neill. 2013. Beyond insecticides: New thinking on an ancient problem. Nat. Rev. Microbiol. 11: 181–193.

de Mendiburu, F., and R. Simon. 2015. Agricolae - ten years of an open source statistical tool for experiments in breeding, agriculture and biology. PeerJ Prepreprints.

Morchang, A., J. Panaampon, and A. Suttitheptumrong. 2013. Biochemical and Biophysical Research Communications Role of cathepsin B in dengue virus-mediated apoptosis. Biochem. Biophys. Res. Commun. 438: 20–25.

Ocampo, C. B., P. A. Caicedo, G. Jaramillo, R. Ursic Bedoya, O. Baron, I. M. Serrato, D. M. Cooper, and C. Lowenberger. 2013. Differential Expression of Apoptosis Related Genes in Selected Strains of *Aedes aegypti* with Different Susceptibilities to Dengue Virus. PLoS One. 8(4): e61187.

Panjwani, A., and A. Wilson. 2016. What Is Stopping the Use of Genetically Modified Insects for Disease Control? PLoS Pathog. 12(10): e1005830.

Rueden, C. T., J. Schindelin, M. C. Hiner, B. E. DeZonia, A. E. Walter, E. T. Arena, and K. W. Eliceiri. 2017. ImageJ2: ImageJ for the next generation of scientific image data. BMC Bioinformatics. 18(1): 529.

Team, R. C. 2018. R: A Language and Environment for Statistical Computing.

West, K., K. C. Ernst, S. Haenchen, K. Dickinson, M. S. Doyle, K. Walker, A. J. Monaghan, M. H. Hayden, and O. Town. 2015. Awareness and Support of Release of Genetically Modified “Sterile” Mosquitoes, Key West, Florida, USA. Emerg. Infect. Dis. 21(2): 320-324.

Wickham, H. 2016. ggplot2: Elegant Graphics for Data Analysis. Springer-Verlag, New York.

Yu, Z., M. Ren, Z. Wang, B. Zhang, Y. S. Rong, R. Jiao, and G. Gao. 2013. Highly efficient genome modifications mediated by CRISPR/Cas9 in *Drosophila*. Genetics. 195: 289–291.

Zhang, L., and R. D. Reed. 2017. A Practical Guide to CRISPR/Cas9 Genome Editing in Lepidoptera, pp. 155–172. In Sekimura, T., Nijhout, H. (eds.), Divers. Evol. Butterfly Wing Patterns. Springer, Singapore.

Tables

Table 5.1 CRISPR guide RNA names and sequences. Guides were created using the Zhang Lab and MIT's CRISPR designe tool (crispr.mit.edu) to target exons (in order to disrupt translation) within two genes of interest: *xylosyltransferase* (AAEL007409) and *cathepsin-b* (AAEL007585) in *Aedes aegpyti*.

Construct name	Sequence (5' → 3')
Xylosyltransferase g1	AltR1/rArGrArGrUrUrUrGrCrArGrCrArUrUrUrCrCrGrGrGrUrUrUrUrArGrArGrCrUrArUrGrCrU/AltR2
Xylosyltransferase g2	AltR1/rGrCrUrArGrArGrUrUrUrGrCrArGrCrArUrUrUrCrGrUrUrUrUrArGrArGrCrUrArUrGrCrU/AltR2
Cathepsin-b g1	AltR1/rUrGrCrCrArGrCrCrUrCrUrCrCrCrUrGrUrCrGrGrGrUrUrUrUrArGrArGrCrUrArUrGrCrU/AltR2
Cathepsin-b g2	AltR1/rUrUrCrCrArCrCrGrArCrArGrGrGrArGrArGrGrCrGrUrUrUrUrArGrArGrCrUrArUrGrCrU/AltR2
Cathepsin-b g3	AltR1/rGrGrGrUrUrGrCrCrGrUrGrGrArGrGrUrArCrUrCrGrUrUrUrUrArGrArGrCrUrArUrGrCrU/AltR2

Table 5.2 Primer names and sequences designed to flank at least 100bp of the cut site for both *cathepsin-b* (AAEL007585) and *xylosyltransferase* (AAEL007409). The For1 and For2 primers for *cathepsin-b* are RNase H-dependant PCR (rhPCR) primers, while the rest of the primers are traditional PCR primers.

Name	Sequence
AAEL007585_For1	TCATTTTCGGATCTTTGGATCTGrUTGTCC/3SpC3/
AAEL007585_Rev1	GGACCTCCCGAAGAAAGAC
AAEL007585_Rev2	ATCTCTCAGTTGTAGCCATACC
AAEL007585_For2	CACCTATTTGGATCTACACGCrCTACAC/3SpC3/
AAEL007585_Rev2	ATCTCTCAGTTGTAGCCATACC
*Xylo*_F	CTCAGCAACTGGGAGCTCAA
*Xylo*_R	GTAGAGCCGCTTGCTCAGAT

Table 5.3 Measured continuous fitness parameters (pupal lifespan, time to hatching, larval lifespan, adult male lifespan, adult female lifespan and number of males and females hatched) from the *cathepsin-b* CRISPR-Cas9 injection experiment. Each line represents one biological replicate (separate injection experiment) for each of our four experimental treatments: wildtype control (un-injected, not handled), handled control (un-injected, handled), buffer injected (injected, handled), and *cathepsin-b* RNP injected (injected, handled). Injection date is included to aid in the separation of biological replicates.

Treatment	Injection date	Pupal lifespan (days)	Time to hatching (days)	Larval lifespan (days)	Adult male lifespan (days)	Adult female lifespan (days)	Number of males hatched	Number of females hatched
wildtype control	18-Sep	1.5	NA	NA	15	25.2	1	6
wildtype control	19-Sep	NA	NA	NA	NA	NA	1	2
wildtype control	20-Sep	NA	NA	NA	NA	NA	NA	NA
wildtype control	23-Sep	NA	NA	NA	NA	NA	NA	NA
wildtype control	26-Sep	NA	14	NA	NA	NA	NA	NA
wildtype control	27-Sep	NA	9	NA	NA	NA	NA	NA
wildtype control	3-Oct	2.75	12	NA	13.6	26.75	3	4
wildtype control	5-Oct	2	5	4	12.5	NA	4	3
wildtype control	6-Oct	2.66	9	4	26.8	NA	7	0
wildtype control	10-Oct	2.5	9	NA	27	NA	2	0
wildtype control	11-Oct	1.5	NA	NA	15.3	14	4	2
wildtype control	12-Oct	NA	NA	NA	NA	NA	1	NA
wildtype control	16-Oct	NA	4	NA	NA	NA	NA	NA
wildtype control	19-Oct	2	11	NA	20.5	27	12	7
wildtype control	24-Oct	3	NA	NA	NA	37	0	1
wildtype control	31-Oct	2.25	NA	NA	22	NA	1	3
wildtype control	1-Nov	2	NA	NA	19.3	20.5	4	2
CRISPR injected	07-Sep	2	2	3	18	16	1	1
CRISPR injected	12-Sep	2	2	6	NA	15	NA	1
CRISPR injected	13-Sep	2	2	5	17	8	2	1
CRISPR injected	14-Sep	NA	NA	NA	NA	NA	NA	NA

CRISPR injected	18-Sep	NA	NA	NA	NA	NA	NA	NA
CRISPR injected	20-Sep	4	2	3	27	NA	1	NA
CRISPR injected	21-Sep	NA	NA	NA	NA	NA	NA	NA
CRISPR injected	22-Sep	NA	NA	NA	NA	NA	NA	NA
CRISPR injected	23-Sep	NA	NA	NA	NA	NA	NA	NA
CRISPR injected	24-Sep	1	2	5	17	NA	1	NA
CRISPR injected	26-Sep	4	2	4	9	NA	2	NA
CRISPR injected	27-Sep	NA	NA	NA	NA	NA	NA	NA
CRISPR injected	28-Sep	NA	NA	NA	NA	NA	NA	NA
CRISPR injected	02-Oct	NA	NA	NA	NA	NA	NA	NA
CRISPR injected	03-Oct	4	2	10.3	8	24	1	1
CRISPR injected	04-Oct	NA	NA	NA	NA	NA	NA	NA
CRISPR injected	05-Oct	4	2	10	32	23	1	1
CRISPR injected	06-Oct	1	2	9	21	27	3	4
CRISPR injected	10-Oct	4	2	10	12	NA	1	NA
CRISPR injected	11-Oct	4	2	4	18	27	4	6
CRISPR injected	12-Oct	4	2	4	16	NA	2	NA
CRISPR injected	16-Oct	4	2	5	14	73	2	4
CRISPR injected	17-Oct	NA	NA	NA	NA	NA	NA	NA
CRISPR injected	18-Oct	4	3	4	NA	NA	1	NA
CRISPR injected	19-Oct	4	3	4	27	37	4	4
CRISPR injected	23-Oct	4	2	7	10	NA	1	NA
CRISPR injected	24-Oct	NA	NA	NA	NA	NA	NA	NA
CRISPR injected	25-Oct	NA	NA	NA	NA	NA	NA	NA
CRISPR injected	26-Oct	NA	NA	NA	NA	NA	NA	NA
CRISPR injected	27-Oct	NA	NA	NA	NA	NA	NA	NA
CRISPR injected	31-Oct	NA	2	4	NA	31	NA	1
buffer	31-Aug	NA	NA	NA	NA	NA	NA	NA
handled control	31-Aug	NA	NA	NA	NA	NA	NA	NA
buffer	2017-09-06	NA	NA	NA	NA	NA	NA	NA

handled control	2017-09-06	NA	NA	NA	NA	NA	NA	NA
buffer	2017-09-12	NA	NA	NA	NA	NA	NA	NA
handled control	2017-09-13	NA	NA	NA	NA	NA	NA	NA
buffer	2017-09-13	NA	NA	NA	NA	NA	NA	NA
handled control	2017-09-14	NA	NA	NA	NA	NA	NA	NA
buffer	2017-09-14	NA	NA	NA	NA	NA	NA	NA
handled control	2017-09-18	NA	NA	NA	NA	NA	NA	NA
handled control	2017-09-19	NA	NA	NA	NA	NA	NA	NA
buffer	2017-09-20	NA	NA	NA	NA	NA	NA	NA
handled control	2017-09-20	NA	NA	NA	NA	NA	NA	NA
handled control	2017-09-21	NA	NA	NA	NA	NA	NA	NA
buffer	2017-09-21	NA	NA	NA	NA	NA	NA	NA
buffer	2017-09-22	NA	NA	NA	NA	NA	NA	NA
handled control	2017-09-22	NA	NA	NA	NA	NA	NA	NA
handled control	2017-09-23	NA	NA	NA	NA	NA	NA	NA
handled control	2-Oct	3	18	NA	19	33.24	1	3
buffer	2-Oct	NA	NA	NA	NA	NA	NA	NA
handled control	03-Oct	2.5	7	NA	31	16.5	5	7
handled control	04-Oct	NA	NA	NA	NA	NA	NA	NA
handled control	05-Oct	3.3	5	NA	13.25	28.4	8	10
handled control	06-Oct	3	4	NA	11.125	16.8	7	5
buffer	06-Oct	NA	NA	NA	NA	NA	NA	NA
handled control	10-Oct	2	4	NA	20.15	26.7	14	12
buffer	10-Oct	2.5	9	NA	29.5	NA	2	0
handled control	11-Oct	2	NA	NA	15.75	23.75	4	5
buffer	11-Oct	NA	NA	NA	NA	NA	NA	NA
handled control	12-Oct	2.3	NA	NA	25.7	23.3	6	5
buffer	12-Oct	NA	NA	NA	NA	NA	NA	NA
handled control	16-Oct	1.5	4	NA	21.7	24.5	7	3
buffer	16-Oct	NA	NA	NA	NA	NA	NA	NA

handled control	17-Oct	2.5	NA	NA	24.25	27.15	3	6
buffer	17-Oct	NA	NA	NA	NA	NA	NA	NA
handled control	18-Oct	2	NA	NA	27.5	NA	3	0
buffer	18-Oct	NA	NA	NA	NA	NA	NA	NA
handled control	19-Oct	2	11	NA	24.3	19	4	3
buffer	19-Oct	2	11	NA	NA	17	0	2
handled control	23-Oct	2	NA	NA	16.3	23	7	6
buffer	23-Oct	NA	NA	NA	NA	NA	NA	NA
buffer	24-Oct	NA	NA	NA	NA	NA	NA	NA
handled control	24-Oct	2	NA	NA	18.75	12.5	5	4
handled control	27-Oct	3	NA	NA	NA	25	0	3
buffer	27-Oct	2.5	20	NA	29.6	26	0	2
handled control	31-Oct	1.7	NA	NA	19.3	9	4	5
buffer	01-Nov	NA	NA	NA	NA	NA	NA	NA
handled control	01-Nov	NA	4	NA	NA	NA	NA	NA
buffer	09-Nov	NA	NA	NA	NA	NA	NA	NA
handled control	09-Nov	NA	NA	NA	NA	NA	NA	NA

Table 5.4 Measured proportional fitness parameters (proportion of larvae hatched, proportion of pupae emerged, proportion of adults that ecolsed) from the *cathepsin-b* CRISPR-Cas9 injection experiment. Each line represents one biological replicate (separate injection experiment) for each of our four experimental treatments: wildtype control (un-injected, not handled), handled control (un-injected, handled), buffer injected (injected, handled), and *cathepsin-b* RNP injected (injected, handled).

Treatment	Proportion of larvae that hatched	Proportion of pupae that emerged	Proportion of adults that eclosed
wildtype control	0.24	0.64	1
wildtype control	0.1	1	1
wildtype control	0.22	1	1
wildtype control	0.03	1	1
wildtype control	0.53	1	1
wildtype control	0.07	1	1
wildtype control	0.14	0.88	1
wildtype control	0.21	0.89	0.88
wildtype control	0.13	1	1
wildtype control	0.13	1	0.67
wildtype control	0.08	1	1
wildtype control	0.01	1	1
wildtype control	0.01	1	1
wildtype control	0.42	0.96	0.95
wildtype control	0.01	1	1
wildtype control	0.07	1	0.8
wildtype control	0.06	1	1
CRISPR injected	0.03	1	1
CRISPR injected	0	1	1
CRISPR injected	0.01	1	1
CRISPR injected	0	NA	NA
CRISPR injected	0	NA	NA
CRISPR injected	0	1	1
CRISPR injected	0	NA	NA
CRISPR injected	0	NA	NA
CRISPR injected	0	NA	NA
CRISPR injected	0.01	1	1
CRISPR injected	0.01	1	1
CRISPR injected	0	NA	NA
CRISPR injected	0	NA	NA
CRISPR injected	0	NA	NA
CRISPR injected	0.01	0.67	1
CRISPR injected	0	NA	NA
CRISPR injected	0.01	1	1
CRISPR injected	0.03	1	0.88

CRISPR injected	0	1	1
CRISPR injected	0.03	1	1
CRISPR injected	0.01	1	1
CRISPR injected	0.02	1	1
CRISPR injected	0	NA	NA
CRISPR injected	0.01	1	1
CRISPR injected	0.04	1	1
CRISPR injected	0.01	0.5	1
CRISPR injected	0	NA	NA
CRISPR injected	0	NA	NA
CRISPR injected	0	NA	NA
CRISPR injected	0	NA	NA
CRISPR injected	0	1	1
buffer	0	NA	NA
handled control	0	NA	NA
buffer	0	NA	NA
handled control	0	NA	NA
buffer	0	NA	NA
handled control	0	NA	NA
buffer	0	NA	NA
handled control	0	NA	NA
buffer	0	NA	NA
handled control	0	NA	NA
handled control	0	NA	NA
buffer	0	NA	NA
handled control	0	NA	NA
handled control	0	NA	NA
buffer	0	NA	NA
buffer	0	NA	NA
handled control	0	NA	NA
handled control	0	NA	NA
handled control	0.09	1	1
buffer	0	NA	NA
handled control	0.15	0.92	1
handled control	0	NA	NA
handled control	0.41	0.95	0.95
handled control	0.31	0.25	1
buffer	0	NA	NA
handled control	0.52	1	0.96
buffer	0.04	1	1
handled control	0.12	1	1
buffer	0	NA	NA
handled control	0.18	1	1

buffer	0	NA	NA
handled control	0.33	0.93	1
buffer	0	NA	NA
handled control	0.16	1	1
buffer	0	NA	NA
handled control	0.07	1	1
buffer	0	NA	NA
handled control	0.13	1	1
buffer	0.07	1	1
handled control	0.27	0.88	0.87
buffer	0	NA	NA
buffer	0	NA	NA
handled control	0.1	1	0.9
handled control	0.04	1	1
buffer	0.13	1	1
handled control	0.14	0.9	1
buffer	0	NA	NA
handled control	0	NA	NA
buffer	0	NA	NA
handled control	0	NA	NA

Table 5.5 Measured egg-laying parameters (number of gonotrophic cycles per female, number of eggs from each gonotrophic cycle per female (1st, 2nd, and 3rd, and average egg size of eggs from each gonotrophic cycle (1st, 2nd, and 3rd) from the *cathepsin-b* CRISPR-Cas9 injection experiment. Each line represents one biological replicate (separate mating pair(s)) for each of our four experimental treatments: wildtype (wt) control (un-injected, not handled), handled control (un-injected, handled), buffer injected (injected, handled), and *cathepsin-b* RNP injected (injected, handled). The buffer injected, and handled pair mates remained within treatment (i.e. only buffer males and females mated, and only handled males and females mated). To create separate *cathepsin-b* KO lines (homozygous KO, heterozygous KO), *cathepsin-b* injected individuals were out-crossed with wt males or females.

Treatment	Number of Gonotrophic Cycles/Female	Number of eggs from the 1st gonotrophic cycle/Female	Number of eggs from the 2nd gonotrophic cycle/Female	Number of eggs from the 3rd gonotrophic cycle/Female	Average egg size from 1st gonotrophic cycle eggs	Average egg size from 2nd gonotrophic cycle eggs	Average egg size from 3rd gonotrophic cycle eggs
CRISPR injected F x CRISPR injected M	2	30	17	NA	0.4966	0.5504	NA
wt F x CRISPR injected M	0	NA	NA	NA	NA	NA	NA
CRISPR injected F x wt M	0	NA	NA	NA	NA	NA	NA
CRISPR injected F x CRISPR injected M	0	NA	NA	NA	NA	NA	NA
wt F x CRISPR injected M	0	NA	NA	NA	NA	NA	NA
wt F x CRISPR injected M	0	NA	NA	NA	NA	NA	NA
wt F x CRISPR injected M	1	4	NA	NA	0.4992	NA	NA
wt F x CRISPR injected M	0	NA	NA	NA	NA	NA	NA
wt F x CRISPR injected M	1	2.5	NA	NA	0.3712	NA	NA
wt F x CRISPR injected M	1	42	NA	NA	0.4946	NA	NA
wt F x CRISPR injected M	2	6.6	15.8	NA	0.4567	0.5058	NA
CRISPR injected F x wt M	1	30	NA	NA	0.5214	NA	NA
CRISPR injected F x wt M	0	NA	NA	NA	NA	NA	NA
CRISPR injected F x CRISPR injected M	1	7	NA	NA	0.3372	NA	NA
wt F x CRISPR injected M	0	NA	NA	NA	NA	NA	NA
CRISPR injected F x CRISPR injected M	2	2	1	NA	0.4955	0.584	NA

wt F x CRISPR injected M	3	79	76	54.5	0.4834	0.4644	0.4958
CRISPR injected F x CRISPR injected M	3	35	5	7	0.4702	0.4356	0.4594
CRISPR injected F x CRISPR injected M	1	73	NA	NA	0.5006	NA	NA
wt F x CRISPR injected M	2	73	12	NA	0.46	0.4538	NA
CRISPR injected F x CRISPR injected M	0	NA	NA	NA	NA	NA	NA
wt F x CRISPR injected M	1	56	NA	NA	0.4855	NA	NA
wt F x CRISPR injected M	0	NA	NA	NA	NA	NA	NA
CRISPR injected F x CRISPR injected M	0	NA	NA	NA	NA	NA	NA
CRISPR injected F x wt M	1	113	NA	NA	0.4018	NA	NA
CRISPR injected F x CRISPR injected M	0	NA	NA	NA	NA	NA	NA
CRISPR injected F x CRISPR injected M	1	94	NA	NA	0.4701	NA	NA
CRISPR injected F x CRISPR injected M	1	9	NA	NA	0.4204	NA	NA
CRISPR injected F x CRISPR injected M	0	NA	NA	NA	NA	NA	NA
wt F x CRISPR injected M	1	79	NA	NA	0.4594	NA	NA
CRISPR injected F x CRISPR injected M	3	72	12	26	0.5736	0.4114	0.4766
CRISPR injected F x CRISPR injected M	3	93	14	70	0.4688	0.494	0.5004
CRISPR injected F x CRISPR injected M	3	94	44	60	0.548	0.5777	0.472
CRISPR injected F x CRISPR injected M	3	72	47	21	0.4566	0.423	0.5978
wt F x CRISPR injected M	2	7	NA	NA	0.4988	NA	NA
CRISPR injected F x wt M	3	55	40	16	0.4716	0.552	0.5266
CRISPR injected F x wt M	0	NA	NA	NA	NA	NA	NA
CRISPR injected F x wt M	3	52	55	41	0.5656	0.4822	0.4118

CRISPR injected F x wt M	2	57	116	NA	0.481	0.493	NA
wt F x wt M	2	4	35.7	NA	0.5686	0.5706	NA
wt F x wt M	2	26.5	12	NA	0.5004	0.4689	NA
wt F x wt M	2	24	15.5	NA	0.492	0.517	NA
wt F x wt M	2	15	12	NA	0.563	0.4468	NA
wt F x wt M	3	47	27	40	0.5212	0.5152	0.5118
buffer F x buffer M	0	NA	NA	NA	NA	NA	NA
buffer F x buffer M	2	74	53	NA	0.4648	0.3778	NA
buffer F x buffer M	1	74	NA	NA	0.4648	NA	NA
buffer F x buffer M	0	NA	NA	NA	NA	NA	NA
handled F x handled M	2	64	59	NA	0.4188	0.515	NA
handled F x handled M	0	NA	NA	NA	NA	NA	NA
handled F x handled M	2	49	12	NA	0.503	0.5084	NA
handled F x handled M	1	43	NA	NA	0.4212	NA	NA
handled F x handled M	1	42	NA	NA	0.5858	NA	NA
handled F x handled M	0	NA	NA	NA	NA	NA	NA

Table 5.6 Statistical analyses completed on the fitness parameter data collected from *cathepsin-b* CRISPR-Cas9 injection experiment. All statistical analyses were completed using R (Team 2018). Panel **A** represents results from one-way ANOVAs completed on continuous data that passed Levene's Test for Homogeneity of Variance (time to hatching, number of eggs from each gonotrophic cycle, size of eggs from each gonotrophic cycle, larval lifespan, male lifespan, female lifespan, and pupal lifespan). Panel **B** shows the results from one-way ANOVAs completed on generalized linear model (family = quasibinomial, link=logit) results used to analyze proportional data (proportion of males and female, proportion of pupae hatched, proportion of adults hatched, proportion of larvae hatched). A generalized linear model (family=poisson, link=log) with another one-way ANOVA was used to investigate the number of gonotrophic cycles per females. *denotes statistically significant ($p<0.05$) parameters.

A.

Fitness Parameter Tested	dF	F value	Pr (>F)
Time to Hatching	3	2.737	0.0609
Number of eggs in the 1st gonotrophic cycle	5	1.352	0.27
Number of eggs in the 2nd gonotrophic cycle	5	2.103	0.122
Number of eggs in the 3rd gonotrophic cycle	3	0.239	0.866
Size of eggs in the 1st gonotrophic cycle	5	0.93	0.475
Size of eggs in the 2nd gonotrophic cycle	5	1.045	0.427
Size of eggs in the 3rd gonotrophic cycle	3	0.158	0.92
Larval lifespan	1	0.867	0.365
Male lifespan	3	2.418	0.0827
Female lifespan	3	0.577	0.635
Pupal lifespan	3	4.551	0.00777*

B.

Fitness Parameter Tested	dF	LR Chisq	Pr (>Chisq)
Proportion of males and females hatched	3	1.0812	0.7816
Proportion of pupae hatched	3	1.5903	0.6616
Proportion of adults hatched	3	4.4247	0.2191
Number of gonotrophic cycles	5	5.9397	0.3121
Proportion of larvae hatched	3	54.662	$8.107e^{-12}$ *

Figures

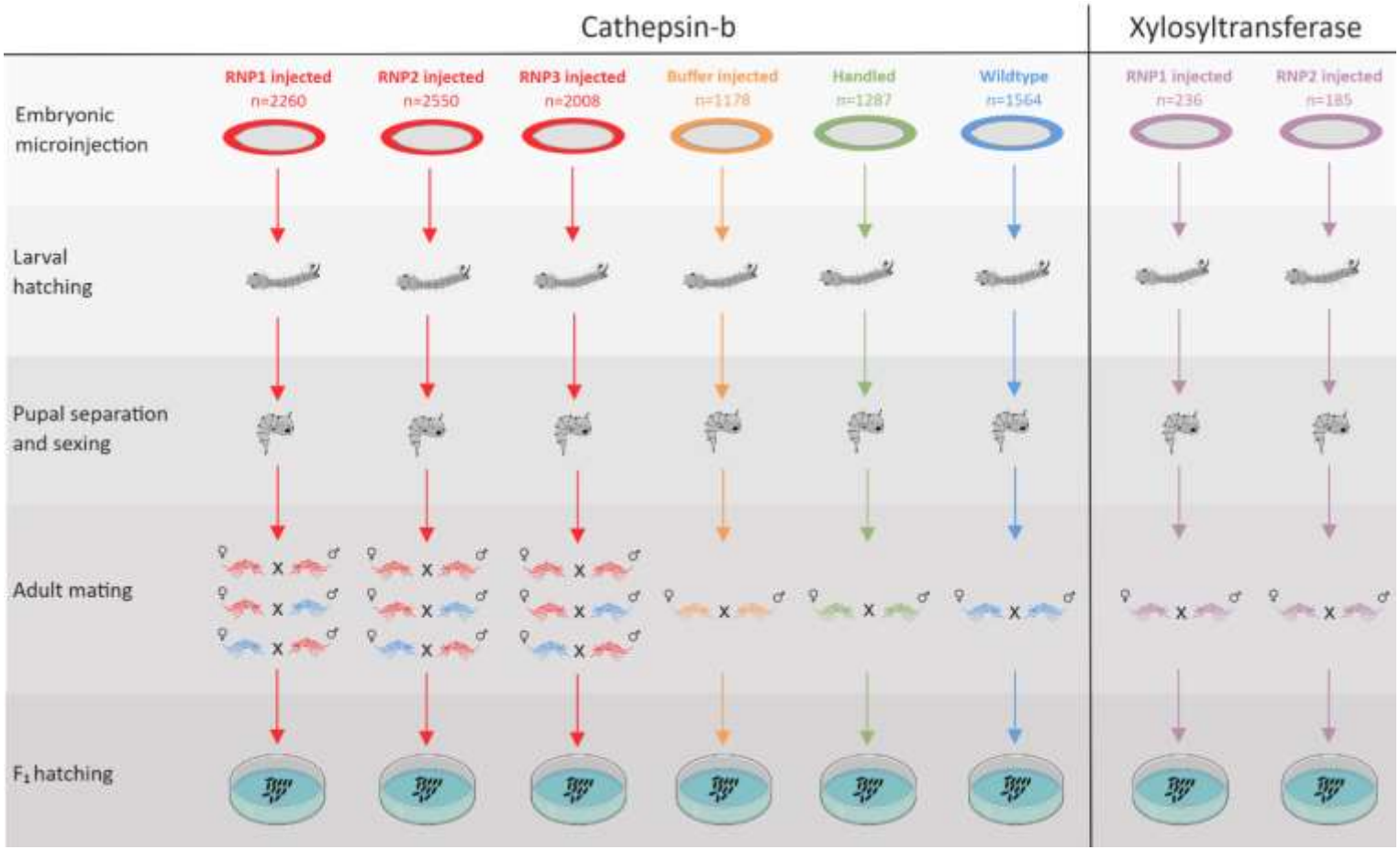

Figure 5.1 Methods flowchart detailing *Aedes aegpyti* CRISPR-Cas9 embroyonic injection experiments. All the steps in the *cathepsin-b* RNP injection experiment were completed at Simon Fraser University, while the embro injections for the *xylosyltransferase* RNP injection experiment were completed at the Insect Transformation Facility at the University of Maryland. Red denotes the *cathepsin-b* RNP injected treatment, orange is the buffer injected treatment, green is the handled treatment control, blue is the wildtype (uninjected, unhandled) treatment control, and purple is the *xylosyltransferase* RNP injected treatment.

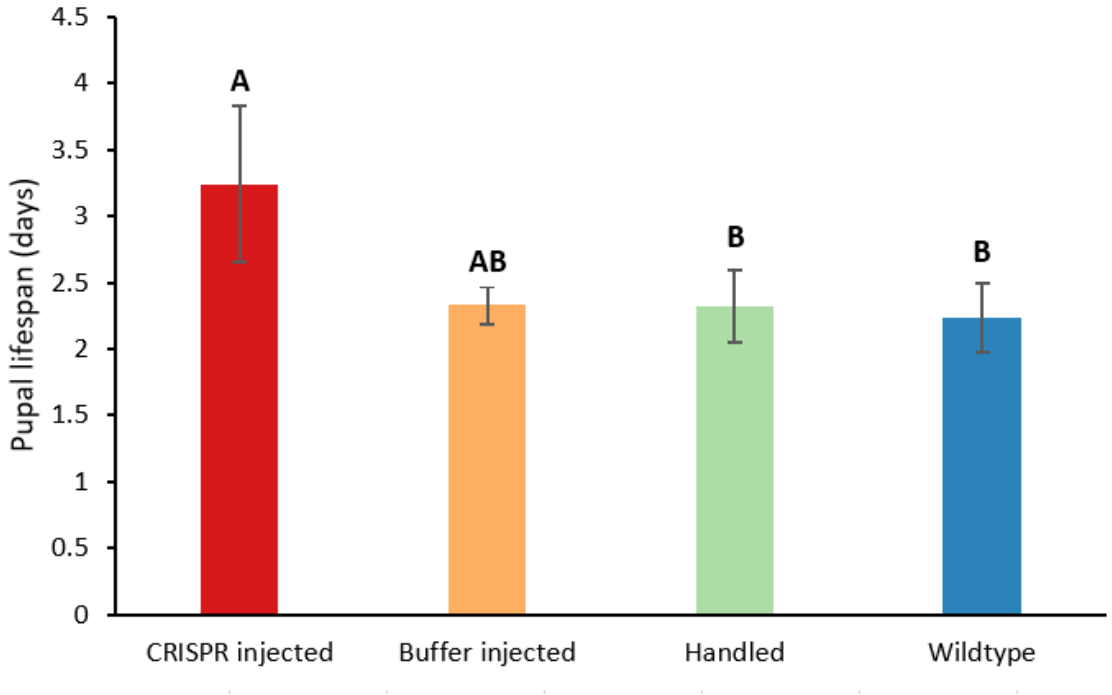

Figure 5.2 A one-way ANOVA with Tukey's post-hoc test was used to investigate differences between pupal lifespan (in days) across treatments in the *cathepsin-b* injection experiment (df=3, F=4.551, p<0.01).

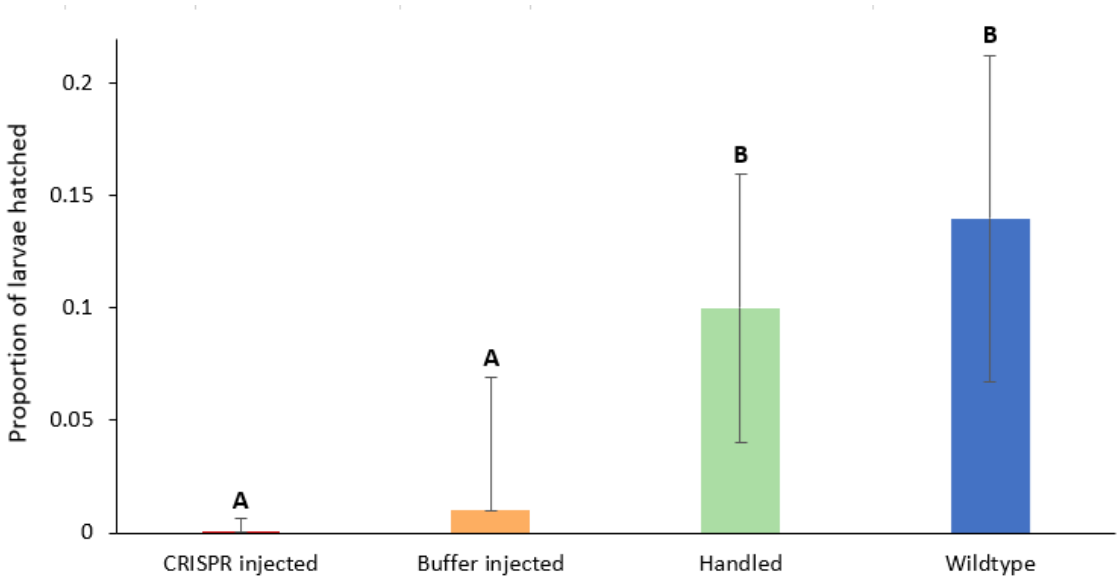

Figure 5.3 A generalized linear quasibinomial model with a logit link function was used to analyze differences between the proportion of larvae hatched across treatments in the *cathepsin-b* embryo injection experiment (df=3, p<0.001).

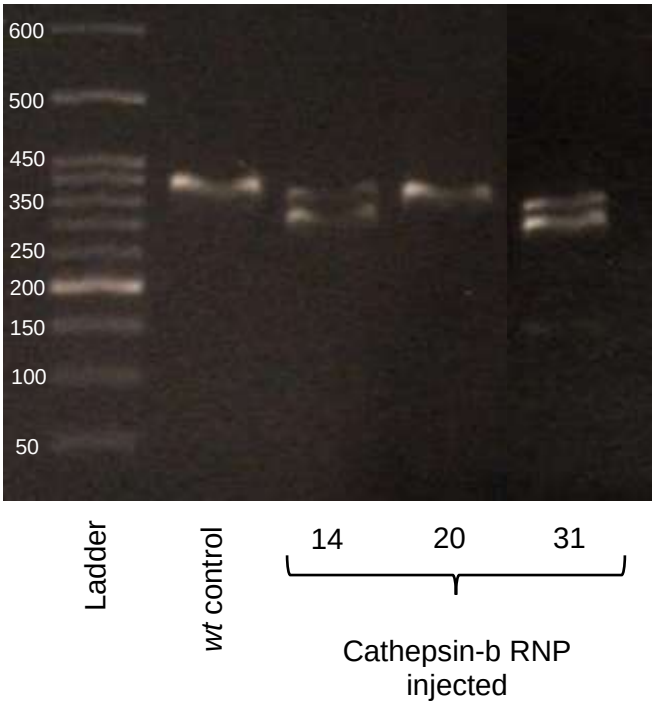

Figure 5.4 Heteroduplex assay (Alt-R Genome Editing Detection Kit, IDT) analyzing *cathepsin-b* gRNA targets. The leftmost lane is a 100bp ladder (100bp Opti-DNA Marker, abm), while the other four lanes each represent one individual mosquito. The *wt* control is an uninjected Liverpool *Aedes aegypti.* PCR projects were seperated in a 3% agarose gel. *Cathepsin-b* RNP injected individuals 14 and 31 show multiple bands (heteroduplexes), while the *wt* control and catepsin-b RNP injected individual 20 only show one band (homoduplexes).

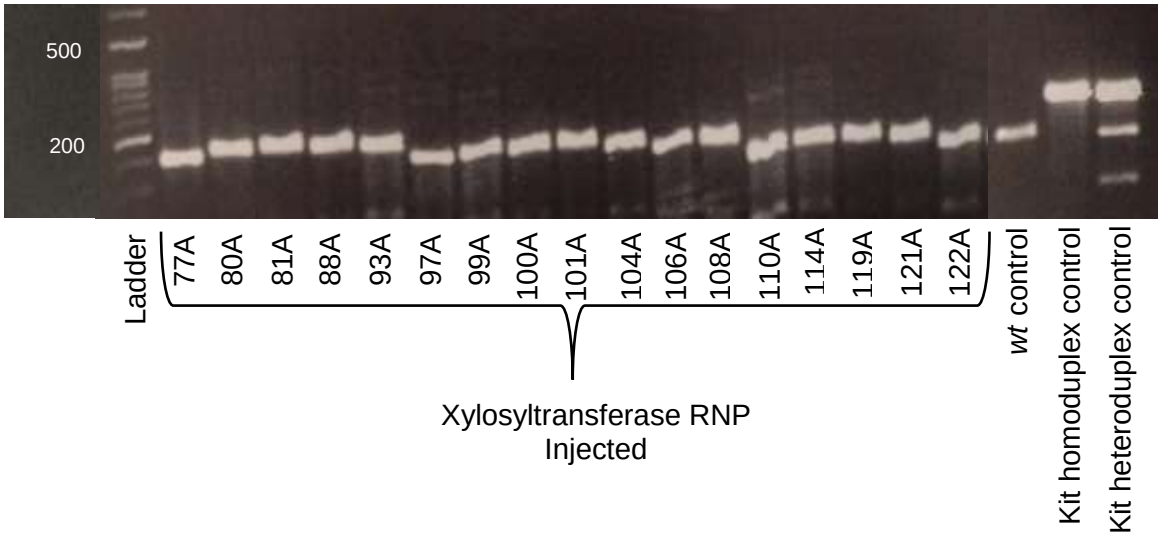

Figure 5.5 Heteroduplex assay (Alt-R Genome Editing Detection Kit, IDT) analyzing *xylosyltransferase* gRNA targets. The leftmost lane is a 100bp ladder (100bp Opti-DNA Marker, abm), while the other lanes each represent one individual mosquito injected with *xylosyltransferase* gRNA 1. The *wt* control is an uninjected Liverpool *Aedes aegypti*. PCR projects were seperated in a 3% agarose gel. *Xylosyltransferase* RNP injected individuals 93A, 97A, 99A, 106A, 108A, 110A, 114A and 122A show multiple bands (heteroduplexes), while the *wt* control and remaining *xylo*syltrasferase RNP injected individuals only show one band (homoduplexes). The kit homoduplex control shows one single band, while the kit heteroduplex control shows multiple bands.

Chapter 6. Conclusions

6.1. Summary

Dengue is an arthropod-borne viral disease that currently affects 390 million people worldwide (Bhatt et al. 2013). As the effects of climate change and urbanization continue to mount, and our human population continues to grow, the number of individuals at risk of dengue infection will increase dramatically (Kraemer et al. 2019). We do not have any means to treat infected individuals, nor do we have any preventative drugs or vaccines against dengue. As such, dengue control and prevention target the primary viral vector, *Aedes aegypti*. These vector control techniques aim to reduce mosquito populations by widespread insecticide sprays, sterile insect releases and via creating genetically modified mosquitoes with skewed sex ratios (McGraw and O'Neill 2013, Kyrou et al. 2018). Newer, more ecologically friendly, methods of control aim to replace dengue-transmitting mosquitoes with non-dengue transmitting mosquitoes via the insertion of a maternally inherited bacterium, *Wolbachia*, into adult female mosquito ovaries (McMeniman et al. 2009, McGraw and O'Neill 2013).

This dissertation aimed to characterize a naturally dengue-refractory *Aedes aegypti* mosquito strain found in and around the city of Cali, Colombia (Cali-MIB) (Ocampo and Wesson 2004). In order to characterize the Cali-MIB strain, we used a combination of molecular biology and bioinformatic tools to compare the Cali-MIB strain against a dengue-susceptible strain from the same geographical area (Cali-S). We then aimed to engineer a dengue-refractory strain based on these results.

We found the strongest evidence for a genetic basis of vector competence in our Cali-MIB mosquitoes, as assessed by our RNA sequencing (Chapter 2) and genome wide association study (GWAS) (Chapter 3). This genetic basis has been noted in other *Ae. aegypti* populations or colonies with varying degrees of refractoriness towards dengue (Bosio et al. 2000). In our GWAS study, we saw an accumulation of missense variants and in-frame insertions in Cali-MIB mosquitoes in genes (*xylosyltransferase oxt* and *heparan sulfate N-deacetylase/N-sulfotransferase*) involved in the biosynthesis of heparan sulfate. Heparan sulfate is a linear polysaccharide that has been implicated as a binding site for dengue viruses (Germi et al. 2002). We hypothesize that the variants present in both *xylosyltransferase oxt* and *heparan sulfate N-deacetylase/N-*

sulfotransferase halt the production of *heparan sulfate*, thus inhibiting dengue from entering midgut epithelial cells in *Ae. aegypti*. This midgut infection barrier (MIB) was observed by our midgut immunofluorescence assays and is the functional basis of the Cali-MIB phenotype.

In order to test this further, we completed RNAi based knock-downs for both *xylosyltransferase oxt* (*xylo*) and *heparan sulfate N-deacetylase/N-sulfotransferase* (*HS*) (Appendix B). We successfully induced a knock-down of both *xylo* and *HS* (Appendix B). Unfortunately based on logistical issues, we were unable to test whether these knock-downs or affected the vector competence of *Aedes aegypti*.

RNAi based functional knock-downs (testing the effect of the knock-downs on *Ae. aegypti* vector competence) were completed for multiple genes identified as significantly differentially expressed in Chapter 2 (Caicedo et al. 2018). These genes were also differentially expressed (Cali-MIB vs. Cali-S) at 30h post infectious blood feeding in a separate microarray study (Caicedo et al. 2018). Caicedo et al. 2018 found that RNAi based knock-downs of a *cathepsin-b*, a keratinocyte lectin, gram negative binding protein, and Niemann Pick Type-C2 in Cali-S mosquitoes reduced the titre of DENV-2, indicating that these four genes are involved in dengue infection in *Ae. aegypti*. None of the knock-downs completely eliminated dengue from the midgut of *Ae. aegypti*, suggesting that vector-competence in Cali-MIB mosquitoes may be the result of a multi-gene effect.

We found no evidence to suggest that the endogenous midgut microbiota of these mosquitoes contributes to their dengue-refractory nature, as the gut microbiomes of Cali-S and Cali-MIB mosquitoes were not significantly different (Chapter 4). This study was completed using sugar-fed mosquito guts and might not be representative of the bacterial community upon infectious blood feeding. It is also possible that small differences in abundance or species richness have large effects on secondary metabolites, which have been shown to play a role in dengue competence in *Ae. aegypti* (Angleró-Rodríguez et al. 2017).

Using results from our RNA sequencing study (Chapter 2), and our genome wide association study (Chapter 3), we attempted to create knock-out lines of *Ae. aegypti* using CRISPR-Cas9 as a genome editing tool. We completed in house RNP injections targeting *cathepsin-b* and sent off RNPs targeting *xylosyltransferase* to be injected at the Insect

Transformation Facility (Rockville, MD, USA). For both RNP constructs (*cathepsin-b* and *xylo*), we were able to create double-stranded breaks and modify the genome, creating indels in *cathepsin-b* and *xylo* (Chapter 5). New genetically modified individuals created with these constructs can now be exposed to dengue to test if our knock-outs change the vector competence of *Ae. aegypti*.

6.2. Future directions

This thesis identified multiple genes that should be investigated further as they may play pivotal roles in determining the dengue refractory and/or susceptible phenotypes that we have observed. It is highly likely that apoptosis and autophagy related genes also contributed to determining these phenotypes. These data suggest that multiple genes are expressed in both strains at different time points post infection. Some of these genes are downstream pathway effectors, while others are pathway inhibitors or indirectly involved in cell death processes. As such, future studies should aim to complete a time-course protein expression analysis on dengue infected Cali-MIB and Cali-S midguts to determine the ultimate outcome of cell death responses.

Our GWAS study identified some markers that could be used in simple one-step PCR reactions to quickly, and cost-effectively, identify Cali-MIB and Cali-S mosquitoes. Creating these PCR based identification assays would be paramount to obtaining pure dengue refractory and susceptible *Ae. aegypti* lines. Future work should incorporate the use of these assays into already established selection protocols. Notably, these assays should include males and females instead of the traditional female focused approach that has used previously. This will assist in understanding the genotype of future progeny and hopefully increase the proportion of dengue refractory individuals in our Cali-MIB colony.

The knock-out lines created through this work could be expanded significantly, incorporating fluorescent markers, a continuously expressed Cas9 protein, and a gene drive mechanism. Although these approaches have already been accomplished in *Ae. aegypti* (Dong et al. 2015, Kistler et al. 2015, Li et al. 2017), these changes have yet to target a gene that alters the vector competence of the mosquito. When used together, these changes could create a new, population replacement based, vector control strategy that may well dampen dengue transmission.

6.3. The challenges of vector control

Creating new, modified *Ae. aegypti* is not a trivial task. Paratransgenic techniques such as the insertion of *Wolbachia* into *Ae. aegypti* took thousands of attempts to complete (Walker et al. 2011). Multiple strains of *Wolbachia* infected *Ae. aegypti* were created (wMel, wMelPop, wMelPop-CLA) in order to overcome initial issues arising from negative fitness consequences associated with *Wolbachia* infection (Kambris et al. 2009). Despite the release of *Wolbachia* infected mosquitoes in Australia, Indonesia, Brazil, Vietnam, and Colombia, we are still unsure if there has been a decrease in dengue incidence (World Mosquito Program).

Genetically modified mosquitoes, such as Oxitec's OX513A *Ae. aegypti,* have also been released in Brazil, the Cayman Islands, Panama and India. These mosquitoes have been modified so that they are dependant on the antibiotic tetracycline for survival. Without tetracycline, the cellular development of the mosquito is impeded via interference with ubiquitin-dependent proteolysis (Gong et al. 2005). Oxitec releases a large number of antibiotic-deficient males into the target environment, who then mate with wildtype females. The resultant offspring do not develop properly, and pass away as larvae, thus decreasing the overall population of *Ae. aegypti*. The release of these self-limiting mosquitoes has decreased target *Ae. aegypti* populations in the Cayman Islands and in Brazil (Carvalho et al. 2015).

While releasing these modified mosquitoes seems like our current best option for vector control, co-ordinating these releases has proven difficult. Although research into methods and models to modify economically, medically and agriculturally important insects is moving forward (Buchman et al. 2018, Chaverra-Rodriguez et al. 2018), regulatory bodies such as the World Health Organization, the US Food and Drug Administration and the Environmental Protection Agency lag behind in developing policies to implement these new vector control approaches (Cumberland 2009). Compounding this lag are the perceptions by the public concerning genetically modified and paratransgenic insects. Some concerns are based on science and not wanting to remove a species from the ecosystem, while others are rooted in a mis-understanding of how these technologies work, and a fear of the unknown. Public support to implement these novel vector control strategies is paramount, as modified mosquitoes must be mass-produced and released in a vast number of highly populated urban areas.

As science continues to generate new methods of control, we need to create educational programs and government policies in parallel with scientific discoveries. Mitigating, preventing and managing dengue requires a collaborative global effort spanning numerous disciplines. We will only be able to achieve elimination goals by incorporating knowledge from scientific literature, regional health associations, and local residents. The data contained in this thesis may contribute to developing scientifically sound, and community acceptable approaches to dampen the transmission of dengue and other mosquito-borne pathogens.

6.4. References

Angleró-Rodríguez, Y., O. A. C. Talyuli, B. J. Blumberg, S. Kang, C. Demby, A. Shields, J. Carlson, N. Jupatanakul, and G. Dimopoulos. 2017. An *Aedes aegypti*-associated fungus increases susceptibility to dengue virus by modulating gut trypsin activity. Elife. 6: e28844.

Bhatt, S., P. W. Gething, O. J. Brady, J. P. Messina, A. W. Farlow, C. L. Moyes, J. M. Drake, J. S. Brownstein, A. G. Hoen, O. Sankoh, M. F. Myers, D. B. George, T. Jaenisch, G. R. William Wint, C. P. Simmons, T. W. Scott, J. J. Farrar, and S. I. Hay. 2013. The global distribution and burden of dengue. Nature. 496: 504–507.

Bosio, C., R. Fulton, M. Salasek, B. Beaty, and W. Iv. 2000. Quantitative trait loci that control vector competence for dengue-2 virus in the mosquito *Aedes aegypti*. Genetics. 156: 687–698.

Buchman, A., J. M. Marshall, D. Ostrovski, T. Yang, and O. Akbari. 2018. Synthetically engineered Medea gene drive system in the worldwide crop pest *Drosophila suzukii*. PNAS. 115: 4725–4730.

Caicedo, P. A., I. M. Serrato, S. Sim, G. Dimopoulos, H. Coatsworth, C. Lowenberger, and C. B. Ocampo. 2018. Immune response-related genes associated to blocking midgut dengue virus infection in *Aedes aegypti* strains that differ in susceptibility. Insect Sci. 26: 635–648.

Carvalho, D. O., A. R. McKemey, L. Garziera, R. Lacroix, C. A. Donnelly, L. Alphey, A. Malavasi, and M. L. Capurro. 2015. Suppression of a Field Population of *Aedes aegypti* in Brazil by Sustained Release of Transgenic Male Mosquitoes. PLoS Negl. Trop. Dis. 9(7): e0003864.

Chaverra-Rodriguez, D., V. M. Macias, G. L. Hughes, S. Pujhari, Y. Suzuki, D. R. Peterson, D. Kim, S. McKeand, and J. L. Rasgon. 2018. Targeted delivery of CRISPR-Cas9 ribonucleoprotein into arthropod ovaries for heritable germline gene editing. Nat. Commun. 9: 3008.

Cumberland, S. 2009. Mosquito wars. Bull. World Health Organ. 87: 167–168.

Dong, S., J. Lin, N. L. Held, R. J. Clem, A. L. Passarelli, and A. W. E. Franz. 2015. Heritable CRISPR/Cas9-mediated genome editing in the yellow fever mosquito, *Aedes aegypti.* PLoS One. 10(3): 1–13.

Germi, R., J.-M. Crance, D. Garin, J. Guimet, H. Lortat-Jacob, R. Ruigrok, J.-P. Zarski, and E. Drouet. 2002. *Heparan sulfate*-Mediated Binding of Infectious Dengue Virus Type 2 and Yellow Fever Virus. Virology. 168: 162–168.

Gong, P., M. J. Epton, G. Fu, S. Scaife, A. Hiscox, K. C. Condon, G. C. Condon, N. I. Morrison, D. W. Kelly, T. Dafa'alla, P. G. Coleman, and L. Alphey. 2005. A dominant lethal genetic system for autocidal control of the Mediterranean fruitfly. Nat. Biotechnol. 23: 453–456.

Kambris, Z., P. E. Cook, H. K. Phuc, and S. P. Sinkins. 2009. Immune activation by life-shortening *Wolbachia* and reduced filarial competence in mosquitoes. Science. 326(5949): 134–136.

Kistler, K. E., L. B. Vosshall, and B. J. Matthews. 2015. Genome engineering with CRISPR-Cas9 in the mosquito *Aedes aegypti*. Cell Rep. 11: 51–60.

Kraemer, M. U. G., R. C. J. Reiner, O. J. Brady, J. P. Messina, M. Gilbert, D. M. Pigott, D. Yi, K. Johnson, L. Earl, L. B. Marczak, S. Shirude, D. Weaver N., D. Bisanzio, T. A. Perkins, S. Lai, X. Lu, P. Jones, G. E. Coelho, R. G. Carvalho, W. Van Bortel, C. Marsboom, G. Hendrickx, F. Schaffner, C. G. Moore, H. H. Nax, L. Bengtsson, E. Wetter, A. J. Tatem, J. S. Brownstein, D. L. Smith, L. Lambrechts, S. Cauchemex, C. Linard, N. R. Faria, O. G. Pybus, T. W. Scott, W. Liu, H. Yu, G. R. W. Wint, S. I. Hay, and N. Golding. 2019. Past and future spread of the arbovirus vectors *Aedes aegypti* and *Aedes albopictus*. Nat. Microbiol. May 4: 845–863.

Kyrou, K., A. M. Hammond, R. Galizi, N. Kranjc, A. Burt, A. K. Beaghton, T. Nolan, and A. Crisanti. 2018. A CRISPR – Cas9 gene drive targeting doublesex causes complete population suppression in caged *Anopheles gambiae* mosquitoes. Nat. Biotechnol. 36(11): 1062-1066.

Li, M., M. Bui, T. Yang, C. S. Bowman, B. J. White, and O. S. Akbari. 2017. Germline Cas9 expression yields highly efficient genome engineering in a major worldwide disease vector, *Aedes aegypti*. Proc. Natl. Acad. Sci. 114(49): E10540-E10549.

McGraw, E. A., and S. L. O'Neill. 2013. Beyond insecticides: New thinking on an ancient problem. Nat. Rev. Microbiol. 11: 181–193.

McMeniman, C. J., R. V. Lane, B. N. Cass, A. W. Fong, M. Sidhu, Y. F. Wang, and S. L. O'Neill. 2009. Stable Introduction of a Life-Shortening *Wolbachia* Infection into the Mosquito *Aedes aegypti*. Science. 323(5910): 141–144.

Ocampo, C. B., and D. M. Wesson. 2004. Population dynamics of *Aedes aegypti* from a dengue hyperendemic urban setting in Colombia. Am. J. Trop. Med. Hyg. 71: 506–513.

Walker, T., P. H. Johnson, I. I. Ormaetxe, F. D. Frenitu, C. J. McMeniman, Y. S. Leong, Y. Dong, J. Axford, P. Kriesner, A. L. Lloyd, S. A. Ritchie, S. L. O'Neill, and A. a Hoffmann. 2011. The wMel *Wolbachia* strain blocks dengue and invades caged *Aedes aegypti* populations. Nature. 476: 450–453.

Appendix A. Supplementary data for Chapter 2

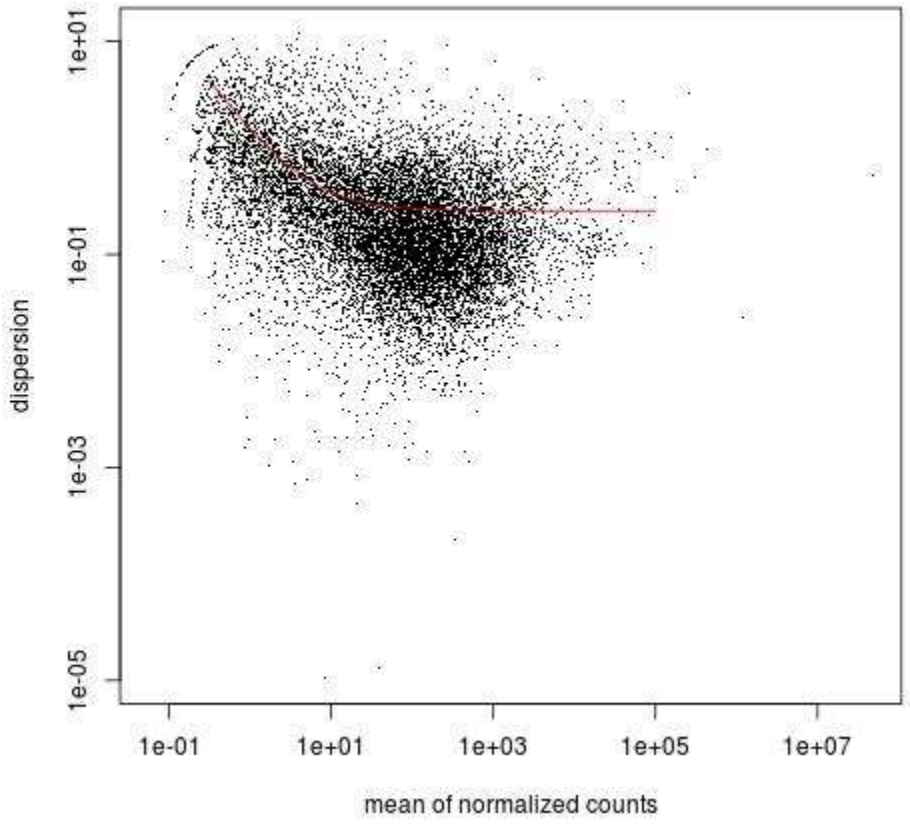

Figure A1. RNA-seq heteroskedastic mean and variation distribution. The homoscedastic data test results are shown displaying the correlation between variance within data and mean. Each black point represents a gene expression count, and the red line represents the mean fitted value.

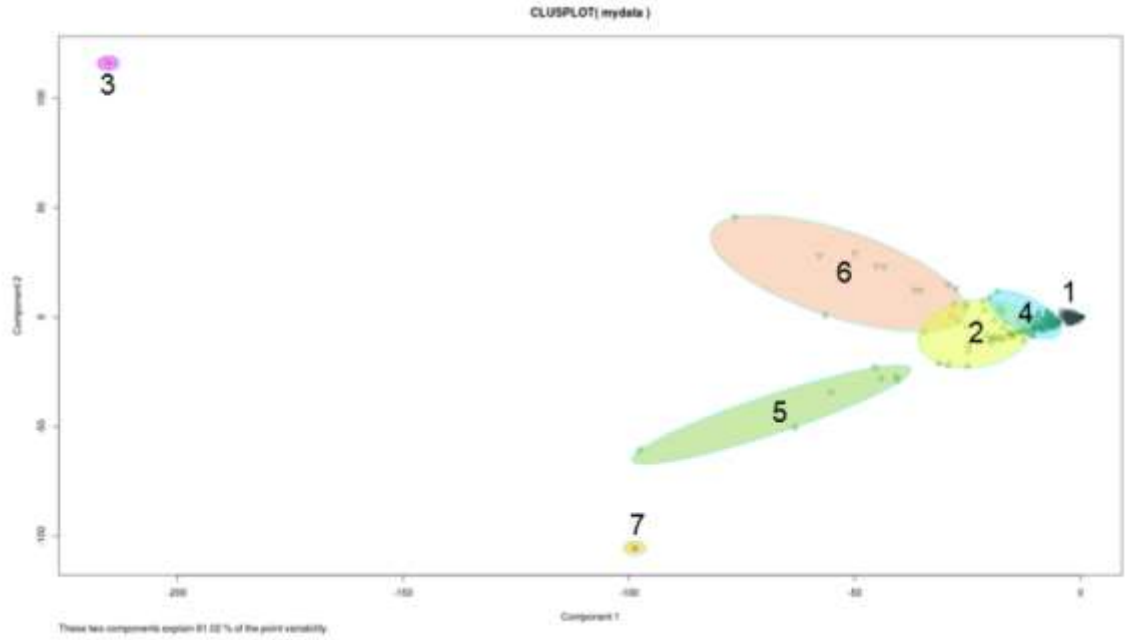

Figure A2. K-means (partitioning) clustering on all gene expression data using R (v. 3.1.1). Cluster 1 (purple) represented a wide variety of functional classes, Clusters 2 (yellow) and 4 (teal) were associated with ribosomal intracellular and translation functions, Clusters 3 (fuc*HS*ia), 6 (red) and 7 (orange) all related to serine-type peptidase activity, and Cluster 5 (green) was made up of mostly metallopeptidases.

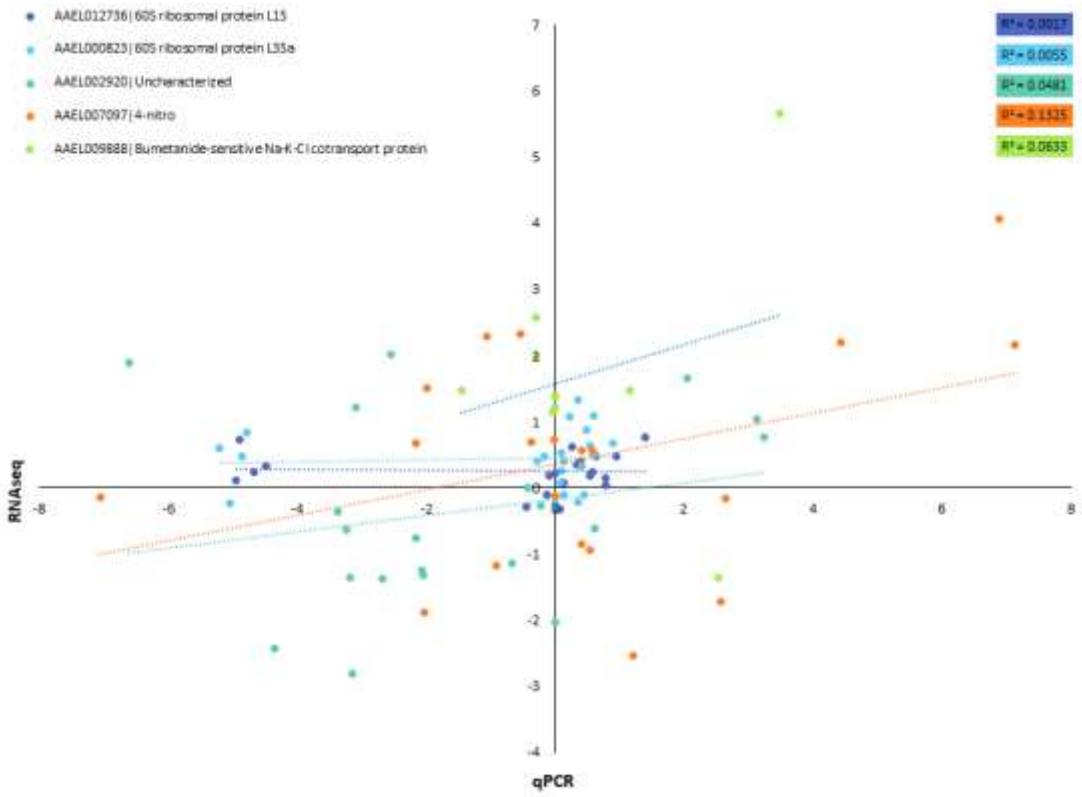

Figure A3. Comparison between qPCR validation and RNAseq data. A scatter plot of qPCR (y-axis) and GFOLD RNAseq values (x-axis) displays the expression values for selected candidate and non-candidate genes. An R2 value and line of best fit of these relationships is shown on the figure displaying the overall concordance between the two datasets for each gene.

Table A1. An overview of all 24 differential expression analyses completed. A list of what samples were compared under each different analysis type, separating out the effect of time, virus and strain.

Type of Differential Analysis	Samples to Compare		Biological Replicates
time series (within condition and strain) - isolating the effect of time	S1 (Sb24)	S2 (Sb36)	No
	S2 (Sb36)	S3 (Sb48)	No
	S1(Sb24)	S3 (Sb48)	No
	S4 (Sv24)	S5 (Sv36)	No
	S5 (Sv36)	S6 (Sv48)	No
	S4 (Sv24)	S6 (Sv48)	No
	R7 (Rb24)	R8 (Rb36)	No
	R8 (Rb36)	R9 (Rb48)	No
	R7 (Rb24)	R9 (Rb48)	No
	R10 (Rv24)	R11 (Rv36)	No
	R11 (Rv36)	R12 (Rv48)	No
	R10 (Rv24)	R12 (Rv48)	No
time points (between conditions within strain) - isolating the effect of virus	S1 (Sb24)	S4 (Sv24)	No
	S2 (Sb36)	S5 (Sv36)	No
	S3 (Sb48)	S6 (Sv48)	No
	R7 (Rb24)	R10 (Rv24)	No
	R8 (Rb36)	R11 (Rv36)	No
	R9 (Rb48)	R12 (Rv48)	No
time points (within condition and across strain) - isolating the effect of strain	S4 (Sv24)	R10 (Rv24)	No
	S5 (Sv36)	R11 (Rv36)	No
	S6 (Sv48)	R12 (Rv48)	No
between conditions (across all times and within a strain) - isolating the effect of virus	S1 (Sb24),S2 (Sb36),S3 (Sb48)	S4 (Sv24),S5 (Sv36),S6 (Sv48)	Yes
	R7 (Rb24), R8 (Rb36), R9 (Rb48)	R10 (Rv24), R11 (Rv36), R12 (Rv48)	Yes
between strains (across all times and within a condition) - isolating the effect of strain	S4 (Sv24), S5 (Sv36), S6 (Sv48)	R10 (Rv24), R11 (Rv36), R12 (Rv48)	Yes

Table A2. The list of genes classified as immune related, as mined from ImmunoDB. Only genes with a confirmed and high confidence status (A and B) were kept for classification.

Gene ID	Name	Subfamily	Family
AAEL013815	*APG10*	APHAG	Autophagy Genes
AAEL009089	*APG12*	APHAG	Autophagy Genes
AAEL013063	*APG18A*	APHAG	Autophagy Genes
AAEL013995	*APG18B*	APHAG	Autophagy Genes
AAEL003799	*APG2*	APHAG	Autophagy Genes
AAEL000955	*APG3*	APHAG	Autophagy Genes
AAEL010516	*APG4A*	APHAG	Autophagy Genes
AAEL007228	*APG4B*	APHAG	Autophagy Genes
AAEL002286	*APG5*	APHAG	Autophagy Genes
AAEL010427	*APG6*	APHAG	Autophagy Genes
AAEL010641	*APG7A*	APHAG	Autophagy Genes
AAEL012306	*APG7B*	APHAG	Autophagy Genes
AAEL007162	*APG8*	APHAG	Autophagy Genes
AAEL009105	*APG9*	APHAG	Autophagy Genes
AAEL001521	*BUFFY*	APHAG	Autophagy Genes
AAEL001515	*DEBCL*	APHAG	Autophagy Genes
AAEL000693	*TOR*	APHAG	Autophagy Genes
AAEL015246	*AGO1A*	Argonaute	Small Regulatory RNA Path
AAEL012410	*AGO1B*	Argonaute	Small Regulatory RNA Path
AAEL007823	*AGO3*	Argonaute	Small Regulatory RNA Path
AAEL000872	*ARK*	ARK	Caspase Activators
AAEL010693	*ARM1*	Armitage	Small Regulatory RNA Path
AAEL010696	*ARM2*	Armitage	Small Regulatory RNA Path
AAEL003389	*ATT*	Attacin	AMPs
AAEL000709	*CACT*	CACT	TOLLPAT*HS*
AAEL014738	*CASPAR1*	CASPAR	IMDPAT*HS*
AAEL003579	*CASPAR2*	CASPAR	IMDPAT*HS*
AAEL014148	*CASPL1*	CASPL	Caspases
AAEL011562	*CASPL2*	CASPL	Caspases
AAEL005963	*CASPS15*	CASPS	Caspases
AAEL005956	*CASPS16*	CASPS	Caspases
AAEL003439	*CASPS18*	CASPS	Caspases
AAEL003444	*CASPS19*	CASPS	Caspases
AAEL014658	*CASPS20*	CASPS	Caspases
AAEL014348	*CASPS8*	CASPS	Caspases
AAEL013407	*CAT1B*	CAT	Catalases
AAEL000627	*CECA*	Cecropin	AMPs
AAEL004223	*CECB*	Cecropin	AMPs
AAEL000598	*CECD*	Cecropin	AMPs
AAEL000611	*CECE*	Cecropin	AMPs
AAEL000625	*CECF*	Cecropin	AMPs
AAEL015515	*CECG*	Cecropin	AMPs

AAEL000775	*CECI*	Cecropin	AMPs
AAEL000777	*CECJ*	Cecropin	AMPs
AAEL000621	*CECN*	Cecropin	AMPs
AAEL002601	*CLIPA1*	CLIPA	CLIPs
AAEL001675	*CLIPA10*	CLIPA	CLIPs
AAEL002126	*CLIPA15*	CLIPA	CLIPs
AAEL008404	*CLIPA16*	CLIPA	CLIPs
AAEL007006	*CLIPA17*	CLIPA	CLIPs
AAEL005718	*CLIPA3*	CLIPA	CLIPs
AAEL000074	*CLIPB1*	CLIPB	CLIPs
AAEL003243	*CLIPB13A*	CLIPB	CLIPs
AAEL003253	*CLIPB13B*	CLIPB	CLIPs
AAEL014349	*CLIPB15*	CLIPB	CLIPs
AAEL005648	*CLIPB16*	CLIPB	CLIPs
AAEL000059	*CLIPB19*	CLIPB	CLIPs
AAEL001084	*CLIPB21*	CLIPB	CLIPs
AAEL008668	*CLIPB22*	CLIPB	CLIPs
AAEL012785	*CLIPB23*	CLIPB	CLIPs
AAEL014140	*CLIPB24*	CLIPB	CLIPs
AAEL014137	*CLIPB25*	CLIPB	CLIPs
AAEL003280	*CLIPB26*	CLIPB	CLIPs
AAEL007993	*CLIPB27*	CLIPB	CLIPs
AAEL013245	*CLIPB28*	CLIPB	CLIPs
AAEL006674	*CLIPB29*	CLIPB	CLIPs
AAEL000760	*CLIPB30*	CLIPB	CLIPs
AAEL006161	*CLIPB31*	CLIPB	CLIPs
AAEL000086	*CLIPB32*	CLIPB	CLIPs
AAEL000099	*CLIPB33*	CLIPB	CLIPs
AAEL000028	*CLIPB34*	CLIPB	CLIPs
AAEL000037	*CLIPB35*	CLIPB	CLIPs
AAEL005431	*CLIPB37*	CLIPB	CLIPs
AAEL003628	*CLIPB38*	CLIPB	CLIPs
AAEL003632	*CLIPB39*	CLIPB	CLIPs
AAEL003614	*CLIPB40*	CLIPB	CLIPs
AAEL003631	*CLIPB41*	CLIPB	CLIPs
AAEL006168	*CLIPB42*	CLIPB	CLIPs
AAEL014354	*CLIPB43*	CLIPB	CLIPs
AAEL005060	*CLIPB44*	CLIPB	CLIPs
AAEL001077	*CLIPB45*	CLIPB	CLIPs
AAEL005093	*CLIPB46*	CLIPB	CLIPs
AAEL005064	*CLIPB5*	CLIPB	CLIPs
AAEL000038	*CLIPB6-B36*	CLIPB	CLIPs
AAEL003625	*CLIPB8*	CLIPB	CLIPs
AAEL003610	*CLIPB9*	CLIPB	CLIPs
AAEL011991	*CLIPC1*	CLIPC	CLIPs
AAEL011593	*CLIPC11*	CLIPC	CLIPs

AAEL012711	*CLIPC12*	CLIPC	CLIPs
AAEL012712	*CLIPC13*	CLIPC	CLIPs
AAEL004948	*CLIPC14*	CLIPC	CLIPs
AAEL010270	*CLIPC15*	CLIPC	CLIPs
AAEL012713	*CLIPC16*	CLIPC	CLIPs
AAEL007593	*CLIPC2*	CLIPC	CLIPs
AAEL007597	*CLIPC3*	CLIPC	CLIPs
AAEL004518	*CLIPC5A*	CLIPC	CLIPs
AAEL004524	*CLIPC5B*	CLIPC	CLIPs
AAEL004540	*CLIPC6*	CLIPC	CLIPs
AAEL007796	*CLIPD1*	CLIPD	CLIPs
AAEL015109	*CLIPD10*	CLIPD	CLIPs
AAEL011375	*CLIPD11*	CLIPD	CLIPs
AAEL004979	*CLIPD2*	CLIPD	CLIPs
AAEL002997	*CLIPD3*	CLIPD	CLIPs
AAEL002124	*CLIPD6*	CLIPD	CLIPs
AAEL015439	*CLIPD7*	CLIPD	CLIPs
AAEL005906	*CLIPD8*	CLIPD	CLIPs
AAEL000238	*CLIPD9*	CLIPD	CLIPs
AAEL010773	*CLIPE10*	CLIPE	CLIPs
AAEL005800	*CLIPE11*	CLIPE	CLIPs
AAEL005644	*CLIPE12*	CLIPE	CLIPs
AAEL005792	*CLIPE8*	CLIPE	CLIPs
AAEL001233	*CLIPE9*	CLIPE	CLIPs
AAEL009338	*CTL10*	CTL	C-Type Lectins
AAEL008299	*CTL11*	CTL	C-Type Lectins
AAEL008681	*CTL12*	CTL	C-Type Lectins
AAEL004679	*CTL13*	CTL	C-Type Lectins
AAEL011453	*CTL14*	CTL	C-Type Lectins
AAEL012353	*CTL15*	CTL	C-Type Lectins
AAEL000533	*CTL16*	CTL	C-Type Lectins
AAEL011446	*CTL17*	CTL	C-Type Lectins
AAEL005482	*CTL18*	CTL	C-Type Lectins
AAEL011404	*CTL19*	CTL	C-Type Lectins
AAEL011407	*CTL20*	CTL	C-Type Lectins
AAEL011408	*CTL21*	CTL	C-Type Lectins
AAEL011609	*CTL22*	CTL	C-Type Lectins
AAEL006456	*CTL23*	CTL	C-Type Lectins
AAEL002524	*CTL24*	CTL	C-Type Lectins
AAEL000556	*CTL25*	CTL	C-Type Lectins
AAEL003119	*CTL6*	CTL	C-Type Lectins
AAEL010992	*CTL8*	CTL	C-Type Lectins
AAEL013748	*CTL9*	CTL	C-Type Lectins
AAEL011402	*CTL26*	CTL+OTHER	C-Type Lectins
AAEL011078	*CTLGA1*	CTLGA	C-Type Lectins
AAEL013566	*CTLGA2*	CTLGA	C-Type Lectins

AAEL011070	*CTLGA3*	CTLGA	C-Type Lectins
AAEL005641	*CTLGA5*	CTLGA	C-Type Lectins
AAEL009209	*CTLGA6*	CTLGA	C-Type Lectins
AAEL011610	*CTLGA7*	CTLGA	C-Type Lectins
AAEL011619	*CTLGA8*	CTLGA	C-Type Lectins
AAEL014385	*CTLGA9*	CTLGA	C-Type Lectins
AAEL011079	*CTLMA10*	CTLMA	C-Type Lectins
AAEL000543	*CTLMA11*	CTLMA	C-Type Lectins
AAEL011455	*CTLMA12*	CTLMA	C-Type Lectins
AAEL011621	*CTLMA13*	CTLMA	C-Type Lectins
AAEL014382	*CTLMA14*	CTLMA	C-Type Lectins
AAEL000563	*CTLMA15*	CTLMA	C-Type Lectins
AAEL000283	*CTLMA16*	CTLMA	C-Type Lectins
AAEL011612	*CTLMA6*	CTLMA	C-Type Lectins
AAEL008929	*CTLSE1*	CTLSE	C-Type Lectins
AAEL014356	*CTLSE2*	CTLSE	C-Type Lectins
AAEL003841	*DEFA*	*Defensin*	AMPs
AAEL003832	*DEFC*	*Defensin*	AMPs
AAEL003857	*DEFD*	*Defensin*	AMPs
AAEL003849	*DEFE*	*Defensin*	AMPs
AAEL001612	*DCR1*	Dicer	Small Regulatory RNA Path
AAEL006794	*DCR2*	Dicer	Small Regulatory RNA Path
AAEL004833	*DPT*	Diptericin	AMPs
AAEL012471	*DOME*	DOME	JAKSTATs
AAEL008592	*DROSHA*	Drosha	Small Regulatory RNA Path
AAEL001932	*FADD*	FADD	IMDPAT*HS*
AAEL009326	*FMR1*	FMR	Small Regulatory RNA Path
AAEL010131	*FREP1*	FREP	Fibrinogen-Related Proteins
AAEL009723	*FREP11*	FREP	Fibrinogen-Related Proteins
AAEL011634	*FREP12*	FREP	Fibrinogen-Related Proteins
AAEL011009	*FREP13*	FREP	Fibrinogen-Related Proteins
AAEL007942	*FREP14*	FREP	Fibrinogen-Related Proteins
AAEL000508	*FREP15*	FREP	Fibrinogen-Related Proteins
AAEL011633	*FREP16*	FREP	Fibrinogen-Related Proteins
AAEL006704	*FREP18*	FREP	Fibrinogen-Related Proteins
AAEL001713	*FREP2*	FREP	Fibrinogen-Related Proteins
AAEL000726	*FREP20*	FREP	Fibrinogen-Related Proteins
AAEL000749	*FREP22*	FREP	Fibrinogen-Related Proteins
AAEL008104	*FREP23*	FREP	Fibrinogen-Related Proteins
AAEL013417	*FREP24*	FREP	Fibrinogen-Related Proteins
AAEL005194	*FREP26*	FREP	Fibrinogen-Related Proteins
AAEL003156	*FREP28*	FREP	Fibrinogen-Related Proteins
AAEL013506	*FREP29*	FREP	Fibrinogen-Related Proteins
AAEL003294	*FREP3*	FREP	Fibrinogen-Related Proteins
AAEL010103	*FREP32*	FREP	Fibrinogen-Related Proteins
AAEL006702	*FREP33*	FREP	Fibrinogen-Related Proteins

AAEL010117	*FREP35*	FREP	Fibrinogen-Related Proteins
AAEL011400	*FREP36*	FREP	Fibrinogen-Related Proteins
AAEL011007	*FREP37*	FREP	Fibrinogen-Related Proteins
AAEL015428	*FREP38*	FREP	Fibrinogen-Related Proteins
AAEL009384	*FREP5*	FREP	Fibrinogen-Related Proteins
AAEL004156	*FREP9*	FREP	Fibrinogen-Related Proteins
AAEL003840	*GALE11*	GALE	Galactoside-Binding Lectins
AAEL009842	*GALE12*	GALE	Galactoside-Binding Lectins
AAEL009845	*GALE13*	GALE	Galactoside-Binding Lectins
AAEL009850	*GALE14*	GALE	Galactoside-Binding Lectins
AAEL012135	*GALE2*	GALE	Galactoside-Binding Lectins
AAEL004196	*GALE3*	GALE	Galactoside-Binding Lectins
AAEL005294	*GALE6A*	GALE	Galactoside-Binding Lectins
AAEL012003	*GALE6B*	GALE	Galactoside-Binding Lectins
AAEL005293	*GALE8A*	GALE	Galactoside-Binding Lectins
AAEL012001	*GALE8B*	GALE	Galactoside-Binding Lectins
AAEL004522	*GAM*	Gambicin	AMPs
AAEL007626	*GNBPA1*	GNBPA	GNBPs
AAEL000652	*GNBPA2*	GNBPA	GNBPs
AAEL003889	*GNBPB1*	GNBPB	GNBPs
AAEL009176	*GNBPB3*	GNBPB	GNBPs
AAEL009178	*GNBPB4*	GNBPB	GNBPs
AAEL003894	*GNBPB5*	GNBPB	GNBPs
AAEL007064	*GNBPB6*	GNBPB	GNBPs
AAEL012069	*GPXH1*	GPX	Peroxidases
AAEL008397	*GPXH2*	GPX	Peroxidases
AAEL000495	*GPXH3*	GPX	Peroxidases
AAEL012553	*HOP*	HOP	JAKSTATs
AAEL003933	*DBLOX*	HPX	Peroxidases
AAEL007563	*DUOX*	HPX	Peroxidases
AAEL006014	*HPX1*	HPX	Peroxidases
AAEL013171	*HPX2*	HPX	Peroxidases
AAEL005416	*HPX3*	HPX	Peroxidases
AAEL000376	*HPX4*	HPX	Peroxidases
AAEL002354	*HPX5*	HPX	Peroxidases
AAEL012481	*HPX6*	HPX	Peroxidases
AAEL004401	*HPX7*	HPX	Peroxidases
AAEL004388	*HPX8A*	HPX	Peroxidases
AAEL004390	*HPX8B*	HPX	Peroxidases
AAEL004386	*HPX8C*	HPX	Peroxidases
AAEL009074	*IAP1*	IAP	IAPs
AAEL006633	*IAP2*	IAP	IAPs
AAEL014251	*IAP5*	IAP	IAPs
AAEL012446	*IAP6*	IAP	IAPs
AAEL012512	*IAP9*	IAP	IAPs
AAEL003245	*IKK1A*	IKKb	IMDPAT*HS*

AAEL010548	*IKK1B*	IKKb	IMDPAT*HS*
AAEL012510	*IKK2*	IKKg	IMDPAT*HS*
AAEL010083	*IMD*	IMD	IMDPAT*HS*
AAEL004392	*IMP*	IMP	Caspase Activators
AAEL008687	*LOQS*	Loquacious	Small Regulatory RNA Path
AAEL003712	*LYSC10*	LYSC	Lysozymes
AAEL003723	*LYSC11*	LYSC	Lysozymes
AAEL010100	*LYSC7A*	LYSC	Lysozymes
AAEL015404	*LYSC7B*	LYSC	Lysozymes
AAEL009670	*LYSC9*	LYSC	Lysozymes
AAEL005988	*LYSC6*	LYS-long	Lysozymes
AAEL014196	*Michelob_x*	Michelob_x	Caspase Activators
AAEL004120	*ML1*	ML	MD2-Like Receptors
AAEL015135	*ML10*	ML	MD2-Like Receptors
AAEL006854	*ML13*	ML	MD2-Like Receptors
AAEL009553	*ML14A*	ML	MD2-Like Receptors
AAEL015516	*ML14B*	ML	MD2-Like Receptors
AAEL009555	*ML15A*	ML	MD2-Like Receptors
AAEL009556	*ML15B*	ML	MD2-Like Receptors
AAEL015140	*ML16*	ML	MD2-Like Receptors
AAEL009557	*ML17*	ML	MD2-Like Receptors
AAEL012064	*ML2*	ML	MD2-Like Receptors
AAEL015137	*ML20*	ML	MD2-Like Receptors
AAEL007592	*ML20B*	ML	MD2-Like Receptors
AAEL009760	*ML21*	ML	MD2-Like Receptors
AAEL015139	*ML22A*	ML	MD2-Like Receptors
AAEL009954	*ML22B*	ML	MD2-Like Receptors
AAEL007591	*ML26A*	ML	MD2-Like Receptors
AAEL013835	*ML26B*	ML	MD2-Like Receptors
AAEL001654	*ML30*	ML	MD2-Like Receptors
AAEL001661	*ML31*	ML	MD2-Like Receptors
AAEL001634	*ML32*	ML	MD2-Like Receptors
AAEL001650	*ML33*	ML	MD2-Like Receptors
AAEL015136	*ML6*	ML	MD2-Like Receptors
AAEL015138	*ML9A*	ML	MD2-Like Receptors
AAEL009953	*ML9B*	ML	MD2-Like Receptors
AAEL009531	-	ML	MD2-Like Receptors
AAEL007768	*MYD88*	*MYD88*	TOLLPAT*HS*
AAEL002478	*PASHA*	Pasha	Small Regulatory RNA Path
AAEL006571	*PELLE*	PELLE	TOLLPAT*HS*
AAEL012380	*PGRPLA*	PGRPL	PGRPs
AAEL010171	*PGRPLB*	PGRPL	PGRPs
AAEL014640	*PGRPLC*	PGRPL	PGRPs
AAEL011608	*PGRPLD*	PGRPL	PGRPs
AAEL013112	*PGRPLE*	PGRPL	PGRPs
AAEL009474	*PGRPS1*	PGRPS	PGRPs

AAEL007037	*PGRPS4*	PGRPS	PGRPs
AAEL007039	*PGRPS5*	PGRPS	PGRPs
AAEL008076	*PIWI1*	PIWI	Small Regulatory RNA Path
AAEL008098	*PIWI2*	PIWI	Small Regulatory RNA Path
AAEL013692	*PIWI3*	PIWI	Small Regulatory RNA Path
AAEL007698	*PIWI4*	PIWI	Small Regulatory RNA Path
AAEL013233	*PIWI5*	PIWI	Small Regulatory RNA Path
AAEL013227	*PIWI6*	PIWI	Small Regulatory RNA Path
AAEL006287	*PIWI7*	PIWI	Small Regulatory RNA Path
AAEL013498	*PPO1*	PPO	Prophenoloxidases
AAEL011764	*PPO10*	PPO	Prophenoloxidases
AAEL013499	*PPO2*	PPO	Prophenoloxidases
AAEL011763	*PPO3*	PPO	Prophenoloxidases
AAEL013501	*PPO4*	PPO	Prophenoloxidases
AAEL013492	*PPO5*	PPO	Prophenoloxidases
AAEL014544	*PPO6*	PPO	Prophenoloxidases
AAEL013493	*PPO7*	PPO	Prophenoloxidases
AAEL013496	*PPO8*	PPO	Prophenoloxidases
AAEL014837	*PPO9*	PPO	Prophenoloxidases
AAEL011753	*R2D2*	R2D2	Small Regulatory RNA Path
AAEL007696	*REL1A*	REL1	REL
AAEL006930	*REL1B*	REL1	REL
AAEL007624	*REL2*	REL2	REL
AAEL001317	*RM62A*	Rm62	Small Regulatory RNA Path
AAEL001769	*RM62B*	Rm62	Small Regulatory RNA Path
AAEL002083	*RM62C*	Rm62	Small Regulatory RNA Path
AAEL002351	*RM62D*	Rm62	Small Regulatory RNA Path
AAEL004978	*RM62E*	Rm62	Small Regulatory RNA Path
AAEL008738	*RM62F*	Rm62	Small Regulatory RNA Path
AAEL010402	*RM62G*	Rm62	Small Regulatory RNA Path
AAEL010787	*RM62H*	Rm62	Small Regulatory RNA Path
AAEL013985	*RM62I*	Rm62	Small Regulatory RNA Path
AAEL001914	*SCRAC1*	SCRA	Scavenger Receptors
AAEL015308	*SCRAL1*	SCRA	Scavenger Receptors
AAEL009192	*SCRASP1*	SCRA	Scavenger Receptors
AAEL010655	*SCRASP2*	SCRA	Scavenger Receptors
AAEL014367	*SCRASP3*	SCRA	Scavenger Receptors
AAEL005374	*SCRB1*	SCRB	Scavenger Receptors
AAEL007748	*SCRB10*	SCRB	Scavenger Receptors
AAEL008370	*SCRB17*	SCRB	Scavenger Receptors
AAEL005987	*SCRB2*	SCRB	Scavenger Receptors
AAEL005979	*SCRB3*	SCRB	Scavenger Receptors
AAEL011222	*SCRB5*	SCRB	Scavenger Receptors
AAEL002741	*SCRB6*	SCRB	Scavenger Receptors
AAEL000234	*SCRB7*	SCRB	Scavenger Receptors
AAEL000227	*SCRB8*	SCRB	Scavenger Receptors

AAEL000256	*SCRB9*	SCRB	Scavenger Receptors
AAEL009420	*SCRBQ1*	SCRB	Scavenger Receptors
AAEL009423	*SCRBQ2*	SCRB	Scavenger Receptors
AAEL009432	*SCRBQ3*	SCRB	Scavenger Receptors
AAEL006355	*SCRC1*	SCRC	Scavenger Receptors
AAEL006361	*SCRC2*	SCRC	Scavenger Receptors
AAEL014091	*CuSOD1*	SOD-Cu-Zn	Superoxide Dismutatses
AAEL006271	*CuSOD2*	SOD-Cu-Zn	Superoxide Dismutatses
AAEL011498	*CuSOD3*	SOD-Cu-Zn	Superoxide Dismutatses
AAEL000259	*CuSOD4*	SOD-Cu-Zn	Superoxide Dismutatses
AAEL004823	*MnSOD1*	SOD-Mn-Fe	Superoxide Dismutatses
AAEL005108	*MnSOD2*	SOD-Mn-Fe	Superoxide Dismutatses
AAEL013235	*SPNE*	Spindle_E	Small Regulatory RNA Path
AAEL000499	*SPZ1A*	SPZ	Spaetzle-like Proteins
AAEL013434	*SPZ1B*	SPZ	Spaetzle-like Proteins
AAEL013433	*SPZ1C*	SPZ	Spaetzle-like Proteins
AAEL001435	*SPZ2*	SPZ	Spaetzle-like Proteins
AAEL008596	*SPZ3A*	SPZ	Spaetzle-like Proteins
AAEL014950	*SPZ3B*	SPZ	Spaetzle-like Proteins
AAEL007897	*SPZ4*	SPZ	Spaetzle-like Proteins
AAEL001929	*SPZ5*	SPZ	Spaetzle-like Proteins
AAEL012164	*SPZ6*	SPZ	Spaetzle-like Proteins
AAEL014079	*SRPN1*	SRPN-INHIB	Serine Protease Inhibitors
AAEL007765	*SRPN10a*	SRPN-INHIB	Serine Protease Inhibitors
AAEL007765	*SRPN10b*	SRPN-INHIB	Serine Protease Inhibitors
AAEL007765	*SRPN10c*	SRPN-INHIB	Serine Protease Inhibitors
AAEL007765	*SRPN10d*	SRPN-INHIB	Serine Protease Inhibitors
AAEL014138	*SRPN16*	SRPN-INHIB	Serine Protease Inhibitors
AAEL014078	*SRPN2*	SRPN-INHIB	Serine Protease Inhibitors
AAEL002720	*SRPN20*	SRPN-INHIB	Serine Protease Inhibitors
AAEL002730	*SRPN21*	SRPN-INHIB	Serine Protease Inhibitors
AAEL002715	*SRPN22*	SRPN-INHIB	Serine Protease Inhibitors
AAEL005665	*SRPN3*	SRPN-INHIB	Serine Protease Inhibitors
AAEL013936	*SRPN4a*	SRPN-INHIB	Serine Protease Inhibitors
AAEL013933	*SRPN4b*	SRPN-INHIB	Serine Protease Inhibitors
AAEL013937	*SRPN4c*	SRPN-INHIB	Serine Protease Inhibitors
AAEL013934	*SRPN4d*	SRPN-INHIB	Serine Protease Inhibitors
AAEL014141	*SRPN5*	SRPN-INHIB	Serine Protease Inhibitors
AAEL010769	*SRPN6*	SRPN-INHIB	Serine Protease Inhibitors
AAEL002699	*SRPN7*	SRPN-INHIB	Serine Protease Inhibitors
AAEL011777	*SRPN8*	SRPN-INHIB	Serine Protease Inhibitors
AAEL008364	*SRPN9*	SRPN-INHIB	Serine Protease Inhibitors
AAEL003686	*SRPN11*	SRPN-nonINHIB	Serine Protease Inhibitors
AAEL003653	*SRPN12*	SRPN-nonINHIB	Serine Protease Inhibitors
AAEL002731	*SRPN14*	SRPN-nonINHIB	Serine Protease Inhibitors
AAEL003697	*SRPN17*	SRPN-nonINHIB	Serine Protease Inhibitors

AAEL006137	*SRPN19*	SRPN-nonINHIB	Serine Protease Inhibitors
AAEL002704	*SRPN23*	SRPN-nonINHIB	Serine Protease Inhibitors
AAEL007420	*SRPN25*	SRPN-nonINHIB	Serine Protease Inhibitors
AAEL003182	*SRPN26*	SRPN-nonINHIB	Serine Protease Inhibitors
AAEL009692	*STAT*	STAT	JAKSTATs
AAEL007035	*TAK1*	TAK1	IMDPAT*HS*
AAEL012267	*TEP13*	TEP	Thio-Ester Containing Proteins
AAEL014755	*TEP15*	TEP	Thio-Ester Containing Proteins
AAEL001794	*TEP20*	TEP	Thio-Ester Containing Proteins
AAEL001802	*TEP21*	TEP	Thio-Ester Containing Proteins
AAEL000087	*TEP22*	TEP	Thio-Ester Containing Proteins
AAEL001163	*TEP23*	TEP	Thio-Ester Containing Proteins
AAEL004000	*TOLL10*	TOLL	TOLLs
AAEL009551	*TOLL11*	TOLL	TOLLs
AAEL007613	*TOLL1A*	TOLL	TOLLs
AAEL003507	*TOLL1B*	TOLL	TOLLs
AAEL007619	*TOLL5A*	TOLL	TOLLs
AAEL000057	*TOLL5B*	TOLL	TOLLs
AAEL000671	*TOLL6*	TOLL	TOLLs
AAEL002583	*TOLL7*	TOLL	TOLLs
AAEL000633	*TOLL8*	TOLL	TOLLs
AAEL013441	*TOLL9A*	TOLL	TOLLs
AAEL011734	*TOLL9B*	TOLL	TOLLs
AAEL013528	*TPX1*	TPX	Peroxidases
AAEL004112	*TPX2*	TPX	Peroxidases
AAEL014548	*TPX3*	TPX	Peroxidases
AAEL002309	*TPX4*	TPX	Peroxidases
AAEL009051	*TPX5*	TPX	Peroxidases
AAEL011363	*TRAF6*	TRAF6	TOLLPAT*HS*
AAEL000293	*TSN*	TSN	Small Regulatory RNA Path
AAEL007642	*TUBE*	TUBE	TOLLPAT*HS*
AAEL008073	*VIG*	VIG	Small Regulatory RNA Path

Table A3. Summary of unmapped and mapped RNA-seq reads. Samstat output summaries and averages of the number of mapped reads under each treatment, as well as the quality statistics for the mapping process. The number of unmapped reads is also noted.

	% from just Aligned Reads	# of Reads			% of All Reads		
Treatment	% MAPQ>30	MAPQ>30	Unmapped	Total	MAPQ>30	Unmapped	Mapped
Rb24	64.5	11090415	2650685	19833635	56%	13%	87%
Rb36	69.1	10521787	2738074	17969751	59%	15%	85%
Rb48	81.6	12400943	4317882	19512721	64%	22%	78%
Rv24	82.4	12309730	2914234	17856949	69%	16%	84%
Rv36	82.3	10686847	2587216	15577074	69%	17%	83%
Rv48	78.8	9778127	2562484	14969762	65%	17%	83%
Sb24	65.5	11392189	3210246	20596883	55%	16%	84%
Sb36	67.5	6097545	1776032	10807060	56%	16%	84%
Sb48	83.5	11759988	4255288	18331302	64%	23%	77%
Sv24	73	10150845	2543240	16455363	62%	15%	85%
Sv36	79.4	11870160	3085770	18044646	66%	17%	83%
Sv48	80.8	15412758	3257884	22330650	69%	15%	85%

Table A4. Significantly overrepresented ($p<0.05$) Gene Ontology (GO) terms and asso-ciation number as identified by the Ontologizer (v2.0). Three treatment comparisons are displayed: Cali-S blood fed (Sb) versus Cali-S virus fed (Sv), Cali-R blood fed (Rb) versus Cali-R virus fed (Rv), and Cali-S virus fed (Sv) versus Cali-R virus fed (Rv) at all three time points, 24, 36 and 48 hours. Overrepresented upregulated terms appear as green, while downregulated terms appear in red.

A. Molecular function associated GO terms

	Sb vs Sv			**Rb vs Rv**			**Sv vs Rv**		
GO term accession and description	24	36	48	24	36	48	24	36	48
GO:0097159|organic cyclic compound binding									
GO:0097367|carbohydrate derivative binding									
GO:1901265|nucleoside phosphate binding									
GO:1901360|organic cyclic compound metabolic process									
GO:1901363|heterocyclic compound binding									
GO:0000287|magnesium ion binding									
GO:0003723|RNA binding									
GO:0003735|structural constituent of ribosome									
GO:0003779|actin binding									
GO:0003824|catalytic activity									
GO:0005488|binding									
GO:0005506|iron ion binding									
GO:0005515|protein binding									
GO:0008092|cytoskeletal protein binding									
GO:0008234|cysteine-type peptidase activity									
GO:0008238|exopeptidase activity									
GO:0008289|lipid binding									
GO:0009055|electron carrier activity									
GO:0016616|oxidoreductase activity, acting on the CH-OH group of donors, NAD or NADP as acceptor									
GO:0016667|oxidoreductase activity, acting on a sulfur group of donors									
GO:0016740|transferase activity									

GO:0016817|hydrolase activity, acting on acid anhydrides											
GO:0022804|active transmembrane transporter activity											
GO:0036094|small molecule binding											
GO:0043167|ion binding											
GO:0043168|anion binding											
GO:0043492|ATPase activity, coupled to movement of substances											
GO:0046906|tetrapyrrole binding											
GO:0048037|cofactor binding											
GO:0051540|metal cluster binding											

B. Biological process associated GO terms

	Sb vs Sv			**Rb vs Rv**			**Sv vs Rv**		
GO term accession and description	24	36	48	24	36	48	24	36	48
GO:0065009|regulation of molecular function									
GO:0070887|cellular response to chemical stimulus									
GO:0071702|organic substance transport									
GO:0071826|ribonucleoprotein complex subunit organization									
GO:0071840|cellular component organization or biogenesis									
GO:0098660|inorganic ion transmembrane transport									
GO:1901564|organonitrogen compound metabolic process									
GO:1901700|response to oxygen-containing compound									
GO:0005975|carbohydrate metabolic process									
GO:0006091|generation of precursor metabolites and energy									
GO:0006366|transcription from RNA polymerase II promoter									
GO:0006396|RNA processing									
GO:0006412|translation									
GO:0006793|phosphorus metabolic process									
GO:0006812|cation transport									
GO:0006818|hydrogen transport									
GO:0006950|response to stress									
GO:0007167|enzyme linked receptor protein signaling pathway									

GO:0008150|biological_process	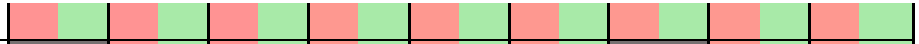
GO:0008152|metabolic process	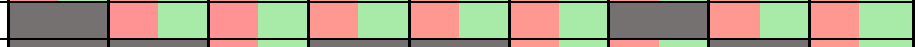
GO:0009056|catabolic process	
GO:0009058|biosynthetic process	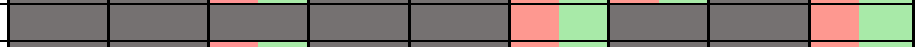
GO:0009987|cellular process	
GO:0010033|response to organic substance	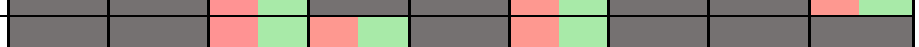
GO:0010467|gene expression	
GO:0010608|posttranscriptional regulation of gene expression	
GO:0010646|regulation of cell communication	
GO:0016052|carbohydrate catabolic process	
GO:0016568|chromatin modification	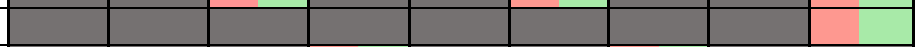
GO:0019538|protein metabolic process	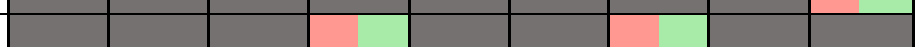
GO:0022613|ribonucleoprotein complex biogenesis	
GO:0023051|regulation of signaling	
GO:0030203|glycosaminoglycan metabolic process	
GO:0033036|macromolecule localization	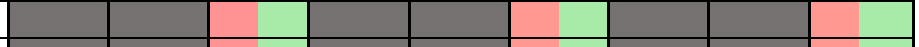
GO:0034660|ncRNA metabolic process	
GO:0035556|intracellular signal transduction	
GO:0043412|macromolecule modification	
GO:0043623|cellular protein complex assembly	
GO:0044281|small molecule metabolic process	
GO:0048583|regulation of response to stimulus	
GO:0051179|localization	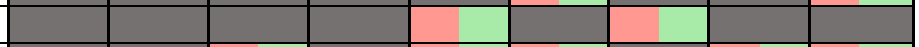
GO:0051641|cellular localization	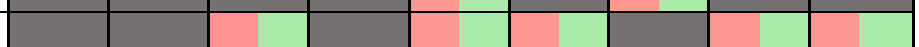
GO:0065008|regulation of biological quality	

C. Cellular component associated GO terms

	Sb vs Sv			**Rb vs Rv**			**Sv vs Rv**		
GO term accession and description	24	36	48	24	36	48	24	36	48
GO:1990204|oxidoreductase complex									
GO:0000502|proteasome complex									
GO:0005622|intracellular									
GO:0005623|cell									
GO:0005737|cytoplasm									
GO:0005852|eukaryotic translation initiation factor 3 complex									
GO:0015629|actin cytoskeleton									
GO:0016020|membrane									
GO:0016469|proton-transporting two-sector ATPase complex									
GO:0030529|ribonucleoprotein complex									
GO:0031974|membrane-enclosed lumen									
GO:0031975|envelope									
GO:0032991|macromolecular complex									
GO:0043226|organelle									
GO:0043228|non-membrane-bounded organelle									
GO:0044422|organelle part									
GO:0044428|nuclear part									

Appendix B. RNAi mediated knock down of *Aedes aegypti xylosyltransferase oxt*, *heparan sulfate N-deacetylase/N-sulfotransferase*, and clip-domain serine protease easter 34, family B

Author Contributions

Carl Lowenberger and Heather Coatsworth conceived the study. Carl Lowenberger, Heather Coatsworth, Jaime Chalissery, and William Shen completed sample preparation and collection. Heather Coatsworth and Laura Barth completed sample processing and analysis. Heather Coatsworth completed statistical analyses. Heather Coatsworth and Carl Lowenberger wrote the chapter.

Abstract

Aedes aegypti is the principal vector of dengue viruses. In Cali, Colombia, approximately 30% of field collected *Ae. aegypti* are dengue-refractory, possessing a midgut infection barrier (Cali-MIB), while the remaining 70% are dengue-susceptible (Cali-S). Previous research investigating gene expression differences between these phenotypes using RNA sequencing (Chapter 2), as well as studies examining DNA sequence differences between the phenotypes using genome wide association studies (GWAS) (Chapter 3) identified two candidate genes of interest, *xylosyltransferase*, and *CLIPB34* that might contribute to the Cali-MIB and Cali-S phenotypes, respectively. *Xylosyltransferase* is a gene with a variant that was found to be statistically associated with the Cali-MIB phenotype (Chapter 3). *CLIPB34* is a gene that was found to be differentially expressed in Cali-S compared with Cali-MIB after bloodfeeding (Chapter 2). We used RNAi approaches to demonstrate that knock-downs of these genes is achievable.

Keywords: *Aedes aegypti*, gene-knockdowns, RNAi

Introduction

Vector-borne pathogens, many of which are transmitted by mosquitoes, are responsible for a large proportion of the world's most debilitating and devasting diseases (Mairuhu et al. 2004). Of these, dengue is the most widespread of the arthropod-borne viruses, infecting 390 million people each year throughout tropical and sub-tropical regions (Bhatt et al. 2013). Dengue viruses (DENV) are primarily transmitted by the anthropophilic mosquito *Aedes aegypti* (Halstead et al. 1997). Although *Ae. aegypti* is the principal vector of dengue viruses, not all females transmit dengue. Naturally dengue refractory strains have been found, and in Cali, Colombia, approximately 30% of field collected *Ae. aegypti* are refractory to all 4 dengue serotypes (Ocampo and Wesson 2004, Serrato et al. 2017) through a midgut infection barrier (MIB) in which DENV is unable to enter or replicate within midgut cells (Ocampo et al. 2013). We used multiple approaches to discern that differences between the Cali-MIB and Cali-S strains were based on differential gene expression in the midguts of the strains (Barón et al. 2010, Ocampo et al. 2013, Caicedo et al. 2018, Chapter 2), and differences in coding regions of DNA (Chapter 3). We determined that the phenotype is likely not due to differences in midgut microbiota (Coatsworth et al. 2018, Chapter 4). From these studies, we identified two genes of interest: *xylosyltransferase oxt* (*xylo*, AAEL007409) and clip-domain serine protease easter 34, family B, (*CLIPB34*, AAEL000028).

A variant predicted to affect the transcription of *xylo* was identified in our GWAS study (Chapter 3) as being statistically associated with the Cali-MIB phenotype. We also observed numerous other SNPs present in the Cali-MIB gene sequence of *xylo* (that Cali-S mosquitoes did not posses). Functionally, *xylosyltransferase* is an enzyme necessary for heparan and chondroitin sulfate production (Esko et al. 1985), substrates deemed essential for viral binding and entry into Vero and BHK (baby hamster kidney) cells (Germi et al. 2002). Mutations in *xylosyltransferase* in dengue-refractory individuals may render downstream substrates such as heparin and chondroitin sulfate non- or sub-functional, preventing viral entry into midgut epithelial cells. As such, we were interested in knocking-down both *xylosyltransferase*, and one of its downstream substrates, *heparan sulfate N-deacetylase/N-sulfotransferase* (*HS*, AAEL012539), to examine what effects these genes have on dengue entry, replication and dissemination in *Ae. aegypti*.

We found higher expression of *CLIPB34* in Cali-S blood and dengue-fed mosquitoes (compared to Cali-MIB blood and dengue-fed mosquitoes) (Chapter 2). We hypothesized that this higher expression might facilitate dengue entry into midgut cells, either directly, by acting as a protein substrate or cell-mediated binding protease, or indirectly, via immune pathway activation or secondary metabolite production. The larger family of CLIP domain proteases has well characterized immune functions against *Plasmodium* in *Anopheles* sp. (Zou et al. 2011). As such, we wanted to knock-down the expression of *CLIPB34* and see if these knock-downs contributed to dengue vector-competence in *Ae. aegypti*.

In order to examine the contribution of each of these three genes to vector competence to dengue in *Ae. aegypti* we first sought out to ensure we could create gene knock-downs for each gene. To do this we used a traditional RNAi technique, injecting dsRNA complementary to each of our genes of interest into adult female blood-fed *Ae. aegypti*. The efficacy of the knock-downs was assessed using quantitative real-time PCR.

Methods

Mosquito maintenance

Adult mosquitoes were maintained under standard laboratory conditions: 27˚C, 70% relative humidity, and a 12:12 hour light: dark cycle, and fed daily with a 10% sucrose solution.

Synthesis of double-stranded RNA

Primers were designed for all three of our genes of interest (Table 1), as well as for a silencing control (*Arabidopsis thaliana* Integrase-type DNA-binding superfamily protein (ANT), AT4G37750). Primer design was completed using NCBI's BLASTn and Primer Blast (Geer et al. 2009) functions in order to create the most unique and specific ~500bp sequence as possible (based on previous experimental successes from our research group). *Aedes aegypti* cDNA from previous experiments was used as a template to generate the dsRNA product. First, the gene-specific ~500bp product was amplified in a standard PCR reaction using 2X Taq Master Mix (ABM, Richmond, BC). This amplicon was purified and sequenced to ensure we had amplified the desired DNA fragment. A T7

overhang was subsequently added to both ends of the product using gene-specific + T7 primers (Table 1). Finally, T7 primers were used to amplify the gene-specific + T7 product to generate sufficient template for dsRNA synthesis. All products were size visualized in a 1% agarose gel. A TranscriptAid T7 High Yield Transcription Kit (Thermo Scientific, Waltham, MA, USA) was used to synthesize dsRNA for our three genes of interest (*CLIPB34*, *xylo* and *HS*), as well as for our injection control (ANT) following the manufacturer's instructions. dsRNA products were ethanol precipitated and visualized in a 1% agarose-bleach gel. The concentration of each product was assessed using a Nanodrop 1000 spectrophotometer (Thermo Fisher Scientific, Waltham, MA, USA), and diluted to 100ng/47nL. This concentration of dsRNA has proved successful based on previous experiments completed in our lab (Caicedo et al. 2018).

Mosquito microinjections

Adult female *Aedes aegypti* (Liverpool strain) were injected with 100ng of treatment-specific dsRNA delivered through a single pulse of 47nL using a Drummond 'Nanoject' injection unit (Broomall, PA, USA). Five females were injected/dsRNA treatment at 24, 48 and 72 hours post blood feeding. Needles used for injection were created in house using aluminosilicate glass and a Sutter Instrument P-1000 Micropipette Puller (Novato, CA, USA) (heat = 510, velocity = 30, delay = 25, pull = 20, pressure = 500). Mosquitoes were anesthetized with CO_2 and kept on ice for immobilization until they were injected. A weak vacuum was used to hold each mosquito by it's notum. Once in place, the needle was inserted into the thorax through the soft membrane behind the head of the insect. Injected mosquitoes were placed in cartons covered with mesh and maintained as previously described.

Mosquito dissections

The midgut of each injected mosquito was extracted 24, 48, or 72 hours post injection. Each midgut was placed individually in tubes containing 200µL of Trizol reagent and stored at -80°C. Similarly, the remaining carcass from each mosquito was placed individually in Trizol reagent and stored at -80˚C.

RNA extraction and cDNA synthesis

Carcass and midgut tissues were homogenized using sterilized plastic pestles and an electronic homogenizer. RNA was extracted from the resultant homogenate using the Trizol (Ambion, Thermo Fisher Scientific, Waltham, MA, USA) RNA extraction protocol provided by the manufacturer. RNA samples were resuspended in 10µL of DEPC treated water, and their concentrations were measured on a Nanodrop 1000 spectrophotometer (Thermo Fisher Scientific, Waltham, MA, USA). First strand cDNA synthesis was performed in 20µL reactions containing 0.5µg of total RNA using an oligo dT primer (MGdT) with the OneScript cDNA Synthesis Kit (ABM, Richmond, BC, Canada) using an extension time of 50 mins. The subsequent cDNA was diluted 1:10 with DEPC water. One (1) µL of each synthesized cDNA was used in a standard PCR reaction using *β-actin* primers (Table 1) to confirm that the cDNA synthesis had been successful.

Knockdown assessment

Quantitative real-time PCR (qPCR) was used to determine expression levels of our genes of interest: *xylosyltransferase*, *heparan sulfate N-deacetylase/N-sulfotransferase* and *CLIPB34*. Briefly, 12µL reactions containing 6.0µ SYBR Green (Quanta BioSciences Inc., Beverly, MA, USA), 3.0µ nuclease-free water, 300mM of each primer (See Table 1) as well as 1µL of cDNA were run in duplicate in a Rotor-Gene 3000 (Corbett Research, Cambridge, UK). Resultant melt curves were analyzed to ensure that a single peak was present in samples containing target DNA, that there was no evidence of primer dimers, and that no peaks were present in the no template control reactions. Direct cycle threshold (Ct) values were compared, and any technical duplicates exceeding a standard deviation of 0.5 were re-run for accuracy. Comparisons were made using the $2^{-\Delta\Delta Ct}$ method (Livak and Schmittgen 2001, Schmittgen and Livak 2008), using 2 housekeeping genes, *β-actin* (LOC5574526) and *40S ribosomal protein S7* (*RPS7*, LOC5572090) as the first internal calibrators. The expression levels of *xylosyltransferase oxt* (*xylo*), *heparan sulfate N-deacetylase/N-sulfotransferase* (*HS*), and clip-domain serine protease easter 34, family B (*CLIPB34*) were compared between dsRNA injected insects and their injection controls (dsANT or water). Resultant ΔCt values were compared in R (v. 3.3.2) (Team 2011, 2018) between treatments for statistical differences using a Student's two-way homoscedastic t-test at $\alpha = 0.05$.

Results

Mosquito microinjections

No female mosquitoes injected with the ds*xylo* construct survived past the 24hour timepoint. As such, subsequent ds*xylo* analyses were only completed at the 24h post injection timepoint. No morbidity was noted in any other dsRNA injected treatment.

Knockdown assessment

After normalization to the housekeeping genes (*RPS7* and *β-actin*, ΔCt), the expression levels of *xylo*, *HS* and *CLIPB34* were directly compared to their injection control treatments (dsANT for *xylo* and *HS*, water for *CLIPB34*) to examine whether the knockdowns were effective (Figures B1-B3). We observed a knockdown effect on *HS* at 24 and 72 hours after injection of ds*HS* (Figure B1), and *CLIPB34* after injection with ds*CLIPB34* (Figure B3), although no differences in expression were observed 48 hours post injection. There was also a knockdown of *HS* 24 hours after injection with ds*xylo* (Figure B1). Injections with ds*xylo* and ds*HS* however increased the expression of *xylo* 24 hours post injection (Figure B2). There was also an increase in *xylo* expression at all three timepoints (24, 48 and 72 hours post injection) for the ds*HS* treatment (Figure B2). These trends however were not statistically significant (from the injection controls) (p-value > 0.05).

Discussion

We observed a knockdown of *HS* in both the ds*HS* and ds*xylo* treatments, although these knockdown effects were not statistically significant (Figure B1), likely due to the large standard deviation present in each experiment due to a low number of replicates (n=3). Future studies should aim to include more replicates. In our ds*xylo* treatment, we saw an increase in the expression of both *xylo* and *HS* at 24 hours post injection (Figures B1 and B2). We also saw an increase in the expression of *xylo* at 24, 48 and 72 hours post injection in the ds*HS* treatment (Figure B2). *Xylo* is required for the creation of the tetrasaccharide backbone, the first step in the glycosaminoglycan synthesis pathway (which produces *heparan sulfate*) (Avirutnan et al. 2007) (Figure B4), while *HS* is required to catalyze N-deacetylation and the N-sulfation of glucosamine to create

heparan sulfate. The expression of *xylo* may have increased as the mosquito noticed a decrease in *heparan sulfate* levels due to the effects of the ds*HS* knockdown. In an effort to remedy this knockdown, the mosquito might be upregulating *xylosyltransferase* expression to create more *heparan sulfate* to restore pre-knockdown levels, although the role of *xylosyltransferase* in *Ae. aegypti* is not well known. However, a homolog of *Ae. aegypti xylosyltransferase* in *Anopheles gambiae* modifies *heparan sulfate* and chondroitin proteoglycans (Armistead et al. 2011), suggesting this may also be possible in *Ae. aegypti*.

Our data suggest that *xylosyltransferase* is essential for adult female *Ae. aegypti* survival, as ds*xylo* injections were lethal to mosquitos by 48 hours post injection. Other experiments targeting mosquito midgut *xylosyltransferase*s in *Culex* sp. however were not lethal (Brackney 2015), which may suggest a dsRNA dose dependant or species-specific response to *xylosyltransferase*.

Glycosaminoglycans have been identified as parasite recognition ligands in the midguts of *An. gambiae* (Dinglasan et al. 2007). Furthermore, *heparan sulfate* glycosaminoglycans were identified as important receptors for salivary gland entry by *Plasmodium falciparum* (Armistead et al. 2011). Dengue viruses use glycosaminoglycans as cell-surface binding sites, and cells lacking both *xylosyltransferase* and *heparan sulfate* showed a 50-70% reduction in DENV NS1 binding (Avirutnan et al. 2007). Results from our GWAS study (Chapter 3) suggest that there are multiple SNPs in both *xylosyltransferase* and *HS* in dengue-refractory mosquitoes which may render the resultant proteins non-functional, thus contributing to the dengue refractory phenotype that we have observed.

We also had a knock-down effect of *CLIPB34* in the ds*CLIPB34* treatment at 24 and 72 hours post injection, although this effect was not statistically significant (p-value >0.05) (Figure B3). As noted above, this lack of statistical significance is likely due to the large standard deviation present as a result of a low number of replicates (n=3). Future studies should include more replicates to overcome this issue. CLIPs are serine proteases involved in immune and developmental processes and are well known for their role in anti-*Plasmodium* responses, initiating melanization and pathogen lysis cascades (Zou et al. 2011). Members of the CLIPB family in mosquitoes have been annotated functionally as melanization proteases (Zou et al. 2011). We observed a higher expression of *CLIPB34*

in our dengue-susceptible mosquitoes (Chapter 2). This may be a result of immune activation due to the continued presence of dengue in our susceptible strain. As the virus is unable to bind to and enter cells in our refractory strain, refractory mosquitoes might not need to upregulate traditional immune-related gene families such as the CLIP subfamily of genes.

For all three of the genes investigated in this experiment, future studies should be completed to assess their role in the Cali-S and Cali-MIB dengue phenotypes. These knockdown studies should be repeated prior to exposing adult females to dengue via an artificial blood meal. Traditional immunofluorescence assays then can be used to screen for the presence or absence of dengue in both the midgut and salivary gland tissues, furthering our knowledge regarding genes that are important for *Ae. aegypti* vector competence towards dengue viruses.

References

Armistead, J. S., I. B. Wilson, T. H. van Kuppervelt, and R. R. Dinglasan. **2011**. A role for *heparan sulfate* proteoglycans in *Plasmodium falciparum* sporozoite invasion of anopheline mosquito salivary glands. Biochem J. 438: 475–483.

Avirutnan, P., L. Zhang, N. Punyadee, A. Manuyakorn, and C. Puttikhunt. **2007**. Secreted NS1 of Dengue Virus Attaches to the Surface of Cells via Interactions with *Heparan sulfate* and Chondroitin Sulfate E. PLoS Pathog. 3(11): e183.

Barón, O. L., R. J. Ursic-Bedoya, C. A. Lowenberger, and C. B. Ocampo. **2010**. Differential Gene Expression from Midguts of Refractory and Susceptible Lines of the Mosquito, *Aedes aegypti* , Infected with Dengue-2 Virus. J. Insect Sci. 10: 1–23.

Bhatt, S., P. W. Gething, O. J. Brady, J. P. Messina, A. W. Farlow, C. L. Moyes, J. M. Drake, J. S. Brownstein, A. G. Hoen, O. Sankoh, M. F. Myers, D. B. George, T. Jaenisch, G. R. William Wint, C. P. Simmons, T. W. Scott, J. J. Farrar, and S. I. Hay. **2013**. The global distribution and burden of dengue. Nature. 496: 504–507.

Brackney, D. E. 2015. Characterization of mosquito midgut protein and glycan determinants mediating susceptibility to flaviviruses.

Caicedo, P. A., I. M. Serrato, S. Sim, G. Dimopoulos, H. Coatsworth, C. Lowenberger, and C. B. Ocampo. **2018**. Immune response-related genes associated to blocking midgut dengue virus infection in *Aedes aegypti* strains that differ in susceptibility. Insect Sci. 26: 635–648.

Coatsworth, H., P. A. Caicedo, T. Van Rossum, C. B. Ocampo, and C. Lowenberger. **2018**. The Composition of Midgut Bacteria in *Aedes aegypti* (Diptera : Culicidae) That Are Naturally Susceptible or Refractory to Dengue Viruses. J. Insect Sci. 18(6).

Dinglasan, R. R., A. Alaganan, A. K. Ghosh, A. Saito, T. H. Van Kuppevelt, and M. Jacobs-lorena. **2007**. *Plasmodium falciparum* ookinetes require mosquito midgut chondroitin sulfate proteoglycans for cell invasion. PNAS. 104(40): 15882-15887.

Esko, J. D., T. O. D. E. Stewart, and W. H. Taylor. **1985**. Animal cell mutants defective in glycosaminoglycan biosynthesis. Proc Natl Acad Sci. 82: 3197–3201.

Geer, L. Y., A. Marchler-Bauer, R. C. Geer, L. Han, J. He, S. He, C. Liu, W. Shi, and S. H. Bryant. **2009**. The NCBI BioSystems database. Nucleic Acids Res. 38: 492–496.

Germi, R., J.-M. Crance, D. Garin, J. Guimet, H. Lortat-Jacob, R. Ruigrok, J.-P. Zarski, and E. Drouet. **2002**. *Heparan sulfate*-Mediated Binding of Infectious Dengue Virus Type 2 and Yellow Fever Virus. Virology. 168: 162–168.

Halstead, S. B., D. J. Gubler, and G. Kuno. **1997**. Dengue and dengue hemorrhagic fever. Handb. Zoonoses. 8: 45–60.

Livak, K. J., and T. D. Schmittgen. **2001**. Analysis of relative gene expression data using real-time quantitative PCR and the $2^{-\Delta\Delta CT}$ method. Methods. 25: 402–408.

Mairuhu, A. T. A., J. Wagenaar, D. P. M. Brandjes, and E. C. M. Van Gorp. **2004**. Dengue: An arthropod-borne disease of global importance. Eur. J. Clin. Microbiol. Infect. Dis. 23: 425–433.

Ocampo, C. B., P. A. Caicedo, G. Jaramillo, R. Ursic Bedoya, O. Baron, I. M. Serrato, D. M. Cooper, and C. Lowenberger. **2013**. Differential Expression of Apoptosis Related Genes in Selected Strains of *Aedes aegypti* with Different Susceptibilities to Dengue Virus. PLoS One. 8(4): e61187.

Ocampo, C. B., and D. M. Wesson. **2004**. Population dynamics of *Aedes aegypti* from a dengue hyperendemic urban setting in Colombia. Am. J. Trop. Med. Hyg. 71: 506–513.

Schmittgen, T. D., and K. J. Livak. **2008**. Analyzing real-time PCR data by the comparative CT method. Nat. Protoc. 3: 1101–1108.

Serrato, I. M., P. A. Caicedo, Y. Orobio, C. Lowenberger, and C. B. Ocampo. **2017**. Vector competence and innate immune responses to dengue virus infection in selected laboratory and field-collected *Stegomyia aegypti* (= *Aedes aegypti*). Med. Vet. Entomol. 31: 312–319.

Team, R. C. 2018. R: A Language and Environment for Statistical Computing.

Team, R. D. C. 2011. R: A language and environment for statistical computing.

Zou, Z., J. Souza-Neto, Z. Xi, V. Kokoza, S. W. Shin, G. Dimopoulos, and A. Raikhel. **2011**. Transcriptome analysis of *Aedes aegypti* transgenic mosquitoes with altered immunity. PLoS Pathog. 7(11): e1002394.

Tables

Table B1. Primer names and sequences used to amplify a ~500 bp DNA template for subsequent dsRNA synthesis. Gene-specific primers were created for three genes of interest: clip-domain serine protease easter family B, (*CLIPB34*, AAEL000028), *xylosyltransferase oxt* (*xylo*, AAEL007409), and *heparan sulfate N-deacetylase/N-sulfotransferase* (*HS*, AAEL012539) and for an plant injection control, *Arabidopsis thaliana* Integrase-type DNA-binding superfamily protein (ANT, AT4G37750). The T7 promotor region included in the primers (underlined region) was added to the 5' end of each primer for subseqeunt dsRNA production.

Primer Name	Primer Sequence	Product Length (bp)
*CLIPB34*500 Forward	GGCCGTCGAGCAAATAATCG	422
*CLIPB34*500 Reverse	GTCCAAAGCTCACAATACCG	
*CLIPB34*500 Forward + T7	GTAATACGACTCACTATAGGGCGAATTGGGCCGTCGAGCAAATAATCG	478
*CLIPB34*500 Reverse + T7	GTAATACGACTCACTATAGGGCGAATTGGTCCAAAGCTCACAATACCG	
*HS*500 Forward	ATTCGTCTGAAGGGGAACGG	516
*HS*500 Reverse	GTTGGCCTGATCTTATAGTAGACG	
*HS*500 Forward + T7	GTAATACGACTCACTATAGGGCGAATTGATTCGTCTGAAGGGGAACGG	572
*HS*500 Reverse +T7	GTAATACGACTCACTATAGGGCGAATTGGTTGGCCTGATCTTATAGTAGACG	
*Xylo*500 Forward	GCTCCAGATTCCCGTTTCCG	557
*Xylo*500 Reverse	ATTCACTAGAGTACTGAACTCCG	
*Xylo*500 Forward + T7	GTAATACGACTCACTATAGGGCGAATTGGCTCCAGATTCCCGTTTCCG	613
*Xylo*500 Reverse + T7	GTAATACGACTCACTATAGGGCGAATTGATTCACTAGAGTACTGAACTCCG	
ANT500 Forward	GGTGGAGGATTTCTTTGGGACC	516
ANT500 Reverse	ACGCCTCGGTATTGAGAAGTTCG	
ANT500 Forward + T7	GTAATACGACTCACTATAGGGCGAATTGGGTGGAGGATTTCTTTGGGACC	572
ANT500 Reverse + T7	GTAATACGACTCACTATAGGGCGAATTGACGCCTCGGTATTGAGAAGTTCG	
T7	GTAATACGACTCACTATAGGGCGAATTG	N/A

Table B2. Primers used in this study for quantitative real-time PCR (qPCR) analysis of gene expression. Gene-specific primers that amplified products ~ 150 bp were designed for three genes of interest: clip-domain serine protease easter family B, (*CLIPB34*, AAEL000028), *xylosyltransferase oxt* (*xylo*, AAEL007409), and *heparan sulfate N-deacetylase/N-sulfotransferase* (*HS*, AAEL012539) and for two housekeeping genes, *β-actin* (LOC5574526) and *40S ribosomal protein S7* (*RPS7*, LOC5572090).

Primer Name	Primer Sequence	Product Length (bp)
*CLIPB34*200 Forward	CAAGCAATGTCAAGCTGAAGG	173
*CLIPB34*200 Reverse	GCGATCCAATTTGGTCAACG	
*HS*200 Forward	TGTTGCGTTGAAGAATGAGTGC	157
*HS*200 Reverse	CCGGTGCGACGTTATTTTGC	
*Xylo*200 Forward	GAACGAGTTGGAGTTTGTGCC	169
*Xylo*200 Reverse	CCCATTCGGACAAAAGTTGGG	
β-actin Forward	CGTTCGTGACATCAAGGAAA	175
β-actin Reverse	GAACGATGGCTGGAAGAGAG	
RPS7 Forward	TCAGTGTACAAGAAGCTGACCGGA	118
RP7 Reverse	TTCCGCGCGCGCTCACTTATTAGATT	

Figures

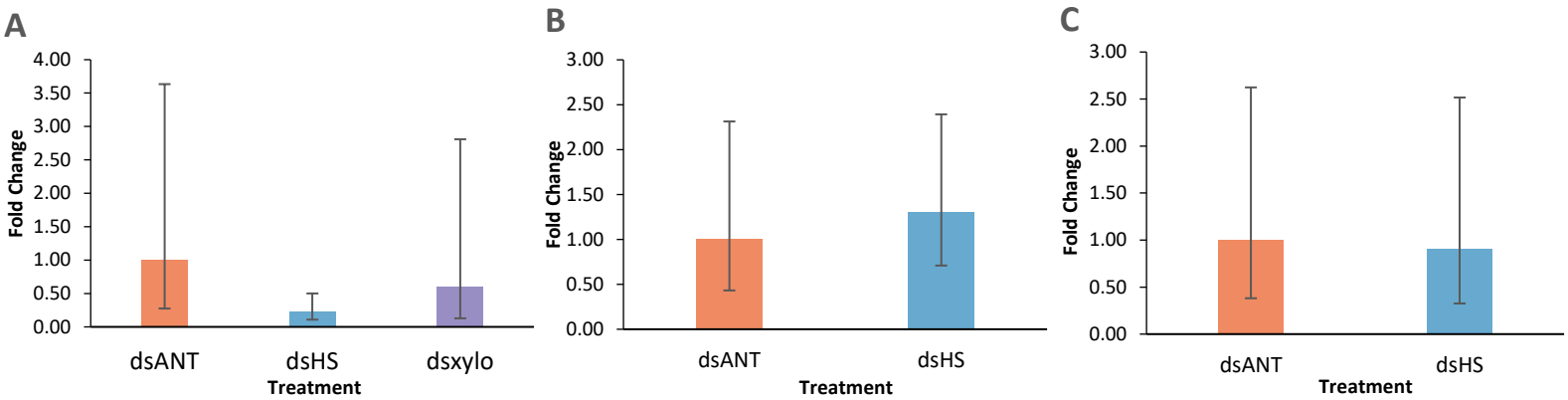

Figure B1. Relative expression of *heparan sulfate N-deacetylase/N-sulfotransferase* (*HS*) (AAEL012539) in *Aedes aegypti* females injected with dsRNA targeting *HS* (blue), an upstream regulator of *HS*, *xylosyltransferase oxt* (*xylo*) (AAEL007409) (purple), and a plant gene control, *Arabidopsis thaliana* Integrase-type DNA-binding superfamily protein (ANT) (AT4G37750) (orange). The vertical axis represents the mean fold change in *HS* expression at (A) 24 hours, (B) 48 hours, and (C) 72 hours post dsRNA injection, measured using quantitative real-time PCR. *HS* expression was normalized using *Ae. aegypti* housekeeping genes *β-actin* (LOC5574526) and *40S ribosomal protein S7* (*RPS7*, LOC5572090). We used the $2^{-\Delta\Delta Ct}$ method using the dsANT treatment as the second calibrator (arbitrarily set to 1) to visualize relative fold changes. Error bars represent standard error (SE), calculated as per Livak and Schmittgen (2001). No measurements were carried out on ds*xylo* injected insects at 48 and 72 hours, as no ds*xylo* injected mosquitoes survived to these timepoints.

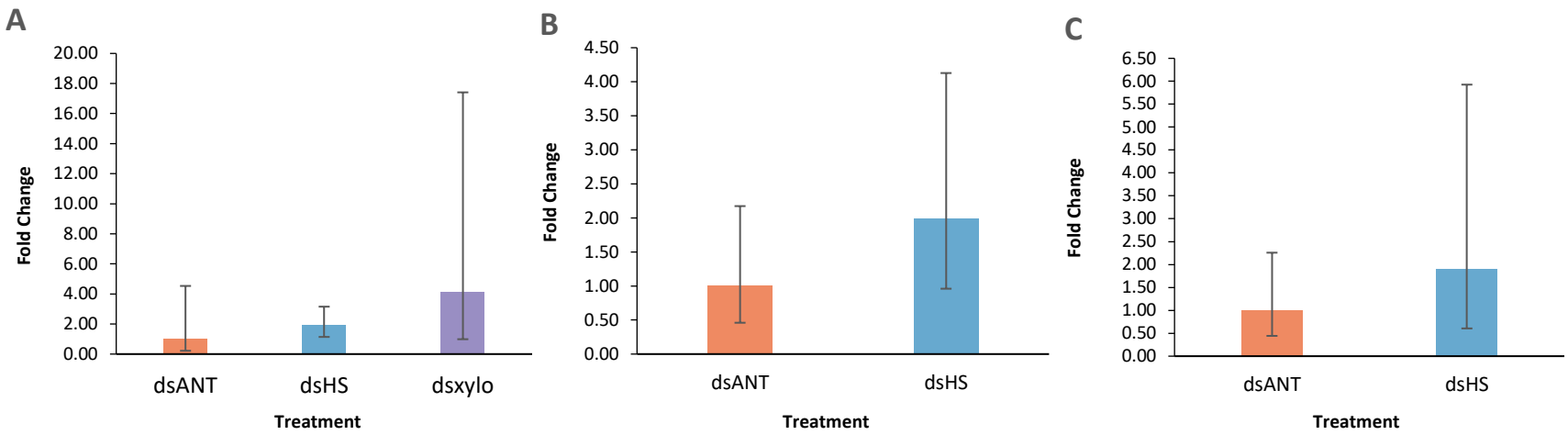

Figure B2. Relative expression of *xylosyltransferase oxt* (*xylo*) (AAEL007409) in *Aedes aegypti* females injected with dsRNA targeting *xylo* (purple), a down stream gene thought to be regulated by *xylo*, *heparan sulfate N-deacetylase/N-sulfotransferase* (*HS*) (AAEL012539) (blue), and a plant gene control, *Arabidopsis thaliana* Integrase-type DNA-binding superfamily protein (ANT) (AT4G37750) (orange). The vertical axis represents the mean fold change in *xylo* expression at (A) 24 hours, (B) 48 hours, and (C) 72 hours post dsRNA injection, measured using quantitative real-time PCR. *Xylo* expression was normalized using *Ae. aegypti* housekeeping genes *β-actin* (LOC5574526) and *40S ribosomal protein S7* (*RPS7*, LOC5572090). We used the $2^{-\Delta\Delta Ct}$ method using the dsANT treatment as the second calibrator (arbitrarily set to 1) to visualize relative fold changes. Error bars represent standard error (SE), calculated as per Livak and Schmittgen (2001). No measurements were carried out on ds*xylo* injected insects at 48 and 72 hours, as no ds*xylo* injected mosquitoes survived to these timepoints.

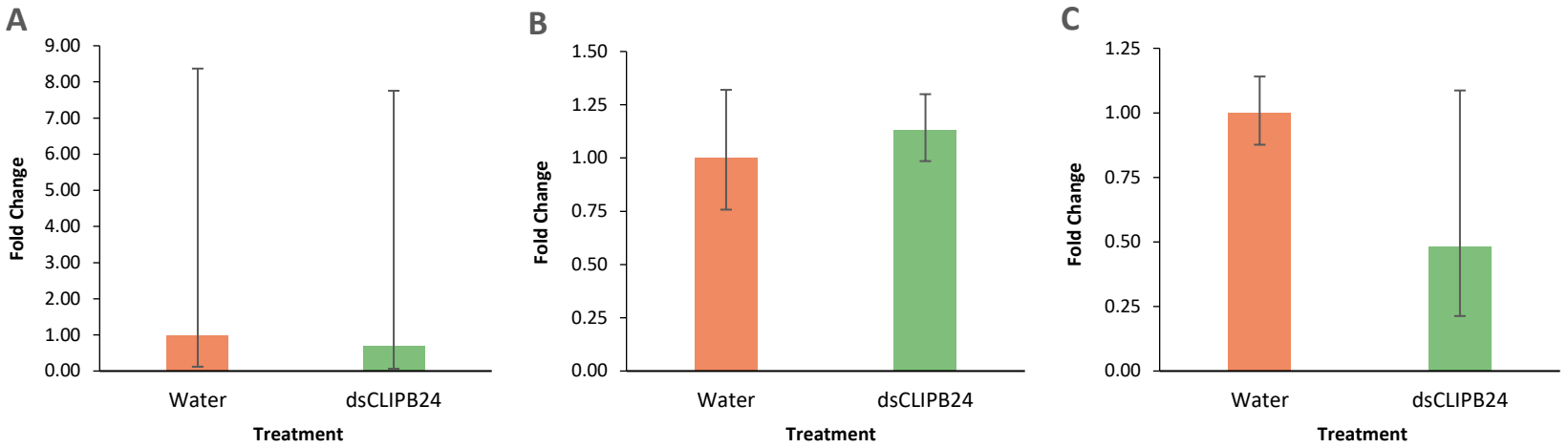

Figure B3. Relative expression of a clip-domain serine protease easter family B, (*CLIPB34*) (AAEL000028) in *Aedes aegypti* females injected with dsRNA targeting *CLIPB34* (green), or an injection control of water (orange). The vertical axis represents the mean fold change in *CLIPB34* expression at (A) 24 hours, (B) 48 hours, and (C) 72 hours post dsRNA or water injection, measured using quantitative real-time PCR. CLIB34 expression was normalized using *Ae. aegypti* housekeeping genes *β-actin* (LOC5574526) and *40S ribosomal protein S7* (*RPS7*, LOC5572090). We used the $2^{-\Delta\Delta Ct}$ method using the water treatment as the second calibrator (arbitrarily set to 1) to visualize relative fold changes. Error bars represent standard error (SE), calculated as per Livak and Schmittgen (2001).

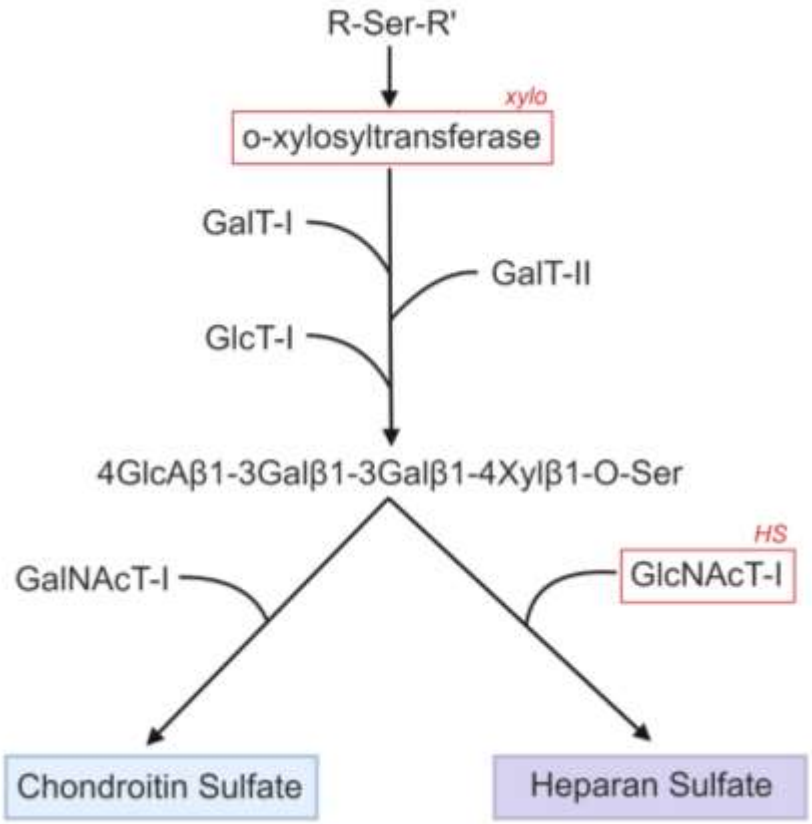

Figure B4. Glycoanaminoglycan biosynthesis in *Aedes aegpyti.* This figure was modified from (Dinglasan et al. 2007), incorperating information from KEGG pathway aag00534 (Glycosaminoglycan biosynthesis - heparan sulfate). Our twos genes of interest are outlined here in red: o-*xylosyltransferase* (*xylo*, AAEL007409), and GlcNAcT-I, *heparan sulfate N-deacetylase/N-sulfotransferase* (*HS*, AAEL012539). *Xylo* is involved in creating the linking reigon tetrasaccharide of heparan sulfate, while *HS* catalyzes the N-deacetylation and the N-sulfation of glucosamine (GlcNAc) of the glycosaminoglycan in heparan sulfate. Both *xylo* and *HS* are considered necessary for the synthesis of heparan sulfate.